

MINISTRY OF URBAN DEVELOPMENT (MoUD)  
MINISTRY OF HOME AFFAIRS (MoHA)  
MINISTRY OF FEDERAL AFFAIRS AND LOCAL DEVELOPMENT (MoFALD)  
DEPARTMENT OF MINES AND GEOLOGY (DMG)  
FEDERAL DEMOCRATIC REPUBLIC OF NEPAL

**THE PROJECT FOR  
ASSESSMENT OF EARTHQUAKE  
DISASTER RISK  
FOR THE KATHMANDU VALLEY  
IN  
NEPAL**

**FINAL REPORT  
VOLUME 2: MAIN REPORT**

**APRIL 2018**

**JAPAN INTERNATIONAL COOPERATION AGENCY**

**ORIENTAL CONSULTANTS GLOBAL CO., LTD.  
OYO INTERNATIONAL CORPORATION**

<b>GE</b>
<b>JR</b>
<b>18-061</b>

**MINISTRY OF URBAN DEVELOPMENT (MoUD)  
MINISTRY OF HOME AFFAIRS (MoHA)  
MINISTRY OF FEDERAL AFFAIRS AND LOCAL DEVELOPMENT (MoFALD)  
DEPARTMENT OF MINES AND GEOLOGY (DMG)  
FEDERAL DEMOCRATIC REPUBLIC OF NEPAL**

**THE PROJECT FOR  
ASSESSMENT OF EARTHQUAKE  
DISASTER RISK  
FOR THE KATHMANDU VALLEY  
IN  
NEPAL**

**FINAL REPORT  
VOLUME 2: MAIN REPORT**

**APRIL 2018**

**JAPAN INTERNATIONAL COOPERATION AGENCY**

**ORIENTAL CONSULTANTS GLOBAL CO., LTD.  
OYO INTERNATIONAL CORPORATION**

## COMPOSITION OF THE FINAL REPORT

Volume 1: Summary

Volume 2: Main Report

Volume 3: Map Book

Volume 4: Appendix (Materials supplement to main report, on DVD)

Volume 5: Attachment (Outcomes of pilot activities including BBB RR plan, LDCRP, SOP and CBDRRM, report of subcontract, technical notes and risk assessment manual, etc., on DVD)

Volume 6: GIS Data (Seismic Hazard and Risk Assessment, on DVD)

The following foreign exchange rate is applied on this report

US\$1.00 = NPR108.44

(December 2016)

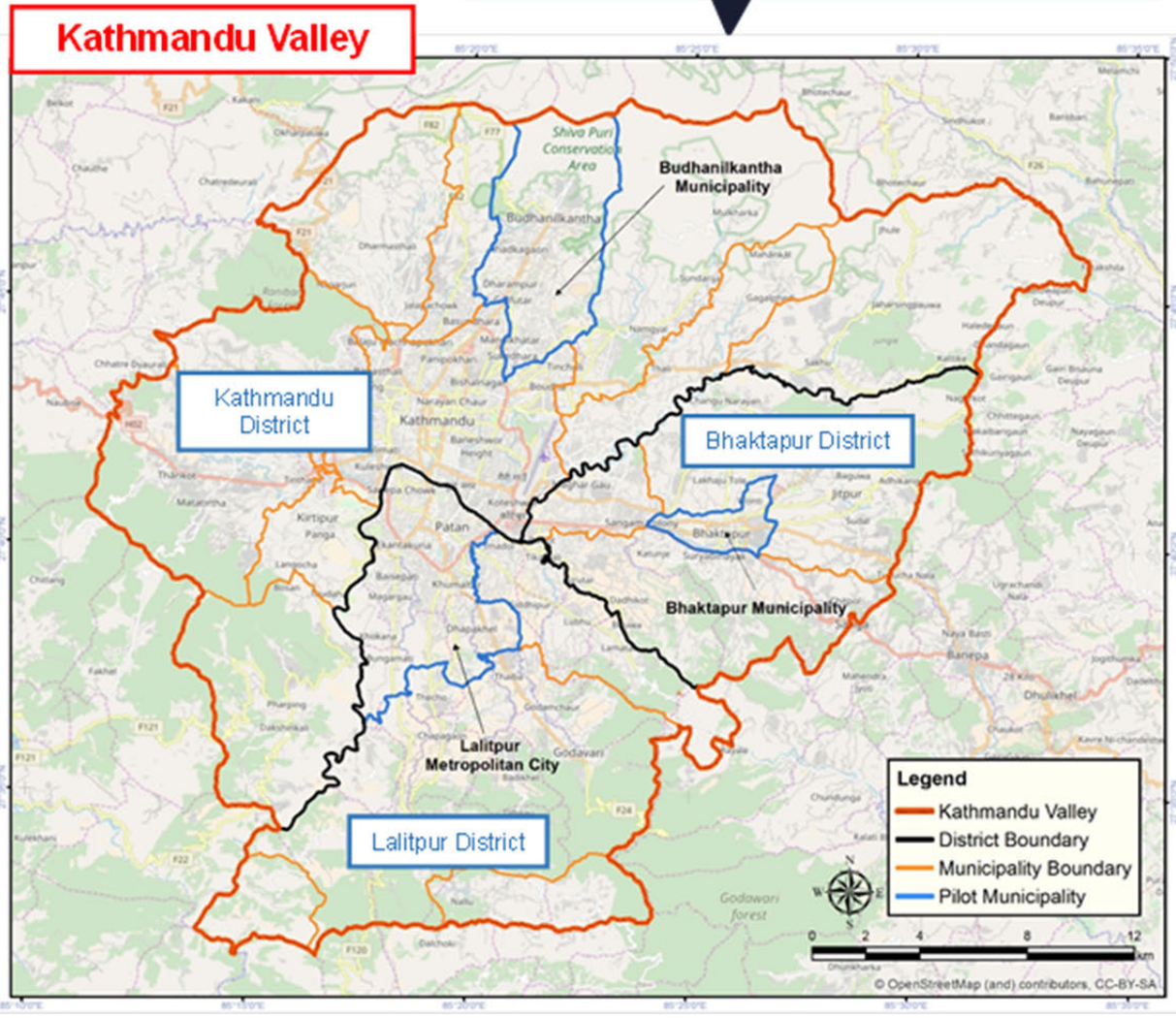


## Table of Contents

### Location Map of the Project

	Page
Chapter 1 Outline of the Project.....	1-1
1.1 Background.....	1-1
1.2 Summary of the Project.....	1-2
1.2.1 Name of the Project.....	1-2
1.2.2 Target Areas.....	1-2
1.2.3 Overall Aim.....	1-3
1.2.4 Project Goal.....	1-3
1.2.5 Project Output.....	1-3
1.2.6 Counterparts.....	1-3
1.2.7 Beneficiaries.....	1-3
1.3 Project Objective.....	1-3
1.4 Implementation Organization.....	1-4
1.4.1 Structure of the Implementation Organization.....	1-4
1.4.2 Structure of Working Groups.....	1-4
1.4.3 Members of the JICA Project Team and Assignments to be covered.....	1-5
1.5 JCC (Joint Coordinating Committee) Meeting.....	1-6
1.5.1 List of the Principal Meetings.....	1-6
1.5.2 JCC (Joint Coordinating Committee).....	1-8
Chapter 2 Basic Information Collection and Analysis.....	2-1
2.1 Natural conditions.....	2-1
2.1.1 Outline of geomorphology.....	2-1
2.1.2 Geology.....	2-2
2.1.3 Earthquake Activity.....	2-6
2.2 Social Information.....	2-11
2.2.1 Buildings.....	2-11
2.2.2 Transportation Infrastructure.....	2-25
2.2.3 Lifeline.....	2-27
2.2.4 Population.....	2-33
2.2.5 Economy.....	2-37
Chapter 3 Seismic Hazard Assessment.....	3-1
3.1 Items of Contents.....	3-2

3.2	Set-up of Scenario Earthquake .....	3-5
3.2.1	Far-Mid Western Nepal Scenario Earthquake.....	3-5
3.2.2	Western Nepal Scenario Earthquake.....	3-6
3.2.3	Central Nepal South Scenario Earthquake.....	3-6
3.3	Collection of Ground Data .....	3-10
3.3.1	Drilling data and geological maps .....	3-10
3.3.2	Altitude data.....	3-13
3.3.3	Preparation of detailed geomorphological map .....	3-14
3.3.4	Tectonic geomorphology .....	3-23
3.3.5	Susceptibility Maps.....	3-27
3.3.6	Depth of rock layer .....	3-29
3.3.7	Geological cross-sections .....	3-31
3.4	Field Survey (Microtremor Measurement) .....	3-33
3.4.1	Tripartite Array Microtremor Measurement .....	3-34
3.4.2	L-shape Array Microtremor Measurement with Three Point Array.....	3-37
3.4.3	Single Point Microtremor Measurement.....	3-41
3.5	Modelling of the Ground.....	3-45
3.5.1	Modeling between rock surface to Klm.....	3-45
3.5.2	Modeling between Klm to ground surface.....	3-45
3.5.3	Integration of ground model .....	3-45
3.6	Calculation of Earthquake Motion at Bedrock.....	3-51
3.7	Calculation of Earthquake Motion at Ground Surface.....	3-53
3.7.1	Input Waveform .....	3-54
3.7.2	Ground Model for Response Analysis .....	3-55
3.7.3	Calculation for Verification Earthquake .....	3-56
3.7.4	Study of Correction Factor .....	3-59
3.7.5	Calculation of Earthquake Motion at Ground Surface for Scenario Earthquake.....	3-61
3.7.6	Calculation of Other Indexes for Earthquake Motion.....	3-64
3.8	Assessment of Liquefaction .....	3-68
3.8.1	Liquefaction history in Kathmandu Valley .....	3-68
3.8.2	Study of liquefaction assessment method.....	3-70
3.8.3	Verification of liquefaction assessment .....	3-77
3.8.4	Liquefaction assessment results for scenario earthquakes.....	3-78
3.8.5	Evaluation method for liquefaction by Architectural Institute of Japan .....	3-81
3.9	Earthquake Induced Slope Failure .....	3-87
3.9.1	Existing Data Collection.....	3-87
3.9.2	Types of Slope Failure .....	3-96
3.9.3	Case Study of Surface Failure using Slope Angle and PGA .....	3-96
3.9.4	Slope Failure Evaluation Results.....	3-99

3.9.5	Slope Failure after Earthquake .....	3-101
3.10	Considerations and Recommendations for the Future in the Seismic Hazard	
	Assessment Performance .....	3-102
3.10.1	Data and assessment method regarding earthquake.....	3-102
3.10.2	Active fault investigation.....	3-103
3.10.3	Ground model .....	3-103
3.10.4	Assessment for slope failure and liquefaction .....	3-104
3.10.5	Human resource development .....	3-104
3.10.6	Results of seismic hazard assessment.....	3-105
Chapter 4	Seismic Risk Assessment.....	4-1
4.1	Necessity and objectives of Seismic Risk Assessment .....	4-5
4.2	Scenario Earthquakes and Their Occurrence Scene.....	4-6
4.2.1	Scenario Earthquakes and Ground Motion Used for Risk Assessment .....	4-6
4.2.2	Earthquake Occurrence Scenes.....	4-7
4.3	Approach and Results of Seismic Risk Assessment.....	4-10
4.3.1	Damage to Buildings .....	4-10
4.3.2	Damage to transportation Infrastructure .....	4-28
4.3.3	Damage to Lifeline Facilities.....	4-39
4.3.4	Human Casualties .....	4-57
4.3.5	Economic Impact Assessment .....	4-65
4.4	Comparative Vulnerability Analysis of KV .....	4-78
4.5	Recommendations for Future Update of Risk Assessment .....	4-81
4.5.1	Recommendations for Technical Aspects of Risk Assessment .....	4-81
4.5.2	Recommendations for Institutional Aspects of Risk Assessment .....	4-84
Chapter 5	Pilot Activities.....	5-1
5.1	Pilot Municipalities .....	5-2
5.1.1	Selection of Pilot Municipalities.....	5-2
5.1.2	Profile of Pilot Municipality .....	5-5
5.2	BBB Recovery and Reconstruction Plan for Pilot Municipalities .....	5-9
5.2.1	Damage survey of pilot municipalities .....	5-10
5.2.2	Case Study of the recovery and reconstruction plan in Japan.....	5-14
5.2.3	Condition setting of the BBB RR Plan .....	5-22
5.2.4	Consideration of the Vision for the BBB RR Plan.....	5-26
5.2.5	Formulation of BBB RR Basic Plan .....	5-29
5.2.6	Land Use Assessment .....	5-35
5.2.7	Formulation of BBB RR Action Plan .....	5-70
5.2.8	Finalization of the BBB RR Plan.....	5-73

5.3	Standard Operation Procedure (SOP) .....	5-76
5.4	Technical Guideline for Formulation of Local Disaster and Climate Resilience Plan (TG LDCRP).....	5-87
5.4.1	Review of Existing Guideline related to Disaster Management Planning.....	5-87
5.4.2	Consideration of Structure of Technical Guideline for Formulation of LDCRP .....	5-93
5.4.3	Formulation of Technical Guideline for Formulation of LDCRP.....	5-98
5.5	Local Disaster and Climate Resilience Plan for Pilot Municipalities .....	5-108
5.5.1	Review of Existing Disaster Risk Management Plan in Municipalities .....	5-108
5.5.2	Information Collection for formulation of LDCRP .....	5-110
5.5.3	Formulation of Local Disaster and Climate Resilience Plan .....	5-111
5.6	Community-based Disaster Risk Reduction and Management (CBDRRM) Activities....	5-139
5.6.1	Background and Situation of CBDRRM Activities in Nepal .....	5-139
5.6.2	Situation of Community's Awareness on DRR in the Pilot Municipalities before the Project activities.....	5-140
5.6.3	Pilot Activities for Enhancing Community Capacities on Disaster Risk Reduction and Management .....	5-144
5.7	Recommendations for Future Disaster Risk Reduction and Management Activities in the Municipal Level and Nationwide Dissemination of Pilot Activities.....	5-165
5.7.1	Recommendations for Future Disaster Risk Reduction and Management Activities in the Municipal Level.....	5-166
5.7.2	Nationwide Dissemination of Pilot Activities.....	5-169
Chapter 6	Capacity Building Activities.....	6-1
6.1	WG and JWG Meeting.....	6-1
6.1.1	WG1 (Working Group 1) Meeting.....	6-1
6.1.2	WG2 (Working Group 2) Meeting.....	6-2
6.1.3	WG3 (Working Group 3) Meeting.....	6-5
6.1.4	JWG (Joint Working Group) Meeting .....	6-9
6.2	Public Seminar .....	6-10
6.2.1	First Public Seminar.....	6-10
6.2.2	Second Public Seminar .....	6-11
6.2.3	Third Public Seminar .....	6-11
6.3	C/P Training in Japan .....	6-13
6.3.1	First C/P Training in Japan .....	6-13
6.3.2	Second C/P Training in Japan .....	6-17
6.3.3	Third C/P Training in Japan.....	6-21



Chapter 7	Contribution to Sendai Framework for Disaster Risk Reduction and Recommendations for achieving Disaster Risk Reduction.....	7-1
7.1	Contribution for Achievement of the target of the Sendai Framework.....	7-1
7.2	Recommendations on Utilization of Risk Assessment Results.....	7-4
7.3	Recommendations for Mainstreaming Seismic Disaster Risk Reduction.....	7-7

**Appendix (on DVD)**

Appendix 1	Review of Related Policies, Plans, Laws and Organization
Appendix 2	Damage of Gorkha Earthquake
Appendix 3	Emergency Response Chronicle Survey of the Gorkha Earthquake in 2015
Appendix 4	Construction of Earthquake Resistant Model Buildings
Appendix 5	DRR Awareness Activities
Appendix 6	Information Collection by Sub-contract
Appendix 7	Development of Building Damage Function
Appendix 8	Seismic Performance Strengthening of Bridge
Appendix 9	Capacity Development and Assessment

**Attachment (on DVD)**

Attachment 1	List of Collected Data
Attachment 2:	Risk Assessment Results of Municipalities
Attachment 3:	Pamphlet for DRR Awareness
Attachment 4:	Radio Programme for DRR Awareness
Attachment 5:	BBB Recovery and Reconstruction Plan for Pilot Municipalities
Attachment 6:	Standard Operation Procedure (SOP) for Pilot Municipalities
Attachment 7:	Technical Guideline for Formulation of LDCRP
Attachment 8:	LDCRP for Pilot Municipalities
Attachment 9:	CBDRRM Plan - Ward Level
Attachment 10:	Ward DRR Carte for CBDRRM
Attachment 11:	Report of Sub-contract
Attachment 12:	Technical Notes for Earthquake Ground Motion Estimation
Attachment 13:	Manual for Seismic Risk Assessment
Attachment 14:	Brochure

## List of Figures

	Page
Figure 1.4.1	Structure of the Implementation Organizations..... 1-4
Figure 1.4.2	Structure of each WG ..... 1-5
Figure 1.4.3	Expert structure of the JICA Project Team and Assignments to be covered..... 1-6
Figure 1.5.1	Original and supplement components of the project ..... 1-8
Figure 1.5.2	1st JCC meeting..... 1-8
Figure 1.5.3	2nd JCC meeting ..... 1-9
Figure 1.5.4	3rd JCC meeting ..... 1-9
Figure 1.5.5	4th JCC meeting ..... 1-10
Figure 1.5.6	5th JCC meeting ..... 1-10
Figure 1.5.7	6th JCC meeting ..... 1-11
Figure 2.1.1	Geomorphological map of the Kathmandu Valley (partly modified from Yoshida and Igarashi, 1984) ..... 2-2
Figure 2.1.2	Geology of the Kathmandu Valley (DMG, Engineering and environmental geological map of the Kathmandu Valley, partly modified from Shrestha et al., 1998) ..... 2-5
Figure 2.1.3	Geology of the Kathmandu Valley, partly modified from Comprehensive Disaster Risk Management Program (UNDP, 2013). ..... 2-5
Figure 2.1.4	Schematic Earthquake Occurrence Model in Nepal from 13th Century ..... 2-8
Figure 2.1.5	Earthquake Activity from 1980 to 2014 ..... 2-9
Figure 2.1.6	Earthquake Activity from 1980 to 2015 ..... 2-9
Figure 2.2.1	The flow of estimation of building distributions by earthquake occurrence scene ..... 2-12
Figure 2.2.2	Three types of thematic maps utilized for area classification..... 2-15
Figure 2.2.3	The result of area classification ..... 2-16
Figure 2.2.4	The estimated results of the building component ratios of ten classified areas..... 2-17
Figure 2.2.5	Building structure component ratio in the entire Kathmandu Valley in 2016 ..... 2-18
Figure 2.2.6	Building structure component ratio in the entire Kathmandu Valley in 2030 without BSPS..... 2-19
Figure 2.2.7	Building structure component ratio in the entire Kathmandu Valley in 2030 with BSPS (five cases) ..... 2-21
Figure 2.2.8	Religious buildings including palace buildings..... 2-24
Figure 2.2.9	Rana building (Keisar Mahal) ..... 2-24
Figure 2.2.10	Elevation of Newari house..... 2-25
Figure 2.2.11	Implemented areas for the Distribution Network Improvement Works ..... 2-29
Figure 2.2.12	The existing sewage distribution network in Kathmandu Valley ..... 2-30

Figure 2.2.13	The classification map of the power distribution service areas in Kathmandu Valley .....	2-31
Figure 2.2.14	Estimated distribution of utility poles in the Kathmandu Valley .....	2-32
Figure 2.2.15	The flow of estimation of urbanization patterns by ward .....	2-35
Figure 2.2.16	Trend of economic growth rate.....	2-38
Figure 2.2.17	Transition of nominal GDP.....	2-38
Figure 2.2.18	GDP ratio of each industry sector.....	2-39
Figure 2.2.19	Transition of growth rate of each sector .....	2-40
Figure 2.2.20	Transition of arrivals and tourism revenue .....	2-40
Figure 2.2.21	Transition of the number of migrant workers and amount of remittance .....	2-41
Figure 2.2.22	Comparison of GDP per capita .....	2-42
Figure 2.2.23	Receiving amounts per person of overseas remittance and GDP ratio of overseas remittance.....	2-43
Figure 3.1.1	Flow of seismic hazard assessment .....	3-2
Figure 3.2.1	Scenario Earthquake Fault Model .....	3-8
Figure 3.2.2	Scenario Earthquake Fault Model in 2002 JICA Project.....	3-9
Figure 3.2.3	Slip Distribution in Fault Area.....	3-9
Figure 3.3.1	Distribution of collected borehole data.....	3-11
Figure 3.3.2	Collected geological maps, (upper) Engineering and Environmental Geology map by DMG, 1998, and (lower) Geology Map by UNDP, 2013 .....	3-12
Figure 3.3.3	Altitude and slope angle distribution using DEM (UNDP).....	3-13
Figure 3.3.4	A pair of aerial photographs for stereo-view nears the Tribhuvan International Airport .....	3-16
Figure 3.3.5	An example of detailed geomorphological classification. Location etc. same as above.....	3-17
Figure 3.3.6	Geomorphological map of the Kathmandu Valley .....	3-20
Figure 3.3.7	Locations of geomorphological map described later. A line of A-B-C represents the location of topographic profile. ....	3-22
Figure 3.3.8	Geomorphological map in the central area of Kathmandu .....	3-22
Figure 3.3.9	Geomorphological map of the northern area of Tribhuvan International Airport.....	3-23
Figure 3.3.10	Geomorphological map in the Suryabinayak area.....	3-23
Figure 3.3.11	Active fault traces of the Chandragiri Fault in the west of Kirtipur Municipality.....	3-25
Figure 3.3.12	Active fault traces in Sunakothi.....	3-25
Figure 3.3.13	A fault scarp around 10m high in the west of Kirtipur Municipality.....	3-26
Figure 3.3.14	A fault scarp in Thankot .....	3-26
Figure 3.3.15	N-S direction topographic profile and distribution of deltaic-lacustrine terraces.....	3-27
Figure 3.3.16	AVS30 map base on geomorphological unit (surface soil softness “Shakability” map).....	3-28

Figure 3.3.17	Liquefaction Susceptibility Map.....	3-28
Figure 3.3.18	Earthquake induced slope failure Susceptibility Map .....	3-29
Figure 3.3.19	Rock depth distribution based on gravity anomaly and drilling data .....	3-30
Figure 3.3.20	Estimated rock depth distribution (2D) .....	3-30
Figure 3.3.21	Estimated rock depth distribution (3D) .....	3-31
Figure 3.3.22	Newly developed Geological cross-sections .....	3-32
Figure 3.4.1	Measurement Points of Tripartite Array Microtremor Measurement .....	3-35
Figure 3.4.2	Results of Tripartite Array Microtremor Measurement .....	3-36
Figure 3.4.3	S-wave Velocity Structure of Deep Ground by Tripartite Array Microtremor Measurement and Soil Layer .....	3-37
Figure 3.4.4	Measurement Points of L-shape Microtremor Measurement .....	3-38
Figure 3.4.5	Relation of AVS30 and Elevation .....	3-39
Figure 3.4.6	Observed S-wave Velocity Profile by Geomorphological Unit.....	3-39
Figure 3.4.7	Relation of Observed S-wave Velocity Profile with Elevation for Alluvial Lowland (al) .....	3-40
Figure 3.4.8	Relation of S-wave Velocity Structure Model in 10m Depth Interval with Elevation for Alluvial Lowland (al).....	3-40
Figure 3.4.9	Measurement Points of Single Point Microtremor Measurement except Existing and L-shape Points .....	3-42
Figure 3.4.10	1st Predominant Period by Single Microtremor Measurement and Rock Depth by Gravity Anomaly .....	3-42
Figure 3.4.11	Predominant Period around 1~2 sec. by Single Microtremor Measurement and Rock Depth by Gravity Anomaly .....	3-43
Figure 3.4.12	Predominant Period less than 1 sec. by Single Microtremor Measurement and Geomorphological Class.....	3-43
Figure 3.4.13	1st Predominant Period by Single Microtremor Measurement except Existing and L-shape Points.....	3-44
Figure 3.4.14	Comparison of Predominant Period by Microtremor Measurement and by Ground Model.....	3-44
Figure 3.5.1	Comparison of Amplification Function Estimated from Earthquake Record (upper), Microtremor Measurement (lower left) and Ground Model (lower right) at DMG point.....	3-47
Figure 3.5.2	Examples of North-South Cross Section of Ground Grid Model.....	3-48
Figure 3.5.3	Estimated AVS30 from Ground Model.....	3-48
Figure 3.5.4	Amplification Factor by Subsurface Soil Layer for Small Input (left) and Large Input (right).....	3-49
Figure 3.5.5	Predominant Period of the Ground by Response Analysis, 1st peak of the transfer function by SH wave multiple reflection theory .....	3-49
Figure 3.5.6	3D Expression of Grid Ground Model .....	3-50

Figure 3.5.7	3D Expression of Soil Layer Boundary, Ground surface (pink), surface of Klm (light blue), Lkl (green), Tarebhir (camel) and Rock (purple). Black bars are drilling logs which reach to rock. ....	3-51
Figure 3.6.1	NGA Attenuation Function for PGA .....	3-52
Figure 3.7.1	Flow of Response Analysis.....	3-54
Figure 3.7.2	Input Waveform for response Analysis, (upper) original, (lower) converted to $V_s=600\text{m/sec}$ rock condition .....	3-55
Figure 3.7.3	PGA of Verification Earthquake (C.F. = $x1/1$ ).....	3-57
Figure 3.7.4	PGA of Gorkha Earthquake (C.F. is set to reproduce the observed PGA) .....	3-57
Figure 3.7.5	PGA of 1934 Bihar-Nepal Earthquake, C.F. = $x1/1$ can explain damage.....	3-58
Figure 3.7.6	PGA of Verification Earthquake (Adopted).....	3-59
Figure 3.7.7	PGV of Verification Earthquake (Adopted).....	3-59
Figure 3.7.8	Comparison of Observed PGA/PGV and Calculated PGA/PGV; (left) PGA, (right) PGV .....	3-60
Figure 3.7.9	PGA of Scenario Earthquake (C.F. = $x1/1$ ) .....	3-63
Figure 3.7.10	PGA of Scenario Earthquakes (Adopted) .....	3-63
Figure 3.7.11	PGV of Scenario Earthquakes (Adopted).....	3-64
Figure 3.7.12	MMI of Verification and Scenario Earthquakes .....	3-66
Figure 3.8.1	Liquefaction history in Kathmandu Valley .....	3-69
Figure 3.8.2	Rate of grids with boreholes or sand layers .....	3-71
Figure 3.8.3	Top depth and thickness of alluvial sand layers .....	3-72
Figure 3.8.4	Relation between N value and depth (alluvial sand layers).....	3-74
Figure 3.8.5	Relation between N value and depth for area division .....	3-74
Figure 3.8.6	N value along depth for each area division.....	3-75
Figure 3.8.7	Liquefaction assessment target grids with area division and ground water level.....	3-77
Figure 3.8.8	Assumed result of liquefaction (rainy season).....	3-80
Figure 3.8.9	Assumed result of liquefaction (dry season) .....	3-81
Figure 3.8.10	Relationship Between Corrected N-Value, Liquefaction Resistance and Dynamic Shear Strain .....	3-84
Figure 3.8.11	Fine Fraction Content and Correction Coefficient for N-Value.....	3-84
Figure 3.8.12	Relationships Among Corrected N-Value, Magnitude, Number of Repetitions and Correction Coefficient .....	3-85
Figure 3.8.13	N-Value Correction Coefficient for Sand/Gravel Ground .....	3-85
Figure 3.9.1	Slope angle comparison between actual and corrected .....	3-88
Figure 3.9.2	Distribution of Corrected Slope Angle (average of the slope angles at the points of 10-meter interval in 250 meter grid, with elevation contour and slope failure history) .....	3-89
Figure 3.9.3	Histogram of Mean Slope Angle classified by Geological Age .....	3-89

Figure 3.9.4	Histogram of Mean Slope Angle for Geomorphological units relating to Surface Slip and Landslide .....	3-90
Figure 3.9.5	<i>N</i> values classified by Geological units (surface 5 meters) .....	3-91
Figure 3.9.6	Histogram of Slope Failure History by Geological Units.....	3-92
Figure 3.9.7	Histogram of Slope Failure History by Slope Angle.....	3-93
Figure 3.9.8	Relationship between PGA and Slope Angle at Slope Failure History Sites.....	3-93
Figure 3.9.9	Slope failure example by the 2015 Gorkha Earthquake (Budanilkantha) .....	3-94
Figure 3.9.10	Road failure by the 2015 Gorkha Earthquake (Bagmati River) .....	3-95
Figure 3.9.11	Road embankment failure by the 2015 Gorkha Earthquake (Bhaktapur road) .....	3-95
Figure 3.9.12	Relationship between Slope Angle and PGA for Safety Factor (F=1.0) .....	3-98
Figure 3.9.13	Proposed Surface Failure Evaluation Criteria .....	3-99
Figure 3.9.14	Assumed results of earthquake induced slope failure due to scenario earthquakes .....	3-100
Figure 4.1.1	Natural disaster trends in the world.....	4-6
Figure 4.2.1	Earthquake occurrence scenes for 2016.....	4-8
Figure 4.2.2	Earthquake occurrence scenes for 2030.....	4-9
Figure 4.3.1	Flow of building risk assessment.....	4-11
Figure 4.3.2	Proposed Damage function for DG 4+ 5 at center area and perimeter area .....	4-11
Figure 4.3.3	Proposed damage function for historical buildings (monuments) .....	4-13
Figure 4.3.4	Result of risk assessment for general building in year 2016 (CNS-2, Left : Damage number, Right : Damage ratio) .....	4-15
Figure 4.3.5	Result of risk assessment for general building in year 2030 (Without BSPPS, CNS-2, Left: Damage number, Right: Damage ratio) .....	4-16
Figure 4.3.6	Building damage ratio (DG 4+5) in 2030 with BSPPS (upper) and ratio of damage reduction (lower) by scenario earthquakes.....	4-19
Figure 4.3.7	Result of risk assessment for school building (distribution).....	4-20
Figure 4.3.8	Result of risk assessment for school buildings (number and ratio) .....	4-20
Figure 4.3.9	Result of risk assessment for medical facilities (distribution).....	4-21
Figure 4.3.10	Result of risk assessment for medical facilities (number and ratio) .....	4-22
Figure 4.3.11	Result of risk assessment for governmental buildings (distribution).....	4-23
Figure 4.3.12	Result of risk assessment for governmental buildings (number and ratio).....	4-23
Figure 4.3.13	Result of risk assessment of historical building at 3 Durbar Squares (total 108 monuments) .....	4-24
Figure 4.3.14	Risk assessment of eleven buildings based on detailed building survey .....	4-25
Figure 4.3.15	Distribution of road link blockage rates on the ETRN due to the debris of collapsed buildings by scenario earthquake (CNS-2).....	4-30
Figure 4.3.16	Reference work for threshold value of response ductility factor .....	4-33
Figure 4.3.17	Distribution maps of possible damaged bridges .....	4-38
Figure 4.3.18	Flow diagram of risk assessment of water supply .....	4-40

Figure 4.3.19	An example of schematic drawing for pipe damage rate summary of each grid.....	4-43
Figure 4.3.20	Estimated damage distribution and the list of number of damage points by municipality for the current water supply network due to CNS-2.....	4-44
Figure 4.3.21	Estimated damage distribution and the list of number of damage points by municipality for the current water supply network due to CNS-2.....	4-45
Figure 4.3.22	Estimated damage distribution and the list of damage length by municipality due to CNS-2 .....	4-48
Figure 4.3.23	Flow Diagram of power outage number calculation due to the utility pole breakage of the power distribution in the area caused by the earthquake .....	4-49
Figure 4.3.24	Estimated distribution of utility pole broken and the list of building number without electricity by municipality due to CNS-2 .....	4-51
Figure 4.3.25	Damage function of the base station antenna .....	4-53
Figure 4.3.26	Amplification when transmitting the building.....	4-53
Figure 4.3.27	Damage function of the entire base station including antenna and building .....	4-56
Figure 4.3.28	Distribution of estimated damage rates by roof-top BTS due to CNS-2 .....	4-57
Figure 4.3.29	Life loss vs building damage for Gorkha Earthquake and those in the world.....	4-59
Figure 4.3.30	Death rate of masonry building .....	4-60
Figure 4.3.31	Death rate of RC building.....	4-61
Figure 4.3.32	Death rate of masonry and RC buildings.....	4-61
Figure 4.3.33	Damage pattern of masonry and RC buildings in the Gorkha Earthquake.....	4-62
Figure 4.3.34	Distribution of number (left) and ratio (right) of death .....	4-63
Figure 4.3.35	School building structure type (left) and building damage (right) .....	4-64
Figure 4.3.36	Comparison of direct damage amounts on each scenario ground motion and GDP in Kathmandu Valley .....	4-72
Figure 4.3.37	Comparison of direct damage amounts on each scenario earthquake ground motion and GDP in Nepal.....	4-73
Figure 4.3.38	Transition of tourist between before earthquake and after earthquake.....	4-74
Figure 4.3.39	Transition of tourist expenditure a day on before or after of earthquake.....	4-75
Figure 4.3.40	Impact for GDP due to earthquake .....	4-77
Figure 4.3.41	Comparison of damage amounts for each scenario earthquake ground motion and GDP in Nepal.....	4-78
Figure 4.4.1	Comparison of vulnerability among municipalities.....	4-80
Figure 4.4.2	Distribution of vulnerability of KV .....	4-81
Figure 5.1.1	Comparison of administrative boundary of municipalities in Kathmandu Valley (Upper: Old, Lower: New) and Locations of the pilot municipalities.....	5-4
Figure 5.1.2	Profile of Lalitpur Metropolitan City .....	5-6
Figure 5.1.3	Profile of Bhaktapur Municipality.....	5-7
Figure 5.1.4	Profile of Budhanilkantha Municipality .....	5-8
Figure 5.2.1	Relationship among BBB RR Plan, LDCRP, and Hazard and Risk Assessment .....	5-9

Figure 5.2.2	Damage Situation caused by the Gorkha Earthquake Based on the Satellite Image .....	5-11
Figure 5.2.3	Satellite image before and after the Gorkha Earthquake at the Bhaktapur Durbar Square (Left: 12 March, 2015 (Before the earthquake), Right: 3 May, 2015 (After the earthquake)) .....	5-12
Figure 5.2.4	Photos of field survey (Left: Bhaktapur (12 June, 2015), Right: Budhanilkantha (30 June, 2015)).....	5-12
Figure 5.2.5	Damage status of cultural heritage in Lalitpur.....	5-14
Figure 5.2.6	Flow of formulation of reconstruction plan after the Great Hanshin-Awaji Earthquake .....	5-16
Figure 5.2.7	Overview of the reconstruction plan of Kobe municipality.....	5-17
Figure 5.2.8	Flow of formulation of reconstruction plan after the Great East Japan Earthquake .....	5-18
Figure 5.2.9	Framework of Reconstruction Agency .....	5-19
Figure 5.2.10	Overview of the reconstruction plan of Iwate Prefecture .....	5-20
Figure 5.2.11	Overview of the reconstruction plan of Sendai Municipality .....	5-21
Figure 5.2.12	Position of the BBB RR Plan.....	5-23
Figure 5.2.13	Period of the BBB RR Plan .....	5-24
Figure 5.2.14	Framework image of the BBB RR Plan .....	5-24
Figure 5.2.15	Structure of the BBB RR Plan .....	5-25
Figure 5.2.16	Cover page of the BBB RR Plan (Left: Lalitpur, Center: Bhaktapur, Right: Budhanilkantha).....	5-25
Figure 5.2.17	Concept of BBB.....	5-26
Figure 5.2.18	Extricated victims and recovered dead bodies by different SAR teams of the Gorkha Earthquake .....	5-28
Figure 5.2.19	Each Vision of the pilot municipalities.....	5-28
Figure 5.2.20	5 Visions (e.g. Lalitpur).....	5-29
Figure 5.2.21	Grand Design of the BBB RR Plan (e.g. Lalitpur) .....	5-31
Figure 5.2.22	Framework of the basic policy (e.g. Lalitpur) .....	5-32
Figure 5.2.23	Format of common action list.....	5-33
Figure 5.2.24	Layout of the basic policy part .....	5-34
Figure 5.2.25	Examples of the basic policy (Left: Life, Right: Safety, e.g. Lalitpur).....	5-34
Figure 5.2.26	Overall Procedure for Land Use Assessment .....	5-37
Figure 5.2.27	Building Density of Lalitpur Sub-metropolitan City.....	5-38
Figure 5.2.28	Building Density of Bhaktapur Municipality .....	5-39
Figure 5.2.29	Building Density of Budhanilkantha Municipality.....	5-40
Figure 5.2.30	Building Damage Map of Lalitpur Sub-metropolitan City.....	5-41
Figure 5.2.31	Building Damage Map of Bhaktapur Municipality .....	5-42
Figure 5.2.32	Overlaid Disaster Stricken Area (blue) on High-density Area (pink).....	5-43



Figure 5.2.33	Disaster Stricken Area (blue) and High-density Area (pink) on Land Use (Lalitpur).....	5-45
Figure 5.2.34	Disaster Stricken Area (blue) and High-density Area (pink) on Land Use (Bhaktapur).....	5-47
Figure 5.2.35	Disaster Stricken Area (blue) and High-density Area (pink) on Land Use (Budhanilkantha) .....	5-49
Figure 5.2.36	Disaster Stricken Area (blue) and High-density Area (pink) on Zoning Plan (Lalitpur).....	5-51
Figure 5.2.37	Disaster Stricken Area (blue) and High-density Area (pink) on Zoning Plan (Bhaktapur).....	5-52
Figure 5.2.38	High-density Area on Zoning Plan (Budhanilkantha) .....	5-53
Figure 5.2.39	High shakability area in Kathmandu Valley .....	5-55
Figure 5.2.40	High liquefiability areas in Kathmandu Valley.....	5-56
Figure 5.2.41	High slope-instability areas in Kathmandu Valley .....	5-57
Figure 5.2.42	Distribution of highly hazardous area in Kathmandu Valley.....	5-59
Figure 5.2.43	Highly Hazardous Areas in Lalitpur Sub-Metropolitan City.....	5-60
Figure 5.2.44	Highly hazardous area in Bhaktapur Municipality .....	5-61
Figure 5.2.45	Highly hazardous areas in Budhanilkantha Municipality .....	5-62
Figure 5.2.46	Development patterns of built-up area in Kathmandu Valley (2000 -2030).....	5-63
Figure 5.2.47	Highly vulnerable areas in Kathmandu Valley .....	5-64
Figure 5.2.48	Highly Vulnerable areas in Lalitpur Sub-metropolitan City.....	5-65
Figure 5.2.49	Highly vulnerable areas in Bhaktapur Municipality.....	5-66
Figure 5.2.50	Highly vulnerable areas in Budhanilkantha.....	5-67
Figure 5.2.51	Framework of the action plan .....	5-72
Figure 5.2.52	Photo of WSs in pilot municipalities (Left: Lalitpur, Right: Budhanilkantha) .....	5-73
Figure 5.4.1	Scope of TG LDCRP .....	5-94
Figure 5.4.2	Position of TG LDCRP .....	5-95
Figure 5.4.3	Structure of TG LDCRP .....	5-95
Figure 5.4.4	Example of reference in TG LDCRP.....	5-96
Figure 5.4.5	Hierarchy of Vision, Mission, Strategies in TG LDCRP.....	5-98
Figure 5.4.6	Cover page of TG LDCRP .....	5-99
Figure 5.4.7	Formulation procedures from VCA and Risk Assessment (Damage Estimation) [Figure in TG LDCRP].....	5-99
Figure 5.4.8	How to set the DRR targets based on the result of risk assessment [Figure in TG LDCRP].....	5-102
Figure 5.4.9	Framework of related organizations [Figure in TG LDCRP].....	5-104
Figure 5.4.10	How to consider the DCR activities [Figure in TG LDCRP].....	5-105
Figure 5.4.11	Major legal framework and national policies related to DCR [Figure in TG LDCRP].....	5-106

Figure 5.5.1	Planning framework and processes of LDCRP .....	5-112
Figure 5.5.2	Photo of 1 <sup>st</sup> workshops for LDCRP and SOP in pilot municipalities .....	5-115
Figure 5.5.3	Rainfall and Temperature 1997 - 2016 (Khumaltar station) (Example of LDCRP for Lalitpur Metropolitan City).....	5-117
Figure 5.5.4	Population Density Map in 2011 (Left) and Household by type of foundation of house at war level in 2011 (Right) (Example of LDCRP for Lalitpur Metropolitan City).....	5-117
Figure 5.5.5	Geological Map (Left) and Geomorphological map (Right) (Example of LDCRP for Lalitpur Metropolitan City).....	5-118
Figure 5.5.6	Heavily Damaged Buildings by 2015 Gorkha Earthquake (Example of LDCRP for Lalitpur Metropolitan City).....	5-118
Figure 5.5.7	AVS30 Map based on Geomorphological Unit (Example of LDCRP for Lalitpur Metropolitan City) .....	5-119
Figure 5.5.8	PGA (Above) and MMI (Below) of Scenario Earthquakes (Example of LDCRP for Lalitpur Metropolitan City).....	5-120
Figure 5.5.9	Liquefaction Susceptibility Map (Left) and Earthquake Induced Slope Failure Susceptibility Map (Right) (Example of LDCRP for Lalitpur Metropolitan City).....	5-121
Figure 5.5.10	Result of risk assessment (1) (Example of LDCRP for Lalitpur Metropolitan City).....	5-122
Figure 5.5.11	Result of risk assessment (2) (Example of LDCRP for Lalitpur Metropolitan City).....	5-123
Figure 5.5.12	Photo of 2 <sup>nd</sup> workshops for LDCRP and SOP in pilot municipalities.....	5-125
Figure 5.5.13	Photo of result of mapping on 2 <sup>nd</sup> workshops in pilot municipalities.....	5-125
Figure 5.5.14	Hazard Map for disasters except earthquakes (Example of LDCRP for Lalitpur Metropolitan City).....	5-128
Figure 5.5.15	Vulnerability Map (Example of LDCRP for Lalitpur Metropolitan City).....	5-129
Figure 5.5.16	Capacity Map (Example of LDCRP for Lalitpur Metropolitan City).....	5-130
Figure 5.5.17	Risk Maps (Example of LDCRP for Lalitpur Metropolitan City).....	5-131
Figure 5.5.18	Photo of 3 <sup>rd</sup> workshops for LDCRP and SOP in pilot municipalities.....	5-136
Figure 5.5.19	Results of 3 <sup>rd</sup> workshop (Left: Open Space Map, Right: Project Activities Map) (Example of LDCRP for Lalitpur Metropolitan City).....	5-137
Figure 5.5.20	Map for Priority Activities (Lalitpur Metropolitan City).....	5-137
Figure 5.5.20	Cover page of LDCRP (Lalitpur Metropolitan City).....	5-138
Figure 5.6.1	Minimum Characteristics of the NRRC Flagship 4.....	5-140
Figure 5.6.2	Ethnic Composition of Each Target Community .....	5-141
Figure 5.6.3	Ratio of Ages of Housing in Each Target Community .....	5-142
Figure 5.6.4	Responders' Knowledge before the Gorkha Earthquake .....	5-142
Figure 5.6.5	Responders' Knowledge after the Gorkha Earthquake .....	5-143

Figure 5.6.6	Responders' Knowledge after the Gorkha Earthquake (by theme).....	5-143
Figure 5.6.7	Implementation Structure of the Pilot Activities .....	5-145
Figure 5.6.8	Steps of Implementation of the CBDRM Activities .....	5-145
Figure 5.6.9	Basic Contents and Flow of the Pilot Activities .....	5-146
Figure 5.6.10	Lecture and Discussion in the Training Program.....	5-147
Figure 5.6.11	Pictures of the 1 <sup>st</sup> Workshop in Each Target Ward.....	5-152
Figure 5.6.12	Drafted Community DRR Map for Each Target Ward .....	5-155
Figure 5.6.13	Pictures of the 2 <sup>nd</sup> Workshop in Each Target Ward.....	5-155
Figure 5.6.14	Pictures of the 3 <sup>rd</sup> Workshop in Each Target Ward .....	5-157
Figure 5.6.15	DRR Carte (front page) and DRR Map of Each Pilot Ward.....	5-159
Figure 5.6.16	Pictures of the Final Handover Program in Each Target Ward.....	5-161
Figure 5.6.17	Certificates of Handover of the DRM Equipment and Tools.....	5-161
Figure 5.6.18	DRR Map Set Up in the Pilot Wards .....	5-162
Figure 5.6.19	Responders' Profiles (exclude invalid answers) .....	5-162
Figure 5.6.20	Evaluation of the ERAKV Community Workshops .....	5-163
Figure 5.6.21	Understanding of Earthquake related Knowledge .....	5-163
Figure 5.6.22	Understanding of DRM Plan and DRR Carte.....	5-164
Figure 6.1.1	Photo of the 1st WG2 Meeting .....	6-3
Figure 6.1.2	Photo of the 2nd WG2 Meeting.....	6-4
Figure 6.1.3	Photo of the 3rd WG2 Meeting .....	6-5
Figure 6.1.4	Photo of the 4th WG2 Meeting.....	6-5
Figure 6.1.5	Photo of 1st WG3 meeting .....	6-6
Figure 6.1.6	Photo of 2nd WG3 meeting .....	6-7
Figure 6.1.7	Photo of 3rd WG3 meeting.....	6-7
Figure 6.1.8	Photo of 5th WG3 meeting.....	6-8
Figure 6.1.9	Photo of 6th WG3 meeting.....	6-8
Figure 6.1.10	Photo of 7th WG3 meeting.....	6-9
Figure 6.1.11	1st JWG meeting .....	6-9
Figure 6.1.12	2nd JWG meeting .....	6-10
Figure 6.2.1	1st Public Seminar .....	6-11
Figure 6.2.2	2nd Public Seminar.....	6-11
Figure 6.3.1	Photos in the 1st Counterpart Training in Japan.....	6-17
Figure 6.3.2	Photos in the 2nd Counterpart Training in Japan.....	6-21
Figure 7.1.1	Contribution to the Priority for Action and Global Target in the Sendai Framework.....	7-3
Figure 7.3.1	Road map for seismic disaster risk reduction .....	7-9

## List of Tables

	Page
Table 1.5.1	List of the principal meetings ..... 1-7
Table 2.1.1	Stratigraphy in the Kathmandu Valley ..... 2-4
Table 2.2.1	Five cases of assumptions for progress levels of BSPS in 2030 ..... 2-20
Table 2.2.2	The number of school buildings by building structure type ..... 2-22
Table 2.2.3	The number of health facility buildings by building structure type..... 2-22
Table 2.2.4	The number of governmental buildings by building structure type..... 2-23
Table 2.2.5	Total length of roads under the jurisdiction of DoR by road class for each district in the Kathmandu Valley ..... 2-25
Table 2.2.6	The number of bridges by structure type ..... 2-27
Table 2.2.7	The summary of the number of consumers and the length of distribution lines for each service area in the Kathmandu Valley..... 2-31
Table 2.2.8	The number of BTSs by structure type..... 2-33
Table 2.2.9	The forecast of the annual population growth rates every half-decade (2016-2031) ..... 2-34
Table 2.2.10	The aggregate result of the change of urbanization pattern during each decade by ward ..... 2-36
Table 2.2.11	The aggregate result of the population growth rate from 2001 to 2011 by the change of urbanization patterns from 2000 to 2012 by ward ..... 2-37
Table 2.2.12	The result of projected populations of the whole Kathmandu Valley in 2016 and 2031 ..... 2-37
Table 2.2.13	Comparison of main indicator of south Asian countries..... 2-42
Table 3.1.1	Comparison of data and methods between this project and the 2002 JICA Study ..... 3-4
Table 3.3.1	Detailed geomorphological classification in the Kathmandu Valley ..... 3-19
Table 3.3.2	<sup>14</sup> C age and altitude of the deltaic-lacustrine terraces..... 3-19
Table 3.6.1	Used GMPE in this Project and 2002 JICA Project..... 3-52
Table 3.7.1	Damage by Historical Earthquakes and Gorkha Earthquake in Kathmandu ..... 3-58
Table 3.7.2	Adopted Correction Factor ..... 3-61
Table 3.8.1	Adopted Correction Factor ..... 3-71
Table 3.8.2	Area division for N value and depth relation..... 3-73
Table 3.8.3	Assumed relation of N value and density ..... 3-76
Table 3.8.4	Assumed $F_c$ for area division ..... 3-76
Table 3.8.5	Assumed ground water level according to the distance from river ..... 3-76
Table 3.8.6	Assessment result of liquefaction for borehole data with $N$ value..... 3-78
Table 3.9.1	Summary Table of Soil Properties (including $C$ and $\phi$ )..... 3-91
Table 4.2.1	Scenario ground motion for risk assessment ..... 4-7

Table 4.2.2	Features of different earthquake occurrence scenes .....	4-9
Table 4.2.3	Earthquake occurrence scenes and risk assessment contents .....	4-10
Table 4.3.1	Category of damage function and structural type .....	4-12
Table 4.3.2	Damage function for central area of KV .....	4-12
Table 4.3.3	Damage function for perimeter area of KV .....	4-12
Table 4.3.4	Estimated building damage (Upper: damage number; Lower: damage ratio) .....	4-14
Table 4.3.5	Building Damage and Loss Amount.....	4-17
Table 4.3.6	Cost Increase of Cases with BSPS to the Case without BSPS .....	4-17
Table 4.3.7	Results of building damage assessment (2016, 2030 and 2030 with 5 cases of BSPS) .....	4-18
Table 4.3.8	Result of risk assessment for school buildings (number and ratio) .....	4-20
Table 4.3.9	Result of risk assessment for medical facilities (number and ratio) .....	4-21
Table 4.3.10	Result of risk assessment for governmental buildings (number and ratio).....	4-23
Table 4.3.11	Summary of lengths of possible damaged road by slope failure and liquefaction .....	4-29
Table 4.3.12	Four period classification of earthquake resistant design code applied for regression analysis .....	4-32
Table 4.3.13	Relation between four periods of groups and coefficient of the regression equation .....	4-33
Table 4.3.14	Bridge inventory and damage of multi-span bridges.....	4-35
Table 4.3.15	Summary of bridge damage estimation .....	4-38
Table 4.3.16	Correction coefficient of the pipe type and joint type .....	4-42
Table 4.3.17	Coefficient of pipe diameter .....	4-42
Table 4.3.18	Coefficient of microtopography.....	4-42
Table 4.3.19	Summary of estimated result of pipeline damage of water supply network.....	4-44
Table 4.3.20	Relation between the damage rate of sewage pipeline and explanatory valuable ....	4-46
Table 4.3.21	Summary of estimated result of pipeline damage for sewage network .....	4-47
Table 4.3.22	Utility pole breakage ratio caused by earthquake motion.....	4-50
Table 4.3.23	Summary of estimated result of utility poles damage for power distribution network .....	4-51
Table 4.3.24	Summary of estimated result of BTS damage for mobile telecommunication network .....	4-57
Table 4.3.25	Results of human casualty estimation.....	4-63
Table 4.3.26	Number of schools and students in KV .....	4-64
Table 4.3.27	Human casualties estimated for 2030 .....	4-65
Table 4.3.28	Items and estimated method of the target of direct loss (target of quantitative evaluation) .....	4-65
Table 4.3.29	Quantitative evaluation items and estimation methodology in tourism sector (2016) .....	4-67

Table 4.3.30	Restoration unit cost of each building structure .....	4-68
Table 4.3.31	Estimated damaged amounts of each scenario earthquake ground motion .....	4-69
Table 4.3.32	Direct loss of school, health and government buildings and historical architecture .....	4-70
Table 4.3.33	Estimated damage amounts of road, bridge, sewage, power distribution and mobile BTS.....	4-70
Table 4.3.34	Restoration unit cost on road structure .....	4-70
Table 4.3.35	Bridge restoration unit cost.....	4-71
Table 4.3.36	Restoration unit cost of mobile BTS, power distribution, sewage and water supply .....	4-71
Table 4.3.37	Direct damage amounts on each scenario ground motion (building, infrastructure) .....	4-71
Table 4.3.38	Transition of employees in the tourism sector on before or after of earthquake .....	4-74
Table 4.3.39	Transition of expenditure a year of tourist on before or after of earthquake .....	4-75
Table 4.3.40	Transition of foreign exchange earnings on before or after of earthquake .....	4-76
Table 4.3.41	Transition of contribution amounts for GDP by tourism sector on before or after of earthquake .....	4-77
Table 4.4.1	Indicators for comparative vulnerability analysis.....	4-78
Table 4.4.2	Score and range of each indicator.....	4-79
Table 4.4.3	Vulnerability score of each municipality .....	4-80
Table 5.1.1	Overview of the pilot municipalities at the beginning of the project .....	5-3
Table 5.1.2	Contents of profile for pilot municipalities .....	5-5
Table 5.2.1	List of sector in PDNA .....	5-13
Table 5.2.2	Example of the result of damage and loss assessment (e.g. Agriculture) .....	5-13
Table 5.2.3	Example of recovery and reconstruction formulated in Japan .....	5-15
Table 5.2.4	Sendai Framework for Disaster Risk Reduction 2015-2030 Priority for Action.....	5-26
Table 5.2.5	Key principles.....	5-27
Table 5.2.6	Each Vision of pilot municipality .....	5-29
Table 5.2.7	Outline of the BBB RR Basic Plan.....	5-30
Table 5.2.8	Sectors of Urban Planning Policy.....	5-35
Table 5.2.9	High-density Area of Lalitpur Sub-metropolitan City.....	5-38
Table 5.2.10	High-density Area of Bhaktapur Municipality .....	5-39
Table 5.2.11	Disaster Stricken Area in Lalitpur Sub-metropolitan City.....	5-41
Table 5.2.12	Disaster Stricken Area in Bhaktapur Municipality .....	5-42
Table 5.2.13	Share of Land Use in Disaster Stricken Area and High-density Area (Lalitpur).....	5-46
Table 5.2.14	Share of Land Use in Disaster Stricken Area and High-density Area (Bhaktapur).....	5-48
Table 5.2.15	Shakability scores .....	5-54
Table 5.2.16	Liquefiability scores .....	5-55

Table 5.2.17	Scoring slope-instability .....	5-57
Table 5.2.18	Colours representing hazard types in highly hazardous areas .....	5-58
Table 5.2.19	Highly hazardous areas in Kathmandu Valley (by type of hazards).....	5-58
Table 5.2.20	Highly Hazardous Areas in Lalitpur Sub-Metropolitan City.....	5-59
Table 5.2.21	Highly hazardous areas in Bhaktapur Municipality .....	5-60
Table 5.2.22	Highly hazardous areas in Budhanilkantha .....	5-61
Table 5.2.23	Development patterns of the built-up area in Kathmandu Valley.....	5-63
Table 5.2.24	Development patterns of the built-up area in Lalitpur Sub-metropolitan City.....	5-65
Table 5.2.25	Development patterns of the built-up area in Bhaktapur .....	5-66
Table 5.2.26	Development patterns of the built-up areas in Budhanilkantha Municipality .....	5-67
Table 5.2.27	Strategies and programs to improve resilience by urban development and hazard types .....	5-69
Table 5.2.28	Land use policies of each municipality .....	5-70
Table 5.2.29	Outline of the BBB RR Action Plan .....	5-71
Table 5.2.30	Main Differences of action plan among pilot municipalities.....	5-72
Table 5.2.31	Progresses of reconstructions .....	5-74
Table 5.2.32	Budgeting of BBB RR Plan (e.g. Lalitpur).....	5-75
Table 5.4.1	Structure and main contents of 2011 guideline.....	5-88
Table 5.4.2	Major issues in 2011 guideline and measures for improvement.....	5-90
Table 5.4.3	Structure and major revised points of LDCRP guideline .....	5-92
Table 5.4.4	List of main meeting with MoFALD and relevant organizations .....	5-93
Table 5.4.5	Table of contents for TG LDCRP .....	5-97
Table 5.4.6	Disaster and Climate Resilience Strategies (Example of Format) [Table in TG LDCRP].....	5-101
Table 5.4.7	Relation between disaster management cycle and priorities for action of Sendai Framework.....	5-103
Table 5.4.8	Example of disaster and climate resilience activities (part of understanding disaster risk) [Table in TG LDCRP] .....	5-107
Table 5.5.1	Collected existing disaster risk management plans .....	5-109
Table 5.5.2	Identified issues by the review of the existing disaster risk reduction and management plan.....	5-110
Table 5.5.3	Collected information for formulation of LDCRP .....	5-111
Table 5.5.4	Contents and Basis of contents for LDCRP.....	5-113
Table 5.5.5	Summary of 1 <sup>st</sup> workshops for LDCRP and SOP in pilot municipalities .....	5-114
Table 5.5.6	Summary of 2 <sup>nd</sup> workshops for LDCRP and SOP in pilot municipalities .....	5-124
Table 5.5.7	Historical Disaster Events in the past around 30 years (Example of LDCRP for Lalitpur Metropolitan City) .....	5-126
Table 5.5.8	Target disasters with priority for pilot municipalities.....	5-127
Table 5.5.9	Disaster and climate resilience strategies in pilot municipalities .....	5-132

Table 5.5.10	Draft of activity list for Lalitpur Metropolitan City .....	5-132
Table 5.5.11	Summary of 3 <sup>rd</sup> workshops for LDCRP and SOP in pilot municipalities.....	5-136
Table 5.5.12	Estimated cost of seismic retrofitting for buildings (Lalitpur Metropolitan City).....	5-138
Table 5.6.1	Target Communities of the Community Baseline Survey .....	5-141
Table 5.6.2	Target Communities for the Pilot CBDRRM Activities .....	5-144
Table 5.6.3	Main Lectures and Discussion in the CBDRRM Training .....	5-147
Table 5.6.4	Major Lectures and Activities in the 1 <sup>st</sup> CBDRRM Workshop.....	5-150
Table 5.6.5	Summary of the HVCA in Each Pilot Ward .....	5-151
Table 5.6.6	Result and Issues for CBDRM activities in the 1 <sup>st</sup> CBDRRM Workshop .....	5-151
Table 5.6.7	Major Lectures and Activities in the 2 <sup>nd</sup> CBDRRM Workshop .....	5-153
Table 5.6.8	Table of Contents of the Ward-level DRM Plan in the Pilot Wards .....	5-153
Table 5.6.9	Result and Issues for CBDRM activities in the 2 <sup>nd</sup> CBDRRM Workshop .....	5-154
Table 5.6.10	Lectures and Activities in the 3 <sup>rd</sup> CBDRRM Workshop .....	5-156
Table 5.6.11	Result and Issues for CBDRM activities in the 3 <sup>rd</sup> CBDRRM Workshop .....	5-156
Table 5.6.12	Priority Actions Designated in the DRM Plan of Each Pilot Ward .....	5-157
Table 5.6.13	Data and Information in the DRR Carte .....	5-158
Table 5.6.14	Lecture and Activities in the Final CBDRRM Workshop.....	5-160
Table 5.7.1	Current situation of staffs in charge of DRRM of municipalities in Japan.....	5-167
Table 5.7.2	Measures for utilization of outcomes of pilot activities to other municipalities.....	5-169
Table 5.7.3	Estimated cost and duration for nationwide dissemination of formulation of LDCRP .....	5-172
Table 6.1.1	Exchange list by presentations and attendance to meetings related to WG 1.....	6-2
Table 6.3.1	The Participants of the 1st Counterpart Training in Japan.....	6-14
Table 6.3.2	Schedule of the 1st Counterpart Training in Japan .....	6-15
Table 6.3.3	The Participants of the 2nd Counterpart Training in Japan .....	6-18
Table 6.3.4	Schedule of the 2nd Counterpart Training in Japan.....	6-19
Table 6.3.5	The participants of the 3rd counterpart training in Japan .....	6-22
Table 6.3.6	Schedule of the 3rd counterpart training in Japan .....	6-23
Table 6.3.7	Technology and policy necessary in Nepal presented by each group at the final presentation.....	6-26
Table 6.3.8	Photos in the 3rd counterpart training in Japan .....	6-27
Table 7.3.1	Recommendations for seismic disaster risk reduction.....	7-10



## Abbreviation

Abbreviation	Official Name
<b>ADB</b>	Asia Development Bank
<b>ADRC</b>	Asian Disaster Reduction Center
<b>ADPC</b>	Asian Disaster Preparedness Center
<b>BBB</b>	Build Back Better
<b>BCP</b>	<b>Business Continuity Plan</b>
<b>BIMS</b>	Building Information Management System
<b>BMS</b>	Bridge Management System
<b>BTS</b>	Base Transceiver Station
<b>CARE</b>	Cooperation for American Relief Everywhere
<b>CBDRRM</b>	<b>Community Based Disaster Risk Reduction and Management</b>
<b>CBS</b>	Central Bureau of Statistics
<b>CCCM</b>	Camp Coordination and Camp Management
<b>CDO</b>	Chief District Officer
<b>CDMC</b>	Community Disaster Management Committee
<b>C.F.</b>	Correction Factor
<b>CNDRC</b>	Central Natural Disaster Relief Committee
<b>CNS-1</b>	Central Nepal South Scenario Earthquake Ground Motion, C.F. = 1/3
<b>CNS-2</b>	Central Nepal South Scenario Earthquake Ground Motion, PGA C.F. = 1/2
<b>CNS-3</b>	Central Nepal South Scenario Earthquake Ground Motion, PGA C.F. = 2/3
<b>C/P</b>	Counterpart
<b>DCC</b>	District Coordination Committee
<b>DDC</b>	District Development Committees
<b>DDRC</b>	District Disaster Relief Committee
<b>DEM</b>	Digital Elevation Model
<b>DEOC</b>	Disaster Emergency Operation Center
<b>DKKV</b>	Deutsches Komitee Katastrophenvorsorge
<b>DM</b>	Disaster Management
<b>DMG</b>	Department of Mines and Geology
<b>DRM</b>	Disaster Risk Management
<b>DRR</b>	Disaster Risk Reduction
<b>DoA</b>	Department of Archeology
<b>DoE</b>	Department of Education
<b>DOH</b>	Department of Health
<b>DoHPP</b>	Department of Housing and Physical Planning
<b>DoHUD</b>	Department of Housing and Urban Development
<b>DoLIDAR</b>	Department of Local Development and Agricultural Roads

<b>DoR</b>	Department of Road
<b>DoS</b>	Department of Survey
<b>DUDBC</b>	Department of Urban Development and Building Construction
<b>ERAKV</b>	The Project for Assessment of Earthquake Disaster Risk for the Kathmandu Valley (This project)
<b>ESS</b>	Earthquake Safety Solutions
<b>ETRN</b>	Emergency Transportation Road Network
<b>EMI</b>	Earthquakes and Megacities Initiative
<b>EMS98</b>	European Macroseismic Scale
<b>ERHQ</b>	Emergency Response Head Quarters
<b>GDP</b>	Gross Domestic Product
<b>GFFO</b>	German Federal Foreign Office
<b>GFL</b>	Ground Floor Level
<b>GIS</b>	Geographic Information System
<b>GMPE</b>	Ground Motion Prediction Equation
<b>GoN</b>	Government of Nepal
<b>GTZ</b>	Technical Cooperation of the Federal Republic of Germany
<b>HFA</b>	Hyogo Framework for Action
<b>HIIS</b>	Health Infrastructure Information System
<b>IASC</b>	Inter-Agency Standing Committee
<b>ICIMOD</b>	International Centre for Integrated Mountain Development
<b>IDNDR</b>	International Decade for Natural Disaster Reduction
<b>IFRC</b>	International Federation of Red Cross and Red Crescent Societies
<b>IOE</b>	Institute of Engineering
<b>IOM</b>	International Organization for Migration
<b>IPPs</b>	Independent Power Producers
<b>ICRC</b>	International Red Cross Society
<b>JASDiM</b>	Japan Association for Slope Disaster Management
<b>JCC</b>	Joint Coordinating Committee
<b>JICA</b>	Japan International Cooperation Agency
<b>JWG</b>	Joint Working Group
<b>KUKL</b>	Kathmandu Upatyaka Khanepani Limited
<b>KVDA</b>	Kathmandu Valley Development Authority
<b>KVRP</b>	Kathmandu Valley Resilient Plan
<b>KVTDC</b>	Kathmandu Valley Town Development Committee
<b>KVWSMB</b>	Kathmandu Valley Water Supply Management Board
<b>LDCRP</b>	Local Disaster and Climate Resilience Plan
<b>LDRC</b>	Local Disaster Relief Committee
<b>LSGA</b>	Local Self Governance Act

<b>LMC</b>	Lalitpur Metropolitan City
<b>LWS</b>	Lutheran World Service
<b>MBT</b>	Main Boundary Thrust
<b>MCT</b>	Main Central Thrust
<b>MDGs</b>	Millennium Development Goals
<b>MFT</b>	Main Frontal Thrust
<b>MHT</b>	Main Himalayan Thrust
<b>MIRA</b>	Multi-cluster Initial Rapid Assessment
<b>M/M</b>	Minutes of Meeting
<b>MMI</b>	Modified Mercalli intensity scale
<b>MoE</b>	Ministry of Education
<b>MoFALD</b>	Ministry of Federal Affairs and Local Development
<b>MoHA</b>	Ministry of Home Affairs
<b>MoHP</b>	Ministry of Health and Population
<b>MoIC</b>	Ministry of Information and Communications
<b>MoPIT</b>	Ministry of Physical Infrastructure and Transport
<b>MoUD</b>	Ministry of Urban Development
<b>Mw</b>	Moment Magnitude
<b>NBC</b>	Nepal National Building Code
<b>NDRF</b>	National Disaster Response Framework
<b>NEA</b>	Nepal Electricity Authority
<b>NEOC</b>	National Emergency Operation Centre
<b>NGA</b>	New Generation Attenuation
<b>NGO</b>	Non-governmental Organization
<b>NHSSP</b>	Nepal Health Sector Support Program
<b>NPC</b>	National Planning Commission
<b>NPR</b>	Nepalese Rupee
<b>NPHA</b>	Nepal Public Health Association
<b>NRA</b>	National Reconstruction Authority
<b>NRAS</b>	National Reconstruction Advisory Council
<b>NRCS</b>	Nepal Red Cross Society
<b>NRRC</b>	Nepal Risk Reduction Consortium
<b>NS</b>	Nepal Scout
<b>NSC</b>	National Seismological Centre
<b>NSDRM</b>	National Strategy for Disaster Risk Management
<b>NSET</b>	National Society for Earthquake Technology Nepal
<b>NTA</b>	Nepal Telecommunication Authority
<b>NTC</b>	Nepal Telecom

<b>NWSC</b>	Nepal Water Supply Corporation
<b>PDDP</b>	Participatory District Development Program
<b>PDNA</b>	Post Disaster Needs Assessment
<b>PGA</b>	Peak Ground Acceleration
<b>PGV</b>	Peak Ground Velocity
<b>PID</b>	Project Implementation Directorate
<b>PSHA</b>	Probabilistic Seismic hazard Analysis
<b>RC</b>	Reinforced-Concrete
<b>RDRC</b>	Regional Disaster Relief Committee
<b>RRNE</b>	The Project on Rehabilitation and Recovery from Nepal Earthquake
<b>RSLUP</b>	Risk Sensitive Land Use Plan
<b>SATREPS</b>	Science and Technology Research Partnership
<b>SDGs</b>	Sustainable Development Goals
<b>Sendai Framework</b>	Sendai Framework for Disaster Risk Reduction
<b>SI</b>	Spectrum Intensity
<b>SOP</b>	Standard Operation Procedure
<b>SRN</b>	Strategic Road Network
<b>SSRN</b>	Statistics of Strategic Road Network
<b>TG LDCRP</b>	Technical Guideline for Formulation of LDCRP
<b>UMN</b>	United Mission to Nepal
<b>UNDP</b>	United Nation Development Program
<b>UNESCO</b>	United Nations Educational, Scientific and Cultural Organization
<b>UNOCHA</b>	United Nation Office for Coordination of Humanitarian Affairs
<b>UNOSAT</b>	United Nations Institute for Training and Research Operational Satellite Applications Program
<b>USAID</b>	United States Agency for International Development
<b>USAIDMN</b>	United States Agency for International Development Mission to Nepal
<b>USGS</b>	United States Geological Survey
<b>UTM</b>	Universal Transverse Mercator
<b>VCA</b>	Vulnerability Capacity Assessment
<b>VDC</b>	Village Development Committees
<b>WB</b>	World Bank
<b>WCDDR</b>	Third UN World Conference on Disaster Risk Reduction
<b>WFP</b>	United Nations World Food Program
<b>WG</b>	Working Group
<b>WGS-84</b>	World Geodetic System 1984
<b>WN</b>	Western Nepal Scenario Earthquake Ground Motion, C.F. = 1
<b>WS</b>	Workshop

## Chapter 1 Outline of the Project

---

### 1.1 Background

Nepal, located in the area where the Indian Plate and Eurasian Plate hit, is one of the most frequent earthquake occurrence areas in the world. Kathmandu Valley (KV), which includes the capital city of Nepal, has experienced several disastrous earthquakes, including the Bihar-Nepal earthquake of magnitude 8.4 in 1934 in which approximately 20% of all buildings in KV were destroyed and 9,040 people were killed. A recent earthquake of magnitude 6.9 in Sikkim India on 18 September 2011, though far from KV, resulted in seven people being killed and 136 being injured.

Considering the high risk of a future earthquake in KV, countermeasures such as retrofitting buildings for seismic resistance, land use control, and observance of the National Building Code (NBC) have not been promoted enough. The main source of risk could be the old buildings in poor condition, extension work on current buildings, and non-engineered buildings constructed without the participation of knowledgeable and skilled architects and engineers. On the other hand, the rapid increase of population in KV would make more people face the risk. The Government of Nepal (GoN) has been tackling the issue with the formulation of laws and strategies but there is a lack of basic risk information for the valley.

The project “The study on Earthquake Disaster Mitigation”, conducted by JICA in 2002, estimated the damage based on the Bihar-Nepal earthquake scenario that 53,000 buildings, which is approximately 21% of all buildings in KV, will be destroyed, 18,000 people, about 1.3% of all population, will be killed, and 53,000, approximately 3.8% of all population will be injured. More than ten years have passed since the 2002 JICA Project, and the population has increased by a factor of 1.5 while the number of buildings has increased up to 1.7 times. The potential damage must be much more serious if the same scenario is considered now, and might be even worse in the future. It becomes a necessary and urgent issue to update the risk assessment for the future development plans and policies, with the primary concern on the disaster risk management. In this circumstance, the GoN requested assistance from the Government of Japan on the implementation of earthquake disaster risk assessment in KV. In response to the request of the GON, JICA conducted a Detailed Planning Survey on the Project in April and September 2014, and, confirmed and signed the minutes of meetings (M/M) on 24 September 2014.

On April 25, 2015, just before the commencement of the project, the Gorkha Earthquake of Mw7.8 (USGS) occurred at the boundary of Indian Plate and Eurasian Plate with its

epicenter approximately 76 km west of Kathmandu. This earthquake brought heavy damages in a wide range of area. 8,790 people were killed, 22,300 people were injured, approximately 500,000 buildings were totally destroyed, and around 250,000 buildings were partially damaged (PDNA). Three experts from this project immediately visited Kathmandu from 6th June. During the visit, the team investigated the damage of buildings, the needs from the GoN for recovery and reconstruction, and had series of discussions with counterparts about the modification of the project component which follows the changed situation.

Through the Gorkha Earthquake caused heavy damages both in and out of KV, the damage is concentrated on the vulnerable buildings, and the infrastructure damage is limited. The damage is considered relatively small compared with other earthquakes having a similar scale of magnitude. It has been recognized by both JICA and GoN that the quick recovery and reconstruction is an urgent issue and, in the meantime, it is necessary to promote the DRR for the future earthquake. On the other hand, the simple recovery, which means constructing the same structures as that of before the quake, must be avoided in order not to re-create the same vulnerability. For this purpose, both the JICA Project Team and counterpart considered a recovery and reconstruction plan with the concept of Build Back Better (BBB) was necessary to be added to the project among the other modifications including the construction of demonstration model for a safe buildings, implementation of disaster risk reduction awareness campaign, damage data collection, detail soil survey, emergency response chronicle survey, and formulation of Standard Operation Procedures (SOP).

As the consequence of the discussion between the Project Team and the counterpart, the First Joint Coordinating Committee (JCC) meeting was held on 18th June 2015, and agreed on the modification on project components and schedule proposed by the Project Team.

## **1.2 Summary of the Project**

### **1.2.1 Name of the Project**

The Project for Assessment of Earthquake Disaster Risk for the Kathmandu Valley

### **1.2.2 Target Areas**

Target areas include:

Risk Assessment: Kathmandu Valley (two Metropolitan Cities, eighteen Municipalities, a part of Rural Municipalities in Kathmandu District, Lalitpur District and Bhaktapur District)

Pilot Activities: Lalitpur Metropolitan City, Bhaktapur Municipality, Budhanilkantha

## Municipality

### 1.2.3 Overall Aim

To reduce the earthquake disaster risk through effective and sustainable measures to be taken based on the disaster risk assessment.

### 1.2.4 Project Goal

To implement the earthquake risk assessment for future scenario earthquakes considering the earthquake environment after the Gorkha Earthquake, and to develop a DRRM plan for concrete and effective promotion on disaster risk management for future earthquakes.

### 1.2.5 Project Output

- Output 1: To conduct seismic hazard analysis based on scenario earthquakes utilizing the latest knowledge and create a detailed ground model for Kathmandu Valley.
- Output 2: To conduct seismic risk assessment based on the results of seismic hazard analysis (Output 1), and summarize as damage estimation by considering several occurrence scenes (time, date, season, etc.)
- Output 3: To enhance skills for updating risk assessment results in accordance with the social environment change in the future.
- Output 4: To formulate a BBB recovery and reconstruction plan utilizing the results of hazard analysis, and a disaster risk reduction and management (DRRM) plan based on the results of the seismic risk assessment for the pilot municipalities.

### 1.2.6 Counterparts

- Main Counterpart: MoUD
- Related Organizations: MoHA, MoFALD, DMG, Local Governments in Kathmandu Valley, and Working Group Members

### 1.2.7 Beneficiaries

- Direct: Central government and local governments in Kathmandu Valley
- Indirect: Residents in Kathmandu Valley (Approx. 2.5 million people)

## 1.3 Project Objective

- 1) To estimate the damages of Kathmandu Valley caused by new scenario earthquakes in

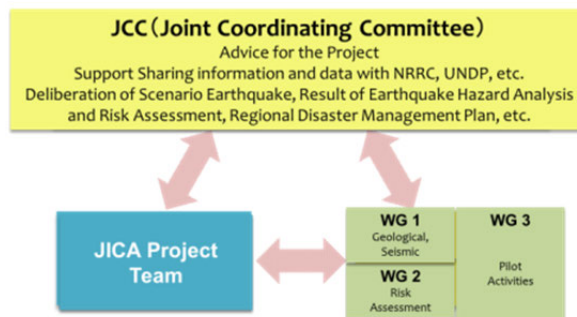
the future after the Gorkha Earthquake through seismic hazard analysis with detailed soil model and seismic risk assessment.

- 2) To formulate a Build Back Better recovery and reconstruction plan and disaster risk reduction and management plan, aiming for a resilient urban structure, based on the results of seismic hazard analysis and risk assessment.
- 3) To contribute to the seismic disaster risk mitigation of Kathmandu Valley by promotion on the implementation of concrete disaster prevention and disaster risk reduction measures through the activities above mentioned.

## 1.4 Implementation Organization

### 1.4.1 Structure of the Implementation Organization

The JCC and three Working Groups (WGs) were established in the project based on the M/M. The structure of the organizations and collaboration system are summarized in Figure 1.4.1. Joint Working Group (JWG) meetings are held as necessary for collaboration among WGs. The detail structure of WGs is shown on 1.4.2, and the meeting information of JCC and WGs are summarized on 1.5.



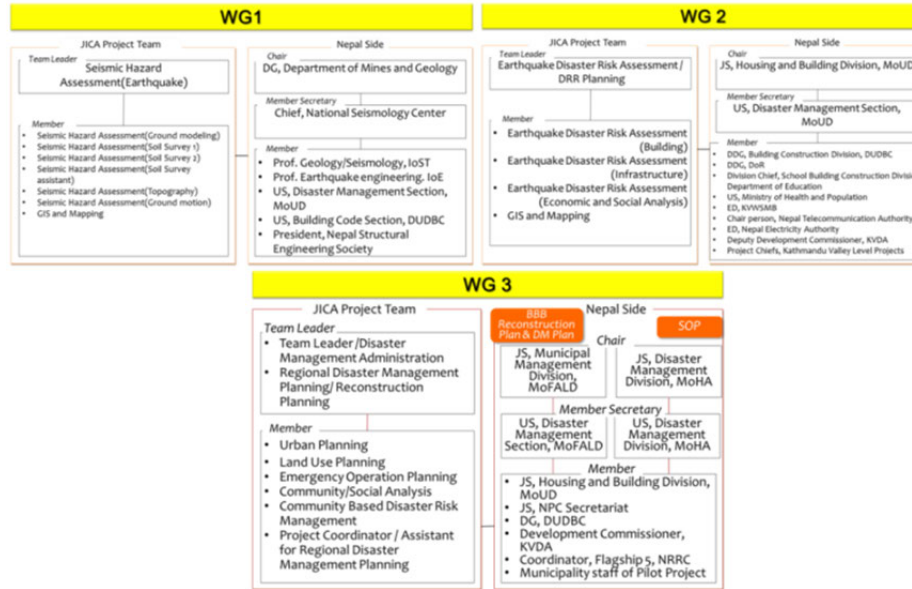
Source: JICA Project Team

**Figure 1.4.1 Structure of the Implementation Organizations**

### 1.4.2 Structure of Working Groups

The JICA Project Team examines the project in collaboration with the WGs. The structure of each WG is summarized in Figure 1.4.2.





Source: JICA Project Team

**Figure 1.4.2 Structure of each WG**

Several researchers and organizations from both Nepal and Japan have researched the earthquakes in KV. Some of them participated in the JCC and WGs, and the JICA Project Team has been asking for their advice while building consensus. The knowledge and information of Japanese researchers have also been shared through the “Science and Technology Research Partnership for Sustainable Development (SATREPS) project” by JICA.

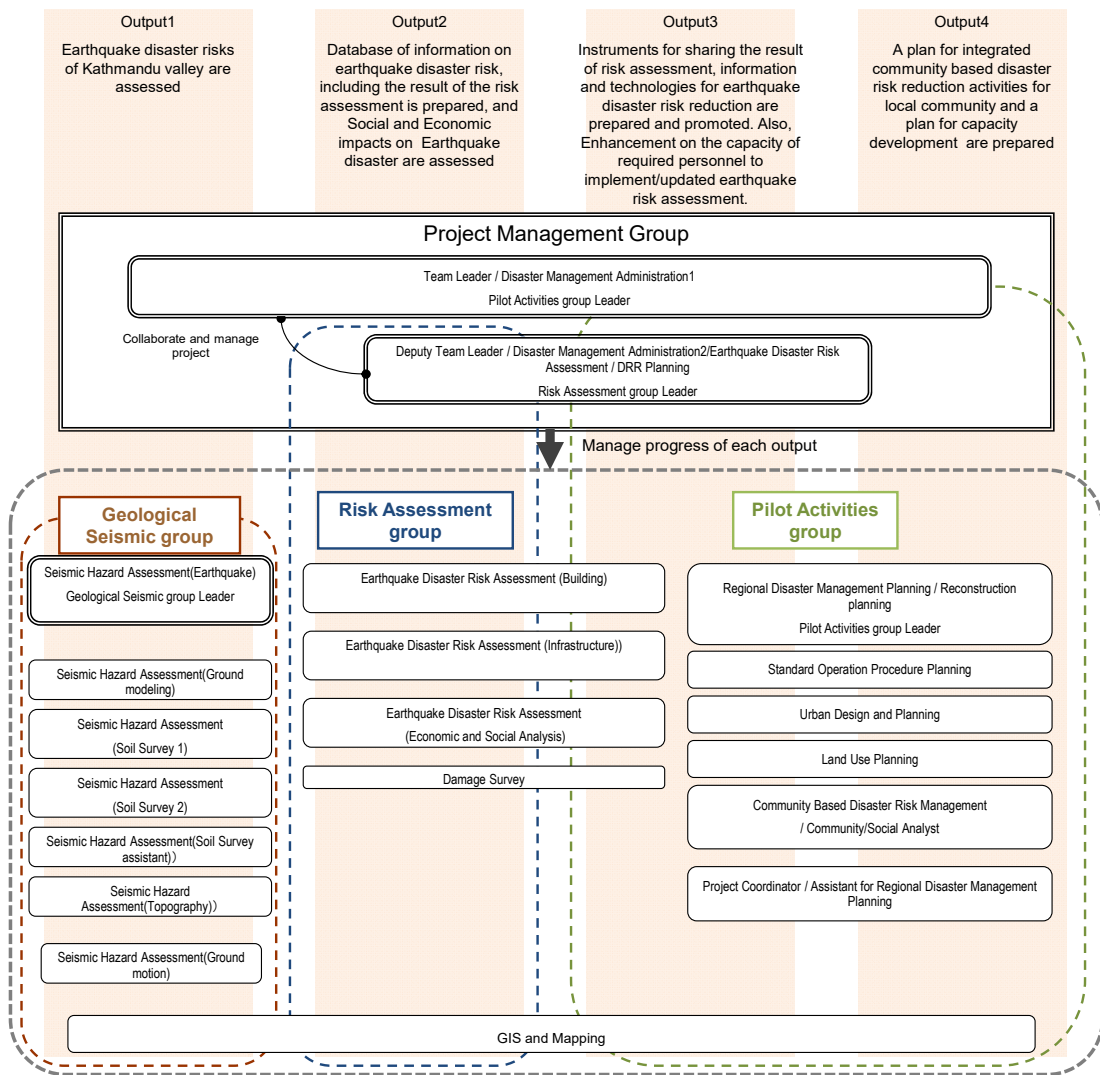
As shown in Figure 1.4.2, the WG members comprises of members from various organizations covering comprehensive needs. Therefore, collaboration within the WG will strengthen the system of DRRM and it will be connected to the sustainability. The Member list of WG is flexibly changed based on the discussion with the Nepalese side. For instance, the National Reconstruction Agency (NRA), which was established after the signing of the M/M of the project, has been invited to the meeting, and a member from NRA actually participated, since it is especially related to the activities of WG3.

Each WG has discussions in a workshop style. The WG meetings are held before the JCC meetings and seminars when essential consensus building is required. Also, in cases when the periodic WG is not enough for the concrete discussion, the extra meetings have been held.

### 1.4.3 Members of the JICA Project Team and Assignments to be covered

The experts list of the JICA Project Team is as shown in Figure 1.4.3. For the effective and efficient project management, the JICA Project Team experts are divided into three groups for four main outputs. The leader of each group coordinates the group, and collaborates

organically. The WGs are “Geological Seismic group” for Output 1, “Risk Assessment group” for Output 2 and 3, and “Pilot Activities group” for Output 3 and 4. Figure 1.4.3 shows members and their assignments for each group. This group structure is corresponded to the WGs of the project.



Source: JICA Project Team

**Figure 1.4.3 Expert structure of the JICA Project Team and Assignments to be covered**

## 1.5 JCC (Joint Coordinating Committee) Meeting

### 1.5.1 List of the Principal Meetings

The list of the principal meetings for JCC and each WG is summarized on Table 1.5.1. Along with those meetings, the regular meetings have been held on a regular basis with the main counterpart MoUD, and other related organizations. As of April 2017, 28 regular meetings have been held. At the regular meetings, progress of the project is shared among participants and the cooperation from organizations is obtained.

**Table 1.5.1 List of the principal meetings**

Date	Meeting	Main Topic	Participants
2015/6/18	1st JCC	<ul style="list-style-type: none"> <li>– Confirmation of modified Project Components, Schedule, and Implementation approach</li> <li>– Confirmation of Pilot Municipalities</li> <li>– Components of Reconstruction Plan</li> <li>– Nominating of Officers for the WG members</li> </ul>	34
2015/7/27	1st WG2	<ul style="list-style-type: none"> <li>– Risk assessment framework</li> <li>– Method of data collection, working group activities, schedule, etc.</li> </ul>	17
2015/8/5	1st WG3	<ul style="list-style-type: none"> <li>– WG3 Framework, Role sharing, Schedule</li> <li>– Vision and TOC of BBB Recovery and Reconstruction (RR) plan, issues and data needed</li> </ul>	26
2015/8/7	1st WG1	<ul style="list-style-type: none"> <li>– Hazard Assessment Framework</li> </ul>	17
2015/11/9	2nd WG1	<ul style="list-style-type: none"> <li>– Progress of Hazard Assessment</li> </ul>	13
2015/12/6	1st JWG	<ul style="list-style-type: none"> <li>– Progress of each WG</li> <li>– Technical transfer</li> </ul>	30
2015/12/16	2nd JCC	<ul style="list-style-type: none"> <li>– Determination of Proposed Scenario Earthquakes</li> <li>– Confirmation of Framework of Recovery and Reconstruction Plan</li> <li>– Determination of Organizations for Technical Transfer</li> </ul>	29
2016/2/8	2nd WG2	<ul style="list-style-type: none"> <li>– Approach of risk assessment</li> <li>– Data collection</li> </ul>	19
2016/3/1	2nd WG3	<ul style="list-style-type: none"> <li>– Contents of the BBB RR plan</li> </ul>	32
2016/4/11	2nd JWG	<ul style="list-style-type: none"> <li>– Progress of the Seismic Hazard Analysis</li> </ul>	28
2016/5/6	3rd WG3	<ul style="list-style-type: none"> <li>– Contents of the BBB RR plan</li> </ul>	28
2016/5/10	3rd JCC	<ul style="list-style-type: none"> <li>– Confirmation of Scenario EQs</li> <li>– Confirmation of Ground Motion by Scenario EQs</li> <li>– Confirmation of BBB Recovery and Reconstruction Plan for Three Pilot Municipalities</li> <li>– Confirmation of Study Area</li> </ul>	36
2016/8/4	3rd WG2	<ul style="list-style-type: none"> <li>– Discussion and confirmation of Approach of risk assessment (building, infrastructure, human and economy) and Earthquake occurrence scene</li> </ul>	26
2016/9/11	3rd WG1	<ul style="list-style-type: none"> <li>– Confirmation of Hazard assessment on Liquefaction and Slope Failure</li> </ul>	18
2016/9/14	4th JCC	<ul style="list-style-type: none"> <li>– Result of Hazard Assessment</li> <li>– Coverage Items for Risk Assessment</li> <li>– Methodology for Risk Assessment</li> <li>– Setting Disaster Occurrence Scenes</li> <li>– Target Scenarios for full Scale Risk Assessment</li> <li>– Activities at Pilot Area</li> </ul>	33
2016/9/16	1st Seminar	<ul style="list-style-type: none"> <li>– Result of Hazard Assessment</li> <li>– Activities at Pilot Area</li> </ul>	162
2016/12/12	5th JCC	<ul style="list-style-type: none"> <li>– Confirmation of Activities in the 2<sup>nd</sup> Phase</li> <li>– Confirmation of methodology for human casualty and remaining data collection for Risk Assessment</li> </ul>	37
2016/12/19	4th WG3	<ul style="list-style-type: none"> <li>– Confirmation of Structure of Disaster Risk Reduction (DRRMP) and Management Plan and SOP</li> <li>– Confirmation of Implementation Schedule of DRRMP, SOP and CBDRRM Activities</li> </ul>	25
2017/2/23	4th WG2	<ul style="list-style-type: none"> <li>– Confirmation of Result of Risk Assessment</li> </ul>	30
2017/4/6	6th JCC	<ul style="list-style-type: none"> <li>– Confirmation of Result of Risk Assessment</li> <li>– Confirmation of Target Ground Motion Level for DRR</li> </ul>	33
2017/4/11	2nd Seminar	<ul style="list-style-type: none"> <li>– Dissemination of Result of Result of Risk Assessment</li> <li>– Dissemination of Progress of the Project</li> </ul>	195
2017/6/7	5th WG3	<ul style="list-style-type: none"> <li>– Confirmation of formulation of Disaster Risk Reduction and Management Plan (DRRM Plan)</li> <li>– Confirmation of formulation of Standard Operation Procedure (SOP)</li> <li>– Confirmation of CBDRRM Activity</li> </ul>	19
2017/9/14	6th WG3	<ul style="list-style-type: none"> <li>– Confirmation of formulation of Guideline for Local Disaster and Climate Resilience Plan (LDCRP) and LDCRP for Pilot Municipalities</li> <li>– Confirmation of formulation of Standard Operation Procedure (SOP)</li> <li>– Confirmation of CBDRRM Activity</li> </ul>	25
2017/12/14	7th WG3	<ul style="list-style-type: none"> <li>– Confirmation of result of formulation of Guideline for Local Disaster and Climate Resilience Plan (LDCRP) and LDCRP for Pilot Municipalities</li> <li>– Confirmation of result of formulation of Standard Operation Procedure (SOP)</li> <li>– Confirmation of result of CBDRRM Activity</li> </ul>	24
2018/2/13	7th JCC	<ul style="list-style-type: none"> <li>– Confirmation of LDCRP Technical Guideline</li> <li>– Confirmation of LDCRP</li> <li>– Confirmation of SOP</li> <li>– Confirmation of AOB</li> </ul>	30
2018/2/15	3rd Seminar	<ul style="list-style-type: none"> <li>– Dissemination of Strengthening of Disaster Risk Reduction and Management Capacity of Municipality</li> <li>– Dissemination of Construction of Robust and Resilient Society against Natural Disaster Risk</li> </ul>	205

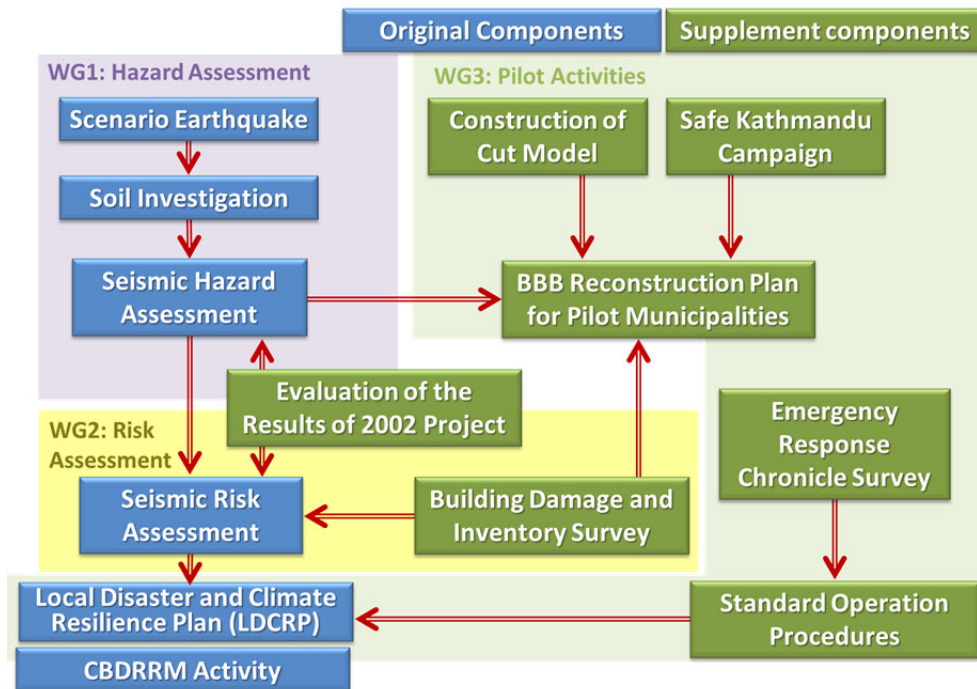
Source: JICA Project Team

### 1.5.2 JCC (Joint Coordinating Committee)

The JCC meetings have been held six times as of April 2017. Summary of each JCC is described below.

#### (1) 1st JCC Meeting

The 1st JCC meeting was held on 18 June 2015, which is approximately two months after the Gorkha Earthquake. In the meeting, the project component was modified, and three pilot municipalities were determined. Originally, this project was planned for Seismic Hazard Assessment, Seismic Risk Assessment and DRRM planning based on the Risk Assessment. However, in order to correspond to the needs after the Gorkha Earthquake, several activities were added as shown in Figure 1.5.1.



Source: JICA Project Team

**Figure 1.5.1 Original and supplement components of the project**



Source: JICA Project Team

**Figure 1.5.2 1st JCC meeting**

## (2) 2nd JCC Meeting

The 2nd JCC meeting was held on 16 December 2015. The activities of the WGs were presented by a Nepali representative of each WG with JICA Project Team members. Scenario Earthquakes were determined, and the framework for BBB Recovery and Reconstruction (RR) Plan was confirmed among participants.



Source: JICA Project Team

**Figure 1.5.3 2nd JCC meeting**

## (3) 3rd JCC Meeting

The 3rd JCC meeting was held on 10th May 2016. The activities of the WGs were presented by a Nepali representative of each WG with JICA Project Team members. Proposed Scenario Earthquakes and Seismic Motion were determined, and the finalization of BBB RR Plan for Pilot Municipalities was confirmed.



Source: JICA Project Team

**Figure 1.5.4 3rd JCC meeting**

**(4) 4th JCC Meeting**

The 4th JCC meeting was held on 14th September 2016. The activities of the WGs were presented by a Nepali representative of each WG with JICA Project Team members. The confirmed items of the JCC were; result of hazard assessment, Coverage Items for Risk Assessment and Remaining Data Collection, Methodology for Risk Assessment, Setting Disaster Occurrence Scenes, Selection of Target Scenarios for Full Scale Risk Assessment, and Activities at Pilot Municipalities in the second phase.



Source: JICA Project Team

**Figure 1.5.5 4th JCC meeting**

**(5) 5th JCC Meeting**

The 5th JCC meeting was held on the occasion of commencement of the 2nd phase of the project on 19 December 2016. In the meeting, contents of the activities for the 2nd phase of the project, and methodology for human casualty and remaining data collection for School, Hospital, and Governmental Buildings were confirmed, and agreed to implement risk assessment based on the proposed methodology.



Source: JICA Project Team

**Figure 1.5.6 5th JCC meeting**

**(6) 6th JCC Meeting**

The 6th JCC meeting was held on the occasion of completion of Risk Assessment on 6 April 2017. Based on the consensus made on the result of risk assessment at 4th WG2 Meeting held on 23 February 2017, at 6th JCC, result of risk assessment was confirmed by JCC members. And, utilization of result for pilot activities, and level of ground motion to be targeted for DRR in Kathmandu Valley were discussed and basically agreed to target the level of CNS-2 for critical facilities (important buildings such as school, hospital, governmental building, high-rise buildings, large scale commercial building, and important infrastructure such as bridges), and CNS-1 for other facilities such as low-rise residential buildings, small commercial and residential buildings.



Source: JICA Project Team

**Figure 1.5.7 6th JCC meeting**

**(7) 7th JCC Meeting**

The 7th (final) JCC meeting was held on 12th February 2018. The meeting confirmed the pilot activity outcomes, including LDCRP Technical Guideline, LDCRP, SOP and CBDRRM activities and the completion of all the activities of the project. The meeting also discussed on the actions that should be taken after the project completion by Nepal government, such as expansion of the pilot activities to KV and whole country, GIS data and hazard and risk assessment results sharing and revision mechanism of risk assessment in the future. The handed over of the equipment used by the project to MoUD is mentioned.



**Figure 1.5.8 7th JCC meeting**

## Chapter 2 Basic Information Collection and Analysis

---

This chapter focuses on the data collection and analysis, which will be the base for seismic hazard and risk assessment. The implementation policies and methods for conducting each activity of the project are based on the collected data. The data collection was firstly started with the interviews with governmental organizations and municipal offices. In parallel, the technical reports, related plans, publications, project documents of I/NGOs or other donors were collected. However, the collected data are not sufficient for performing the assessment. The project made site survey, sub-contracting or estimation to supplement the lack of data.

### 2.1 Natural conditions

#### 2.1.1 Outline of geomorphology

The geomorphology of the Kathmandu Valley is divided into deltaic-lacustrine terraces, fluvial surfaces (modern flood plains), mountainous slopes, hills, landslides etc. (Figure 2.1.1).

As described in the chapter of preparation of the detailed geomorphological map, most areas of the Kathmandu Valley stand on the deltaic-lacustrine terraces. These were formed under the environment of the Paleo-Kathmandu Lake (Sakai et al., 2012). The Paleo-Kathmandu Lake appeared ~one million years BP by the uplift of the Mahabharat range and disappeared ~10,000 years BP. The terraces are subdivided into T1 to T7 by the altitudes of the distribution which depend on the lake-water level at that time. According to  $^{14}\text{C}$  dating of charred materials included in the terrace deposits, T1 to T4 terraces were formed after ~50,000 years BP. T5 to T7 terraces are somewhat older than T1 to T4 terraces. These were uplifted tectonically which resulted in the distribution at higher altitudes than T1 to T4 terraces. The frame of the present topography of the Kathmandu Valley was created after the last ~50,000 years BP in the history of the Paleo-Kathmandu Lake which reaches up to ~one million years.

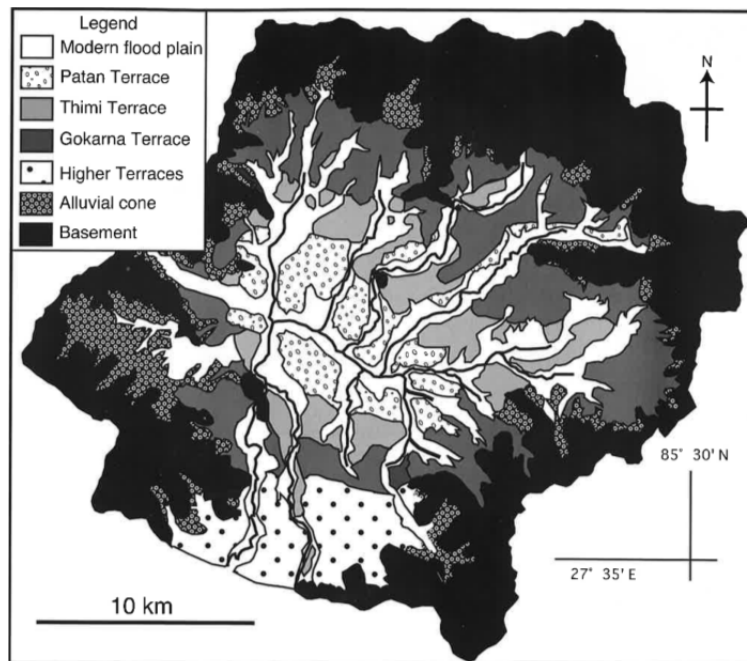
The terrace surfaces in the northern region and in the southern region are inclined to the south and to the north, respectively. This suggests that the terraces were formed by the fluvial process, when the lake reduced and became shallow, though under the environment of the Paleo-Kathmandu Lake. Therefore, the terrace deposits are composed mainly of gravels which are weakly consolidated as compared to the alluvial deposits mentioned later.

The fluvial surfaces (modern flood plains) were formed by the fluvial process as the deltaic-lacustrine terraces were eroded by modern rivers after disappearance of the



Paleo-Kathmandu Lake ~10,000 years BP. The fluvial surfaces are subdivided into alluvial lowland, valley plain, former river course, back marsh, natural levee, alluvial fan, lower terrace, and higher terrace. The ground conditions on these topographies are likely to amplify strong seismic motions and cause liquefaction. In Kathmandu Valley, residential areas traditionally stand on the deltaic-lacustrine terraces forming urban areas. However, residential areas have developed into the modern flood plains with bad ground conditions due to the rapid increase of population.

The Chandragiri Fault with WNW-ESE direction crosses from Kirtipur to Sunakothe in the southwestern region of the Kathmandu Valley (Saijo et al., 1995; Yagi et al., 2000; Asahi, 2003; Sakai et al., 2012). This fault is active because fault scarps are recognized on the alluvial fan, and T2 (Thimi) terrace is tilted tectonically.



Source: Sakai et al., 2012 (partly modified from Yoshida and Igarashi, 1984)

**Figure 2.1.1 Geomorphological map of the Kathmandu Valley (partly modified from Yoshida and Igarashi, 1984)**

## 2.1.2 Geology

The stratigraphy in the Kathmandu Valley is shown in Table 2.1.1, and the geological map is shown in Figure 2.1.2 and Figure 2.1.3. The stratigraphy is divided into the Paleozoic-Precambrian basement, the Pleistocene “Kathmandu Basin Group”, the Late Pleistocene deltaic-lacustrine terrace deposits, and the Holocene alluvium (Stocklin, 1980; Sakai et al., 2012).

### (1) Basement

The basement is distributed at the base of the Kathmandu basin and the surrounding

mountainous areas. It is composed of the Kathmandu Nappe (rock bodies transferred from another place by thrusts) and its underlying Tethyan sediments. The Kathmandu Nappe is divided into “the Shivapuri gneiss and granite injection complex” (Bs1) in the northern area of the basin and “the Bhimphedi Group” (Bs2) composed of schist, quartzite, phyllite, and marble in the northeastern and southeastern areas of the basin. In the region of the Kathmandu Nappe, many landslides are recognized. The Tethyan sediments are called as “the Phulchauki Group” (Bs3) which consists of weakly metamorphosed sediments of phyllite, slate, sandstone, limestone, and quartzite. The Phulchauki Group is distributed from the central to southern area of the basin. This is composed of relatively hard rocks.

## **(2) Kathmandu Basin Group**

The Kathmandu Basin was formed ~2.5 million years BP. The thickness of the basin-fill deposits is over 600 m. The basal boulder bed and Tarebhir formation were deposited at the bottom of the basin by fluvial process of the Paleo-Bagmati River. These formations are relatively hard. The thickness of the Tarebhir formation occasionally reaches up to 300 m.

The Kathmandu Basin was dammed up and changed to the Paleo-Kathmandu Lake ~one million years BP, and the Lukundol and Kalimati formations were deposited. The former is the weakly consolidated fluvial and flood plain/oxbow lake deposits, deposited during the early stage of Paleo-Kathmandu Lake. The latter is lake-fill deposits composed mainly of unconsolidated dark grey to black clay deposited at the middle stage when the lake expanded and deepened. The maximum thickness reaches up to 200 m.

## **(3) Deltaic-lacustrine deposits**

The deltaic-lacustrine deposits were formed at the final stage when the lake reduced and became shallow after ~50,000 years BP. These are subdivided into Patan, Thimi, Gokarna, Tokha, Boregaon, Chapagaon, and Pyangaon terrace deposits which are composed mainly of weakly consolidated gravel layers with rounded to sub-rounded pebbles and cobbles.

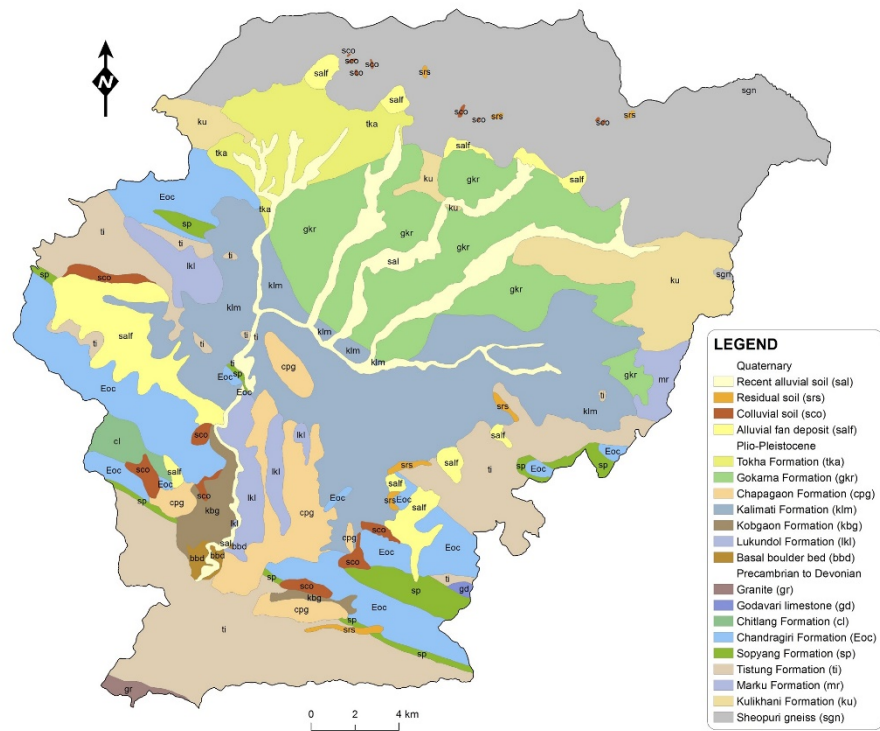
## **(4) Alluvium**

The alluvium is divided into alluvial deposits, fan deposits, and colluvial deposits formed in the Holocene time. These layers are basically composed of unconsolidated silt and sand, likely to amplify strong seismic motion and liquefy because water level is high along rivers.

**Table 2.1.1 Stratigraphy in the Kathmandu Valley**

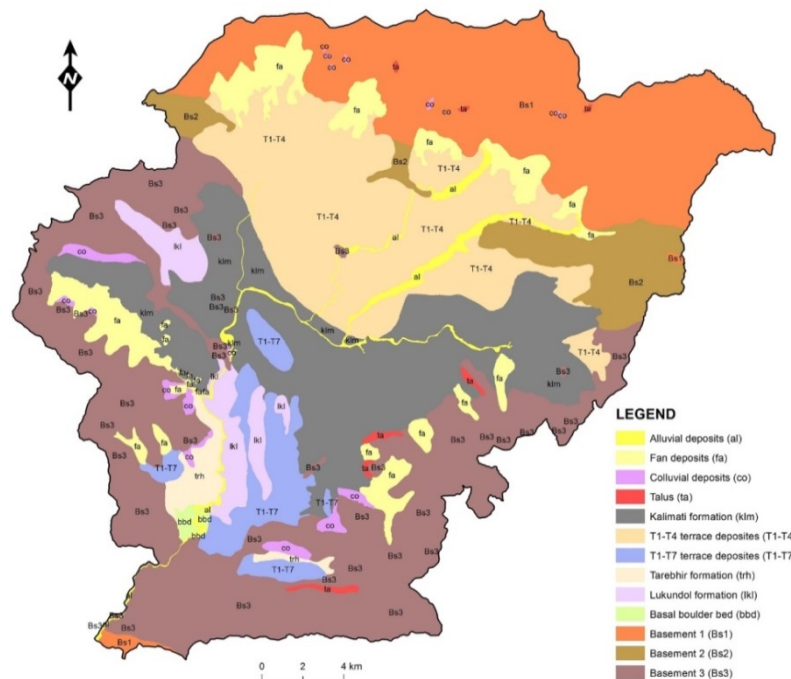
Geological age		Stratigraphy		abbr	Facies	
Cenozoic	Quaternary	Holocene	Alluvium	Alluvial deposits	al	Clay, sand, gravel
				Fan deposits	fa	Poorly sorted gravel with sub-angular to sub-rounded pebbles and cobbles
				Talus	ta	Clay, silt, sand with angular to sub-angular pebbles and cobbles
				Colluvial deposits	co	Clay, silt, sand with angular to sub-angular pebbles and cobbles
		Pleistocene	Deltaic-Lacustrine terrace deposits	Northern region: Patan, Thimi, Gokarna, Tokha terrace deposits	T1-T4	Sand, sandy clay with sub-rounded to rounded pebbles and cobbles
				Southern region: Patan, Thimi, Gokarna, Boregaon, Chapagaon, Pyangaon terrace deposits	T1-T7	Sand, sandy clay with sub-rounded to rounded pebbles and cobbles
			Kathmandu basin group	Kalimati Formation	klm	Dark gray to black clay, organic clay, and fine sand
				Lukundol Formation	lkl	Weakly consolidated and laminated clay, silt, and fine sand with granules
	Tarebhir Formation	trh		Laminated fine sand with sandy clay, silty sand, and gravel		
	Basal boulder bed	bbd		Compact boulder conglomerate		
Paleozoic to Pre-Cambrian	—	Basement	Shivapuri gneiss and granite injection complex	Bs1	Gneiss, granite, schist	
			Bhimphedi Group	Bs2	Schist, quartzite, Phyllite, marble	
			Phulchauki Group	Bs3	Phyllite, slate, sandstone, limestone, quartzite	

Source: JICA Project Team (compiled from several literature sources)



Source: DMG, Shrestha et al., 1998 with some revision

**Figure 2.1.2 Geology of the Kathmandu Valley (DMG, Engineering and environmental geological map of the Kathmandu Valley, partly modified from Shrestha et al., 1998)**



Source: UNDP, 2013 with some revision

**Figure 2.1.3 Geology of the Kathmandu Valley, partly modified from Comprehensive Disaster Risk Management Program (UNDP, 2013).**

### 2.1.3 Earthquake Activity

#### (1) Historical Earthquakes

Almost all the territory of Nepal is located right above the Main Himalayan Thrust (MHT) where the Indian Plate subducts under the Eurasian Plate. The active faults are called Main Frontal Thrust (MFT), Main Boundary Thrust (MBT) and Main Central Thrust (MCT) which run on the ground from east to west of the country (see ). Nepal and its surrounding regions are the most seismically active zone in the world and largest inland historical earthquakes have occurred in this region.

The earthquake activities before the instrumental observation started can generally be studied based on the discovery and analysis of the chronicle of the dynasty, reports of the administrative or personal diaries. It can be traced back to more ancient times and more precisely if the stable domination continued longer period. Because of the geographical features of Nepal, not only in the country but the documents in India, Tibet and England should be studied to know the historical earthquake activity of Nepal. Ambraseys and Douglas (2004) and Szeliga et al. (2010) collected various historical literature sources and compiled a historical earthquake catalog of north India including Nepal. Many historical earthquakes can be discovered by this method, but one earthquake is sometimes documented as different earthquakes of a separate year. The conversion of ancient calendars to the current calendar is sometimes difficult.

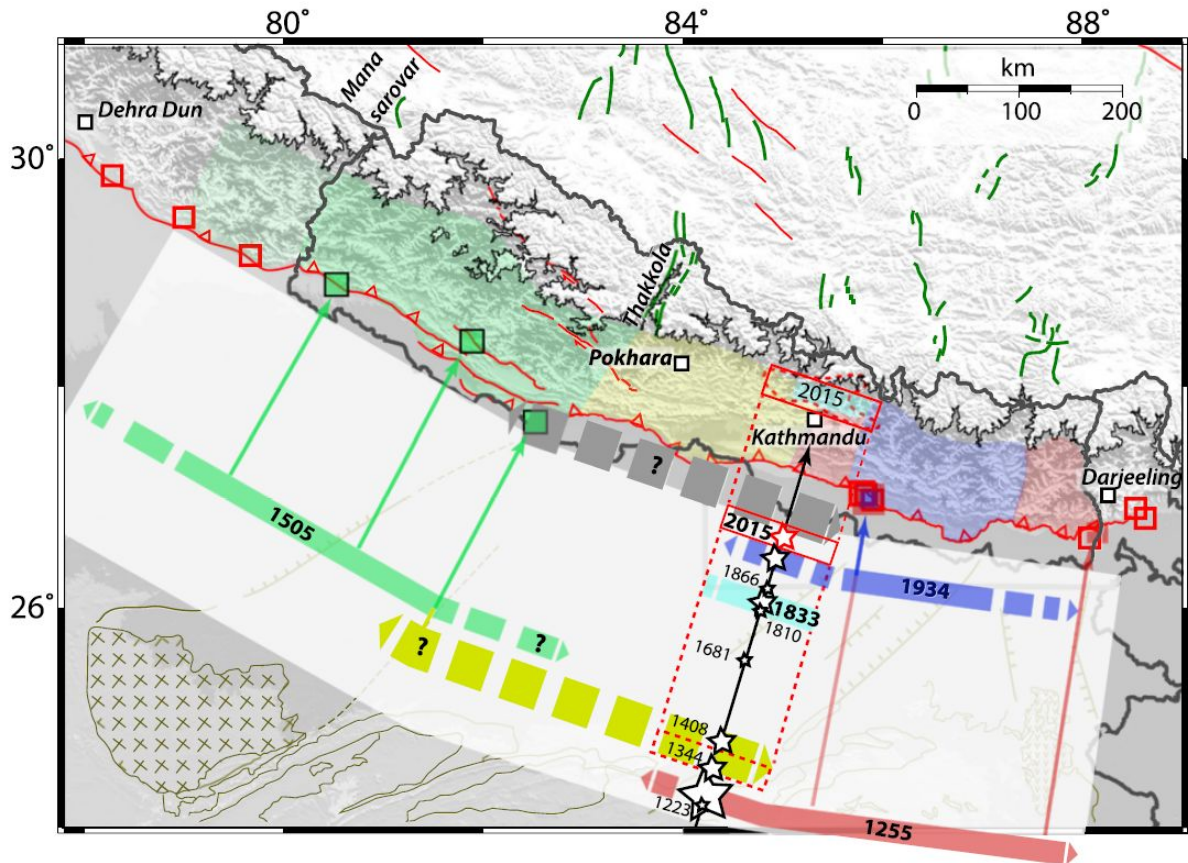
Trenching survey of the fault is another way to study the historical earthquakes directly. Most of the devastating earthquakes in Nepal occurred due to the movement of MHT and traces of the activity can be found along MFT at the surface. Trenching survey is a powerful tool to study the historical earthquakes in Nepal and many researchers from many countries have conducted the survey. The dating analysis of the sample from the trench is necessary to know the age of the activity if the movement is found by trenching, but the uncertainty of the estimation is sometimes large.

Bollinger et al. (2016) proposed the earthquake occurrence model in Nepal from the 13th century up until now as shown in using the earthquake catalog based on the historical literature and trenching survey results. Based on their result, some hundreds of kilometers from Central Nepal to East Nepal was activated in 1255 and one third of the inhabitants of Kathmandu including the king died because of that earthquake. The aftershocks continued for more than four months. The next damaging earthquake occurred in 1344, and the then king was heavily injured and died the next day. As for the earthquakes in 1255 and 1344, only the descriptions of Kathmandu are found in literature. No records of shaking or destruction in other regions have been found so far. The next large reported earthquake may have occurred in 1408 but details are unknown. Bollinger et al. (2006) supposed the section

of MFT from Kathmandu to Pokhara in Central Nepal moved and generated an earthquake in 1344 or in 1408. The great earthquake in 1505 is significantly better documented. It is supposed that 600 km from Far West Nepal to Central Nepal was activated in 1505 but there was no mention of a large event in Kathmandu.

The 19th century earthquakes are better known. Kathmandu was severely damaged by the August 26, 1833 earthquake (Bilham (1995)). The magnitude of this earthquake is supposed to be 7 class and occurred north-northwest of Kathmandu Valley. The May 23, 1866 earthquake affected the area northeast of the Kathmandu Valley, but the damage was not as severe as the 1833 event. The next large earthquake to affect Kathmandu was the January 15, 1934 “Bihar-Nepal” earthquake, the magnitude is estimated 8.1 to 8.4. Central Nepal to East Nepal including Kathmandu was severely damaged by this earthquake. Recent field work and trenching survey in this region found the traces of activity by 1934 and 1255 event along MFT (Sapkota et al. (2013)). The latest devastating earthquake is April 25, 2015 “Gorkha” earthquake ( $M_w=7.8$ ). The estimated length of seismic source area is about 100 km.

Based on the above observation, Bollinger et al. (2016) pointed out that earthquakes occurred in 1255 and in 1934 with an interval of 679 years in Central - East Nepal zone repeatedly, however the West Nepal zone of MFT has been quiet for over 600 years, therefore a large earthquake in West Nepal can be supposed in the near future and the effect to Kathmandu is feared.



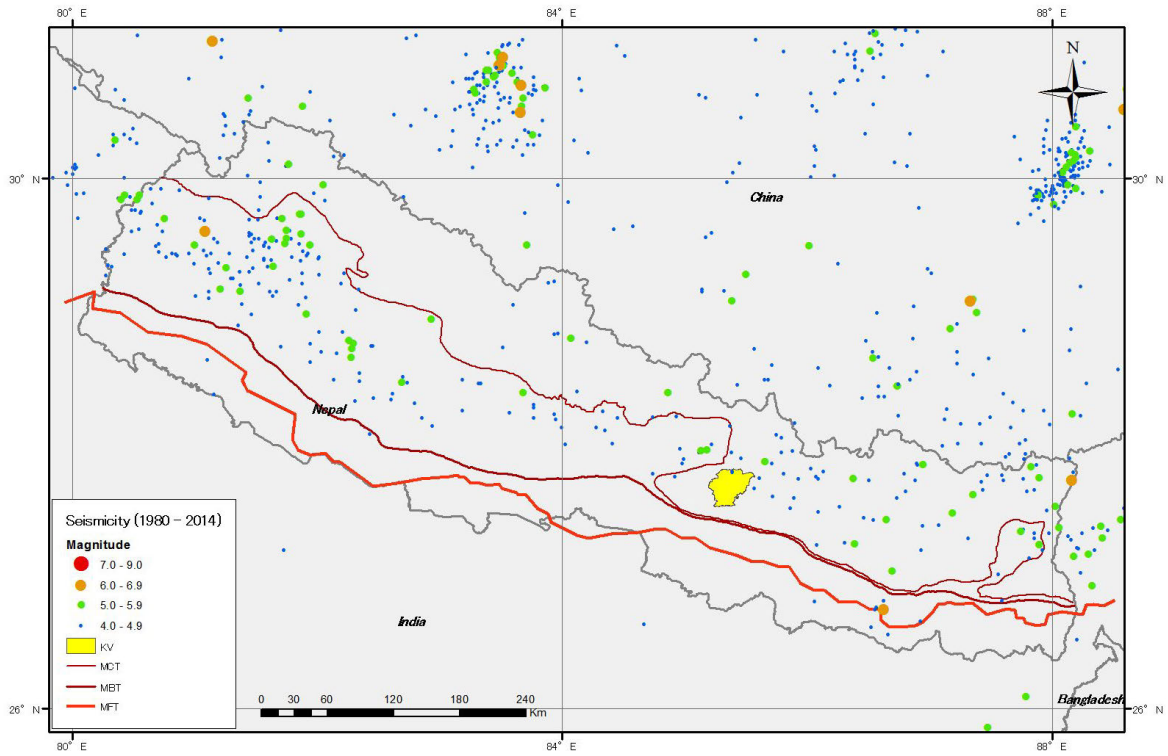
Source: Fig. 5 in Bollinger et al. (2016)

**Figure 2.1.4 Schematic Earthquake Occurrence Model in Nepal from 13th Century**

**(2) Recent Earthquake Activity**

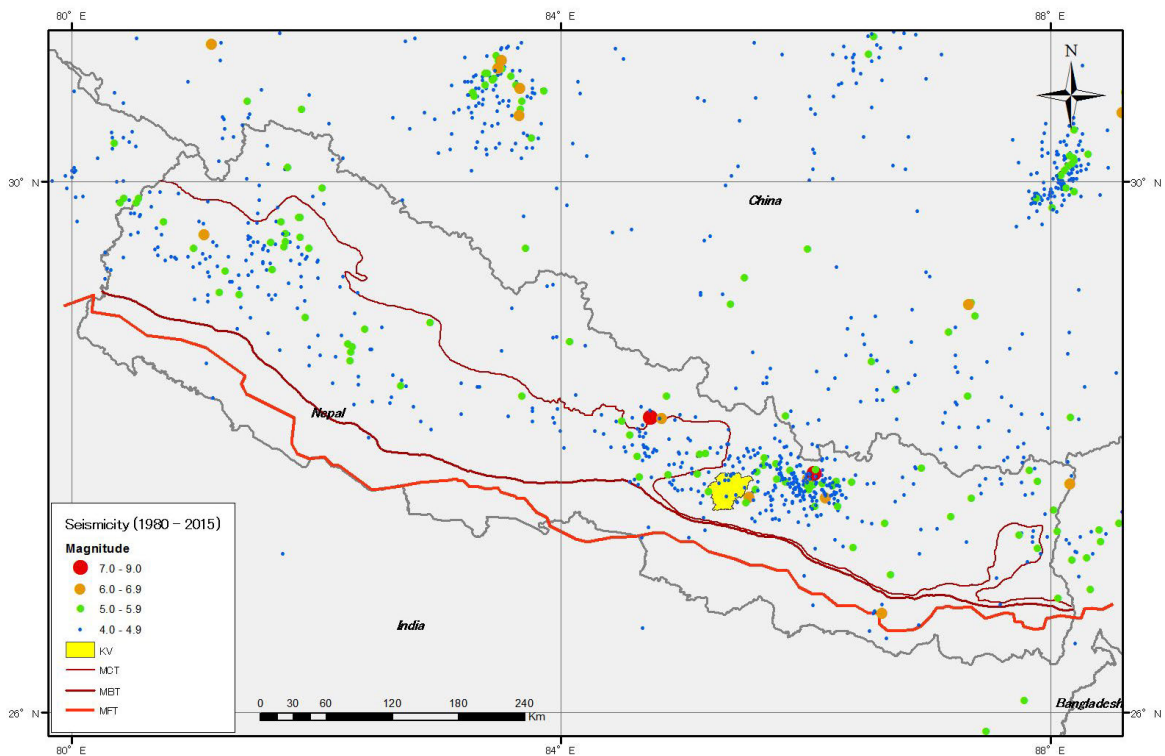
The recently observed earthquake activity from 1980 to 2014 (before the Gorkha Earthquake) and 1980 to 2015 (including Gorkha Earthquake and aftershocks) are shown in and respectively. The earthquake activity is almost limited to north of MFT.

No earthquake of magnitude 7 or larger occurred in Nepal from 1980 till the Gorkha Earthquake, for 35 years. Far West Nepal to Midwest Nepal is comparatively active and the activity in West Nepal is low. The plotted epicenters around Kathmandu Valley in are that of the Gorkha Earthquake and aftershocks. The events larger than magnitude 7 (red circle) are main shock (northwest of KV: Mw 7.8) and largest after shock (east of KV: Mw 7.3).



Source: Plotted by JICA Project Team based on the Earthquake Catalog of USGS and Fault data by DMG

**Figure 2.1.5 Earthquake Activity from 1980 to 2014**



Source: Plotted by JICA Project Team based on the Earthquake Catalog of USGS and Fault data by DMG

**Figure 2.1.6 Earthquake Activity from 1980 to 2015**



## References (2.1)

- Ambraseys, N. N., J. Douglas (2004) Magnitude calibration of north Indian earthquakes, *Geophys. J. Int.*, Vol. 159, pp. 165-206.
- Asahi, K. (2003) Thankot Active Fault in the Kathmandu Valley, Nepal Himalaya. *Jour. Nepal Geol. Soc.*, 28, pp. 1-8.
- Bilham, R. (1995) Location and magnitude of the 1833 Nepal earthquake and its relation to the rupture zones of contiguous great Himalayan earthquakes, *Current Science*, 69(2), pp. 155-187, 25 July 1995.
- Bollinger, L., P. Tapponnier, S. N. Sapkota, and Y. Klinger (2016) Slip deficit in central Nepal: omen for a repeat of the 1344 AD earthquake, *Earth Planets Space*, 68, 12.
- Saijo, K., K. Kimura, T. Komatsubara, and H. Yagi (1995) Active faults in southwestern Kathmandu basin, central Nepal. *Jour. Nepal Geol. Soc.*, 11 (Special Issue), pp. 217-224.
- Sakai, H., T. Sakai, A.P. Gaujrel, and R. Fujii (2012) Guidebook for excursion on geology of Kathmandu Valley. 27th Himalaya-Karakoram-Tibet Workshop (HKT), Kathmandu, 45p.
- Sapkota, S. N., L. Bollinger, Y. Klinger, P. Tapponnier, Y. Gaudemer, and D. Tiwari, (2013) Primary surface ruptures of the great Himalayan earthquakes in 1934 and 1255, *Nat. Geosci.*, 6, pp. 71-76.
- Shrestha, O.M, A. Koirala, S.L. Karmacharya, U.B. Pradhan, and R. Karmacharya (1998) Engineering and environmental geological map of the Kathmandu Valley, scale 1:50,000. Department of Mines and Geology.
- Stocklin, J (1980) Geology of Nepal and its regional frame. *Jour. Geol. Soc. London*, 137, pp. 1-34.
- Szeliga, W., S. Hough, S. Martin, and R. Bilham (2010) Intensity, Magnitude, Location and Attenuation in India for Felt Earthquakes since 1762, *Bull. Seism. Soc. Am.*, Vol. 100, No. 2, pp. 570-584.
- UNDP (2013) Comprehensive Disaster Risk Management Program.
- Yagi, H., H. Maemoku, Y. Ohtsuki, K. Saijo, and T. Nakata (2000), Recent activities of active faults distributed in and around Kathmandu valley, Lower Himalayan Zone. *Proc. Hokudan international symposium and school on active faulting*, Hiroshima University, Hiroshima, pp. 557-560.
- Yoshida, M and Y. Igarashi (1984) Neogene to Quaternary lacustrine sediments in the Kathmandu Valley, Nepal. *Jour. Nepal Geol. Soc.* 4 (Special Issue), pp. 73-100.

## **2.2 Social Information**

Basic data for risk assessment, including building, infrastructure and lifeline inventory, population and economic information are provided herein and please refer Annex 2: Map Book for all of the detail figures.

### **2.2.1 Buildings**

#### **(1) General Buildings**

Three types of earthquake damage scenes such as (i) Current situation in 2016, (ii) Future situation without upgrading the Building Seismic Performance Strengthening (BSPS) in 2030 and (iii) Future situation with BSPS in 2030 were set for the seismic risk assessment of general building damage in the project. Building damage by earthquake occurrence scene was estimated to calculate the number of damaged buildings according to the Peak Ground Acceleration (gal) of the scenario earthquake for each grid by dividing the entire Kathmandu Valley as the study area. The grid size is 250 square meters and the total number of grids in Kathmandu Valley is 11,933. As the preparation of input data for the general building damage estimation, it was necessary to set the number of buildings and building structure component ratios for each grid and all of three types of earthquake occurrence scenes.

When setting the number of buildings and building structure component ratios for each grid, detailed data on the position and structure type of each actual building was required. However, it is difficult to prepare accurate building data for all the buildings in Kathmandu Valley in 2016 without extensive site survey to visit each and every building in the Kathmandu Valley. Building data can be estimated based on assumptions from several types of usable data. In this project, with existing relevant data and the result of damaged building survey implemented after the Gorkha Earthquake in 2015, the estimation of building distribution in entire study area at the time of the Gorkha Earthquake in 2015 was taken as the first step of preparing building data. Then, based on that building distribution in 2015, the building distribution in 2016 was estimated assuming the number of damaged buildings by the Gorkha Earthquake and the status of reconstruction of buildings which were affected by the earthquake. With regard to the building distribution in the future, i.e. in 2030, it was decided to estimate the building distribution in consideration of population growth rates given by Central Bureau of Statistics (CBS) and results of projection of future built-up area distribution prepared by KVDA/UNDP, 2013. And, for the future situation with BSPS in 2030, multiple assumptions for progress levels of BSPS by different status of new building construction and building rehabilitation from 2016 to 2030 were set as cases of earthquake occurrence scenes in 2030 with BSPS. The flow of estimation of building distributions by earthquake occurrence scenes in this project is shown in Figure 2.2.1.

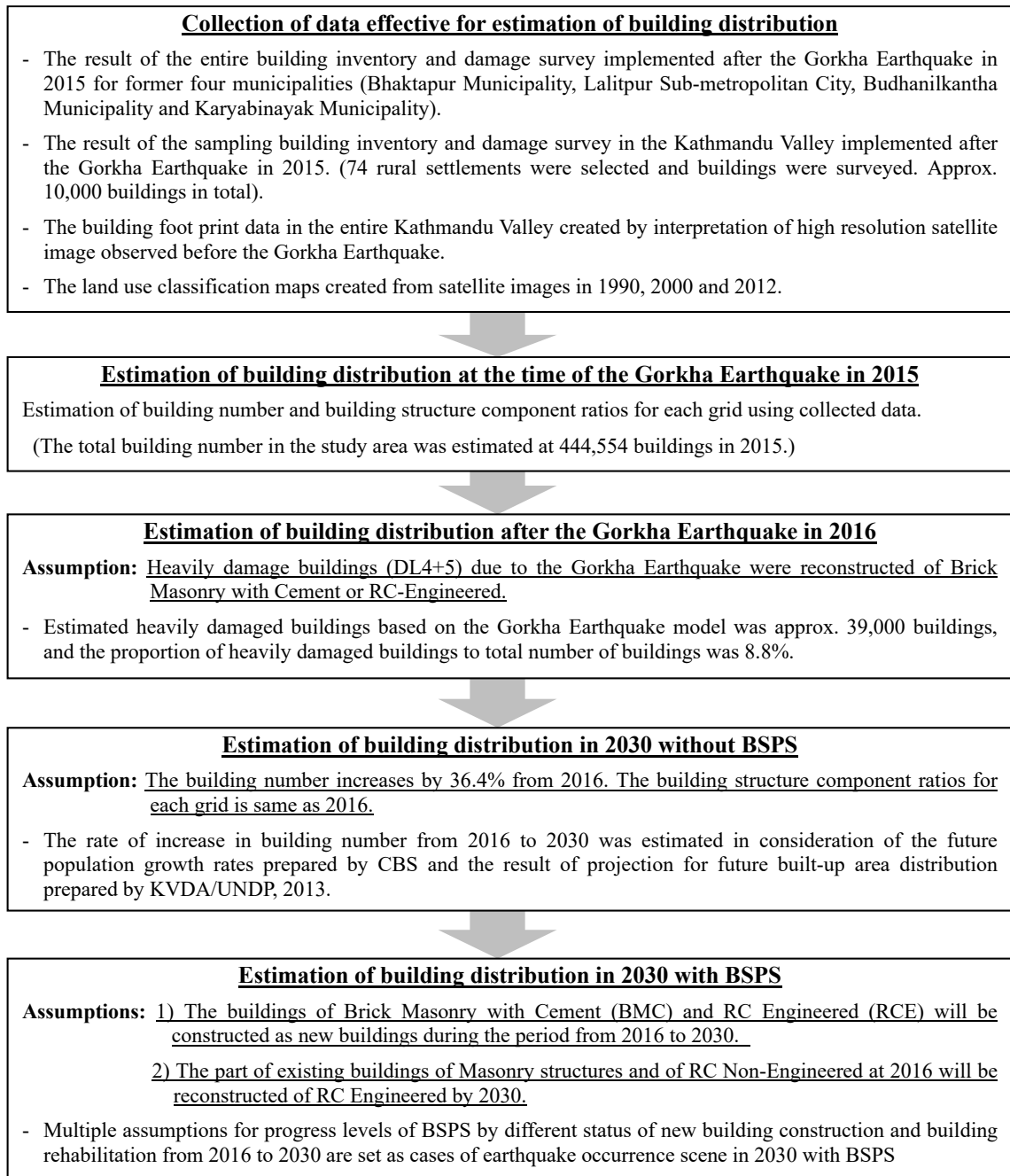


**Figure 2.2.1 The flow of estimation of building distributions by earthquake occurrence scene**

**1) Collection of data effective for estimation of building distribution**

Four types of spatial data were available to be utilized for the estimation procedure of the building distribution before the Gorkha Earthquake in 2015, which are as follows:

- i. The result of the entire building inventory and damage survey implemented after the Gorkha Earthquake in 2015 for former four municipalities (Bhaktapur Municipality, former Lalitpur Sub-metropolitan City, Budhanilkantha Municipality and former Karyabinayak Municipality).

- ii. The result of the sampling building inventory and damage survey in the Kathmandu Valley implemented after the Gorkha Earthquake in 2015. (74 rural settlements were selected and the surveyed buildings are approximately 10,000 buildings in total).
- iii. The building foot print data in the entire Kathmandu Valley created by interpretation of high resolution satellite image observed before the Gorkha Earthquake, in November 2014.
- iv. The land use classification maps created from satellite images in 1990, 2000 and 2012.

As a result of the validation of the building survey results which are listed above as i) and ii), it has been found that the number of buildings and the building component ratio for each area in the Kathmandu Valley show different trends depending on the type of land use, the period of urbanization especially in the central area and the density of buildings especially in rural areas. From the result of pre-validation, the following procedure was adopted as the method of building distribution estimation.

**Step 1: Creation of 250m grid-base thematic maps:** Three types of 250m grid-base thematic maps for the urbanization pattern, the land use pattern and the building density were created from the building foot print data and the land use classification maps in 1990, 2000 and 2012 which are listed above as iii) and iv).

**Step 2: Classification of areas:** Each grid in the entire Kathmandu Valley was classified into multiple areas from the combination of three thematic maps.

**Step 3: Estimation of building number by grid:** The correlation equation between exact building numbers by grid collected by the field survey and the density of building foot prints area by grid at the four municipalities for each classified area was determined. Then the estimated building number by grid was calculated to plug the density of building foot print area by grid into the correlation equation selected based on the classified area of target grid.

**Step 4: Estimation of building component ratio by classified area:** The building component ratio by classified area was calculated from the exact building component ratio collected by the field survey at the four municipalities and sampling area in the Kathmandu Valley.

## 2) Estimation of building distribution at the time of the Gorkha Earthquake in 2015

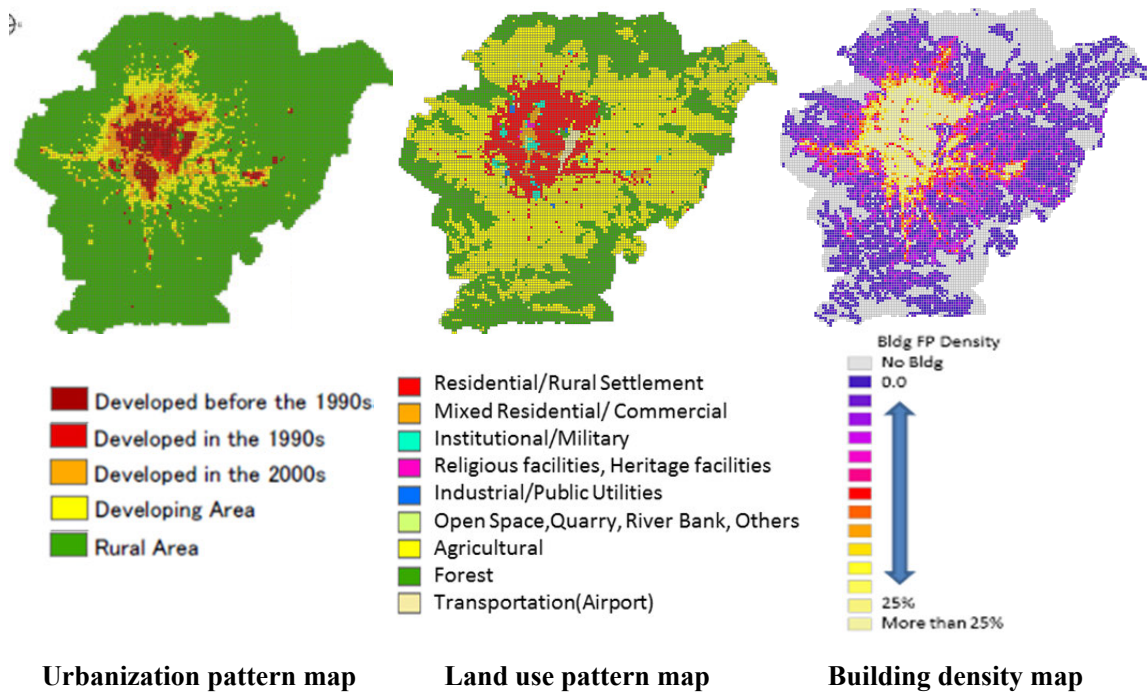
Based on the four steps mentioned above, building number and building structure component ratios for each grid was estimated using collected data.

**a) Step 1: Creation of 250m grid-base thematic maps**

The urbanization pattern map has been created by time-series analysis of built-up area expansion for each grid. Three land cover maps in 1990, 2000 and 2012, that were created in the project "Comprehensive Study of Urban Growth Trend and Forecasting of Land Use in the Kathmandu Valley" undertaken for the UNDP/CDRMP in 2013, were used as the basis of this time-series analysis. All the grids in the entire Kathmandu Valley were classified into five urbanization patterns from the difference in timing of urbanization as following:

- The grids which consist mostly of built-up area in 1990 were defined as "Developed Area before the 1990s".
- The grids which show a significant increase of built-up area between 1990 and 2000 and gentle or no increase of built-up area between 2000 and 2012 were defined as "Developed Area in the 1990s".
- The grids which show very few built-up areas or very gradual increase of built-up area between 1990 and 2000 and a significant increase of built-up area between 2000 and 2012 were defined as "Developed Area in the 2000s".
- The grids which show very few built-up areas in 2000 but a gradual increase of built-up area in 2012 was defined as "Developing Area".
- The grids which consist of no or very few built-up areas in 2012 were defined as "Rural Area"

The land use pattern map classified into nine land use patterns has been created by modifying the land use classification map of 2012. And, the building density map has been created by calculating the density of building foot prints area for each grid. Considering the use of the building density map to classify multiple areas in the "Rural Area" of the urbanization pattern map, the building densities have been divided into five classes using the thresholds set from maximum and minimum densities in "Rural Area". As a result of Step 1, 250m grid-base thematic maps were prepared, which are shown in Figure 2.2.2.



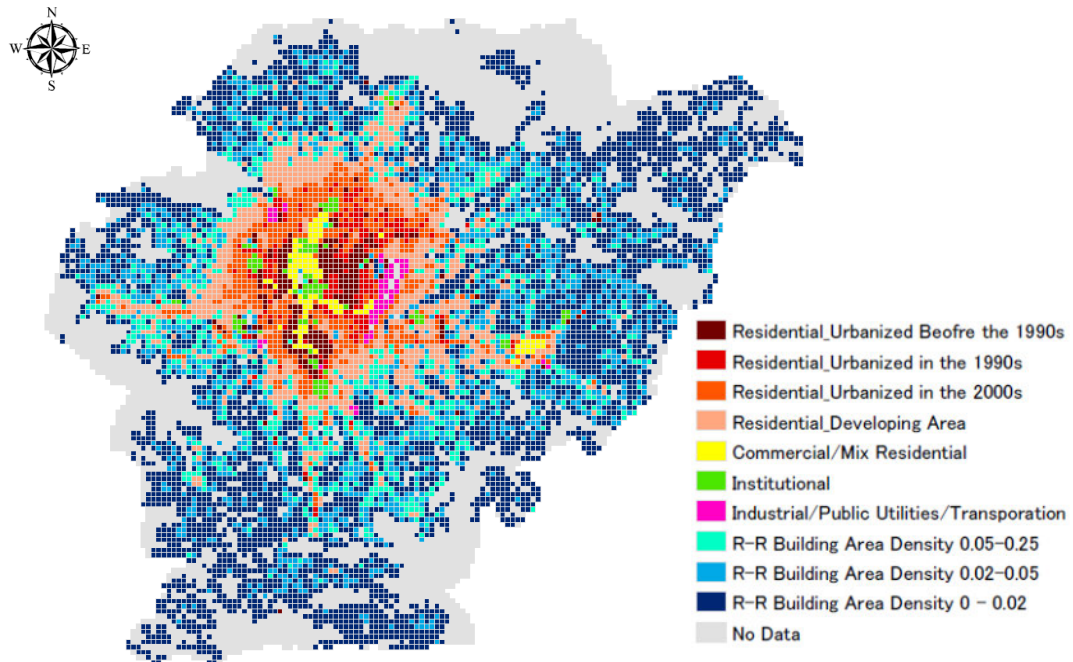
**Urbanization pattern map      Land use pattern map      Building density map**

Source: JICA Project Team, KVDA/UNDP, 2013

**Figure 2.2.2 Three types of thematic maps utilized for area classification**

**b) Step 2: Classification of areas**

Using the three types of thematic maps and results of building survey, listed above as i) and ii), the appropriate number of areas into which to classify all grids in the entire Kathmandu Valley was verified. In particular, the building component ratios in every possible combination of each pattern or class of three thematic maps were estimated. Total number of combinations was 225 (five urbanization patterns, nine land use patterns, five building density classes). Then the similarities of building component ratio for each combination were verified. If some combinations were similar, they were merged. Finally, by repeating this process, each grid in the entire Kathmandu Valley was classified into ten areas from the combination of three thematic maps. The result of area classification is shown in Figure 2.2.3.



Source: JICA Project Team

**Figure 2.2.3 The result of area classification**

**c) Step 3: Estimation of building number by grid**

Based on the classification of ten areas, the correlation equation between exact building numbers by grid collected by the field survey, listed above as i), and the density of building foot print area by grid, listed above as iii) at four municipalities were determined. The reason for determining correlation equations for each area is that the building foot prints number is not the exact building number, as that number was counted from the satellite image, and the difference of building number from exact ones increases with the increasing building density. Therefore, the density of building foot print area was used as a parameter to estimate the building number by grid. After determination of correlation equations for each area, the building number of each grid was calculated by the correlation equation selected based on the classified area of the target grid and the building foot print of the grid was substituted accordingly.

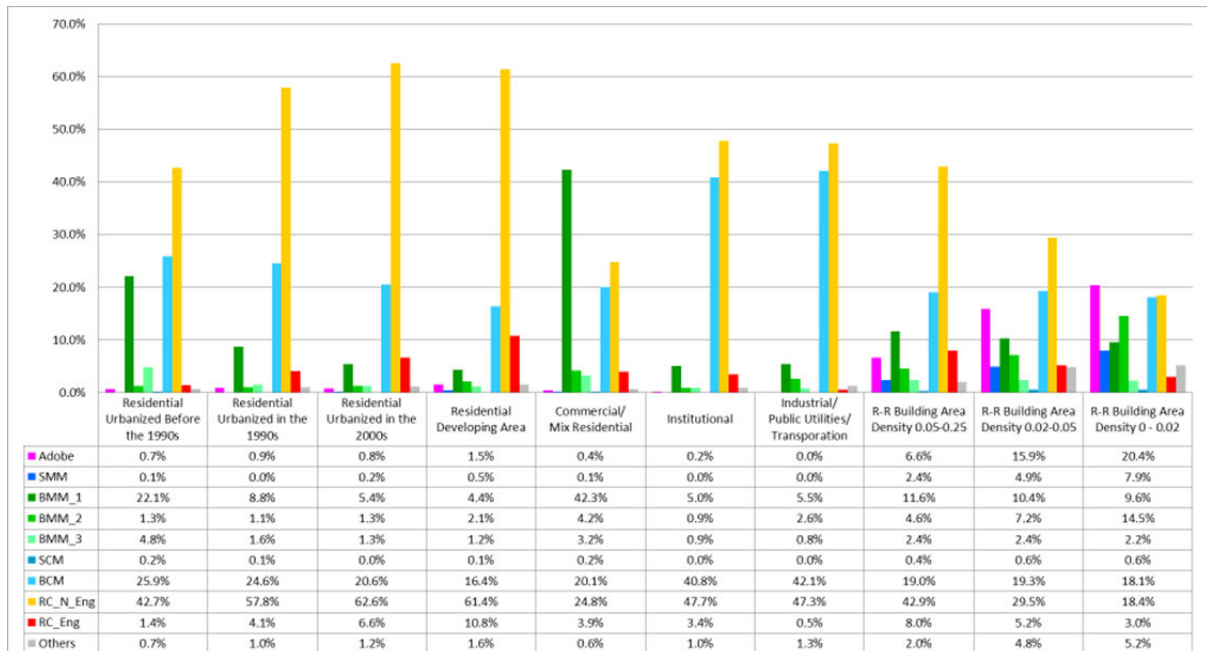
For the former four municipalities in which the entire building survey has been conducted, the correlation coefficient between the estimated building numbers and exact ones for each grid was approximate 0.93 ( $R^2 = 0.8729$ ) and a high correlation between estimated numbers and exact ones was obtained. The total number of buildings in the entire Kathmandu Valley was estimated to be 444,554 buildings at the time of the Gorkha Earthquake in 2015.

**d) Step 4: Estimation of building structure component ratio by classified area**

As explained in the section of Step 2, the building structure component ratios by classified area (the total number of areas is ten) were calculated from the results of the building survey, listed above as i) and ii). The building types to be categorized as the building component ratio are as follows (10 types):

1. Adobe
2. SMM: Stone with mud mortar joint
3. BMM\_1: Brick with mud mortar joint / Flex roof (wooden) / 20 years and over after construction
4. BMM\_2: Brick with mud mortar joint / Flex roof (wooden) / Less than 20 years after construction
5. BMM\_3: Brick with mud mortar joint / Rigid roof (RC structure)
6. SCM: Stone with cement mortar joint
7. BCM: Brick with cement mortar joint
8. RC\_N\_Eng: RC Non-Engineered
9. RC\_Eng: RC Engineered
10. Others

Figure 2.2.4 shows the estimated results of the building component ratios of ten classified areas.



Source: JICA Project Team

**Figure 2.2.4 The estimated results of the building component ratios of ten classified areas**



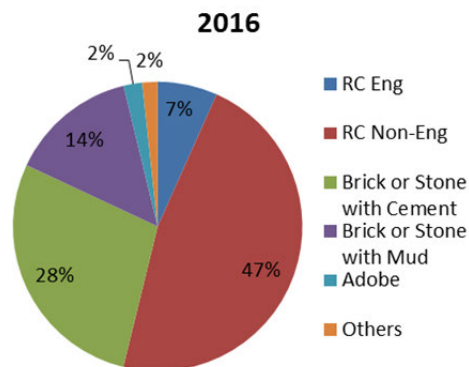
### 3) Estimation of building distribution after the Gorkha Earthquake in 2016

The building distribution in 2016 was estimated assuming the number of damaged buildings by the Gorkha Earthquake and the status of reconstruction of buildings affected by the earthquake. Specifically, based on estimated building distribution at the time of the Gorkha Earthquake in 2015, the building distribution in 2016 was estimated by setting the following assumption.

**[Assumption]:** Heavily damaged buildings (DL4+5) due to the Gorkha Earthquake were reconstructed of Brick Masonry with Cement (BCM) or RC-Engineered (RC\_Eng).

The number of heavily damaged buildings due to the Gorkha Earthquake for each grid was estimated using damage functions by structure type proposed in the project. The building distribution at the time of the Gorkha Earthquake in 2015 and the distribution of Peak Ground Acceleration (gal) reproduced based on the Gorkha Earthquake model were input as parameters of damage functions. Estimated heavily damaged buildings based on the Gorkha Earthquake model was approximately 39,000 buildings, and the proportion of heavily damaged buildings to total number of buildings was 8.8%.

The number of buildings per grid in 2016 was assumed to be same as at the time of the Gorkha Earthquake in 2015. The total number of buildings is 444,554 and the building structure component ratio in the entire Kathmandu Valley is shown in Figure 2.2.5.



Source: JICA Project Team

**Figure 2.2.5 Building structure component ratio in the entire Kathmandu Valley in 2016**

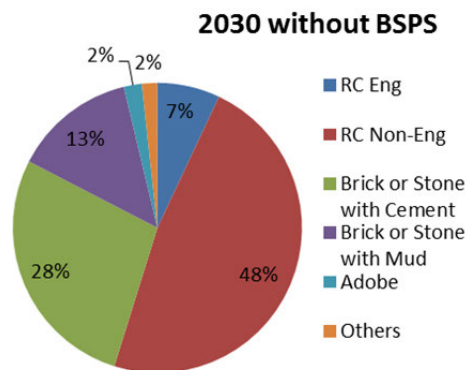
### 4) Estimation of building distribution in 2030 without BSPTS

Based on estimated building distribution in 2016, the building distribution in 2030 without BSPTS (Without promotion on Building Seismic Performance Strengthening) has been estimated by setting the following assumption.

**[Assumption]:** The building number increases by 36.4% from 2016. The building structure component ratios for each grid is same as 2016.

The rate of increase in the number of buildings in 2016 to 2030 for each grid has been estimated based on the future population growth rate prepared by the Central Bureau of Statistics (CBS) and the result of future built-up area distribution predicted by KVDA/UNDP, 2013. The total building number was estimated at 606,506 buildings in 2030.

The building structure component ratios for each grid were assumed to be same as ones in 2016. However, since the rate of increase in the number of buildings from 2016 to 2030 varies depending on the grid, the building structure component ratio in entire the Kathmandu Valley is slightly different from the ratio in 2016. Figure 2.2.6 shows the composition ratio of buildings in 2030 without BSPPS.



Source: JICA Project Team

**Figure 2.2.6 Building structure component ratio in the entire Kathmandu Valley in 2030 without BSPPS**

#### 5) Estimation of building distribution in 2030 with BSPPS

Based on estimated building distribution in 2030 without BSPPS, five types of building distributions in 2030 with BSPPS have been estimated by setting five cases of different assumptions for progress levels of BSPPS in consideration about different status of new building construction and building rehabilitation from 2016 to 2030. The five cases of assumptions for progress levels of BSPPS in detail are shown in Table 2.2.1.

**Table 2.2.1 Five cases of assumptions for progress levels of BSPS in 2030**

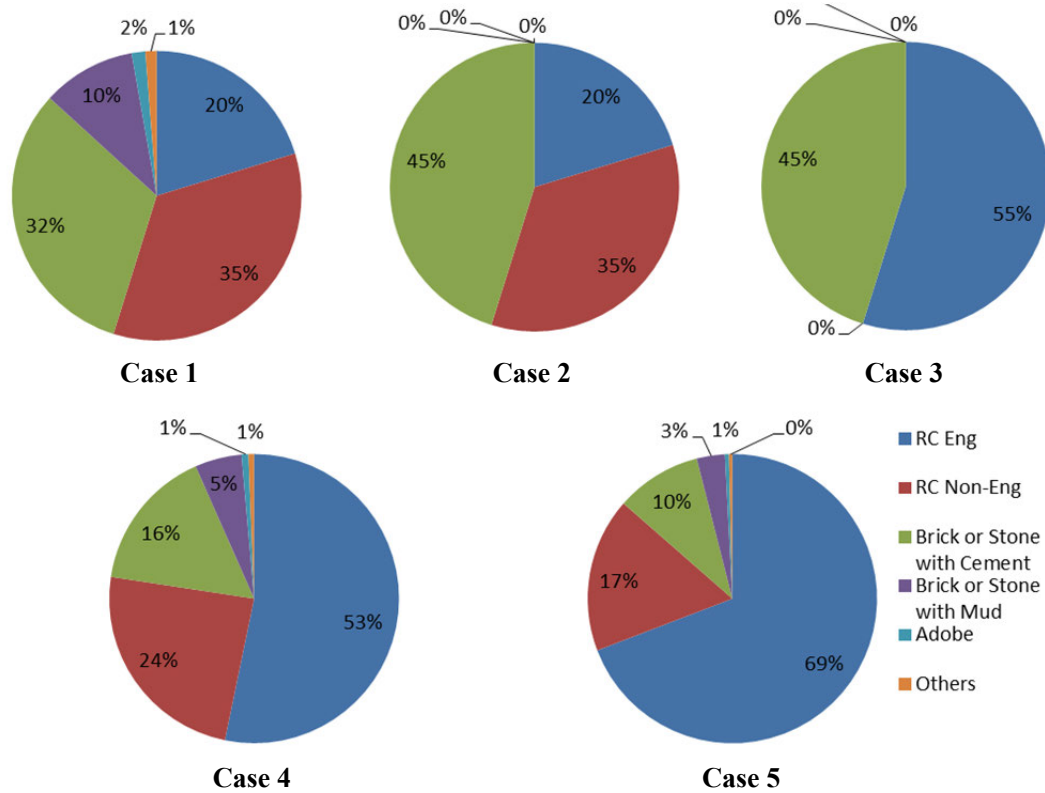
Case-1: Existing buildings in 2016 will not be changed. New build buildings will be BMC and RCE only.																									
<p>i) The buildings of Brick Masonry with Cement (BMC) and RC Engineered (RCE) will be constructed as new buildings during the period from 2016 to 2030. The ratio of BMC and RCE for new buildings was assumed having the same ratio between Masonry<sup>*1</sup> and RC<sup>*2</sup> in 2016.</p>	<table border="1"> <thead> <tr> <th>Category</th> <th>2016</th> <th>2030 Case-1</th> </tr> </thead> <tbody> <tr> <td>Existing Building in 2016 (Total 444,554)</td> <td></td> <td></td> </tr> <tr> <td>Masonry (all kind)</td> <td>46.0%</td> <td>46.0%</td> </tr> <tr> <td>RC non-engineered</td> <td>47.0%</td> <td>47.0%</td> </tr> <tr> <td>RC engineered</td> <td>7.0%</td> <td>7.0%</td> </tr> <tr> <td>New Building by 2030 (Total 161,952)</td> <td></td> <td></td> </tr> <tr> <td>Masonry (Cement)</td> <td>46.0%</td> <td>46.0%</td> </tr> <tr> <td>RC engineered</td> <td>54.0%</td> <td>54.0%</td> </tr> </tbody> </table>	Category	2016	2030 Case-1	Existing Building in 2016 (Total 444,554)			Masonry (all kind)	46.0%	46.0%	RC non-engineered	47.0%	47.0%	RC engineered	7.0%	7.0%	New Building by 2030 (Total 161,952)			Masonry (Cement)	46.0%	46.0%	RC engineered	54.0%	54.0%
Category	2016	2030 Case-1																							
Existing Building in 2016 (Total 444,554)																									
Masonry (all kind)	46.0%	46.0%																							
RC non-engineered	47.0%	47.0%																							
RC engineered	7.0%	7.0%																							
New Building by 2030 (Total 161,952)																									
Masonry (Cement)	46.0%	46.0%																							
RC engineered	54.0%	54.0%																							
Case-2: Seismic performance strengthening for existing buildings made of Masonry <sup>*1</sup> in 2016 will be promoted in addition to Case 1.																									
<p>i) The buildings made of Brick Masonry with Cement Mortar and RC Engineered will be constructed as new buildings by 2030.</p> <p>ii) Existing buildings made of Adobe, Brick Masonry with Mud Mortar and Other materials in 2016 will be reconstructed by Brick masonry with cement mortar.</p>	<table border="1"> <thead> <tr> <th>Category</th> <th>2016</th> <th>2030 Case-2</th> </tr> </thead> <tbody> <tr> <td>Existing Building in 2016 (Total 444,554)</td> <td></td> <td></td> </tr> <tr> <td>Masonry (all kind)</td> <td>46.0%</td> <td>all BMC 46.0%</td> </tr> <tr> <td>RC non-engineered</td> <td>47.0%</td> <td>47.0%</td> </tr> <tr> <td>RC engineered</td> <td>7.0%</td> <td>7.0%</td> </tr> <tr> <td>New Building by 2030 (Total 161,952)</td> <td></td> <td></td> </tr> <tr> <td>Masonry (Cement)</td> <td>46.0%</td> <td>46.0%</td> </tr> <tr> <td>RC engineered</td> <td>54.0%</td> <td>54.0%</td> </tr> </tbody> </table>	Category	2016	2030 Case-2	Existing Building in 2016 (Total 444,554)			Masonry (all kind)	46.0%	all BMC 46.0%	RC non-engineered	47.0%	47.0%	RC engineered	7.0%	7.0%	New Building by 2030 (Total 161,952)			Masonry (Cement)	46.0%	46.0%	RC engineered	54.0%	54.0%
Category	2016	2030 Case-2																							
Existing Building in 2016 (Total 444,554)																									
Masonry (all kind)	46.0%	all BMC 46.0%																							
RC non-engineered	47.0%	47.0%																							
RC engineered	7.0%	7.0%																							
New Building by 2030 (Total 161,952)																									
Masonry (Cement)	46.0%	46.0%																							
RC engineered	54.0%	54.0%																							
Case-3: Seismic performance strengthening for existing buildings of RC Non-Engineered in 2016 will be promoted in addition to Case 2.																									
<p>i) The buildings made of Brick Masonry with Cement Mortar and RC Engineered will be constructed as new buildings by 2030.</p> <p>ii) Existing buildings made of Adobe, Brick Masonry with Mud Mortar and Other materials in 2016 will be reconstructed by Brick masonry with cement mortar.</p> <p>iii) Existing buildings of RC Non-Engineered in 2016 will be reconstructed by RC Engineered.</p>	<table border="1"> <thead> <tr> <th>Category</th> <th>2016</th> <th>2030 Case-3</th> </tr> </thead> <tbody> <tr> <td>Existing Building in 2016 (Total 444,554)</td> <td></td> <td></td> </tr> <tr> <td>Masonry (all kind)</td> <td>46.0%</td> <td>all BMC 46.0%</td> </tr> <tr> <td>RC non-engineered</td> <td>47.0%</td> <td>0%</td> </tr> <tr> <td>RC engineered</td> <td>7.0%</td> <td>100% 54.0%</td> </tr> <tr> <td>New Building by 2030 (Total 161,952)</td> <td></td> <td></td> </tr> <tr> <td>Masonry (Cement)</td> <td>46.0%</td> <td>46.0%</td> </tr> <tr> <td>RC engineered</td> <td>54.0%</td> <td>54.0%</td> </tr> </tbody> </table>	Category	2016	2030 Case-3	Existing Building in 2016 (Total 444,554)			Masonry (all kind)	46.0%	all BMC 46.0%	RC non-engineered	47.0%	0%	RC engineered	7.0%	100% 54.0%	New Building by 2030 (Total 161,952)			Masonry (Cement)	46.0%	46.0%	RC engineered	54.0%	54.0%
Category	2016	2030 Case-3																							
Existing Building in 2016 (Total 444,554)																									
Masonry (all kind)	46.0%	all BMC 46.0%																							
RC non-engineered	47.0%	0%																							
RC engineered	7.0%	100% 54.0%																							
New Building by 2030 (Total 161,952)																									
Masonry (Cement)	46.0%	46.0%																							
RC engineered	54.0%	54.0%																							
Case-4: Seismic performance strengthening for existing buildings in 2016 and new buildings by 2030 will be promoted.																									
<p>i) 50% of existing buildings of Masonry<sup>*1</sup> and 30% of existing buildings of RC Non-Engineered in 2016 will be reconstructed of RC Engineered by 2030.</p> <p>ii) The buildings of Brick Masonry with Cement (BMC) and RC Engineered (RCE) will be constructed as new buildings during the period from 2016 to 2030. The ratio of BMC and RCE for new buildings was assumed having the same ratio between Masonry<sup>*1</sup> and RC<sup>*2</sup> in 2016 at first and then transferred 50% of BMC to RCE.</p>	<table border="1"> <thead> <tr> <th>Category</th> <th>2016</th> <th>2030 Case-4</th> </tr> </thead> <tbody> <tr> <td>Existing Building in 2016 (Total 444,554)</td> <td></td> <td></td> </tr> <tr> <td>Masonry (all kind)</td> <td>46.0%</td> <td>50% 23.0%</td> </tr> <tr> <td>RC non-engineered</td> <td>47.0%</td> <td>50% 32.9%</td> </tr> <tr> <td>RC engineered</td> <td>7.0%</td> <td>30% 44.1%</td> </tr> <tr> <td>New Building by 2030 (Total 161,952)</td> <td></td> <td></td> </tr> <tr> <td>Masonry (Cement)</td> <td>46.0%</td> <td>50% 23.0%</td> </tr> <tr> <td>RC engineered</td> <td>54.0%</td> <td>50% 77.0%</td> </tr> </tbody> </table>	Category	2016	2030 Case-4	Existing Building in 2016 (Total 444,554)			Masonry (all kind)	46.0%	50% 23.0%	RC non-engineered	47.0%	50% 32.9%	RC engineered	7.0%	30% 44.1%	New Building by 2030 (Total 161,952)			Masonry (Cement)	46.0%	50% 23.0%	RC engineered	54.0%	50% 77.0%
Category	2016	2030 Case-4																							
Existing Building in 2016 (Total 444,554)																									
Masonry (all kind)	46.0%	50% 23.0%																							
RC non-engineered	47.0%	50% 32.9%																							
RC engineered	7.0%	30% 44.1%																							
New Building by 2030 (Total 161,952)																									
Masonry (Cement)	46.0%	50% 23.0%																							
RC engineered	54.0%	50% 77.0%																							
Case-5: Seismic performance strengthening for existing buildings in 2016 and new buildings by 2030 will be promoted more actively compared to Case 4.																									
<p>i) 70% of existing buildings of Masonry structures and 50% of existing buildings of RC Non-Engineered in 2016 will be reconstructed of RC Engineered by 2030.</p> <p>ii) The buildings of Brick Masonry with Cement (BMC) and RC Engineered (RCE) will be constructed as new buildings during the period from 2016 to 2030. The ratio of BMC and RCE for new buildings was assumed having the same ratio between Masonry<sup>*1</sup> and RC<sup>*2</sup> in 2016 at first and then transferred 70% of BMC to RCE.</p>	<table border="1"> <thead> <tr> <th>Category</th> <th>2016</th> <th>2030 Case-5</th> </tr> </thead> <tbody> <tr> <td>Existing Building in 2016 (Total 444,554)</td> <td></td> <td></td> </tr> <tr> <td>Masonry (all kind)</td> <td>46.0%</td> <td>70% 13.8%</td> </tr> <tr> <td>RC non-engineered</td> <td>47.0%</td> <td>50% 23.5%</td> </tr> <tr> <td>RC engineered</td> <td>7.0%</td> <td>50% 62.7%</td> </tr> <tr> <td>New Building by 2030 (Total 161,952)</td> <td></td> <td></td> </tr> <tr> <td>Masonry (Cement)</td> <td>46.0%</td> <td>30% 13.8%</td> </tr> <tr> <td>RC engineered</td> <td>54.0%</td> <td>70% 86.2%</td> </tr> </tbody> </table>	Category	2016	2030 Case-5	Existing Building in 2016 (Total 444,554)			Masonry (all kind)	46.0%	70% 13.8%	RC non-engineered	47.0%	50% 23.5%	RC engineered	7.0%	50% 62.7%	New Building by 2030 (Total 161,952)			Masonry (Cement)	46.0%	30% 13.8%	RC engineered	54.0%	70% 86.2%
Category	2016	2030 Case-5																							
Existing Building in 2016 (Total 444,554)																									
Masonry (all kind)	46.0%	70% 13.8%																							
RC non-engineered	47.0%	50% 23.5%																							
RC engineered	7.0%	50% 62.7%																							
New Building by 2030 (Total 161,952)																									
Masonry (Cement)	46.0%	30% 13.8%																							
RC engineered	54.0%	70% 86.2%																							

\*1: Masonry structures include Adobe, Stone with Mud & Cement, Brick Masonry with Mud & Cement and Other materials.

\*2: RC structures include RC Non-Engineered and RC Engineered.

Source: JICA Project Team

The total number of buildings is 606, 506 buildings, number of buildings for each grid are the same as in 2030 without BSPPS. The building structure component ratios for five cases in 2030 with BSPPS are shown in Figure 2.2.7.



Source: JICA Project Team

**Figure 2.2.7 Building structure component ratio in the entire Kathmandu Valley in 2030 with BSPPS (five cases)**

**(2) School buildings**

The seismic risk assessment of the school buildings is based on the estimation of the building damage ratio calculated from damage functions proposed in the project according to the Peak Ground Acceleration (gal) of scenario earthquakes. For damage assessment using damage functions, the coordinate and the structure type for each school building are required. The building inventory survey on schools and health facilities in the Kathmandu Valley was conducted by the Flagship 1 Activity of the Nepal Risk Reduction Consortium (NRRC), and all of building data including locations of schools and structure types for each school building is published on Open Street Map (OSM). In the project, the results of this Flagship 1 Activity and the damage status survey result of the public schools collected after the Gorkha Earthquake that was provided by the Department of Education (DoE) were utilized to carry out the seismic risk assessment of school buildings.

The number of targeted schools in the Kathmandu Valley were 2,115 schools including from

elementary schools to universities for both public and private schools, and the total number of school buildings is 5,731. The number of school buildings by building structure type is shown in Table 2.2.2.

**Table 2.2.2 The number of school buildings by building structure type**

Structure Type	Number of Buildings	Ratio
RC Engineered	490	8.5%
RC Non-Engineered	1,742	30.4%
Brick or Stone with cement mortar joint	2,973	51.9%
Brick or Stone with mud mortar joint	526	9.2%
Total	5,731	100%

Source: JICA Project Team

### (3) Health facility buildings

The seismic risk assessment of the health facility buildings is also based on the estimation of the building damage ratio calculated from damage functions according to the Peak Ground Acceleration (gal) of scenario earthquakes. Also, the coordinate and the structure type for each health facility building were required. In this project, the results of this Flagship 1 Activity of NRRC as well as school buildings and the damage status survey result of public health facilities collected after the Gorkha Earthquake provided by the Nepal Health Sector Support Program (NHSSP) and Ministry of Health (MoH) were utilized to carry out the seismic risk assessment of health facility buildings.

The number of targeted health facilities in the Kathmandu Valley was 363 facilities including from central hospitals to health posts for both private and community facilities, and the total number of health facility buildings is 584. The number of health facility buildings by building structure type is shown in Table 2.2.3.

**Table 2.2.3 The number of health facility buildings by building structure type**

Structure Type	Number of Buildings	Ratio
RC Engineered	53	9.1%
RC Non-Engineered	298	51.0%
Brick or Stone with cement mortar joint	181	31.0%
Brick or Stone with mud mortar joint	52	8.9%
Total	584	100%

Source: JICA Project Team

### (4) Governmental buildings

The seismic risk assessment of governmental buildings as well was based on the estimation of the building damage ratio for each governmental building as well as for schools and health facilities. In this project, the building inventory data including the coordinate and the structure type for each governmental building was prepared from the damage status survey

result of governmental buildings collected after the Gorkha Earthquake that was received from the Department of Urban Development and Building Construction (DUDBC) and drawings of governmental buildings managed by the Building Information Management System (BIMS) in DUDBC. For the building inventory data of municipal offices, the JICA Project Team conducted building surveys to gather data on the location and structure type of the buildings.

The number of targeted governmental buildings in the Kathmandu Valley was 478 buildings including ministry offices, municipal offices, public libraries and public research institutes. The number of governmental buildings by building structure type is shown in Table 2.2.4.

**Table 2.2.4 The number of governmental buildings by building structure type**

Structure Type	Number of Buildings	Ratio
RC Engineered	229	47.9%
RC Non-Engineered	12	2.5%
Brick or Stone with cement mortar joint	173	36.2%
Brick or Stone with mud mortar joint	64	13.4%
Total	478	100%

Source: JICA Project Team

#### **(5) Historical buildings**

Historical buildings are located mainly in the historical cities of Kathmandu, Lalitpur (Patan) and Bhaktapur. Durbar squares, where many cultural buildings included as World Heritage exist, are the centers of these areas, and also, traditional houses are located on the surrounding area of the squares. The Durbar Squares constitutes religious architecture and palace architecture constructed during the 16th century to the 18th century. More than half of these historical buildings were damaged, including heavy damage and collapse, by the 1934 Nepal-Bihar Earthquake, and were reconstructed later. The management of historical buildings is mainly done by DOA (Department of Archaeology). A damage map of the three Durbar Squares has been prepared by the project.

Historical buildings in the Valley are categorized as, 1) Religious buildings including Palace buildings, 2) Rana buildings, and 3) Newari houses

#### **1) Religious buildings including Palace buildings**

Brick masonry with the combination of wooden structure is the main structure of religious buildings. Mud mortar with brick powder is used for the joint mortar of brick masonry. The floor and roof are wooden. Kashthamandap temple, which collapsed due to the 2015 Gorkha Earthquake, is shown in Figure 2.2.8 (a) and similarly, as shown below, the Palace in Bhaktapur (Figure 2.2.8 (b)). Buildings in Lalitpur (Figure 2.2.8 (c)) were also damaged due to the Gorkha Earthquake. The recovery work is done by DOA with the support of UNESCO.

Historical buildings in Durbar Square are classified generally into four categories.

1. Palace and the Palace area (Durbar Square)
2. Temples in the traditional style
3. Temples in the Shikhara style
4. Other buildings of the Palace area



Source: “a) “ECS NEPAL” July-August 2015, b), (c) JICA Project Team

**Figure 2.2.8 Religious buildings including palace buildings**

## 2) Rana buildings

Rana buildings are the buildings constructed during the Rana age, a period which occurred more than 100 years ago, and the external façade of such buildings are like that of the European style palaces. The structure is brick masonry and the floor is wooden. Mortar at the joints of brick masonry is mud mortar including lime and brick powder called Surkhy. Standard size of a brick is 9”x5”x2.5”. Figure 2.2.9 shows a building served for library and governmental office under DOE, namely Keisar Mahal.



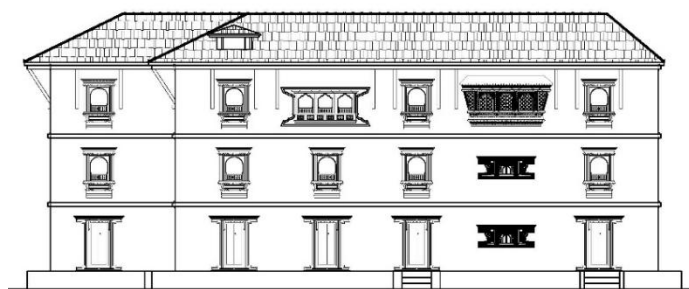
Source: JICA Project Team

**Figure 2.2.9 Rana building (Keisar Mahal)**

## 3) Newari Houses

Newari houses are traditional houses with brick walls, wooden flooring, decorated wooden windows, and wooden diagonal supports for the roof. The floor is wooden and finished with mud mortar. The standard elevation drawing is shown in Figure 2.2.10. Newari houses

located in the Jhatapol area, inside the World Heritage area in the Lalitpur District, were damaged.



Source: ESS (Earthquake Safety Solutions)

**Figure 2.2.10 Elevation of Newari house**

## 2.2.2 Transportation Infrastructure

### (1) Roads

#### 1) Existing road network

According to the Strategic Road Network Statistics 2015-2016 (SSRN 2015-2016) published by the Department of Roads (DoR), the total length of roads under the jurisdiction of DoR in three districts of Kathmandu valley is 646.71 km. The breakdown of road length by district is summarized as 326.05 km in the Kathmandu District, 188.0 km in the Lalitpur District and 132.66 km in the Bhaktapur District. Table 2.2.5 shows the breakdown of road length by road class for each district in the Kathmandu Valley.

**Table 2.2.5 Total length of roads under the jurisdiction of DoR by road class for each district in the Kathmandu Valley**

		(km)
District	Road Classes	Road Length (km)
Kathmandu	National Highway	39.85
	Feeder Road Network	207.85
	Strategic Urban Road	78.35
Lalitpur	National Highway	18.00
	Feeder Road Network	113.39
	Strategic Urban Road	56.61
Bhaktapur	National Highway	14.12
	Feeder Road Network	110.94
	Strategic Urban Road	7.60

Source: DoR

In Nepal, the local road network consists of two types of roads such as district roads and urban roads under the Strategic Road Network. The local roads are basically managed by the Department of Local Development and Agricultural Roads (DOLIDAR), but the cost for construction and maintenance of urban roads is sometimes covered by the budget of the



municipalities. According to the statistics of local roads in 2011-2012 published by DoLIDAR, the total length of local roads in the Kathmandu valley is approximately 1,811km. The breakdown of local roads by district is summarized as 828.30km in the Kathmandu District, 634.56km in the Lalitpur District and 348.23km in the Bhaktapur District.

In this project, the estimation of the road link blockage by collapsed street-side buildings and the transportation impediment due to slope failures or liquefaction are conducted as a part of seismic risk assessment of roads. For this assessment, the detailed road network including that up to urban roads along with road width data for each node is needed as input data. The spatial data of the existing road network collected from DoR and DoLIDAR contains coordinates of each node and pavement status of each road segment but the road width data is not given and the fineness of the road network data is insufficient.

On the other hand, according to the final report of “Comprehensive Study of Urban Growth Trend and Forecasting of Land Use in the Kathmandu Valley” undertaken for the UNDP/CDRMP in 2013, GIS data of detail road network which consists of approximately 5,800km of road network in the Kathmandu Valley was produced by interpretation of the high resolution satellite image. This detailed road network data covers up to the detail of urban roads with pavement types and road widths for each road segment as attribute information. This detail road network data was received from UNDP/CDRMP at the stage of detailed design of this project by JICA, and the approval of use had been given to this project, and it was decided to utilize this detail road network as input data for seismic risk assessment of roads in the project. On the grounds that the detail road network data prepared by UNDP/CDRMP was created based on the satellite image observed in 2012 and this basis image included topographic distortions, so, the road network in the data has been updated and revised based on the newer geo-corrected satellite image observed on 25th October, 2014. In addition, its consistency with the data strategic road network and local roads network collected from DoR and DoLIDAR has been confirmed.

## **2) Emergency Transportation Road Network**

It is essential consideration for proper responses and prompt recovery activities to secure transportation routes of emergency vehicle, relief goods and other necessary resources in the emergency situation. In preparation for possible emergency, it is important to select a road network responsible for emergency transportation and to take measures preferentially such as widening of roads and improvement of roadside environment beforehand.

In the Project on Rehabilitation and Recovery from Nepal Earthquake (RRNE) undertaken by JICA, Emergency Transportation Road Network (ETRN) is being proposed in cooperation with another JICA project known as the project on Urban Transport Improvement for Kathmandu Valley.

The ETRN was selected in consideration of locations of important facilities and places such as ministries office to be emergency headquarters for disaster countermeasures, hospitals that can respond to emergency medical treatment, major evacuation centers and others. The ETRN consists of the National Highway, ring roads, a part of other strategic road networks and a part of a district road network.

**(2) Bridges**

Road bridges are being managed by different organizations who administer each road network. Bridges located on the strategic road network, the district road network and other urban road networks are managed by DoR, DoLIDAR and municipalities respectively.

In this project, all of the bridges located on the strategic road network and utilizable bridges located on the local road network were selected as targeted bridges for seismic risk assessment. For the selection of targeted bridges, first an interpretation of high resolution satellite images was carried out to identify the locations of utilizable bridges in the Kathmandu Valley, and then the Project Team visited all the identified bridges one by one to check exact coordinates and structure types for each bridge. The data of Bridge Management System (BMS) managed by DoR was used as a source to identify bridges located on the strategic road network. The total number of targeted bridges is 145 bridges. The number of bridges by structure type is shown in Table 2.2.6.

**Table 2.2.6 The number of bridges by structure type**

Structure	Multi-Span	Single-Span
RC pier	45	31
RC box culvert	2	-
Masonry	24	42
Timber	1	-
Total	72	73

Source: DoR, JICA Project Team

General drawings on the shape of the superstructure and substructure for the 45 bridges of the RC pier in the multi-span bridge (72 bridges) were created by the measurement at sites of bridges in order to quantitatively analyze bearing force of earthquake resistance based on the dynamic model for the seismic motion of the bridge.

**2.2.3 Lifeline**

**(1) Water supply network**

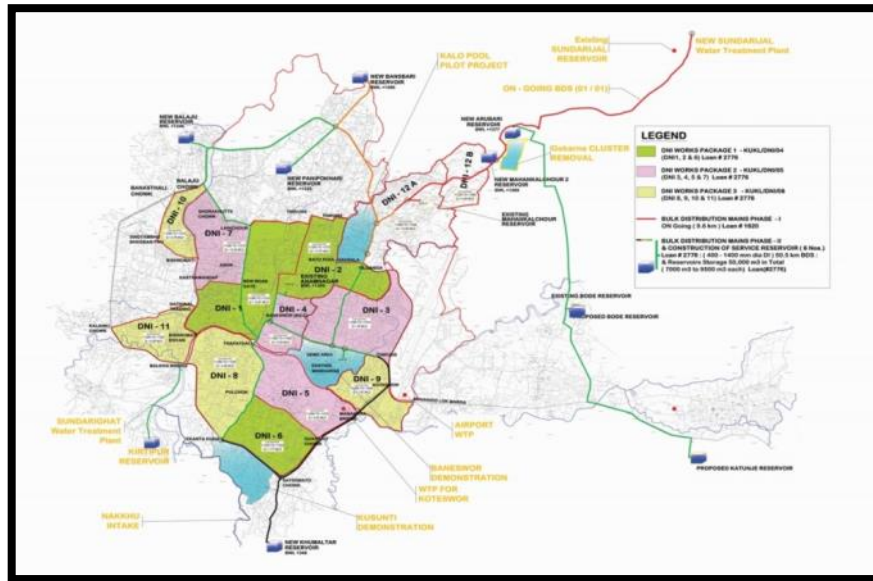
The management and operation of the water and sewerage network in the Kathmandu Valley had been managed by the Nepal Water Supply Corporation (NESC) which was commissioned by the Nepal government. After the reorganization in 2008, the Kathmandu

Valley Water Supply Management Board (KVWSMB) was established as a management and supervisory authority of water and sewerage network in Kathmandu Valley, and, Kathmandu Upatyaka Khanepani Limited (KUKL) became the responsible organization for the operation and maintenance of water supply and sewerage systems by receiving approval from KVWSMB. According to the annual report in 2015 published by KUKL, the water supply service area covers 235 wards in 21 municipalities which numbers were counted based on previous administrative boundaries which were reorganized in 2017. The amount of water supply is 119MLD (Millions of Liters per Day), while on the other hand, the amount of water demand is 375MLD which is three times the amount of water supply in 2014 to 2015.

The spatial data of the existing water supply distribution network was received from KUKL. This data contains the types of pipe materials, diameter of pipes (mm) and construction years by pipe node as attribute information. The six types of pipe materials such as cast-iron pipe (CI), ductile cast-iron pipe (DI), galvanized iron pipe (GI), high density polyethylene pipe (HDPE), polyvinyl chloride pipe (PVC), spun iron pipe (SI) have been used for the existing water supply distribution network.

In order to improve the water supply capacity, the Kathmandu Valley Water Supply Improvement Project has been carried out as a loan assistance project by the Asian Development Bank (ADB). This project consists of two major works, such as, a) Distribution Network Improvement Works and b) laying of Bulk distribution System & Service Reservoirs. According to the Project Implementation Directorate (PID) of this project under KUKL, there is a plan to start an operation of new water supply network in eleven areas, which are shown as DNI 1 to DNI 11 in Figure 2.2.11, as the first phase by 2018. As there was a request from KUKL for implementing the risk assessment for the newly constructed water supply distribution network as well as existing one, it was decided to conduct a risk assessment for both the existing network and the new one. The spatial data of a part of new water supply network was received from KUKL.

It should be pointed out that, after the new water supply network is brought into operation the existing water distribution network will be abandoned leaving only the existing distribution reservoir. In addition, two types of pipes such as ductile cast-iron pipe (DI) and high density polyethylene pipe (HDPE), as major materials, are supposed to be installed and it is expected to improve the seismic capacity of pipe lines as compared to the existing one.



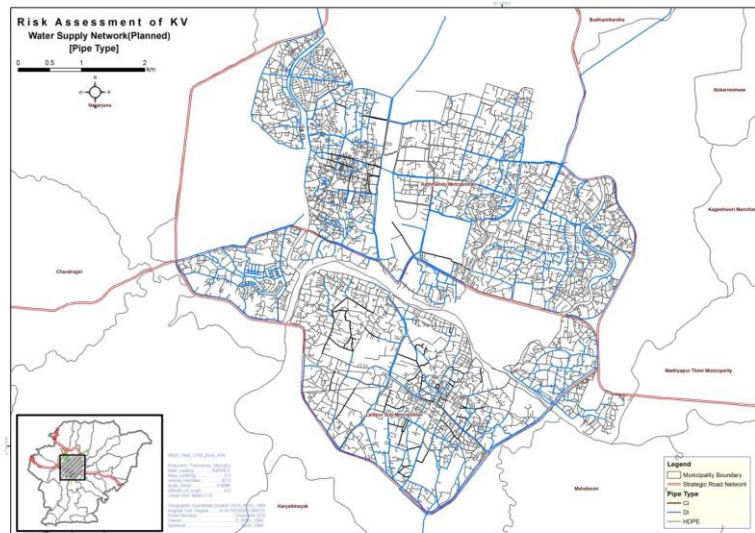
Source: KUKL

Figure 2.2.11 Implemented areas for the Distribution Network Improvement Works

## (2) Sewage network

According to the annual report in 2015 published by KUKL, the service area of the sewage network covers 110 wards, counted based on the previous administrative boundary which was reorganized in 2017 in the five municipalities of Kathmandu, Lalitpur, Bhaktapur, Madhyapur Thimi and Kritipur. The service area is concentrated in the central area of the Kathmandu Valley and is limited compared to the service area for the water supply. The operation and maintenance of the water sewage system is conducted by KUKL, and, the construction of the system is sometimes implemented by municipalities or other organizations.

The spatial data of existing sewage distribution network was received from KUKL (Figure 2.2.12). This data contains the types of pipe materials, pipes diameter (mm), depth of burial (mm) and construction years by pipe node as attribute information. The reinforced concrete is mainly used as the pipe material. In addition, the service zones by sewage network and the coordinates of manholes and drainage points to the river also covered by the spatial data collected from KUKL.



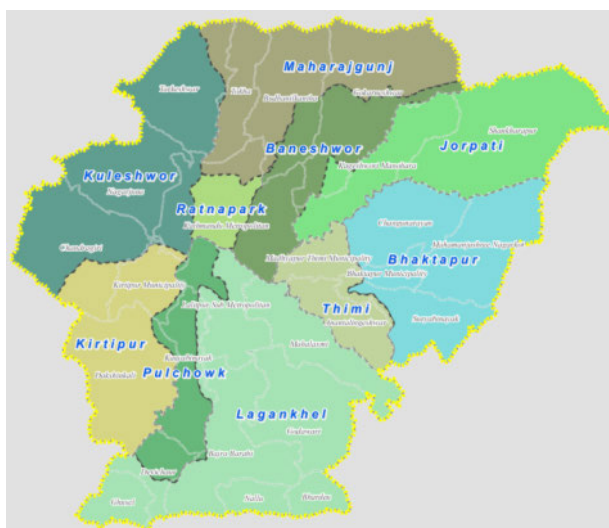
Source: KUKL

**Figure 2.2.12 The existing sewage distribution network in Kathmandu Valley**

### (3) Electricity

In Nepal, the Nepal Electricity Authority (NEA) is the responsible organization for the management and operation of power generation and electricity supply network. According to the annual report of NEA, in 2014, the amount of on-peak energy for nation-wide demand in 2014 is approximately 1,200MW. 50% of the electricity supply for this demand of energy is covered by the supply from the hydroelectric power stations with a few thermal power stations and remaining 50% by the purchased electricity from Independent Power Producers (IPPs) and India.

In the Kathmandu Valley, the power distribution service area is divided into ten divisions. The electricity generated by hydroelectric and thermal power stations is transferred to sub-stations located in ten divisions through transmission lines and facilities. Thereafter, the electricity is delivered to the power consumers in the distribution service area through the distribution network from each sub-station. The classification map of the power distribution service areas in Kathmandu Valley is shown in Figure 2.2.13, and the summary of the number of consumers and the length of distribution lines for each service area is shown in Table 2.2.7.



Source: NEA, Updated by JICA Project Team

**Figure 2.2.13 The classification map of the power distribution service areas in Kathmandu Valley**

**Table 2.2.7 The summary of the number of consumers and the length of distribution lines for each service area in the Kathmandu Valley**

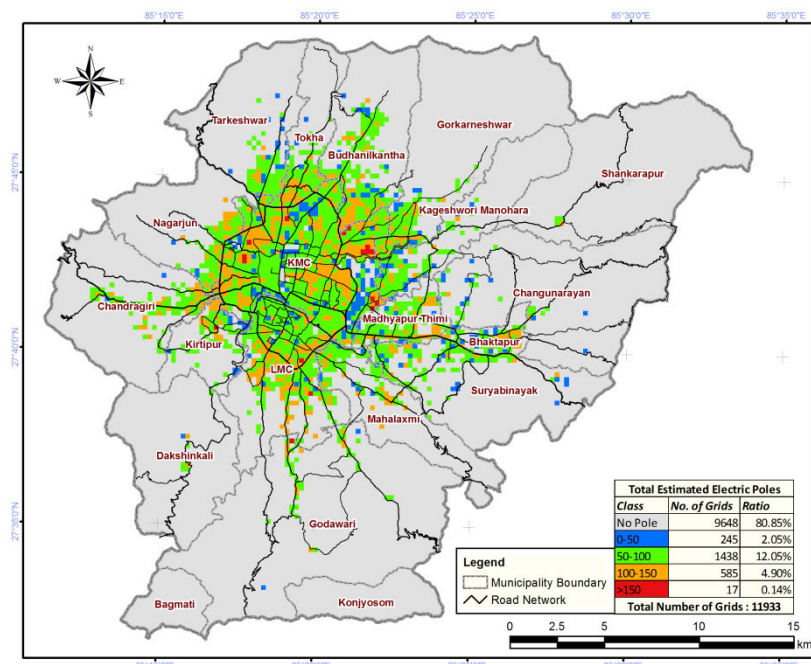
Distribution Area	Total Number of Consumers	Length of 11kv-Distribution Line [ km]	Length of 0.4/0.23 kv- Distribution Line [ km]	Number of Total Distribution Transformers
Lagankhel	54,048	281.00	679.00	548
Kuleshwor	65,779	205.00	535.00	600
Kirtipur	16,899	97.66	327.03	201
Thimi	21,712	71.00	540.00	185
Pulchowk	22,022	78.55	243.32	316
Baneshwor	58,650	217.55	480.00	404
Ratnapark	48,971	237.00	1,415.00	424
Maharajgunj	37,620	155.86	403.20	238
Bhaktapur	31,551	117.02	271.69	349
Jorpati	18,323	93.50	854.90	196

Source: Annual Summary Report of 2072/073 prepared by Kathmandu Regional Office of Nepal, NEA

In this project, the evaluation of the rate of utility pole breakage and the rate of households of power outage based on the rate of utility pole breakage using damage function, has been adopted as the method of seismic risk assessment of electricity. Although it is desirable to utilize detailed data of the power distribution network as an input data of the evaluation, after confirmation with the NEA that there is no spatial data related to such a distribution network, the project team focused on the fact that the distribution network is maintained along the road, and, decided to estimate the power distribution network and the distribution of utility poles by substituting the existing road network data.

According to Figure 2.2.14, the total length of the power distribution network in the Kathmandu Valley is 5,749 km. On the other hand, the total length of the existing road network in the urbanized area is 2,533 km. From the both lengths, the ratio of the power distribution network to the existing road network is 2.27. In addition, after actual measurement of the distance between utility poles at multiple points in the Kathmandu Valley, the average distance was calculated as 30.13m. Using these numerical values, the number of utility poles by grid size is 250 meters square was determined by using the following formula.

$$\begin{aligned} &\text{Number of utility poles in the grid} \\ &= \text{Total length of road network in the grid (km)} \times 2.27 / 30.13 \end{aligned}$$



Source: JICA Project Team

**Figure 2.2.14 Estimated distribution of utility poles in the Kathmandu Valley**

#### (4) Telecommunication network

In 1995, the Nepal Telecommunication Authority (NTA) was established by the government of Nepal for the dissemination and development of the communication services and for the creation of a competitive environment by private communication operators. NTA assumes the role to formulate the policy and standard for development and operation of a communication network by private operators and to issue several licenses to private operators as a supervisory organization. According to the latest report published by NEA in March 2016, the total numbers of mobile subscribers is 28,654,642, fixed-line subscribers and others is 848,673 and 846,967 respectively. Currently, mobile communication is the common telecommunication system in Nepal, and the total number of mobile subscribers is 94% out of the all total telecommunication facility users. And 93% share in the mobile

communication market is taken by NTC (Nepal Telecom) which takes 48% share and Ncell which takes 45% share.

Given the existing status of the telecommunication environment in Nepal, the damage assessment of the mobile telecommunication network is an important component of the earthquake risk assessment. Based on the discussion with NTA, in this project, it was decided to focus on the vulnerability assessment of the Base Transceiver Stations (BTS) which connects each mobile phone and mobile communication network. Specifically, the method of evaluation of seismic vulnerabilities, for both the antenna of BTS and the building where BTS is installed, using damage functions was adapted.

With the cooperation of the NTA, the latest data for locations of BTSs was received from NTC and Ncell. Based on this data, the Project Team visited each BTS site to check the exact location, site status and structure type of the buildings where BTS is installed. The number of BTSs by structure type is shown in Table 2.2.8.

**Table 2.2.8 The number of BTSs by structure type**

Structure Type	NTC GSM	NTC CDMA	Ncell
Roof Top (RC Engineered)	82	15	81
Roof Top (RC Non-Engineered)	381	32	386
Ground based Tower	40	14	12
Total	503	61	479

Source: Ncell, NTC / JICA Project Team

## 2.2.4 Population

### (1) Existing population and growth ratio

According to the result of the CENSUS 2011, the total population in the Kathmandu Valley is 2,517,023 people in 2011, and the breakdown by district is, 1,744,240 people in Kathmandu, 468,132 people in Lalitpur and 304,651 people in Bhaktapur. On the other hand, according to the result of the CENSUS 2001, the total number of population in the Kathmandu Valley is 1,645,091 people and the breakdown by district is as 1,081,845 people in Kathmandu, 337,785 people in Lalitpur and 225,461 people in Bhaktapur. Based on the results of both of the CENSUS, the annual population growth rate from 2001 to 2011 is 4.34%, and the growth of population in ten years is approximately 87 million people. In addition, for the growth of population in the future, CBS made a public forecast of the annual population growth rates by district every half-decade until 2031 (Table 2.2.9).



**Table 2.2.9 The forecast of the annual population growth rates every half-decade (2016-2031)**

Districts	2011-2016	2016-2021	2021-2026	2026-2031
Bhaktapur	2.22%	2.12%	1.58%	1.34%
Lalitpur	2.33%	2.21%	1.62%	1.38%
Kathmandu	2.90%	2.72%	1.85%	2.05%
Kathmandu Valley	2.73%	2.57%	1.79%	1.86%

Source: CBS/ JICA Project Team

**(2) Prediction of population in 2016 and 2030**

For the human casualty estimation based on the scenario earthquake, the prediction of the ward-wise population in 2016 and 2031 has been carried out. In this project, the prediction of the ward-wise population in 2031 has been used as the estimated population in 2030. The population in 2001 and 2011 collected by CENSUS and the forecast result of the annual population growth rates by district every half-decade shown in Table 2.2.9 were used for this prediction.

Also, the degree of population growth in the future could be different depending on the existing urbanized status and the potential of urbanization for the future. Therefore, in this project, it was decided that the difference of the urbanization process ought to be estimated using several types of land use maps from the past to the future, and the estimated urbanization pattern by ward was adopted for the prediction of the future population. Three land use maps in 1990, 2000 and 2012 and two predicted maps of built-up area distribution in 2020 and 2030 prepared by UNDP/CDRMP were used for analysis of the decennial urbanization process by ward. The flow of estimation of urbanization patterns by ward is shown in Figure 2.2.15.

Firstly, the density of built-up area for each year and the decennial increase rate of built-up area were calculated by ward using the built-up area distribution maps in 1990, 2000, 2012, 2020 and 2030. For instance, the decennial increase rate of built-up area in 2000 was calculated to compare the built-up area in 1990 and 2000. Based on the density and increase rate of built-up area, each ward was classified into three categories by following criteria:

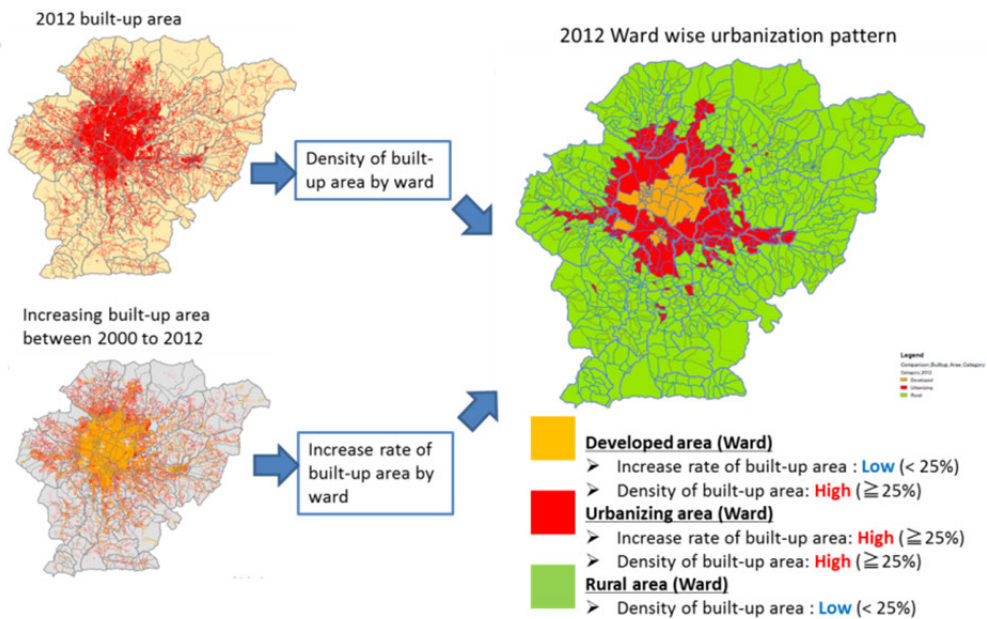
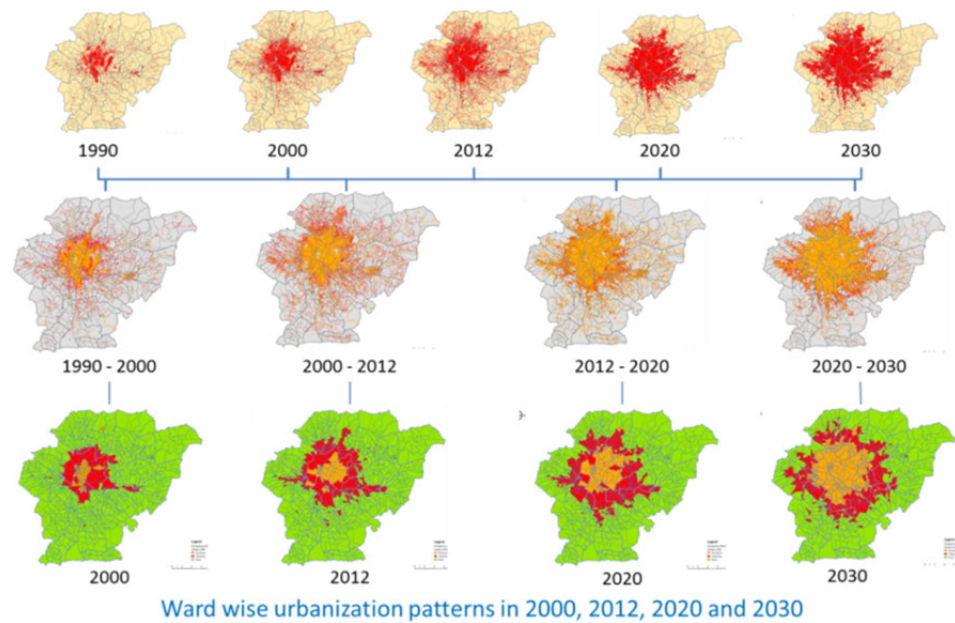
- i. **Developed Area:** the density of the built-up area is high but the decennial increase rate of built-up area is low. It means this ward was already developed ten years ago.
  - The density of built-up area  $\geq 25\%$  (High)
  - The decennial increase rate of built-up area  $< 25\%$  (Low)
- ii. **Urbanizing Area:** the density of the built-up area is high and the decennial increase rate of built-up area is high. It means the urbanization in this ward is still continuing during this decade.

- The density of built-up area  $\geq 25\%$  (High)
- The decennial increase rate of built-up area  $\geq 25\%$  (High)

iii. **Rural Area:** the density of built-up area is low. It means this ward has not changed during this decade. The decennial increase rate of built-up area is not included for the judgment, because the variation of the built-up area is very limited.

- The density of built-up area  $< 25\%$  (Low)
- The decennial increase rate of built-up area: No criteria

The wards are classified into three categories such as Developed Area, Urbanizing Area, or Rural Area at 2000, 2012, 2020 and 2030.



Source: JICA Project Team

**Figure 2.2.15** The flow of estimation of urbanization patterns by ward

Then, the change of urbanization patterns during each decade was organized. For instance, if the ward was Rural Area in 2000 and Urbanizing Area in 2012, this ward urbanized rapidly during the decade from 2000 to 2012, and, it was assumed that the population increase as well was rapid depending on the urbanization. And, if the ward was Urbanizing Area in 2000 and Developed Area in 2012, the urbanization as well as the population increase during decade from 2000 to 2012 was gentle in this ward.

The aggregate result of the change of urbanization pattern during each decade by ward is shown in Table 2.2.10. In the case of 2000-2012, the change of urbanization patterns were as follows; 5% of wards did not change from Developed Area (Developed→Developed), 1% of wards developed more (Developed→Urbanizing). 1% of wards changed from Urbanizing Area to Developed Area (Urbanizing→Developed). 7% of wards did not change from Urbanizing Area (Urbanizing→Urbanizing). 15% of wards changed from Rural Area to Urbanizing Area (Rural→Urbanizing). 71% of ward did not change from Rural Area (Rural→Rural).

**Table 2.2.10 The aggregate result of the change of urbanization pattern during each decade by ward**

Year	Total Wards	Developed		Developed		Urbanizing		Urbanizing		Rural		Rural	
		↓		↓		↓		↓		↓		↓	
		Developed		Urbanizing		Developed		Urbanizing		Urbanizing		Rural	
2000-2012	1001	48	5%	13	1%	14	1%	66	7%	148	15%	714	71%
2012-2020	1001	57	6%	6	1%	40	4%	187	19%	128	13%	585	58%
2020-2030	1001	92	9%	11	1%	155	15%	160	16%	136	14%	449	45%

Source: JICA Project Team

The aggregate result of the population growth rate from 2001 to 2011 by change of urbanization patterns 2000 to 2012 by ward is shown in Table 2.2.11. In the case of 2000-2012, the population growth rate of wards classified as no change from Developed Area (Developed→Developed) is 11.6%, but the growth rate of wards classified as changed from Urbanizing Area to Developed Area (Developed→Developed) is 40.3%, as no change from Urbanizing Area (Urbanizing→Urbanizing) is 79.2% and as changed from Rural Area to Urbanizing Area (Rural→Urbanizing) is 129.4%. It is assumed that the growth rate of population is significantly different depending on the change of urbanization patterns.

**Table 2.2.11 The aggregate result of the population growth rate from 2001 to 2011 by the change of urbanization patterns from 2000 to 2012 by ward**

Urbanization Patterns 2000 to 2012		No. of Ward	Population CENSUS2001	Population CENSUS2011	Growth Rate by Pattern	Relative Growth Ratio by Pattern
<b>Developed</b>	Developed	46	265,855	296,699	11.60%	0.22
<b>Developed</b>	Urbanizing	13	39,117	44,840	14.63%	0.28
<b>Urbanizing</b>	Developed	14	244,602	343,235	40.32%	0.77
<b>Urbanizing</b>	Urbanizing	66	464,172	831,924	79.23%	1.51
<b>Rural</b>	Urbanizing	149	166,487	381,832	129.35%	2.47
<b>Rural</b>	Rural	713	413,339	530,749	28.41%	0.54
<b>Total (All KV Ward)</b>		1,001	1,593,572*	2,429,279*	52.44%	100.0%

Note: The exact population in 2001 and 2011 based on CENSUS is including institutional population. The population in this table is smaller than the exact population based on CENSUS because this aggregate result is not including the institutional population.

Source: CBS, JICA Project Team

As shown in Table 2.2.11, the result of calculation to divide the population growth rates for each change of urbanization patterns based on the CENSUS 2001 and 2011 by the population growth rate of the whole Kathmandu Valley was defined as the relative growth ratio by the change of urbanization patterns at the ward level. By multiplying this ratio with the population growth rate by district every five-decade from 2011 to 2031 forecast by CBS, the population growth rate by the change of urbanization patterns at the ward level every five decades. Furthermore, using this rate, the ward-wise populations in 2016, 2021, 2026 and 2031 were projected based on the population of CENSUS 2011. Table 2.2.12 shows the projected populations of the whole Kathmandu valley in 2016 and 2031.

**Table 2.2.12 The result of projected populations of the whole Kathmandu Valley in 2016 and 2031**

Districts	2016	2031
Bhaktapur	340,066	436,553
Lalitpur	497,240	647,773
Kathmandu	2,011,978	2,792,056
Entire Kathmandu Valley	2,849,284	3,876,382

Source: JICA Project Team

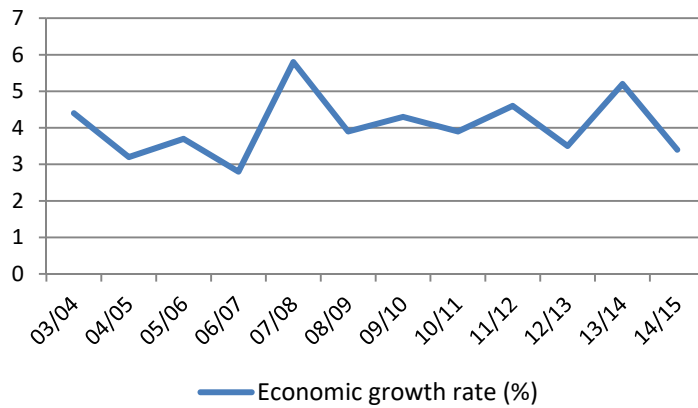
## 2.2.5 Economy

In order to estimate the impact for economy of Nepal and Kathmandu Valley due to the scenario ground motion, the following items were analyzed regarding the scale of economy and structure of current Nepal and Kathmandu Valley.

(1) Scale of Economy

1) Transition of GDP

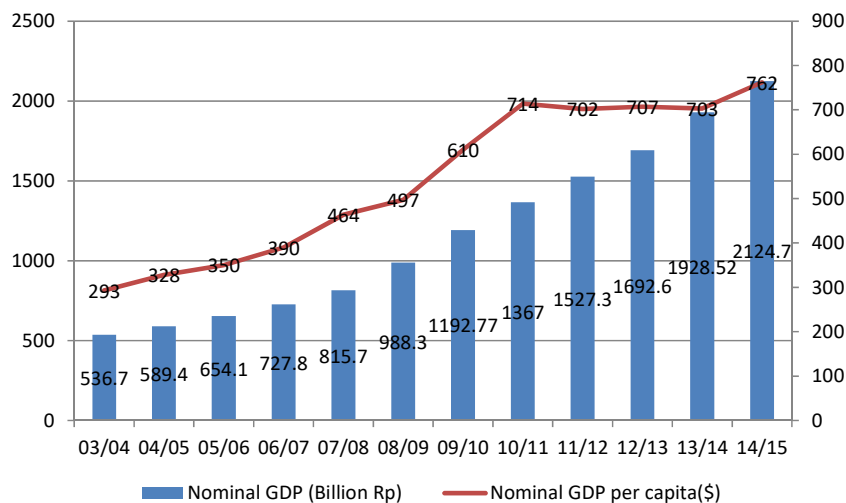
GDP has grown steadily every year, so, the growth rate of the service sector has increased due to the increase of expenditure for the service sector by overseas remittance. In addition to the growth of the agriculture sector, the economic growth rate of 2013/14 year (July 16, 2013-July 16, 2014) reached to 5.2%, increasing by 1.6 points as compared with the previous year. However, the economic growth rate of 2014/15 dramatically decreased to 3.04% in consequence of the earthquakes that occurred in April 25<sup>th</sup> and May 12<sup>th</sup> in 2015.



Source: Central Bureau of Statistics

**Figure 2.2.16 Trend of economic growth rate**

On the other hand, the middle-income group increased in urban areas due to the continuous inflow of overseas remittance. Nominal GDP per capita in 2014/15 year of earthquake occurred increased to 762 dollars from 703 dollars from the previous year in consequence of the rise of consumption of the middle-income group.



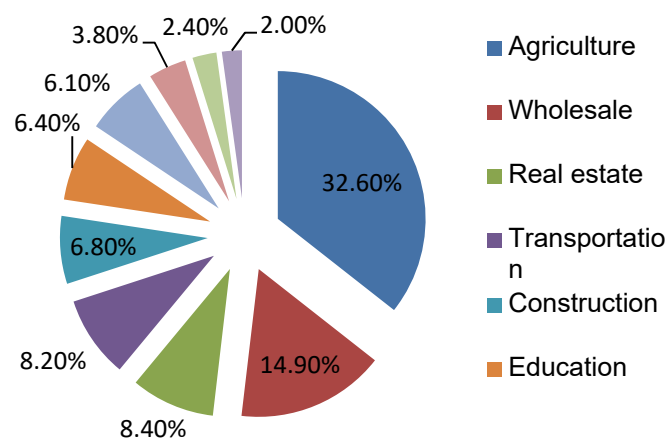
Source: Central Bureau of Statistics

**Figure 2.2.17 Transition of nominal GDP**

The ratio of economic activity in Kathmandu Valley for the GDP is estimated at 23%. The agriculture sector occupies approximately 30% of the GDP of Nepal, but the occupation ratio of agriculture in Kathmandu Valley is only 5% and the service sector in Kathmandu Valley occupies the most part of the GDP.

## 2) Transition of growth rate of each sector

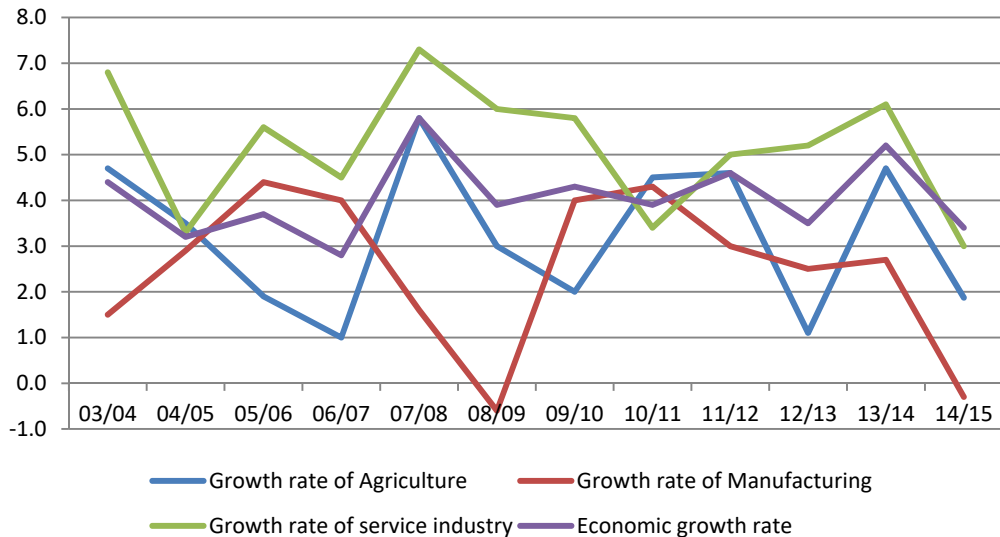
The ratio of GDP of each industrial sector is as follows: Agriculture-32.6%, Wholesale-14.9%, Real estate-8.4% Transportation-8.2%, Construction-6.8%, Education-6.4% Manufacturing-6.1%, Finance business-3.8%, Social service-2.4%, Hotel and Restaurant-2.0%.



Source: Central Bureau of Statistics

**Figure 2.2.18 GDP ratio of each industry sector**

Primary industry occupies 32.6% of the GDP. This ratio is much higher as compared to other South Asian countries. The GDP ratio of the manufacturing sector is 6.1%, which can be read as the cause for the slow progress of industrialization in Nepal. Tertiary industries, sightseeing, information and telecommunication, etc. occupies the most part of the GDP. The service industry exerts traction on Nepal economy judging from the growth rate of service industry (Figure 2.2.19).

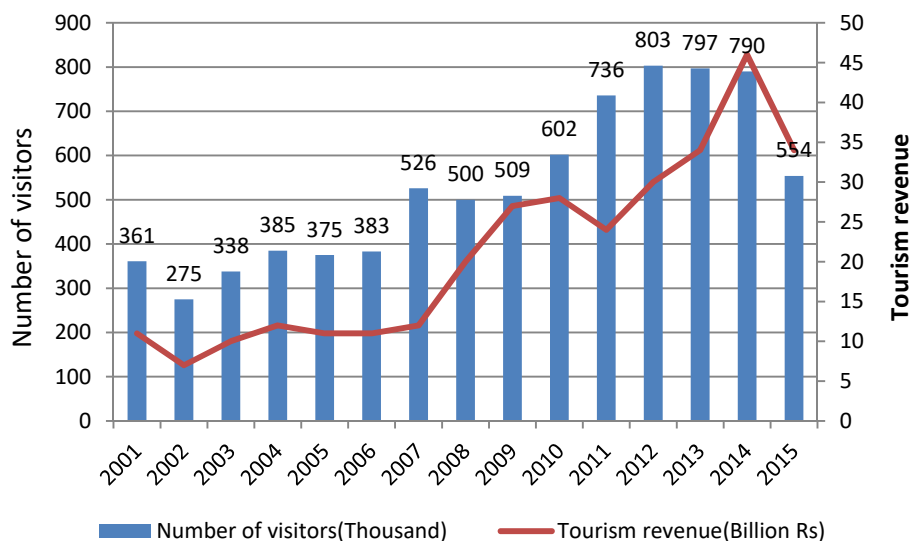


Source: Central Bureau of Statistics

**Figure 2.2.19 Transition of growth rate of each sector**

### 3) Tourism sector

The number of visitors for Nepal is maintained at 500,000 people, as the number of visitors since 2007 is over 500,000. Thanks to the implementation of tourism promotion in 2011, the number of visitors reached 700,000 in 2011 and increased to 800,000 in 2012. Though the number of visitors decreased a little in 2013, many of them continued to visit Nepal. However, the number of visitors decreased from 790,000 in 2014 to 550,000 in 2015 in consequence of the earthquake that occurred in the April of 2015.



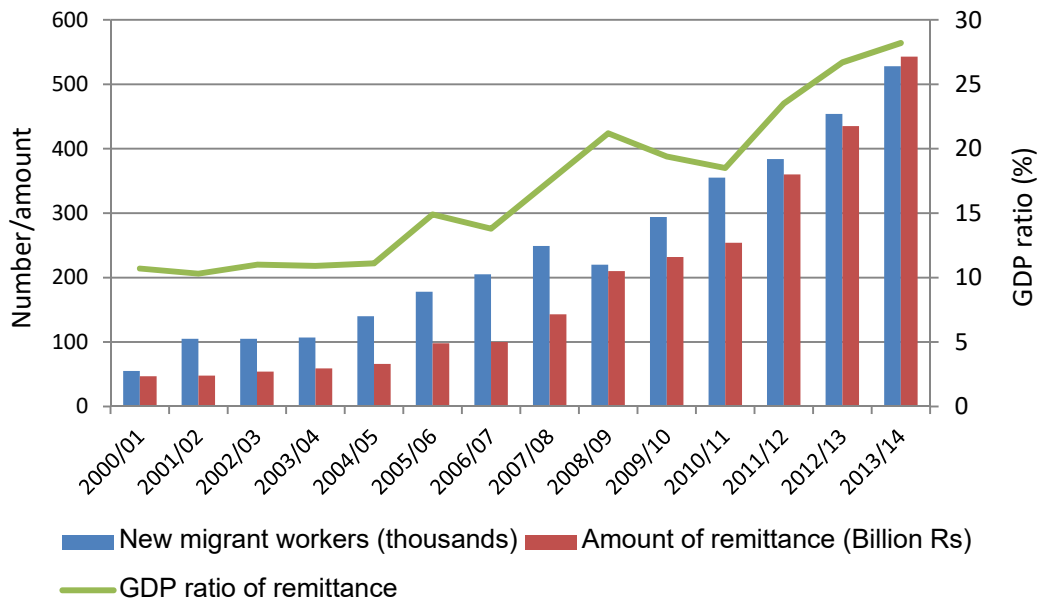
Source: NTB

**Figure 2.2.20 Transition of arrivals and tourism revenue**

### 4) Situation of International migrant work and overseas remittance

The number of international migrant workers from Nepal increased since the 1990s and

reached over 410,000 in the year 2012/13 (middle of July, 2012- middle of July, 2013) (Figure 2.2.21).



Source: Current Macroeconomic Situation in Nepal, NPB

**Figure 2.2.21 Transition of the number of migrant workers and amount of remittance**

Overseas remittance from migrant workers has been steadily growing, and the amount has reached to 434.6 billion NRP (25.5% of GDP). Also, the ratio of households receiving an overseas remittance and the average receiving amount per person has increased. In consequence of the increase in overseas remittance, the GDP ratio of money supply (M2) in Nepal is relatively high among South Asian countries in addition to the improvement of income level of low order by 20%, and, the situation of Nepal holding a lot of cash is caused by overseas remittance.

**(2) Comparison with South Asian countries**

**1) Each sector ratio in GDP**

According to the statistics of ADB, the rate of agriculture in the GDP of Nepal is 33.9% (Bangladesh-16.3%, India-18.4%, Pakistan-25.1%, Sri Lank-10.8%). On the other hand, the ratio of manufacturing in the GDP is 15.2% (Bangladesh-27.6%, India-24.6%, Pakistan-21.1%, Sri Lanka-32.5%) and this low ratio shows the backwardness of industrialization compared with other South Asian countries.



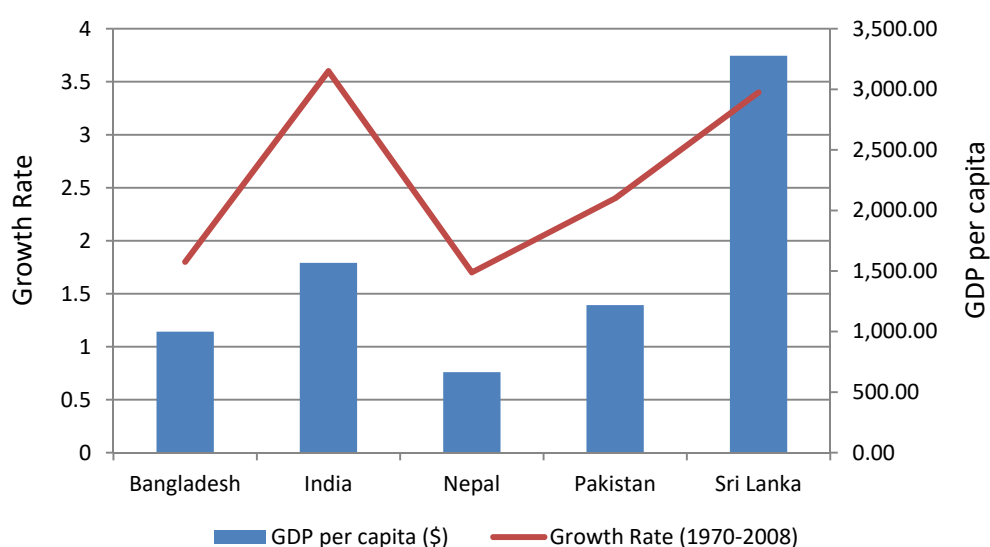
**Table 2.2.13 Comparison of main indicator of south Asian countries**

	Bangladesh	India	Nepal	Pakistan	Sri Lanka
GDP (Billion \$)	153.5	1798.6	18.1	212.6	67.2
GDP growth rate (%)	6	4.9	3.9	3.7	7.3
Ratio of Agriculture (%)	16.3	18.4	33.9	25.1	10.8
Ratio of Manufacturing (%)	27.6	24.7	15.2	21.1	32.5
Ratio of service industry (%)	56.1	57.0	51.0	53.8	56.8

Source: ADB Key indicator 2014

## 2) GDP per capita

As shown in Figure 2.2.22. GDP per capita of Nepal is low compared to other South Asian countries; in addition, the growth ratio is also low.

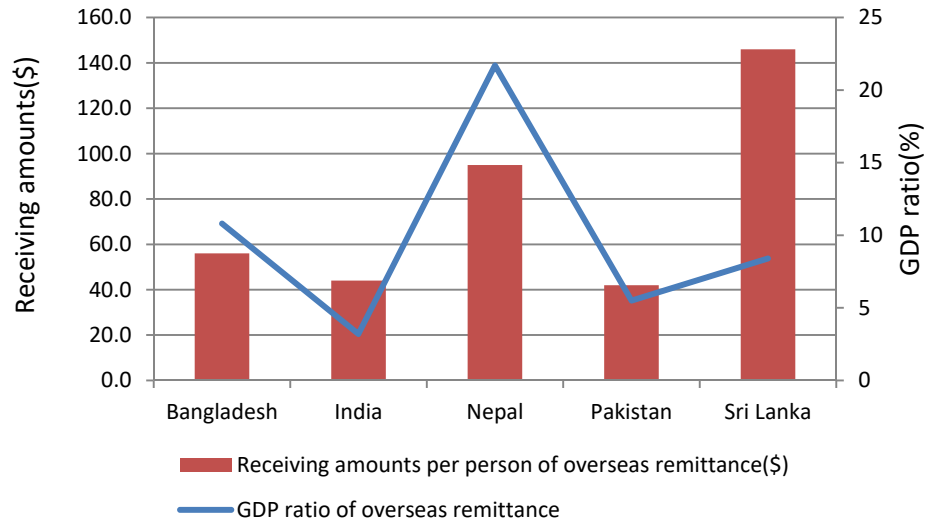


Source: ADB Key Indicator 2014

**Figure 2.2.22 Comparison of GDP per capita**

## 3) Ratio of overseas remittance in GDP

The ratio of overseas remittance for GDP in Nepal, 21.7%, is outstanding among South Asian countries (Figure 2.2.23). This situation shows that the economic structure of Nepal is dependent on the overseas remittance from migrant workers. As a consequence, the GDP ratio of money supply is 77.7% and which is relatively high, and it also shows that the economy of Nepal is rich in cash as compared to the scale of GDP.



Source: ADB key Indicators 2014

**Figure 2.2.23 Receiving amounts per person of overseas remittance and GDP ratio of overseas remittance**

## Chapter 3 Seismic Hazard Assessment

---

In this chapter, seismic hazard assessment conducted prior to the seismic risk assessment and preparation for Disaster Risk Reduction and Management Plan is described. The main content of the seismic hazard assessment in this project is the estimation of the seismic ground motion as the target at the time of planning. The contents of study are arranged (3.1) and assessed along the propagation process of seismic ground motion as follows:

- (1) Set-up of Scenario Earthquake (3.2),
- (2) Modeling of the Ground (3.3-3.5),
- (3) Calculation of Earthquake Motion at Bedrock (3.6),
- (4) Calculation of Earthquake Motion at Ground Surface by Response Analysis (3.7),
- (5) Assessment of Liquefaction and Earthquake Induced Slope Failure (3.8-3.9).

The fundamental flow of the estimation of the seismic motion at the ground surface in this project is the same as the 2002 JICA Study. However, utilization of observed records due to the Gorkha earthquake, newly developed data in the process of ground modeling, and evaluation of S-wave velocity by microtremor survey are greatly different. The items improved in this project are as follows:

- Number of scenario earthquakes is the same, three scenarios, but the verification earthquakes are two scenarios including the 2015 Gorkha Earthquake.
- Attenuation equations are used as the average of the most recent four equations of NGA (New Generation Attenuation).
- Actual observed records due to the Gorkha Earthquake are utilized to study the ground model as well as for input motion for response analysis.
- Approximately 50% more drilling data were collected comparing to 2002 JICA Study.
- Rock depth distribution has been estimated based on the gravity survey results and drilling data.
- Detailed Geomorphological map has been newly developed based on aerial photographs (1: 15,000) and site observation.
- Geological cross-section has been newly prepared (EW- 11, NS- 14 of a total 25 sections) with maximum depth of about 500m.
- Tripartite array microtremor measurement (5 points) was performed to set the S-wave velocity of the deep geological strata.
- L-shaped array microtremor measurement (74 points), 3-point array microtremor measurement (39 points) were carried out for setting the S-wave velocity structure of the

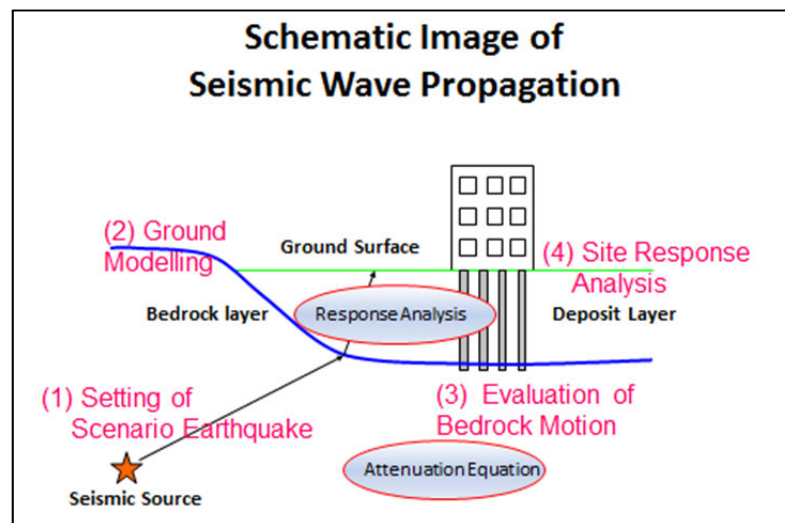
subsurface soil layers in conjunction with geomorphology map, drilling data and geological cross-sections.

- Based on the above, for each  $250\text{m} \times 250\text{m}$  grid (total 11,934), setting of the ground model of up to a maximum depth of about 500m has been done.
- From the results of the single point microtremor measurement (carried out at the 308 points and the existing 210 points), the predominant periods of ground model were confirmed.

During the implementation of seismic hazard assessment, shortages of human resources in the relating fields and necessary data appeared. The interpretation and reproduction of rather peculiar Gorkha Earthquake as well as how to apply the experiences to the scenario earthquakes were added as the big challenges. The recommendations for future improvements regarding to the seismic hazard assessment are summarized at the end (3.10).

### 3.1 Items of Contents

Seismic hazard assessment was implemented basically along the propagation of seismic ground motion, (1) setting scenario earthquake, (2) modeling the ground, (3) estimation of ground motion at bedrock, and (4) evaluation of the response of the subsurface ground and estimation of seismic ground motion at ground surface.



Source: JICA Project Team

**Figure 3.1.1 Flow of seismic hazard assessment**

Seismic ground motion radiated from seismic source propagates through the deep rock layers, and reaches the basement of the target, such as the base of the Kathmandu Valley. Then, it propagates to the subsurface and reaches the ground surface. In this project, first the verification and scenario earthquakes were set and then ground motion at rock surface was estimated using attenuation equation. On the other hand, subsurface soil layers were modeled as ground models from rock surface to ground surface. In parallel with setting the scenario

earthquakes and attenuation equations, based on the collection and compilation of ground information including a variety of ground surveys, ground modeling and response analysis were carried out.

Target earthquakes of this assessment are three scenario earthquakes and two verification earthquakes, described in detail in Clause 3.2. Also, soil model was provided for each grid of 250 meters  $\times$  250 meters unit. Total area of the Kathmandu Valley is about 700 square kilometers, and the total number of grids is 11,934. Maximum depth of ground models is approximately 500m for rock surface as given by drilling data. It should be noted that, in the 2002 JICA Study, the maximum depth of ground model was about 100m in 500m  $\times$  500m grid with total 2,826 grids. The comparison of the data and assessment methods between the 2002 JICA Study and this project is shown in Table 3.1.1 .

Though the basic flow for estimation of seismic motion at ground surface is similar to the 2002 JICA Study, for this project, the study, used data, survey amount and modeling conditions are different. The items that are improved in this project are as follows:

- Number of scenario earthquakes is the same, three, but the verification earthquakes are two including the 2015 Gorkha Earthquake.
- Attenuation equations are used as the average of the most recent four equations of NGA (New Generation Attenuation).
- Actual observed records due to the 2015 Gorkha Earthquake are utilized to study the ground model as well as for input motion for response analysis.
- Approximately 50% more drilling data were collected than in the case of the 2002 JICA Study.
- Rock depth distribution has been estimated based on the gravity survey results and drilling data.
- Detailed Geomorphological map has been newly developed based on aerial photographs (1: 15,000) and site observation.
- Geological cross-section has been newly prepared (EW- 11, NS- 14 of a total 25 sections) with maximum depth of about 500m.
- Tripartite array microtremor measurement (5 points) was performed to set the S-wave velocity of the deep geological strata.
- L-shaped array microtremor measurement (74 points), 3-point array microtremor measurement (39 points) were carried out for setting the S-wave velocity structure of the subsurface soil layers in conjunction with geomorphology map, drilling data and geological cross-sections.
- Based on the above, for each 250m  $\times$  250m grid (total 11,934), setting of the ground model of up to a maximum depth of about 500m has been done.

- From the results of the single point microtremor measurement (carried out at the 308 points and the existing 210 points), the predominant periods of ground models were confirmed.

**Table 3.1.1 Comparison of data and methods between this project and the 2002 JICA Study**

Items	2002 Survey	2015-2016 Survey
Drilling data	300 (rock 36)existing boreholes (5 conducted)	449 (rock 56) existing boreholes
N-value data	61 existing boreholes	124 existing boreholes
PS-logging data	5 conducted	5 existing
Gravity Exploration data	not used	Used for rock depth
Geomorphology map	not available	Newly produced (based on 1:15,000 aerial photos)
Environmental Geology map	used	used
Single point Microtremor	0	308 conducted, 210 existing
L-shape Array Microtremor	0	74 conducted
3-points Array Microtremor	0	39 conducted
Triangle Array Microtremor	0	5 conducted
Geotechnical test	some collected/conducted	some collected
Geological Cross Sections	not available	Newly produced (based on existing information)
Soil Layer and Vs	a Vs-N relation	Vs structure (based on Array Microtremor results)

Items	2002 Survey	2015-2016 Survey
Geomorphology / Geology and Vs	empirical setting	Newly proposed based on Microtremor results
Scenario earthquakes	3 Scenario earthquakes (Mid Nepal, North Bagmati, KV local)	3 Scenario earthquakes (Far-Mid Western Nepal, Western Nepal, Central Nepal South)
Verification earthquakes	1 verification earthquake (1934 Bihar-Nepal EQ)	2 verification earthquakes (1934 Bihar-Nepal EQ, 2015 Gorkha EQ)
Earthquake Records	not available	Newly Recorded by DMG, Hokkaido Univ., USGS
Attenuation equation	1 equation (Boore, 1997)	4 equations (NGA, 2008)
Grid	500mx500m (2826 grids)	250mx250m (11,934 grids)
Base layer and Depth	Kalimati formation (100m depth max)	Rock (maximum depth 500m level)
Response Analysis	1 dimensional	1 dimensional
Input Motion	existing foreign sample	Newly Recorded (at Kirtipur) by DMG, Hokkaido Univ.
Seismic Intensity	PGA, PGV, MMI, Sa(T)	PGA, PGV, MMI, Sa(T), SI
Collateral Hazards	Liquefaction, Slope failure	Liquefaction, Slope failure

Source: JICA Project Team

Among the contents of seismic hazard assessment, the way of calculation and related data for main portions such as Bedrock Motion, Fault Distance and Ground Modelling are summarized as Technical Notes for Earthquake ground Motion Estimation and put in the Volume 5 Attachment-12. The related data and information were already handled to DMG during the project.

### **References (3.1)**

- JICA, The Study on Earthquake Disaster Mitigation in the Kathmandu Valley, Kingdom of Nepal, 2002.

## **3.2 Set-up of Scenario Earthquake**

Set-up of scenario earthquake started on June 2015. The past historical earthquakes, recent earthquake activity, tectonics and active faults were studied and discussed with DMG. The first version of three scenario earthquakes was set in the end of October 2015 after consulting with the researchers of SATREPS (Science and Technology Research Partnership for Sustainable Development) project. In the second JCC which was held in December 2015, DMG requested to have the consensus of the related scientists and experts in Nepal for the scenario earthquakes. DMG posted the comments that the fault size of “Central Nepal South Scenario”, which was set in the south of the Gorkha Earthquake fault zone, should be reduced and the magnitude should be modified to 7.0 from 7.8 accordingly. The Central Nepal South Scenario was modified after this comment. Additionally, DMG posted the comment in the middle of March 2016, after discussion with the related international experts, that the shape of scenario earthquake faults should be modified to cover the gaps between the fault plane, namely change the shape from rectangular to indeterminate form, and return the magnitude of Central Nepal South Scenario to 7.8. Again, the scenario was modified after their comment and finalized. The final scenario earthquakes were formally approved through 2nd JWG (April 11, 2016) and 3rd JCC (May 10, 2016). The approved scenario earthquakes are three scenario earthquakes such as; “Far-Mid Western Scenario Earthquake”, “Western Nepal Scenario Earthquake” and “Central Nepal South Scenario Earthquake” and two earthquakes for verification; 1934 Bihar-Nepal Earthquake and 2015 Gorkha Earthquake including largest aftershock as shown in Figure 3.2.1.

The basis of scenario earthquakes and the relation with historical earthquakes are shown below.

### **3.2.1 Far-Mid Western Nepal Scenario Earthquake**

Large earthquake motion was felt from Far West Nepal to Midwest Nepal in 1505. Nepal, Tibet and India were severely damaged. The reoccurrence of this earthquake was adopted as the scenario to consider the effects to Kathmandu, even though no destruction was reported in Kathmandu at that time. The source area was made following the outcome of SATREPS and the south border of the source fault was clipped at MFT (Main Frontal Thrust) based on the discussion with DMG.

### **3.2.2 Western Nepal Scenario Earthquake**

After the 1344 or 1408 earthquake, no large earthquake has occurred in West Nepal for over 600 years. A large earthquake occurred in 1255 in Central to East Nepal and Kathmandu suffered heavy damage. 679 years after that earthquake, in 1934, again another large earthquake occurred in East Nepal and Kathmandu was severely damaged. If the reoccurrence process in West Nepal is common to that of East Nepal, the next large earthquake in West Nepal is around the corner. The presumed next large earthquake in West Nepal is adopted as the scenario. The source area was made following the outcome of SATREPS and the south border of the source fault was clipped at MFT based on the discussion with DMG.

### **3.2.3 Central Nepal South Scenario Earthquake**

In Central Nepal, a magnitude 7 class earthquake occurred in 1833 and caused damage to Kathmandu and its surroundings. The epicenter of this earthquake is estimated to be north of Kathmandu Valley. In 1866, an earthquake occurred in Kathmandu again, after an interval of 33 years. The magnitude of this earthquake may be almost same to 1833 event and the supposed epicenter is south of Kathmandu Valley.

The epicenter of the 2015 event is located in the Gorkha District, but the earthquake fault extends eastward to north of Kathmandu Valley. The northern part of Central Nepal was activated but no movement was found along MFT in south Central Nepal area. The northern part of MHT (Main Himalayan Thrust) section in Central Nepal may have moved but the southern part was calm during the Gorkha Earthquake (Elliot et al. (2016)). On the analogy of 1833 and 1866 events, an earthquake of almost same magnitude to the Gorkha Earthquake may occur in the near future and the epicenter may be south of Kathmandu Valley. The supposed next large earthquake of the southern area of Central Nepal is adopted as the scenario. The earthquake fault of the Gorkha Earthquake was set based on the distribution of aftershocks by Adhikari et al. (2016). The southern adjacent area was bounded by the Gorkha Earthquake fault area and MFT was modeled.

DMG (Department of Mines and Geology) pointed out that the magnitude of the Central Nepal South Scenario Earthquake is overestimated considering the magnitude of the 1866 event, which is supposed to be 6.5 to 7.4 (Szeliga et al. (2010), Bollinger (2016)) as well as seismo-tectonics features at plate boundary cross section by Sapkota et al. (2012). In this study, the magnitude is set at 7.8, which is the same as the Gorkha Earthquake, based on the fault size and from the view point of disaster management.

The Scenario Earthquake Models in 2002 JICA project are shown in to compare with current models, clearly different from the 2015 Gorkha Earthquake;

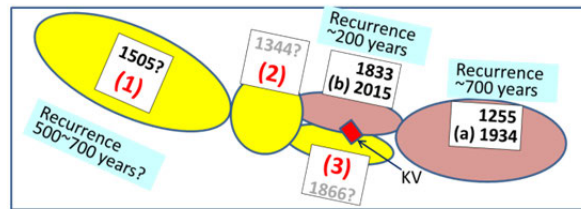
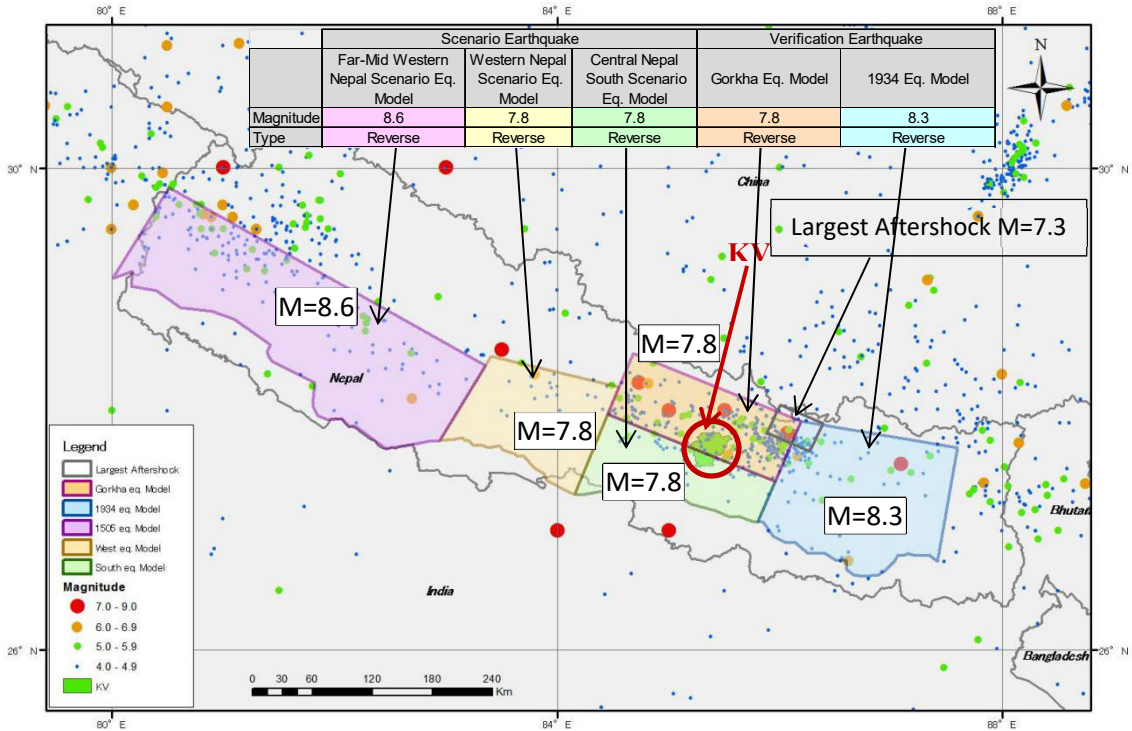


- (1) Mid Nepal Earthquake Model:  $M=8.0$ , west of KV, near to the “Western Nepal Scenario Earthquake Model”
- (2) North Bagmati Earthquake Model:  $M=6.0$ , north of KV,
- (3) Kathmandu Valley Local Earthquake:  $M=5.7$ , modeled from active fault in KV,
- (4) 1934 Bihar-Nepal Earthquake Model:  $M=8.4$ , reoccurrence of 1934 event.

The color and contour line of shows the analyzed slip distribution of the Gorkha Earthquake by Kubo et al. (2016). The larger amplitude slip distributes east of the fault plane. The damage amount and damage ratio caused by the Gorkha Earthquake is reported high in eastern districts of Kathmandu, though the earthquake motion around the epicenter was also estimated to be large. The asperity is also shown in by a red broken line, the size of asperity is almost same to the fault size of largest aftershock ( $M_w=7.3$ ) of the Gorkha Earthquake. The location of “North Bagmati Earthquake Model ( $M=6.0$ )” in the 2002 JICA project almost agrees with the largest slip (red contour) in and the estimated damage amount and distribution is comparable with the Gorkha Earthquake damage; the estimated number of deaths by North Bagmati Earthquake of the 2002 JICA project is around 2,000 in KV for example.

The fault model of scenario earthquakes in the 2002 JICA project are obviously different from the Gorkha Earthquake fault, however the similarity of the 2002 JICA Project results with the Gorkha Earthquake has some interest.

There are issues in academic attention for the 2015 Gorkha Earthquake that the strength of the input ground motion was extremely small as compared with the attenuation equations even though the magnitude 7.8 and short distance from the source fault, and that seismic ground motion rich in long-period component was quite dominant in the central part of the valley.



**Three Scenario Earthquakes**

- (1) Far- Mid Western Nepal Eq., Magnitude = 8.6
- (2) Western Nepal Eq., Magnitude = 7.8
- (3) Central Nepal South Eq., Magnitude = 7.8

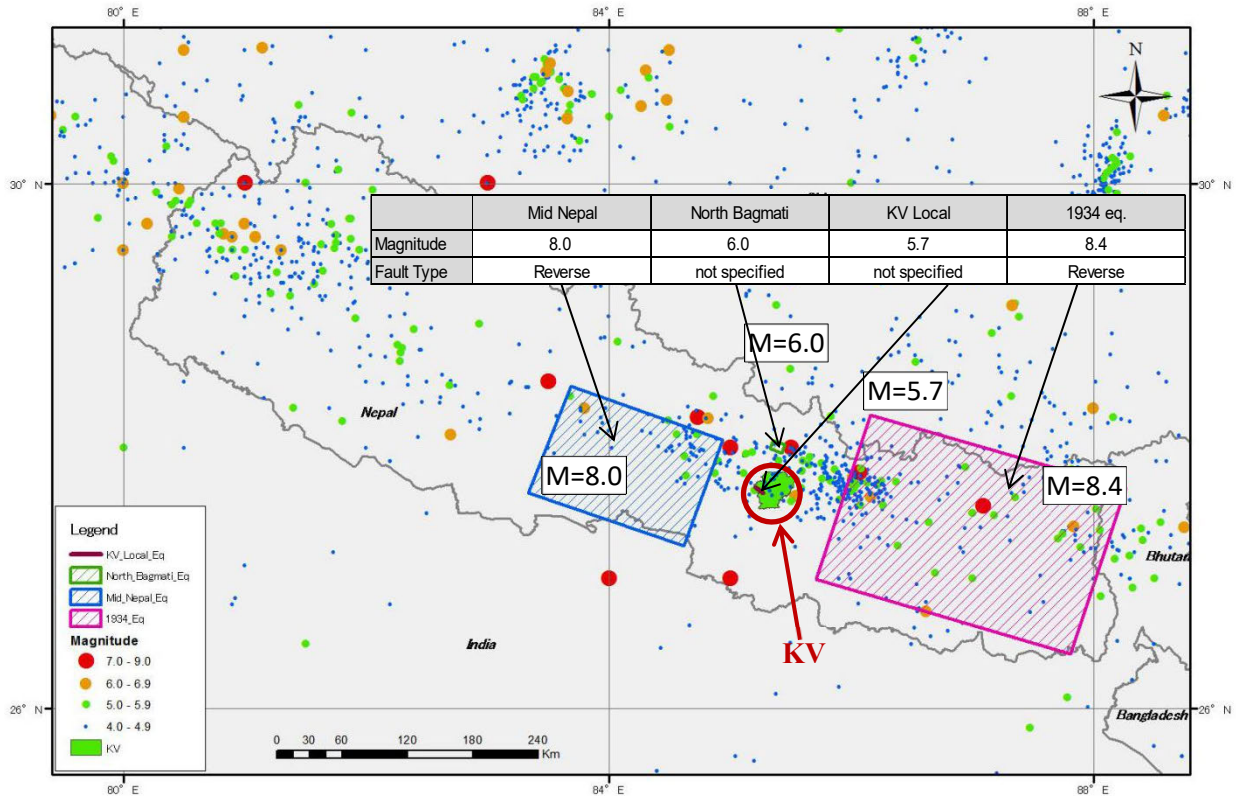
**Two Verification Earthquakes**

- (a) Recurrence of the 1934 Bihar-Nepal earthquake, Magnitude = 8.3
- (b) Recurrence of the 2015 Gorkha earthquake, Magnitude = 7.8, 7.3

Determined after taking into account of comments from Scientific Community

Source: JICA Project Team compiled from JICA (2002)

**Figure 3.2.1 Scenario Earthquake Fault Model**



Source: JICA Project Team compiled from JICA (2002)

**Figure 3.2.2 Scenario Earthquake Fault Model in 2002 JICA Project**

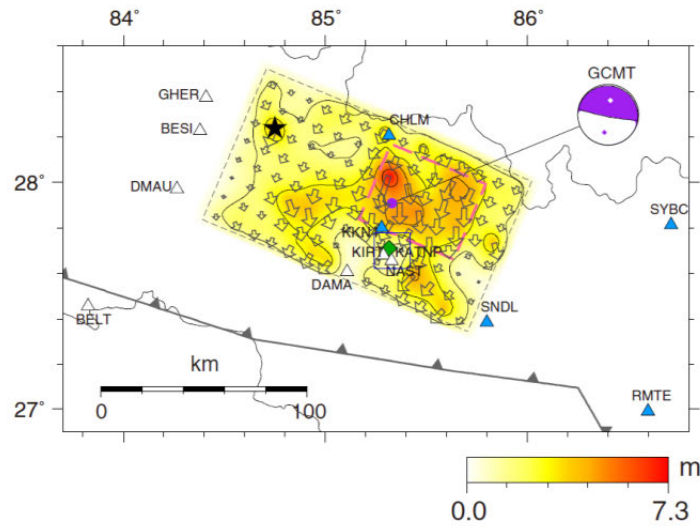


**Fig. 2** Map projection of the final-slip distribution. Contour interval is 1.46 m. Arrows indicate the slip amplitude and direction of the hanging wall relative to the foot wall. Black star indicates the rupture starting point. Broken rectangle represents the assumed fault model. Broken pink rectangle represents the estimated asperity. Focal mechanism represents the GCMT solution of the 2015 Gorkha earthquake

Source: Kubo et al. (2016)

**Figure 3.2.3 Slip Distribution in Fault Area**

### References (3.2)

- Adhikari, L.B., U.P. Gautam, B.P. Koirala, M. Bhattarai, T. Kandel, R.M. Gupta, C. Timsina, N. Maharjan, K. Maharjan, T. Dahal, R. Hoste-Colomer, Y. Cano, M. Dandine, A. Guilhem, S. Merrer, P. Roudil and L. Bollinger (2015) The aftershock sequence of the 2015 April 25 Gorkha–Nepal, *Geophys. J. Int.*, 203, pp. 2119–2124.
- Bollinger, L., P. Tapponnier, S. N. Sapkota, and Y. Klinger (2016) Slip deficit in central Nepal: omen for a repeat of the 1344 AD earthquake ?, *Earth Planets Space*, 68, 12.
- Elliot, J.R., R. Jolivet, P.J. Gonzalez, J.-P. Avouac, J. Hollingsworth, M.P. Searle and V.L. Stevens (2016) Himalayan megathrust geometry and relation to topography revealed by the Gorkha earthquake, *Nature Geoscience*, DOI: 10.1038/NGE 02623.
- JICA (2002) The Study on Earthquake Disaster Mitigation in the Kathmandu Valley Kingdom of Nepal, Final Report, Volume III.
- Kubo, H., Y. P. Dhakal, W. Suzuki, T. Kunugi, S. Aoi and H. Fujiwara (2016) Estimation of the source process of the 2015 Gorkha, Nepal, earthquake and simulation of long-period ground motions in the Kathmandu basin using a one-dimensional basin structure model, *Earth, Planets and Space*, 68:16.
- S. N. Sapkota, S.N., L. Bollinger, Y. Klinger, P. Tapponnier, Y. Gaudemer and D. Tiwari (2012) Primary surface ruptures of the great Himalayan earthquakes in 1934 and 1255, *Nature GeoScience*, DOI: 10.1038/NGEO1669.
- Szeliga, W., S. Hough, S. Martin, and R. Bilham (2010) Intensity, Magnitude, Location and Attenuation in India for Felt Earthquakes since 1762, *Bull. Seism. Soc. Am.*, Vol. 100, No. 2, pp. 570 -584.

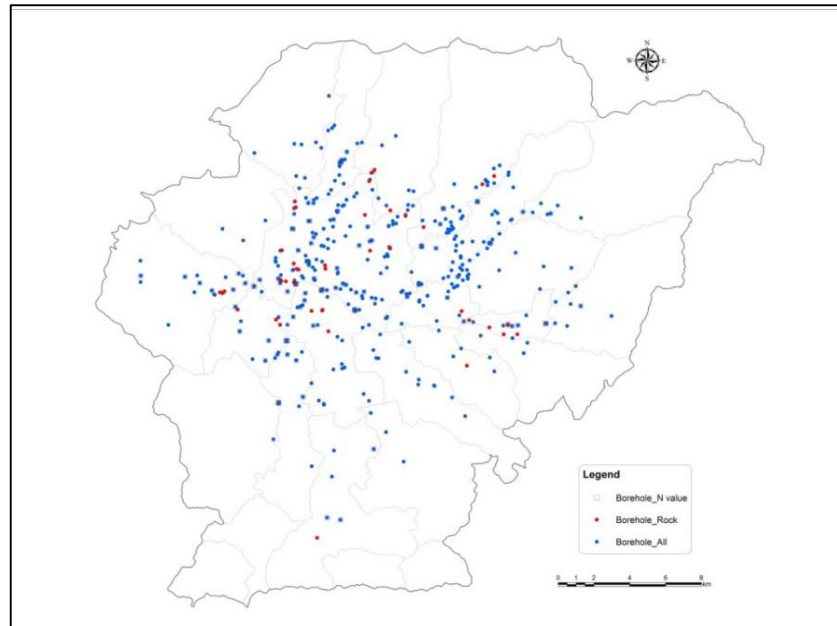
### 3.3 Collection of Ground Data

As ground information, mainly drilling data, geological maps, geological cross-section, altitude data and gravity exploration results were collected. Geomorphological map preparation based on both aerial photo interpretation and field observation, field surveys including microtremor measurement were conducted, as well as the organizing of basic data for ground modelling were performed. The content of the ground information used in this project is explained below.

#### 3.3.1 Drilling data and geological maps

In total 449 drilling data (2002 survey was about 300) were collected. Their distribution is shown in Figure 3.3.1. Collection sources were JICA (2002 Survey), UNDP (United Nations Development Program), DoR (Department of Road), KUKL (Kathmandu Upatyaka Khanepani Limited), and so on. Among them, 124 boreholes have N values (2002 Survey was 61), within those only 36 (2002 Survey was 29) are 20m or more in depth. PS logging was five, same number as the 2002 Survey. 56 boreholes reach rock, increased from 36 at the

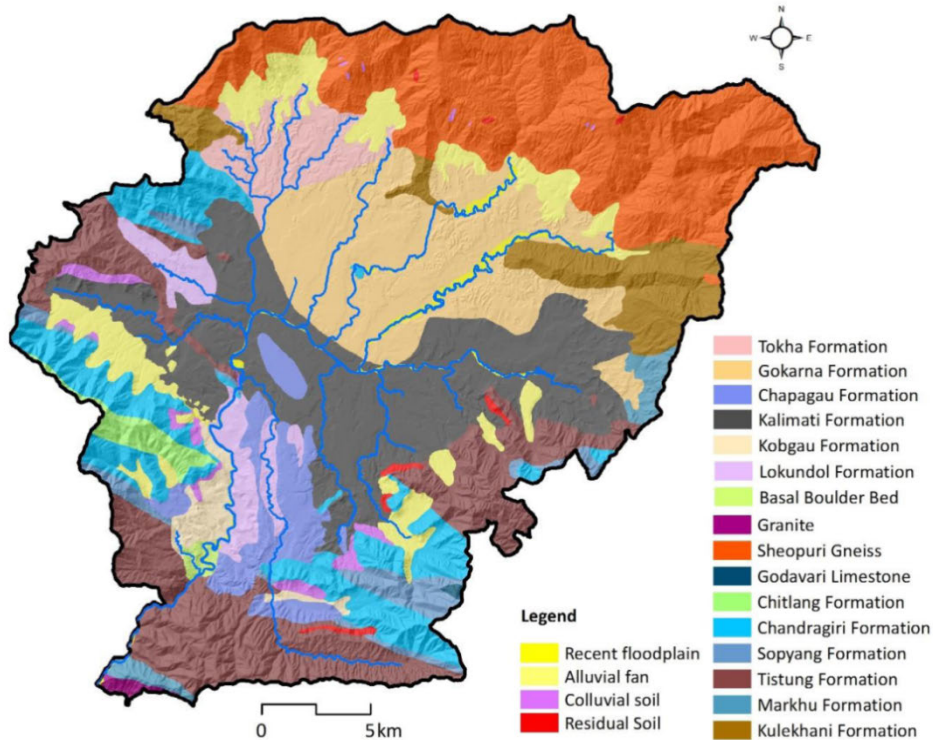
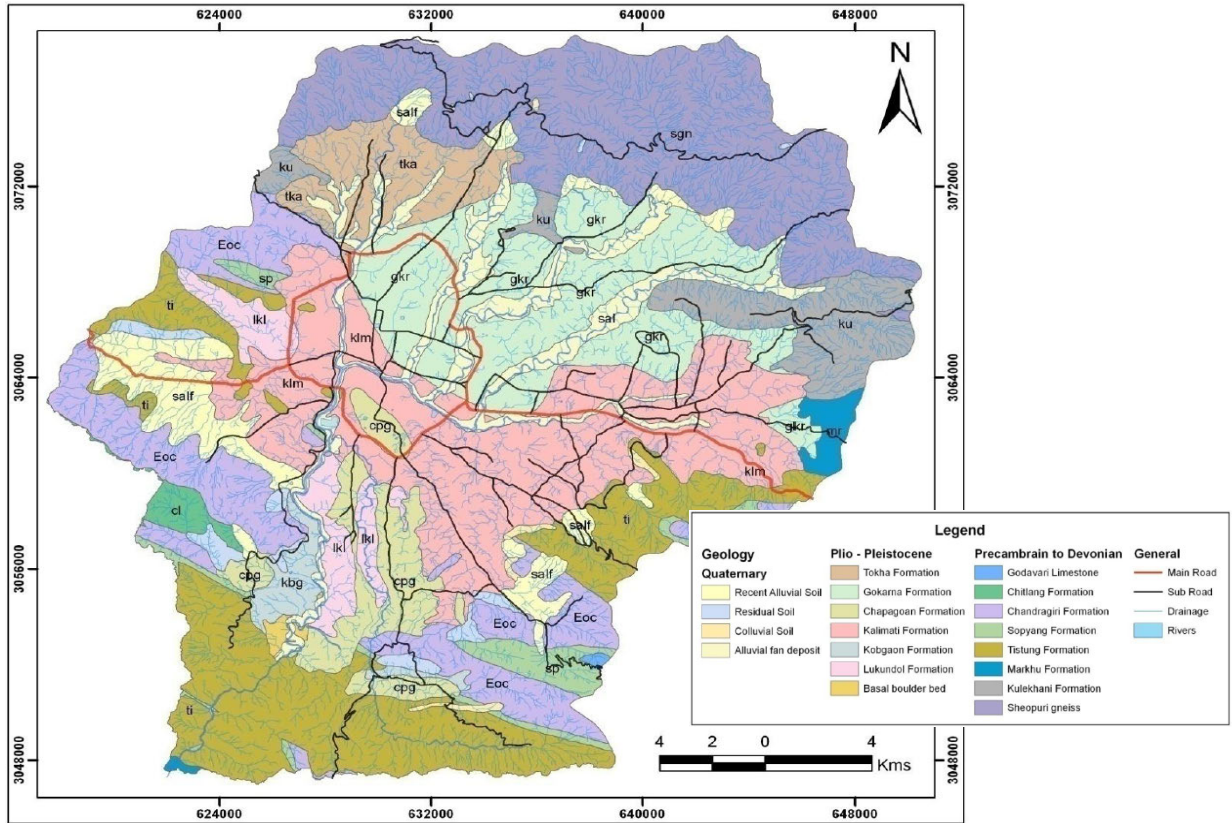
2002 Survey. And soil tests were carried out at 24 holes. In addition, out of 449 boreholes, depths shallower than 50m are 236, 100m or deeper are around 200.



Source: JICA Project Team

**Figure 3.3.1 Distribution of collected borehole data**

For Geological maps, existing Engineering and Environmental Geology Map (DMG, 1998) and Geology Map (UNDP, 2013) were collected as shown in below.

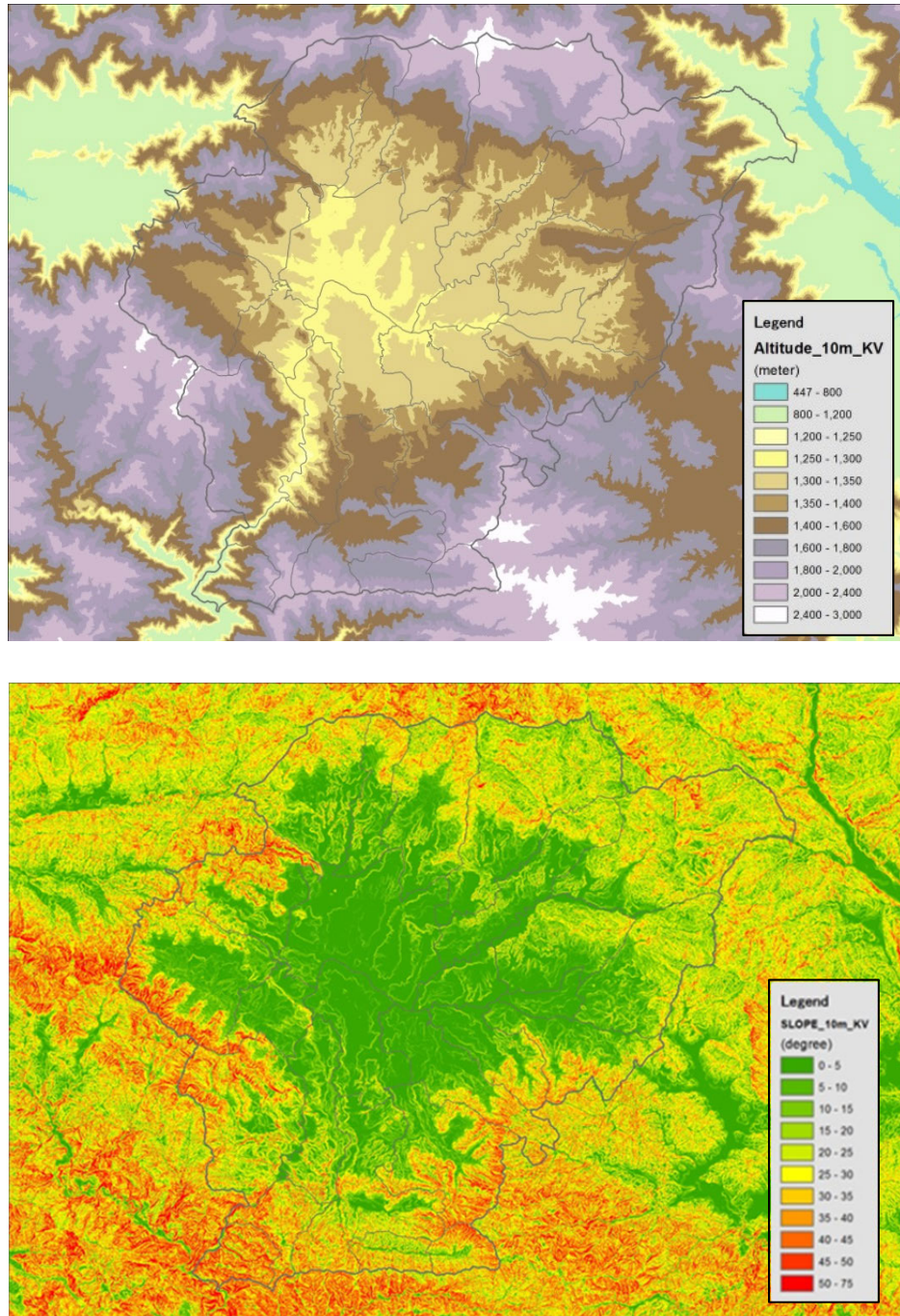


Source: DMG, UNDP

**Figure 3.3.2** Collected geological maps, (upper) Engineering and Environmental Geology map by DMG, 1998, and (lower) Geology Map by UNDP, 2013

### 3.3.2 Altitude data

The altitude data was obtained as a DEM (Digital Elevation Model) derived from recent satellite imagery data from UNDP. Altitude and slope angle distribution were prepared using the DEM as shown in Figure 3.3.3. Also, the topographical maps with scale 25,000 were purchased at the map center, published by DoS (Department of Survey).



Source: JICA Project Team based on UNDP, 2013 data

**Figure 3.3.3 Altitude and slope angle distribution using DEM (UNDP)**

### **3.3.3 Preparation of detailed geomorphological map**

For ground modeling, along with geological information, drilling data and topographical materials, geomorphological map which reflects detailed depositional environment plays an important role. Since existing geomorphological maps in the Valley had not sufficient resolution, new one was to be developed in this project. Therefore, aerial photographs with scale of 1: 15,000, partly 1: 50,000 were purchased from DoS (Department of Survey). Geomorphological interpretation and site reconnaissance survey were implemented, and a new detailed geomorphological map was prepared with DMG participation. Still site survey has not yet perfect, which will be supplemented by DMG, and then, DMG will be supposed to publicize after some further analysis.

#### **(1) Purpose**

The purpose of the preparation of a detailed geomorphological map in the Kathmandu Valley is as follows:

- 1) Modeling of subsurface ground conditions for estimation of strong seismic motion
- 2) Liquefaction assessment
- 3) Evaluation of earthquake-induced landslide and slope failure

#### **1) Modeling of subsurface ground conditions for estimation of strong seismic motion**

It is well known that the same earthquake in the same region causes different seismic motions at the ground surface according to the difference of the subsurface ground conditions. Therefore, it is very important to estimate the ground conditions for seismic hazard assessment. Usually the target area is divided into smaller grids and subsurface soil models are adopted for each grid after performing drilling and physical prospection. However, this process requires a huge number of ground investigation and information in order to achieve modeling in the whole target region. As the subsurface ground conditions and geomorphologies have close relation each other, the same geomorphologies can have similar subsurface ground conditions. If we perform soil investigation for each geomorphology, it would be easy to model the subsurface ground conditions in the whole region. Therefore, the preparation of detailed geomorphological map is important for seismic hazard assessment.

The geomorphology in the Kathmandu Valley consists of mainly the deltaic-lacustrine terraces formed under the paleo-Kathmandu Lake, and the narrow fluvial surfaces except mountainous areas and hills. Traditionally people in the Kathmandu Valley live on the deltaic-lacustrine terraces where urban areas have been built. However, due to the rapid increase of population in recent years, settlements have been expanded even in the fluvial



surfaces with worse ground conditions. Because the fluvial surfaces are likely to amplify the strong seismic motion, the detailed geomorphological classification of the fluvial surfaces is indispensable to model the subsurface ground conditions.

## **2) Liquefaction assessment**

Liquefaction occurrences at several sites have been reported during the 2015 Mw 7.8 Gorkha Earthquake. But during the 1934 Mw 8.1 Bihar Earthquake, various apparent occurrences of liquefaction have been reported. If a large earthquake occurs in the future, fluvial surface areas have a high risk of liquefaction.

The geomorphology in the Kathmandu Valley is mainly divided into the deltaic-lacustrine terrace and fluvial surfaces. Furthermore, the fluvial surfaces are sub-divided to alluvial lowland, natural levee, former river course, back marsh, lower terrace, higher terrace, valley plain and alluvial fan etc. Out of these, the natural levee and former river course consist of sandy materials with higher underground water level, so, liquefaction is likely to occur there. Generally, liquefaction is unlikely to occur on the deltaic-lacustrine terrace. However, there might be a possibility of liquefaction within the valley plains developing on the terraces.

## **3) Evaluation of earthquake-induced landslide and slope failure**

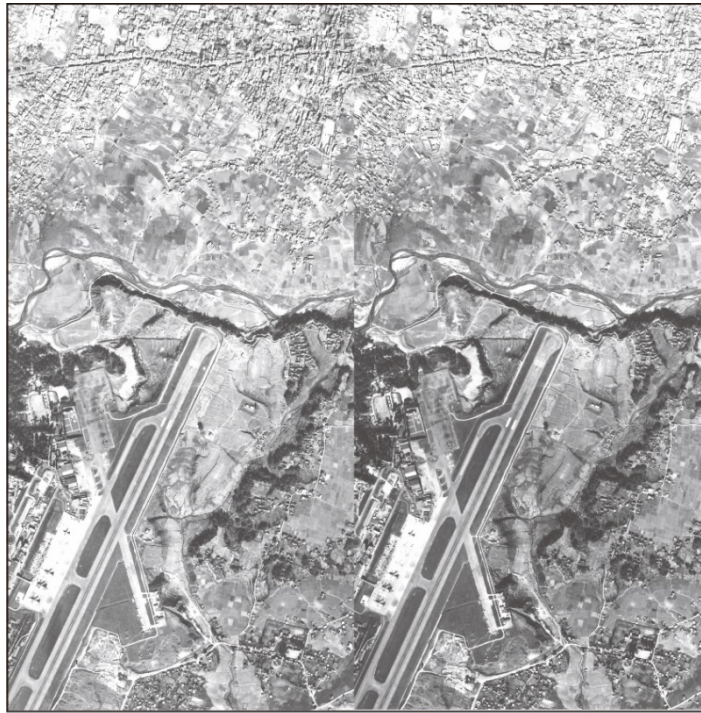
Large-scale landslides and slope failures did not occur in Kathmandu Valley during the 2015 Gorkha Earthquake. However, so far large-scale landslides have occurred during large earthquakes in other regions, for example, the 1999 Mw 7.6 Chi-Chi, Taiwan earthquake, which resulted in a huge damage. There are many clear landslide topographies which have been observed in the mountainous slope of the Kathmandu Valley. If a large earthquake occurs in the future, extensive damage caused by landslides can be expected. Therefore, in the geomorphological classification, it is necessary to detect landslide topographies for the seismic hazard assessment. In addition, the flanks of the terrace surfaces can be eroded and sometimes show steep cliffs. There is a risk of occurrences of rock falls and slope failures at the cliffs.

## **(2) Method**

The detailed geomorphological classification was carried out by stereo-view of large-scale aerial photographs taken in December 1998 (scale about 1:15,000). The aerial photographs are continuously taken in the E-W direction. Nine lines, eighteen photographs per line, are available in the Kathmandu Valley. Most areas of the Kathmandu Valley are covered by these aerial photographs taken in 1998, while large-scale photographs are not available in the western to southwestern margin of the Kathmandu Valley. Therefore, we used complementary small-scale aerial photographs taken in 1992 (scale about 1: 50,000).

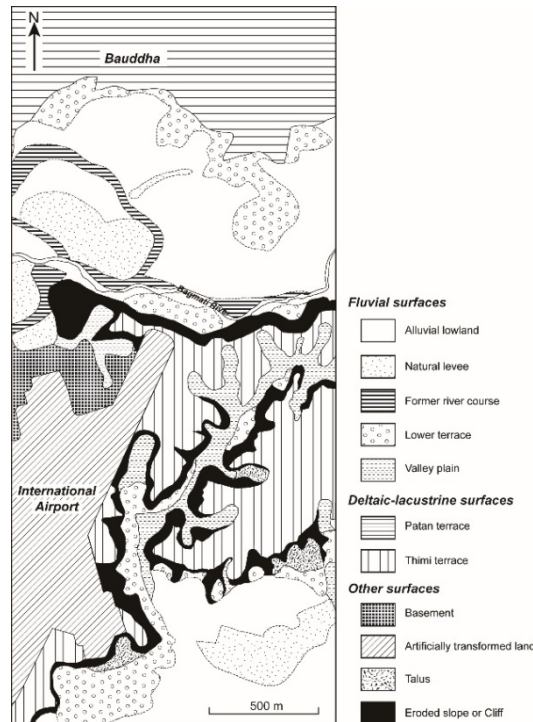
Adjoining photographs overlap within 60% of each other, and the overlapping images were stereo-viewed by a stereo-scope or naked eye. 3D images were useful to observe detailed geomorphologies.

A pair of aerial photographs near the Tribhuvan International Airport is shown in Figure 3.3.4. An example of detailed geomorphological classification made up by stereo-view of aerial photograph is shown in Figure 3.3.5.



Source: JICA Project Team based on DoS data

**Figure 3.3.4** A pair of aerial photographs for stereo-view nears the Tribhuvan International Airport



Source: JICA Project Team based on DoS data

**Figure 3.3.5 An example of detailed geomorphological classification. Location etc. same as above**

### (3) Detailed geomorphological classification

The detailed geomorphological classifications in the Kathmandu Valley are shown in Table 3.3.1. The geomorphology in the Kathmandu Valley was divided into fluvial surfaces (modern flood plain), deltaic-lacustrine terraces, and other surfaces. The detailed geomorphological map is shown in Figure 3.3.6. Refer A0 size original map for details because this map is reduced to A4 size.

#### a) Fluvial surfaces (modern flood plains)

Fluvial surfaces were sub-divided as follows:

- Alluvial lowland (al): Flat lowland along modern rivers. Former river courses and terraces developed on the alluvial lowland.
- Valley plain (vp): Flat plain in the narrow valleys formed by tributaries.
- Former river course (fr): Long and narrow depressions between natural levees and between alluvial lowland and terrace or mountainous slope. It represents a dark grey-blackish color on the aerial photographs.
- Back marsh (bm): Marshes between natural levees and between alluvial lowland and terrace or mountainous slope. It represents a blackish color as well as former river courses on the aerial photographs.

- Natural levee (nl): Long-narrow and slightly hilly area along modern rivers and former river courses (dry river courses). Young topographies are clearer and more recognizable than old ones.
- Alluvial fan (fa): Gentle slopes with concentric contours and a network of streams formed by fluvial process at the outlet of valleys.
- Lower terrace ( $tr_2$ ): Slightly hilly area along modern rivers. It is somewhat higher than natural levees. The river-side flanks of the terraces show cliffs.
- Higher terrace ( $tr_1$ ): Fluvial terrace surfaces on the flank of the deltaic-lacustrine terraces and the hillsides of hills and mountainous slopes. The altitude is different from that of deltaic-lacustrine terrace surfaces. Its distribution is limited.

#### **b) Deltaic-lacustrine terraces**

The deltaic-lacustrine terraces were classified referring to Sakai et al. (2012) and Yamanaka (1982). The deltaic-lacustrine terraces were subdivided into T1 to T7 terraces. The order of T1 to T7 depends on the altitude of the distribution.  $^{14}\text{C}$  age and altitude of terraces are shown in Table 3.3.2. T1, T2, T3, and T4 correspond to Patan, Thimi, Gokarna, and Tokha terraces, respectively. Sakai et al. (2012) defined Tokha terrace as an upper part of the Gokarna terrace formation. However, we subdivided “Gokarna terrace” into two terraces of Gokarna and Tokha terraces because Tokha terrace has an apparent terrace surface. Tokha terrace is at the highest altitude in the northern region of the Kathmandu Valley, while it is younger than Thimi terrace (; Sakai et al., 2012). The altitude of the Gokarna terrace surface in the southern region is higher than that in the northern region because it is uplifted by the activity of the Chandragiri Fault as described later. T5, T6, and T7 are high terraces which are distributed only in the southern margin of the Kathmandu Valley.

#### **c) Other surfaces**

Other surfaces were sub-divided into Talus (ta), Landslides and slope failure (Ls), Eroded slope and cliff (es), Geomorphological basement (Bs), and Artificially transformed land (at).

Usually the basement indicates hills and mountainous slopes where hard rocks are exposed. However, the area where Kalimati formation is directly exposed also shows the topography of the hills and lower mountainous slope. In this study, “geomorphological basement” includes the hilly area where Kalimati formations as well as exposed hard rocks.

**Table 3.3.1 Detailed geomorphological classification in the Kathmandu Valley**

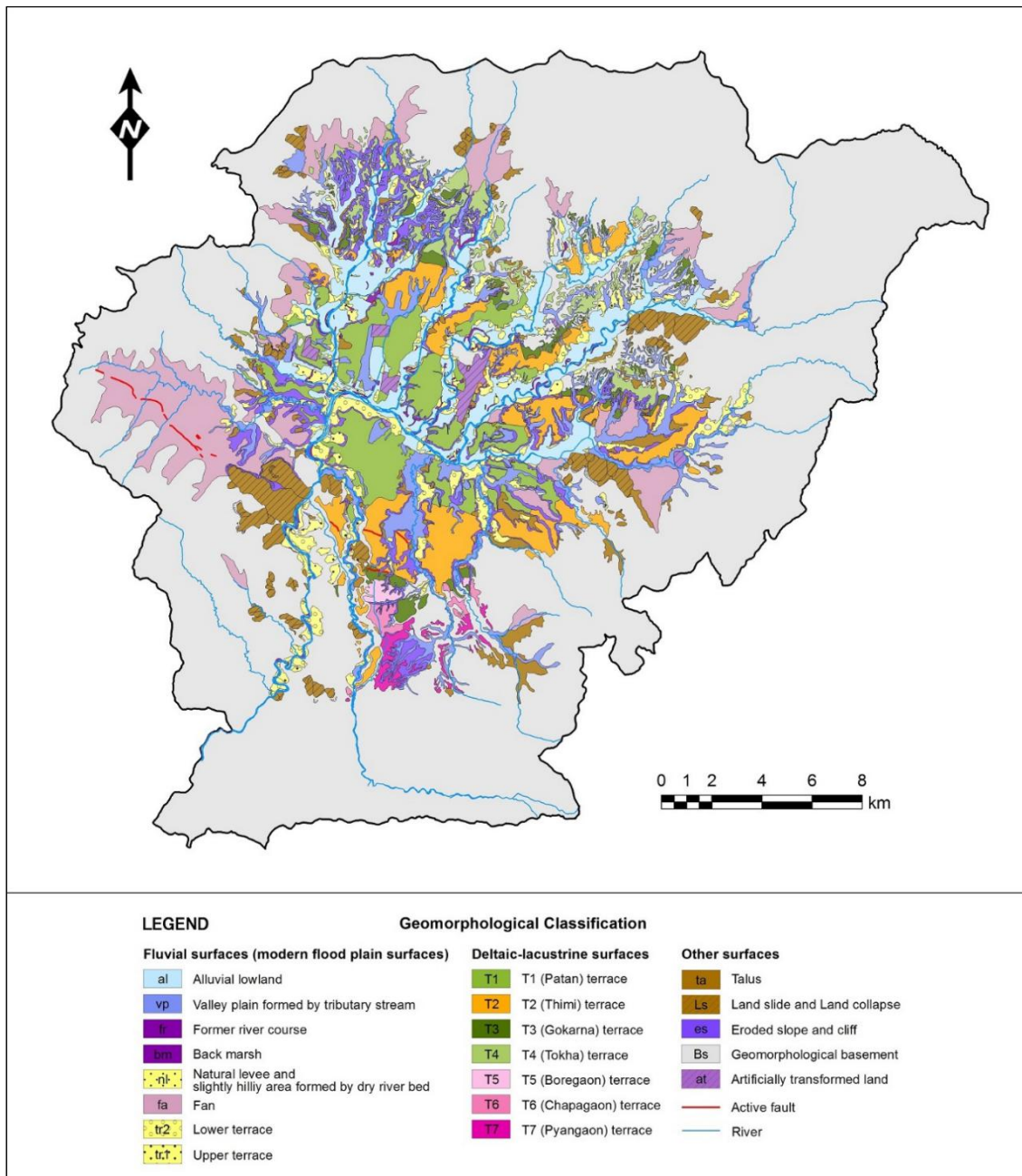
Classification	Detailed classification	abbr	Characteristics
Fluvial surfaces (modern flood plain)	Alluvial lowland	al	Lowland along modern rivers
	Valley plain	vp	Lowland in the narrow valleys
	Former river course	fr	Long and narrow depression
	Back marsh	bm	Marshes between natural levees
	Natural levee	nl	Long-narrow and slightly hilly area
	Alluvial fan	fa	Gentle slope with concentric contours at the exit of valley
	Lower terrace	tr2	Slightly hilly area
	Higher terrace	tr1	Fluvial terraces on the hillside
Deltaic-lacustrine terraces	T1 (Patan) terrace	T1	Terrace formed under the environment of the Paleo-Kathmandu Lake. The terraces are subdivided into T1 to T7 depending on the altitudes (see Table 3.3.2).
	T2 (Thimi) terrace	T2	
	T3 (Gokarna) terrace	T3	
	T4 (Tokha) terrace	T4	
	T5 (Boregaon) terrace	T5	
	T6 (Chapagaon) terrace	T6	
	T7 (Pyangaon) terrace	T7	
Other surfaces	Talus	ta	Relatively steep slope formed by collapse of cliff
	Landslide and slope failure	Ls	Relatively gentle slope formed by sliding of mountainous slope
	Eroded slope and cliff	es	Cliff at the side of terraces
	Geomorphological basement	Bs	Hill and mountainous slope where hard rocks and the Kathmandu basin Group expose
	Artificially transformed land	at	Developed land by bank on the lowland Flat surface by cutting of terraces

Source: JICA Project Team compiled from several literature sources

**Table 3.3.2 <sup>14</sup>C age and altitude of the deltaic-lacustrine terraces**

Terrace	Age of terraces (cal ka years BP)	Altitude of terraces (m above sea level)	
		Northern region	Southern region
T1 (Patan)	17-10	1,300-1,330	1,310-1,330
T2 (Thimi)	35-28	1,330-1,350	1,330-1,360
T3 (Gokarna)	>50-38	1,350-1,390	1,380-1,410
T4 (Tokha)	23-17	1,360-1,390	-
T5 (Boregaon)	>50	-	1,420-1,440
T6 (Chapagaon)	>50	-	1,440-1,460
T7 (Pyangaon)	>50	-	1,470-1,510

Source: Gautam et al. (2009), Sakai et al. (2006), Sakai et al. (2008), Sakai et al. (2012)



Source: JICA Project Team with DMG

**Figure 3.3.6 Geomorphological map of the Kathmandu Valley**

**(4) Examples of detailed geomorphological classification**

The target areas which were described as examples of detailed geomorphological classification are shown in Figure 3.3.7.

**a) Central area of Kathmandu**

The geomorphological map in the central area of Kathmandu is shown in Figure 3.3.8. A long and narrow valley plain with N-S direction is developed, though most of the area consist of T1 (Patan) terrace. Singha Durbar stands on the artificially transformed land which is banked on the alluvial lowland. The ground conditions around Singha Durbar are thought

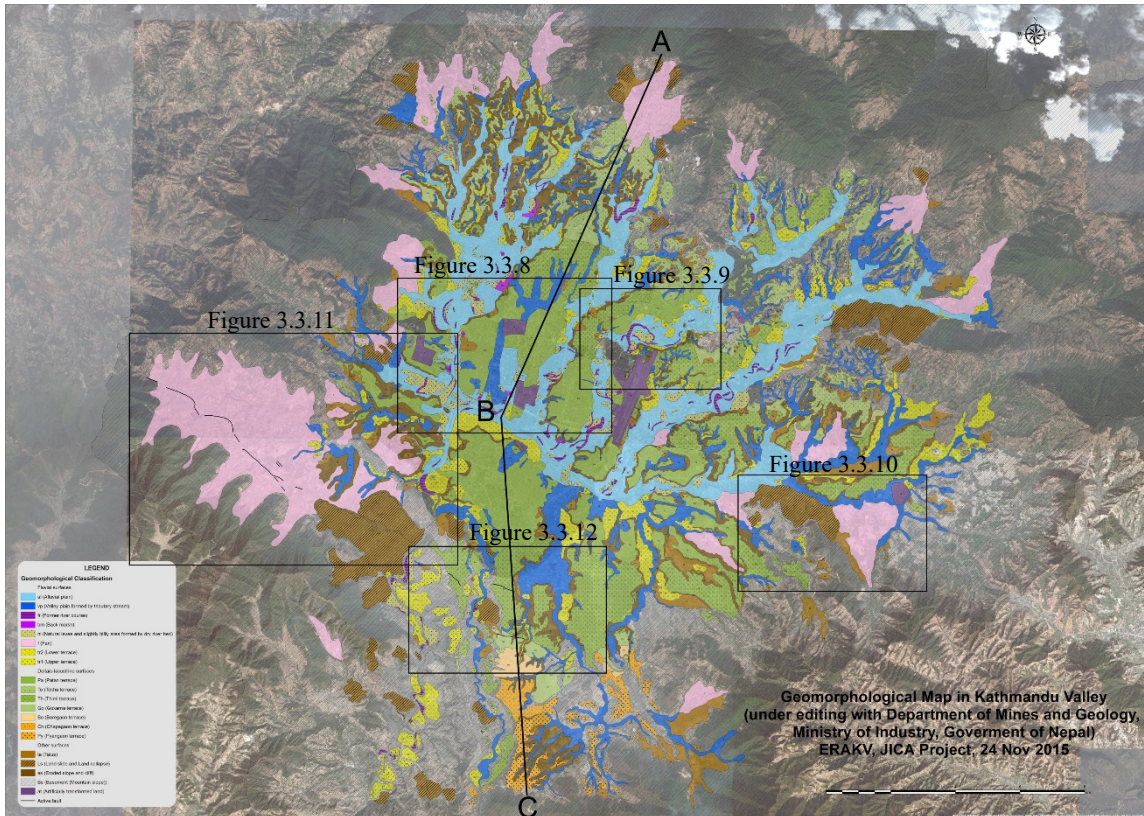
to be not so good because there are back marshes on the western side. The amplification of seismic motions might be large, and liquefaction can be expected if a large earthquake occurs in the future.

**b) Northern area of Tribhuvan International Airport**

The geomorphological map of the northern area of Tribhuvan International Airport is shown in Figure 3.3.9. This area stands on the modern flood plain, and the topographies, such as alluvial lowland, natural levee, and former river course, are developed. According to the aerial photographs taken in December 1998, fewer houses were built at that time on the alluvial lowland. Also, according to the Google Earth image in 2003 there were fewer houses. However, houses are shown closely built together in 2015. This means that settlements have been expanded to the modern flood plain, though ground conditions are worse, due to the rapid increase of population in recent years. As former river courses and natural levees are composed of sandy materials with high groundwater level, liquefaction is likely in that area in the case of a large earthquake in the future.

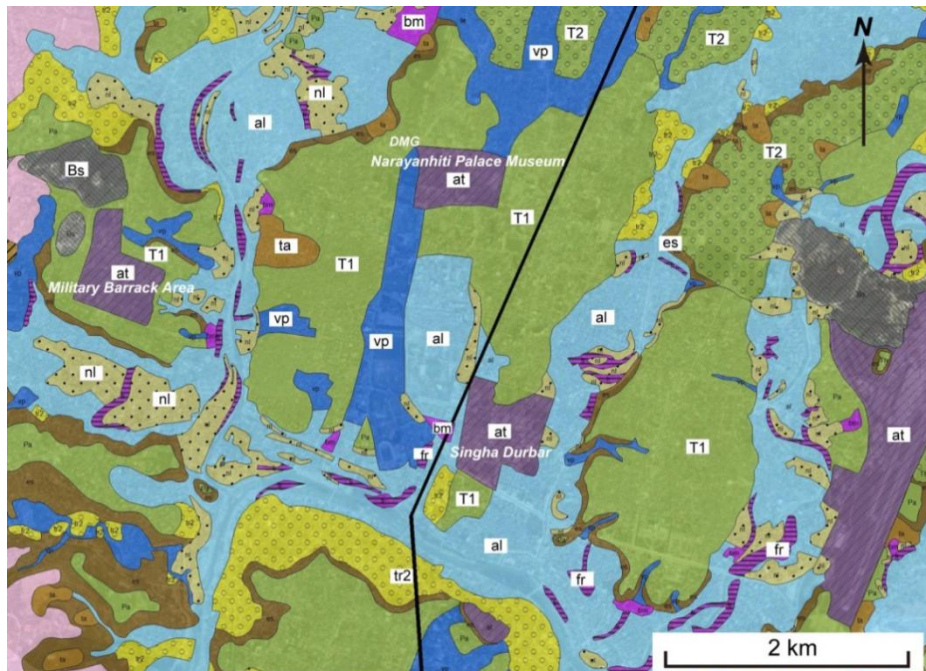
**c) Suryabinayak Area**

The geomorphological map in the Suryabinayak area is shown in Figure 3.3.10. In the northern slope of the Suryabinayak area several apparent landslides with elliptic sliding cliffs were recognized in the aerial photographs. On the eastern side of landslides, a typical alluvial fan has developed. The landslides and slope collapses might have provided the quantity of materials to form the alluvial fan. Also, landslides have been recognized in the northern slope of Changunarayan located at the north of Suryabinayak (Figure 3.3.7).



Source: JICA Project Team

**Figure 3.3.7** Locations of geomorphological map described later. A line of A-B-C represents the location of topographic profile.

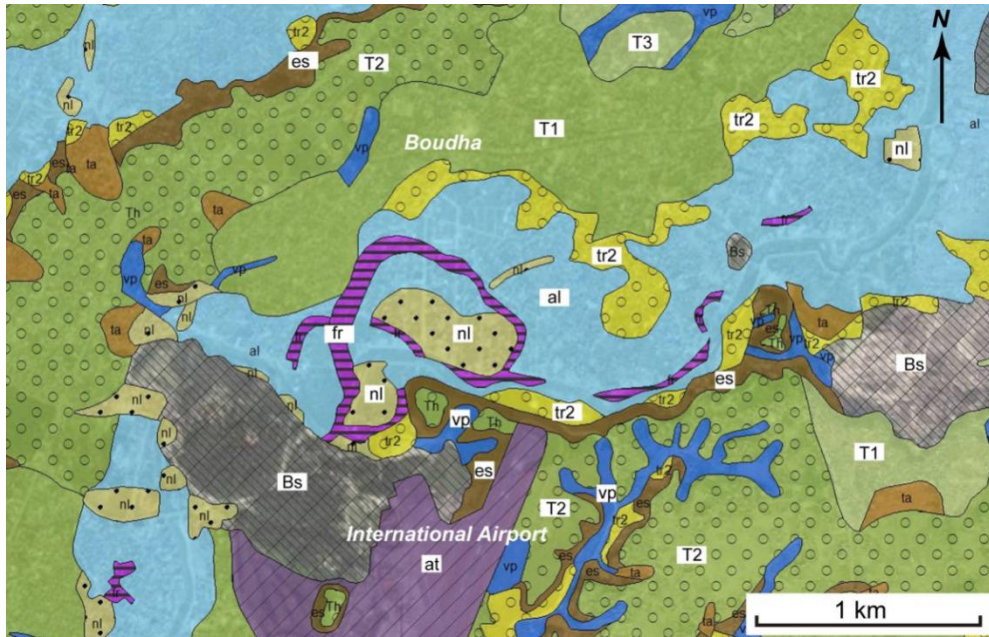


Refer as legend

Source: JICA Project Team

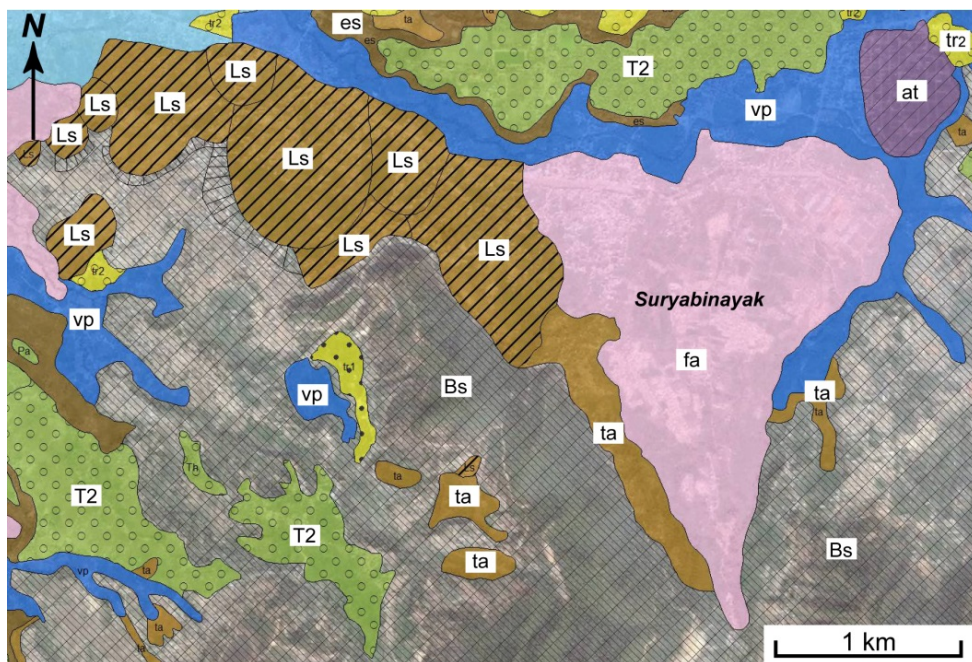
**Figure 3.3.8** Geomorphological map in the central area of Kathmandu





Source: JICA Project Team

**Figure 3.3.9** Geomorphological map of the northern area of Tribhuvan International Airport



Source: JICA Project Team

**Figure 3.3.10** Geomorphological map in the Suryabinayak area

### 3.3.4 Tectonic geomorphology

Previous studies reported the presence of several active faults in the Kathmandu Valley (Saijo et al., 1995; Sakai et al., 2012). However, according to aerial photograph interpretation in this study for the preparation of the detailed geomorphological map, most of these faults do not represent any active fault topographies. The active fault topographies,

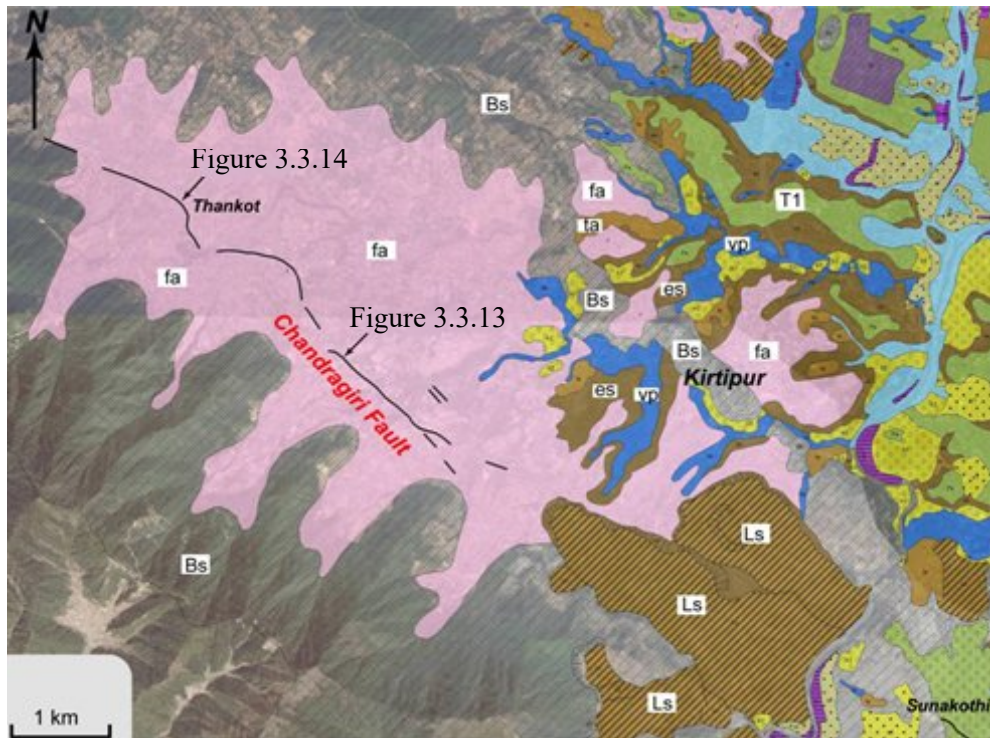
such as fault scarp, folding scarp, and tilting terrace surfaces, are recognized only along the Chandragiri Fault in the southwestern margin of the Kathmandu Valley (Yagi et al., 2000; Asahi, 2003). Yagi et al. (2000) called this fault the Kathmandu South Fault. Asahi (2003) called the western half of this fault the Thankot Fault.

The Chandragiri Fault, which is a WNW–ESE trending reverse fault inclined to the south, extends from Thankot in the west of Kirtipur Municipality to the vicinity of Sunakothi (Figure 3.3.7 and Figure 3.3.11). The fault traces in the west of Kirtipur municipality are shown in Figure 3.3.11. Apparent active fault scarps are recognized along the fault traces (Figure 3.3.11). A fault scarp around 10m high was confirmed in the west of Kirtipur (Figure 3.3.11). A fault scarp with around 2–3m difference was confirmed in Thankot, though it has been modified due to the construction of houses (Figure 3.3.14).

The active fault traces in Sunakothi are shown in Figure 3.3.11. The contour map with 2m intervals are shown as the background of the detailed geomorphological map (Figure 3.3.12). The Chandragiri fault crosses T2 (Thimi) terrace surface and the contours are close on the southern side of the fault (on the hanging wall of the fault). The inclination of the slope is steeper than that of normal terrace surfaces. This means that the southern side of the fault represents around 1km wide folding scarp (flexural scarp). It was confirmed that the T2 (Thimi) terrace surface is tilted to the north with a steeper inclination than that of normal terrace surface in the field.

A topographic profile of line A-B-C (Figure 3.3.7) and the distribution of deltaic-lacustrine terrace surfaces are shown in Figure 3.3.15. The terrace surfaces in both the northern and southern regions are inclined toward the central Bagmati River. This indicates that the terraces in the northern region were formed by the fluvial process originating in the northern range, and the terraces in the southern region were formed by the fluvial process originating in the southern range. The topographic profile demonstrates that the terrace surfaces on the southern side of the Chandragiri Fault are steeper.

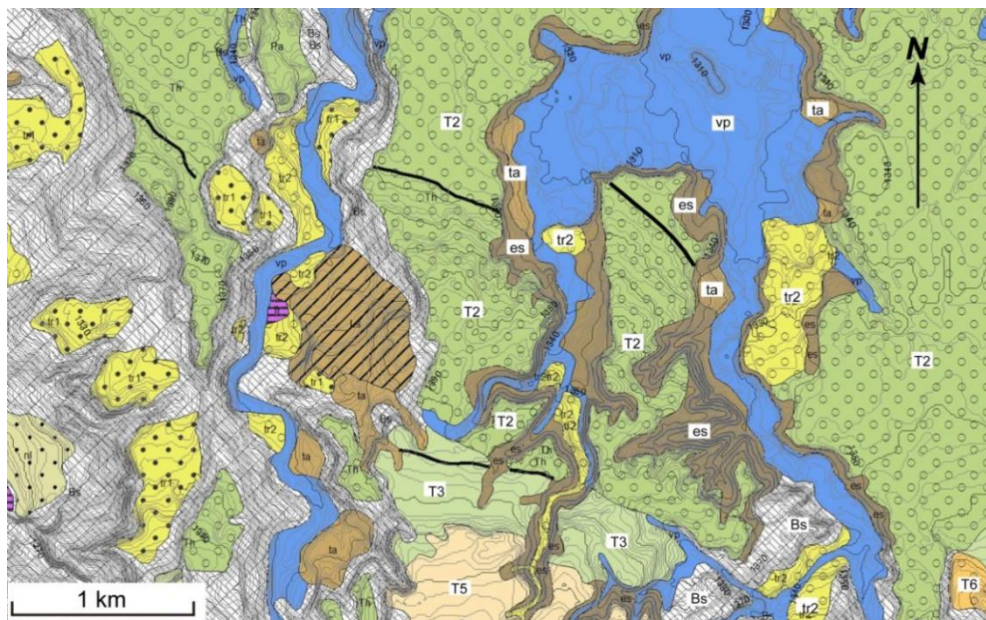
The higher terraces of T5, T6, and T7 (Boregaon, Chapagaon, Pyangaon) are distributed only in the southern edge of the Kathmandu Valley at an altitude of 1,420-1,510 m (Table 3.3.2). The altitude of these terraces in the southern region is about 100 m higher than that of the T4 (Tokha) terrace in the northern region. This suggests that T5 to T7 terraces were uplifted by the activity of the Chandragiri Fault throughout the Late Quaternary time.



Note: Solid lines represent active fault traces. Large landslides are recognized in the south-eastern extension of the fault.

Source: JICA Project Team

**Figure 3.3.11 Active fault traces of the Chandragiri Fault in the west of Kirtipur Municipality**



Note: Solid lines represent active fault traces. The contour map with 2 m intervals (thin solid lines) is shown as the background of the detailed geomorphological map. The contours are close in the southern side of the fault. T2 and T3 terrace surfaces are tilted to the north.

Source: JICA Project Team

**Figure 3.3.12 Active fault traces in Sunakothi**



Note: The location of the photograph is shown in Figure 3.3.11.

Source: JICA Project Team

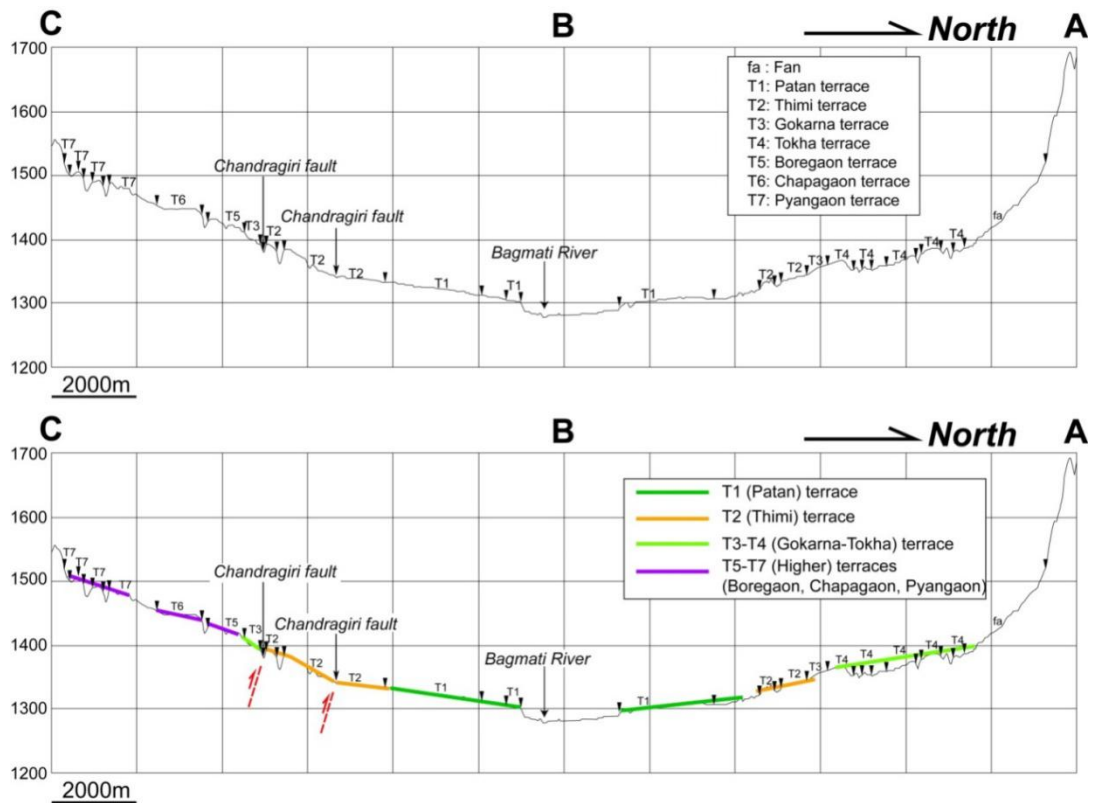
**Figure 3.3.13 A fault scarp around 10m high in the west of Kirtipur Municipality**



Note: The location of the photograph is shown in Figure 3.3.11.

Source: JICA Project Team

**Figure 3.3.14 A fault scarp in Thankot**



Note: The location of the topographic profile is shown in Figure 3.3.7. The vertical axis is exaggerated fifteen times against the horizontal axis. The inclination of the terrace surface in the southern side of the Chandragiri fault is steeper. T5 to T7 terraces in the southern region are around 100m higher than T4 terrace in the northern region. This suggests that T5 to T7 terraces are uplifted by the activity of the Chandragiri fault. Top: original data, Bottom: interpretation of terrace surfaces.

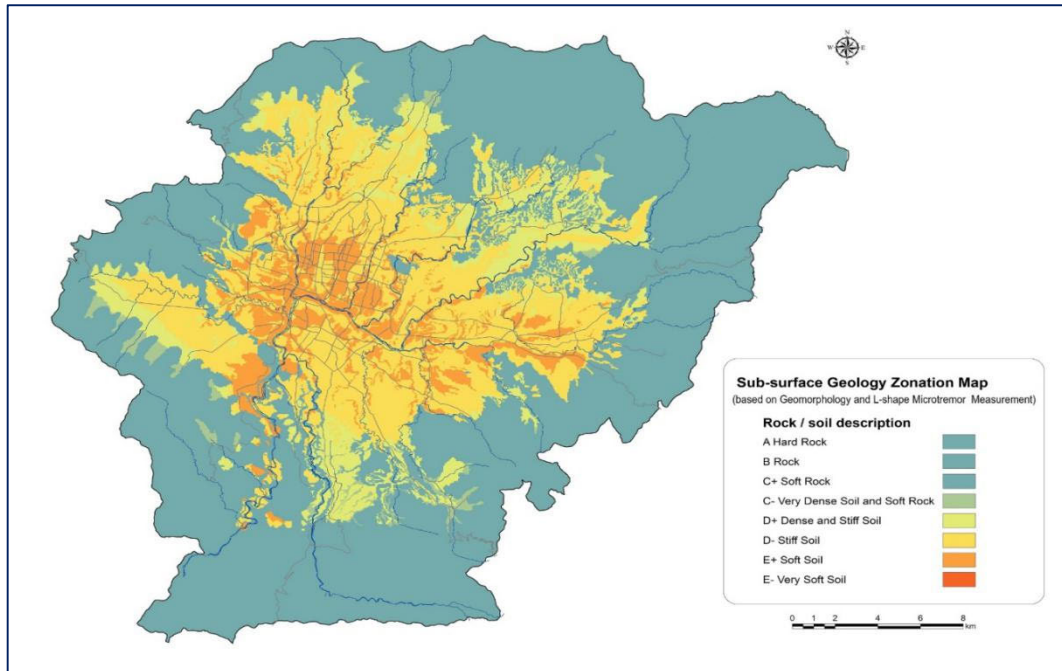
Source: JICA Project Team

**Figure 3.3.15 N-S direction topographic profile and distribution of deltaic-lacustrine terraces**

### 3.3.5 Susceptibility Maps

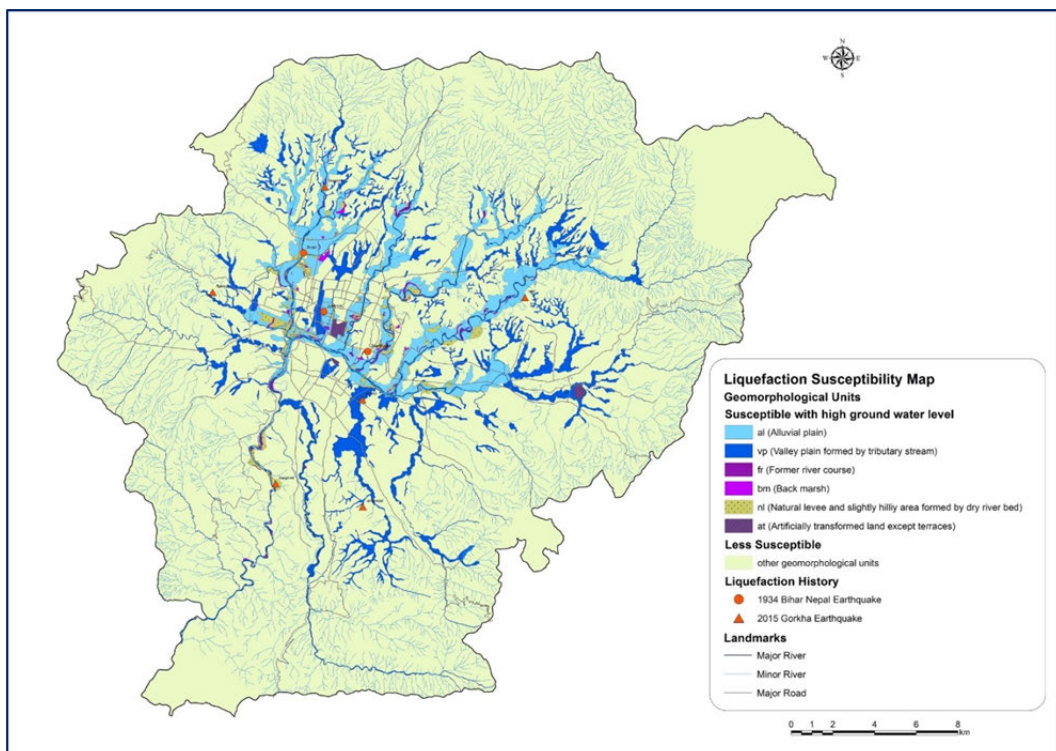
The geomorphological map mentioned above in Figure 3.3.6, has significantly contributed not only to the ground modeling, but also to the understanding of origin, process and distribution of ground formation. In this project, by combining the geomorphological map and a variety of survey results, the maps were developed that show the softness of ground, vulnerability related to liquefaction and slope failure. Specifically, to organize the results of AVS30 obtained from the L-shaped array measurement of microtremor described below (where AVS30 is the average value of the S-wave velocity to a depth of 30m from the surface) for each geomorphological unit, together with the relationship with altitude, AVS30 map or the surface soil softness map, namely “Shakability” map, was developed as in . In addition, the liquefaction susceptibility map including the past liquefaction history (Figure 3.3.17) was prepared. Further, earthquake induced slope failure susceptibility map (Figure 3.3.18) considering slope angle, geomorphological unit, the history of slope failure and the inclination was developed. These susceptibility maps should be valid maps for taking

advantage as basic information at the time of grasping the ground situation of the entire Valley, or development planning, setting land use unit.



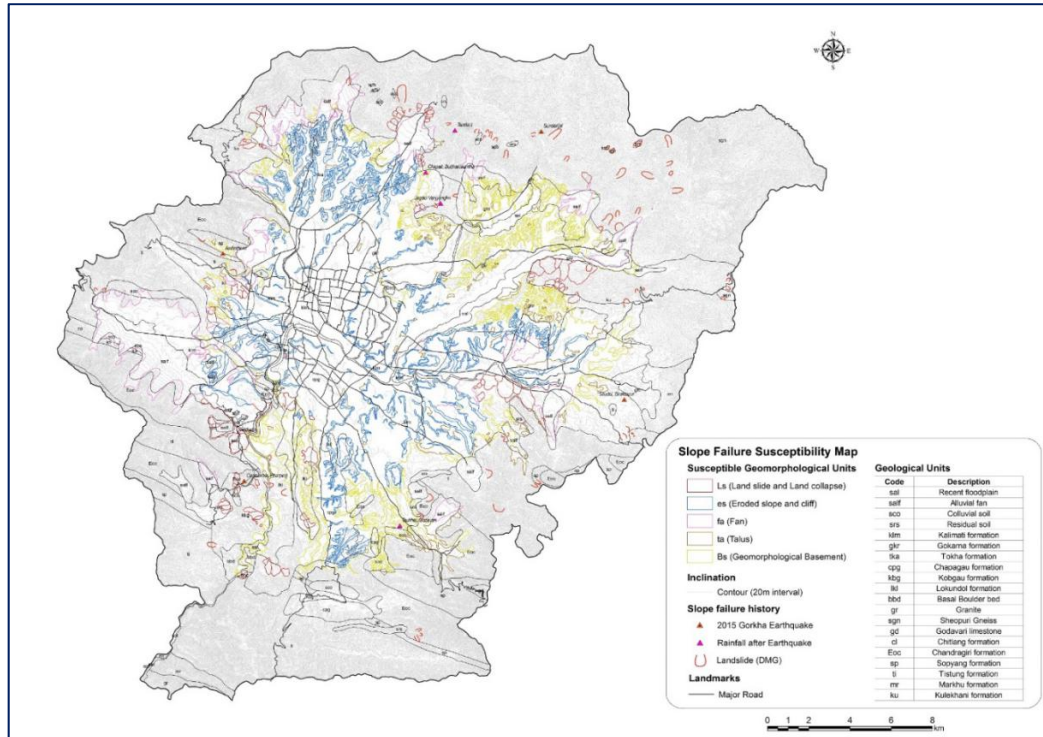
Source: JICA Project Team

**Figure 3.3.16 AVS30 map base on geomorphological unit (surface soil softness “Shakability” map)**



Source: JICA Project Team

**Figure 3.3.17 Liquefaction Susceptibility Map**



Source: JICA Project Team

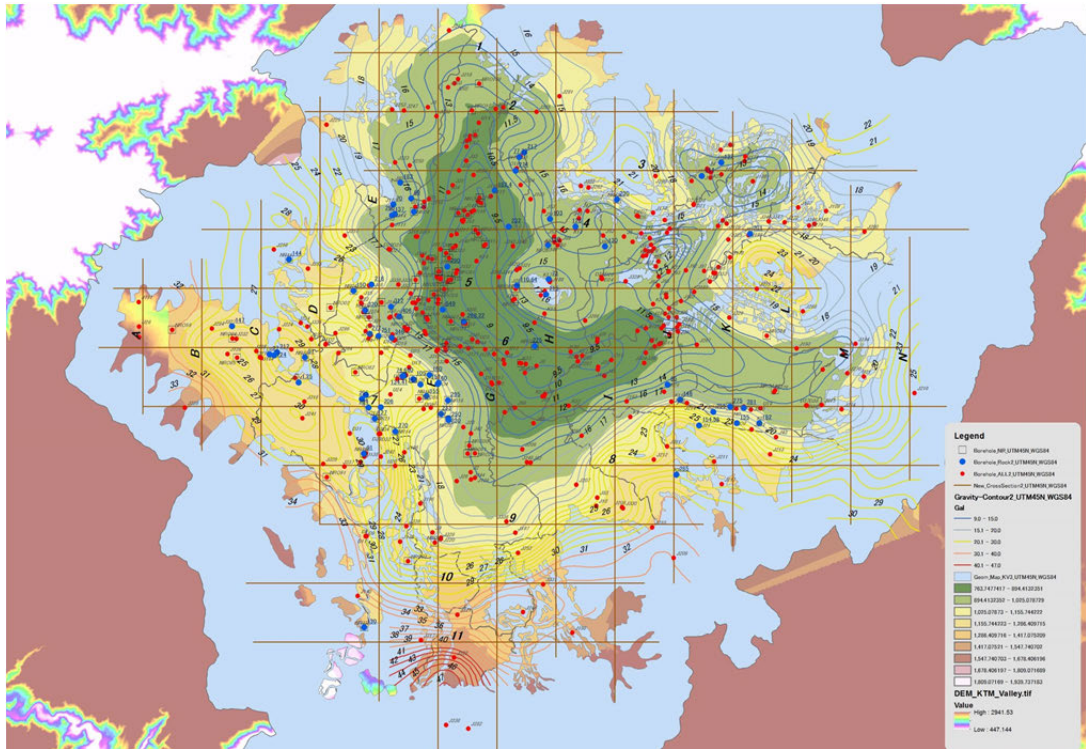
**Figure 3.3.18 Earthquake induced slope failure Susceptibility Map**

### 3.3.6 Depth of rock layer

Since the drilling information as point data that reach rock layer is limited to 56, in order to clarify the distribution or contour of rock depth, the gravity anomaly exploration results (Moribayashi and Maruo, 1980) was utilized. In other words, the relation between the gravity anomaly distribution and rock depth by drilling data was found. Then, together with rock depth by drilling, geomorphological map, geological map etc., the rock depth distribution was developed.

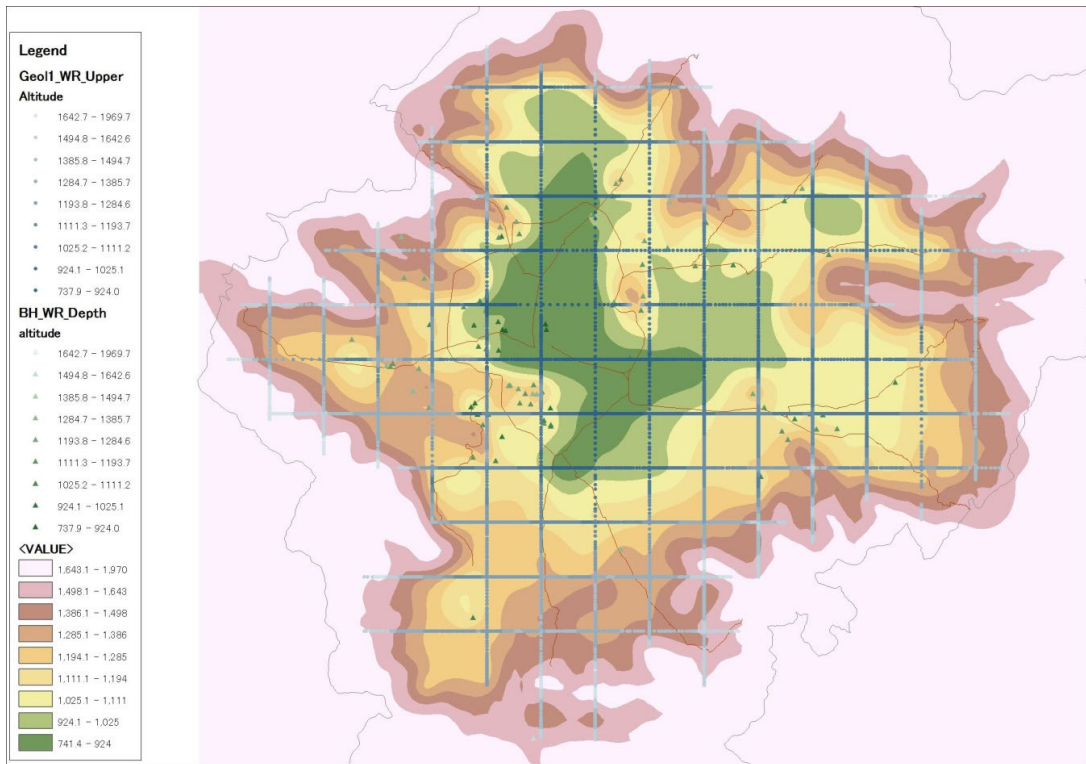
The results are shown in Figure 3.3.19 to Figure 3.3.21. According to the figures, it is easily identified that the internal soil structure variation of the valley is not simple. It should be reflected with the process of the formation of the valley, that the past mountain areas with ridges and valleys settled, next the old lake was produced, and soils were flown in and deposited in the lake from surrounding slopes, as a result the terrace layer was formed along with changes of water level of the old lake. Overall, the topography is quite complex. Though the maximum depth of rock is more than 500m at the central region, there are situations where a face of the rock is exposed at the ground surface and can be observed. Deeper portion of the ground is across the center of Kathmandu City from north to south, southern extension hits Lalitpur Sub-Metropolitan City, bypasses to the east, and is divided into southwest and east portions. East oriented portion passes through the Thimi (Madhyapur) City to Bhaktapur City. In the north of Tribhuvan International Airport there is

Pashupatinath, west of Kathmandu there is Swayambhunath, and in Lalitpur and Kirtipur bedrock appears on the ground surface or at shallow depth.



Source: JICA Project Team

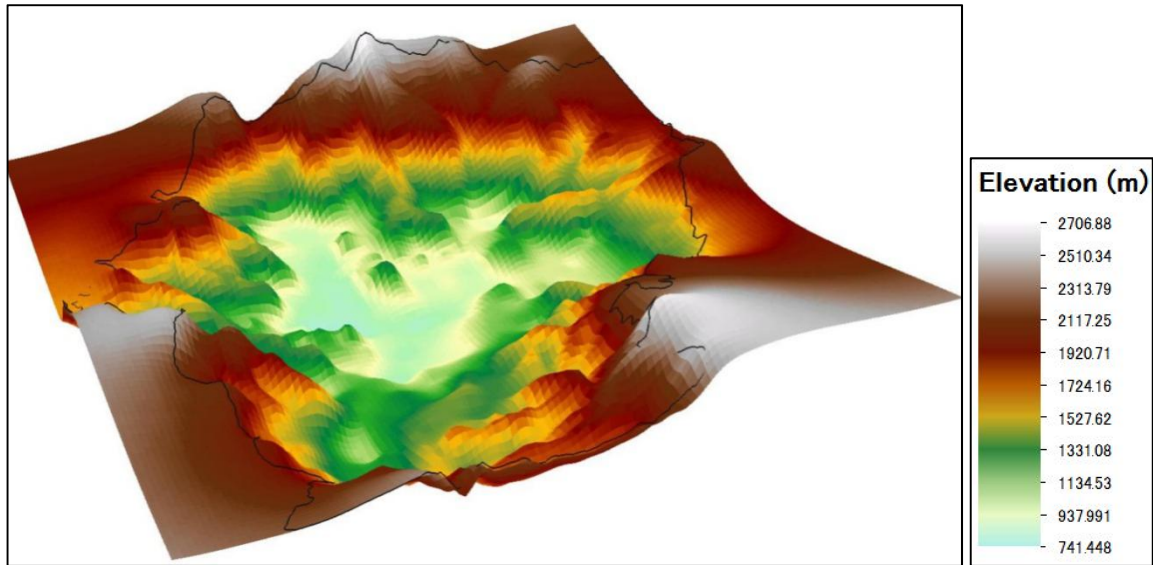
**Figure 3.3.19** Rock depth distribution based on gravity anomaly and drilling data



Source: JICA Project Team

**Figure 3.3.20** Estimated rock depth distribution (2D)





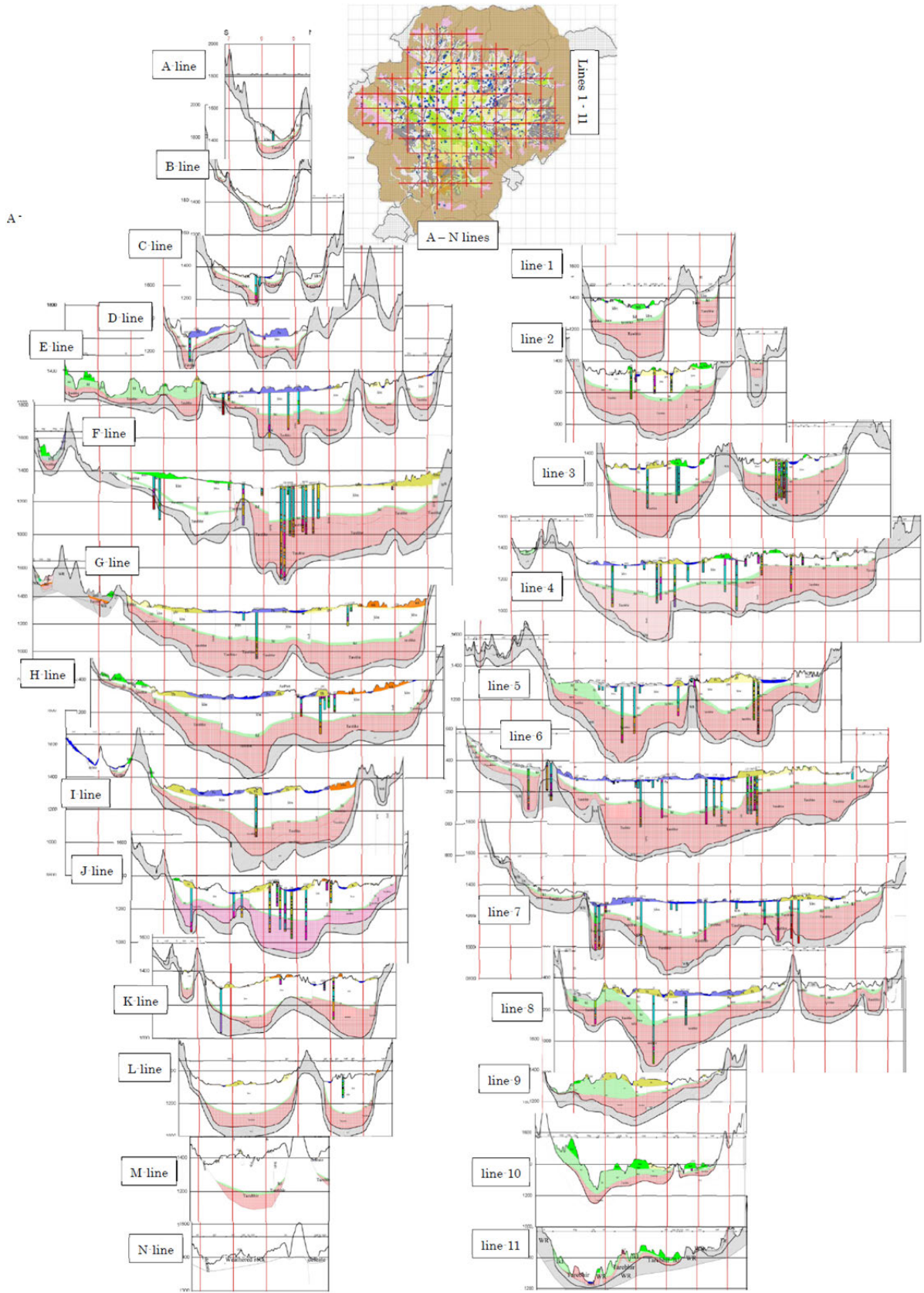
Source: JICA Project Team

**Figure 3.3.21 Estimated rock depth distribution (3D)**

### 3.3.7 Geological cross-sections

Although the preparation survey by JICA introduced a geological cross-section diagram compiled by JICA and ADB (2012), it is still not available to the public. Therefore, no usable geological cross-sections exist for the Kathmandu Valley. The usable geological cross-section is inevitable for soil modeling, so, a new one has been developed for this project. They are a total of 25 sections (14 north-south and 11 east-west) at 2km intervals (Figure 3.3.22). Still the information is insufficient, and it is necessary to supplement and improve it in the future. Basically, the fundamental structure of the geological layers is as following. Referring to the existing geological documentation, under the top soil layers the somewhat thick Kalimati layer mainly composed of relatively soft lacustrine clay was found, under Kalimati the somewhat rigid, thin Lukundol layer (mainly lacustrine clay) and thick Tarebhir layer (lacustrine) were found. This is the main configuration of the cross-section.

However, since the material is not sufficient, assumptions have to be often adopted during the determination of strata, interpolation between the materials and etc. Although the ground modeling in this project have used these cross-sections, in the future, it is expected to prepare more detailed geological cross-sections which can suggest important clues to obtain more accurate ground characteristics, by enriching the ground information.



Source: JICA Project Team

**Figure 3.3.22 Newly developed Geological cross-sections**

### References (3.3)

- Asahi, K. (2003) Thankot Active Fault in the Kathmandu Valley, Nepal Himalaya. *Jour. Nepal Geol. Soc.*, 28, 1-8.
- Department of Mines and Geology (DMG) (1998) Ministry of Industry, Engineering and Environmental Geological maps of Kathmandu Valley, and Pokhara Valley.
- Gautam, P., T. Sakai, K.N. Paudyal, S. Bhandari, B.R. Gyawali, C.N. Gautam, and L.M. Rial (2009) Magnetism and granulometry of Pleistocene sediments of Dhapasi section, Kathmandu (Nepal): implications for depositional age and paleoenvironment. *Bull. Dept. Geol. Trivhivan Univ.*, **12**, 17-28.
- Moribayashi, S., Maruo Y. (1980) Basement Topography of the Kathmandu Valley, Nepal: An Application of Gravitational Method to the Survey of a Tectonic Basin in the Himalayas, *Journal of the Japan Society of Engineering Geology*, 21(2), 80-87.
- Sakai, H., T. Sakai, A.P. Gajurel, and R. Fuji (2012) Guidebook for excursion on geology of Kathmandu Valley. 27<sup>th</sup> Himalaya-Karakoram-Tibet Workshop (HKT), Kathmandu, 2012, 45p.
- Sakai, T., A.P. Gajurel, B.N. Upreti, H. Tabata, N. Ooi, T. Takagawa, and H. Kitagawa (2008) Revised stratigraphy of fluvio-lacustrine sediments in the northern Kathmandu Valley, Nepal. *Nepal. Jour. Nepal Geol. Soc.*, **37**, 25-44.
- Saijo, K., K. Kimura, T. Komatsubara, and H. Yagi (1995) Active faults in southwestern Kathmandu basin, central Nepal. *Jour. Nepal Geol Soc.*, 11 (Special Issue), 217-224.
- Sakai, T., T. Takagawa, A.P. Gajurel, H. Tabata, N. Ooi, and B.N. Upreti (2006) Discovery of sediment indicating rapid lake-level fall in the late Pleistocene Gokarna Formation, Kathmandu Valley, Nepal: implication for lake terrace formation. *Daiyonki Kenkyu (Quaternary Research)*, 45, 1, 99-112.
- United Nations Development Program (UNDP) (2013) Nepal, Comprehensive Disaster Risk Management Program (Report for MoUD/KVDA).
- Yagi, H., H. Maemoku, Y. Ohtsuki, K. Saijo, and T. Nakata (2000) Recent activities of active faults distributed in and around Kathmandu valley, Lower Himalayan Zone. *Proc. Hokudan international symposium and school on active faulting*, Hiroshima University, Hiroshima, 557-560.
- Yamanaka, H. (1982) Classification of geomorphic surfaces in the Kathmandu Valley and it's concerning problems. *Preprint of Congress, Assoc. of Japanese Geog.*, **21**, 58-59 (in Japanese).

### 3.4 Field Survey (Microtremor Measurement)

The outline of ground structure and its distribution can be estimated by geological map, geological cross section, geomorphology map and rock depth which are shown in clause 3.3. The other necessary information to assess the amplification by response analysis is the

physical property of the soil layer. Microtremor measurement was selected as the method of ground survey. Three types of microtremor measurement were conducted for separate purposes. Tripartite Microtremor Measurement was conducted to know the S-wave velocity structure of deep grounds up to several 100 meters. The purpose of the L-shape Array Microtremor was to know the S-wave velocity structure of shallow ground up to 50 meters. Single Microtremor Measurement was conducted to know the predominant period of the point and used for the confirmation of the ground model.

It should be noted that the results of this survey may include an error of 10% due to the inaccuracy of installation, observation and analysis. Also, the limitation of the measurement derives from the balance of power of microtremor and resolution of measuring instruments which is different in time and place. As there was less power of especially longer period of microtremor than expected, the accuracy of the S-wave velocity ( $V_s$ ) of deeper geology is not necessarily sufficient.

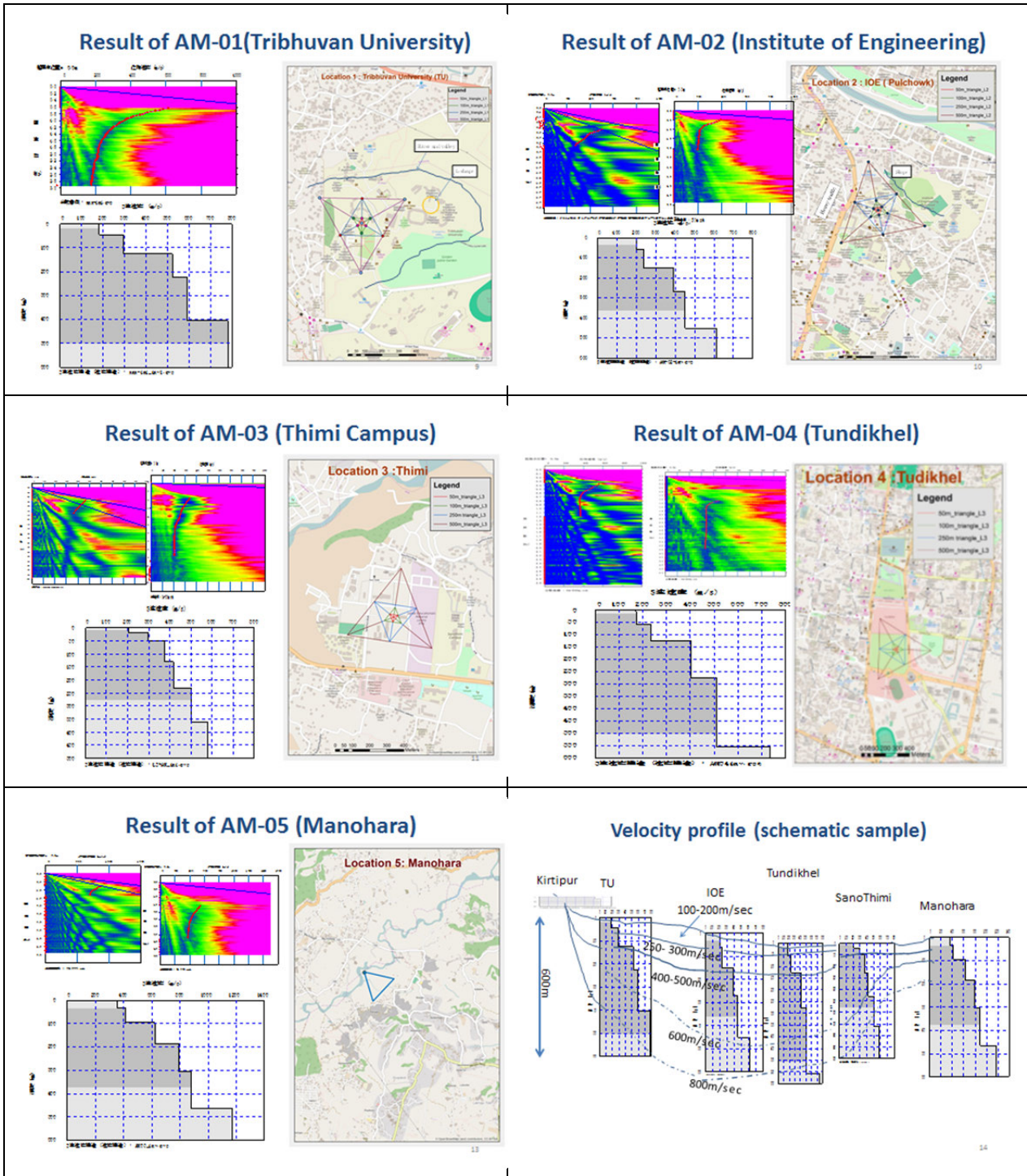
### **3.4.1 Tripartite Array Microtremor Measurement**

The thickness of the soil layer over rock to the ground surface in Kathmandu Valley was estimated around 500m in maximum based on the existing drilling logs and geological information. The S-wave velocity structure of the soil layer is indispensable for response analysis, but almost no information was found so far. For this purpose, tripartite array microtremor measurement was conducted. The length of tripartite was set for 50m, 100m, 250m and 500m. Five points were selected for measurement considering the distribution of strong motion observatory by DMG, USGS and Hokkaido Univ.

Four seismometers were set at the center and the corners of the triangle and the microtremor is observed at the same time. The predominant phase velocity for the frequency of observed microtremor was analyzed and the results are expressed as the dispersion curve. The velocity structure to satisfy the dispersion curve is acquired by inversion analysis. As the result is not unique, the initial model is used in the numerical calculation. The existing bore logs were used for making the initial model in this project. The output of the survey is limited by the observed frequency range. If the velocity of a deeper layer is desired, the range of observed frequency should be longer. In this study, the surveyed depth was 500m in maximum and the S-wave velocity was 600 to 800m/sec with some uncertainty.

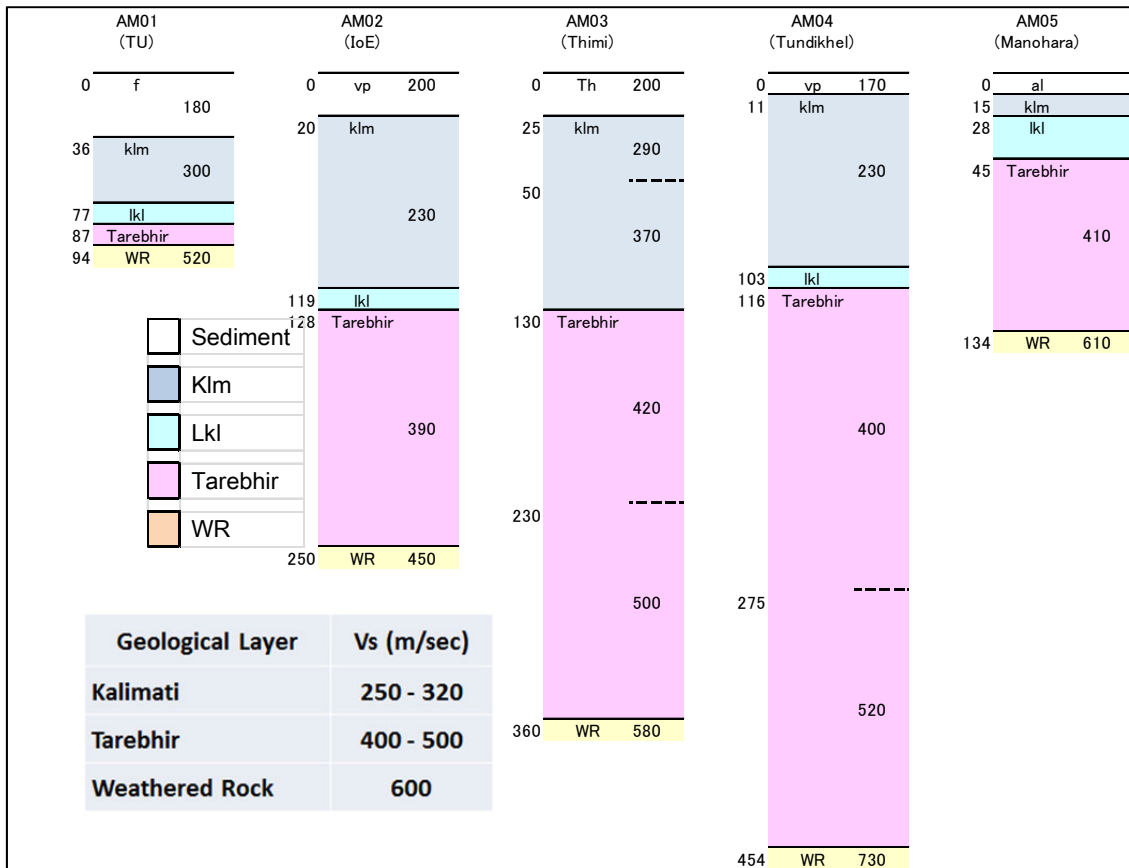
Figure 3.4.1, Figure 3.4.2, and Figure 3.4.3 show the distribution of measurement points, analyzed velocity structure and velocity structure model to fit the geological layer. The results of the survey are summarized as follows. The S-wave velocity of weathered rock, which is the deepest layer in this analysis is 600m/sec, Tarebhir layer shows 400 to 500m/sec and rather soft clayey Kalimati (Klm) layer shows 250 to 320m/sec.





Source: JICA Project Team

Figure 3.4.2 Results of Tripartite Array Microtremor Measurement



Source: JICA Project Team

**Figure 3.4.3 S-wave Velocity Structure of Deep Ground by Tripartite Array  
 Microtremor Measurement and Soil Layer**

### 3.4.2 L-shape Array Microtremor Measurement with Three Point Array

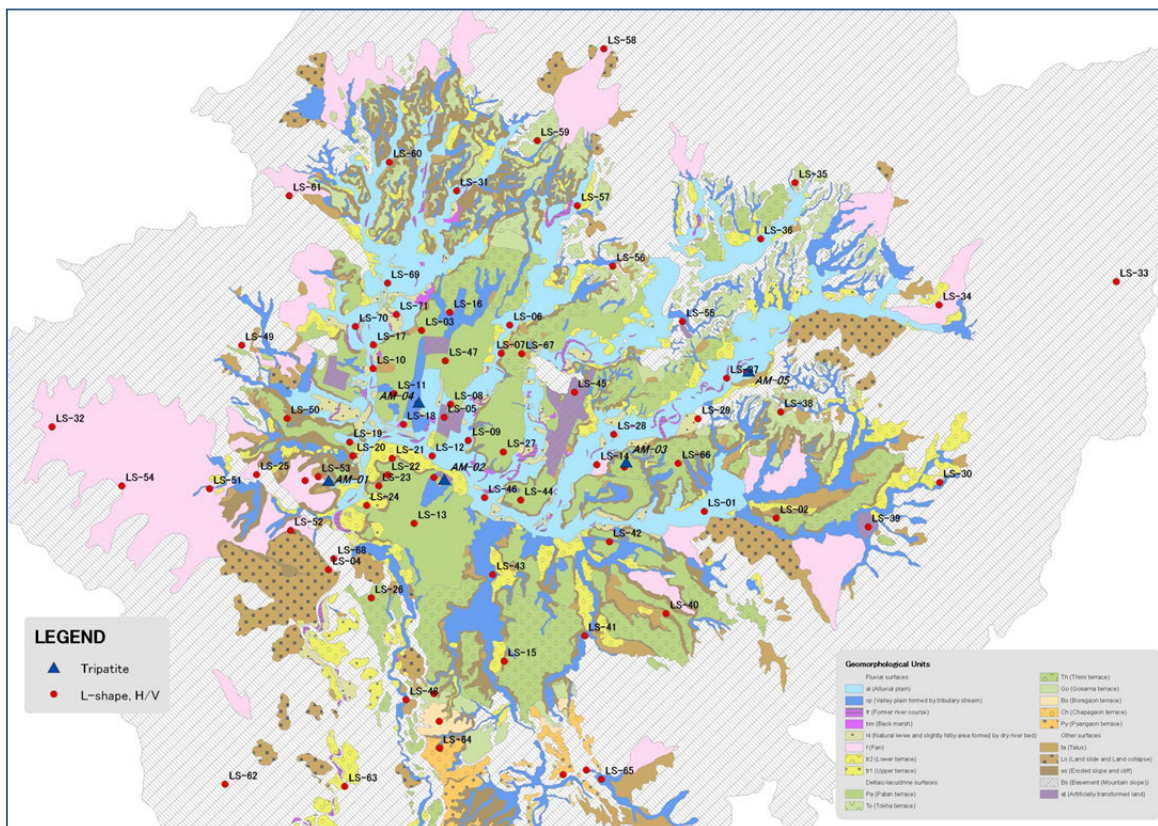
This survey was conducted to know the S-wave velocity structure of the soft surface layer up to 50 meters. In the beginning, it was planned to take measurements at 50 points, but it was increased to 74 points to cover all the geomorphological classes considering the complexity of the structure of subsurface ground than expected (Figure 3.4.4). Before this project, the only available information about S-wave velocity was the results of five PS logging in the 2002 JICA project up to 30 meters in depth. The product of the L-shape array is epoch-making information, although the volume is not enough yet. It is reported that Assistant Professor Chamlagain of Tribhuvan University has conducted an array microtremor measurements with 200m lengths at 40 points in Kathmandu Valley. If the results become available, the combination of two data sets can produce a more precise ground model.

Among the 74 points, three points array microtremor measurements were conducted simultaneously at 39 points and jointly analyzed. The survey depth of L-shape array microtremor measurement was 30m in the initial plan based on the existing information and limitation of usable open area. After the preliminary analysis of first several observations, it

was found that the survey depth should be increased to 50m in some areas.

The average S-wave velocity over 30m depth from ground surface (AVS30) is popularly used to know the general amplification characteristics of the ground, softness or “shakability”. The distribution of AVS30 was calculated in the first step of the analysis and compared with the elevation (Figure 3.4.5). AVS30 and the elevation show positive correlation in general which may be reduced to the difference of sediment period.

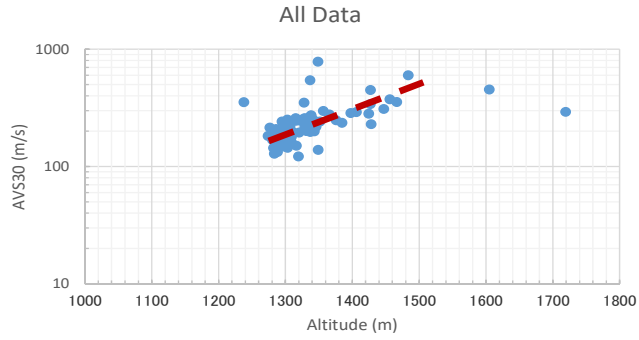
The S-wave velocity profile along the depth was studied next. In Figure 3.4.6, several velocity profiles are plotted in one graph by geomorphological units. Several units show almost the same profile, while several other units show dispersed profiles referring to the difference of elevation. For example, the profiles of alluvial lowland (al) were plotted along the elevation from 1280m to 1340m in Figure 3.4.7. This figure shows that low velocity continues to deep depths if the elevation is low and the low velocity layer becomes thin and the high velocity layer appears from shallower depth if the elevation is high. Figure 3.4.8 is the S-wave velocity structure model for alluvial lowland made from the relation with elevation. The relation of S-wave velocity of 10m depth interval and elevation is modeled in this figure. In ground modeling, the S-wave velocity of shallow layer was decided by this model.



Source: JICA Project Team

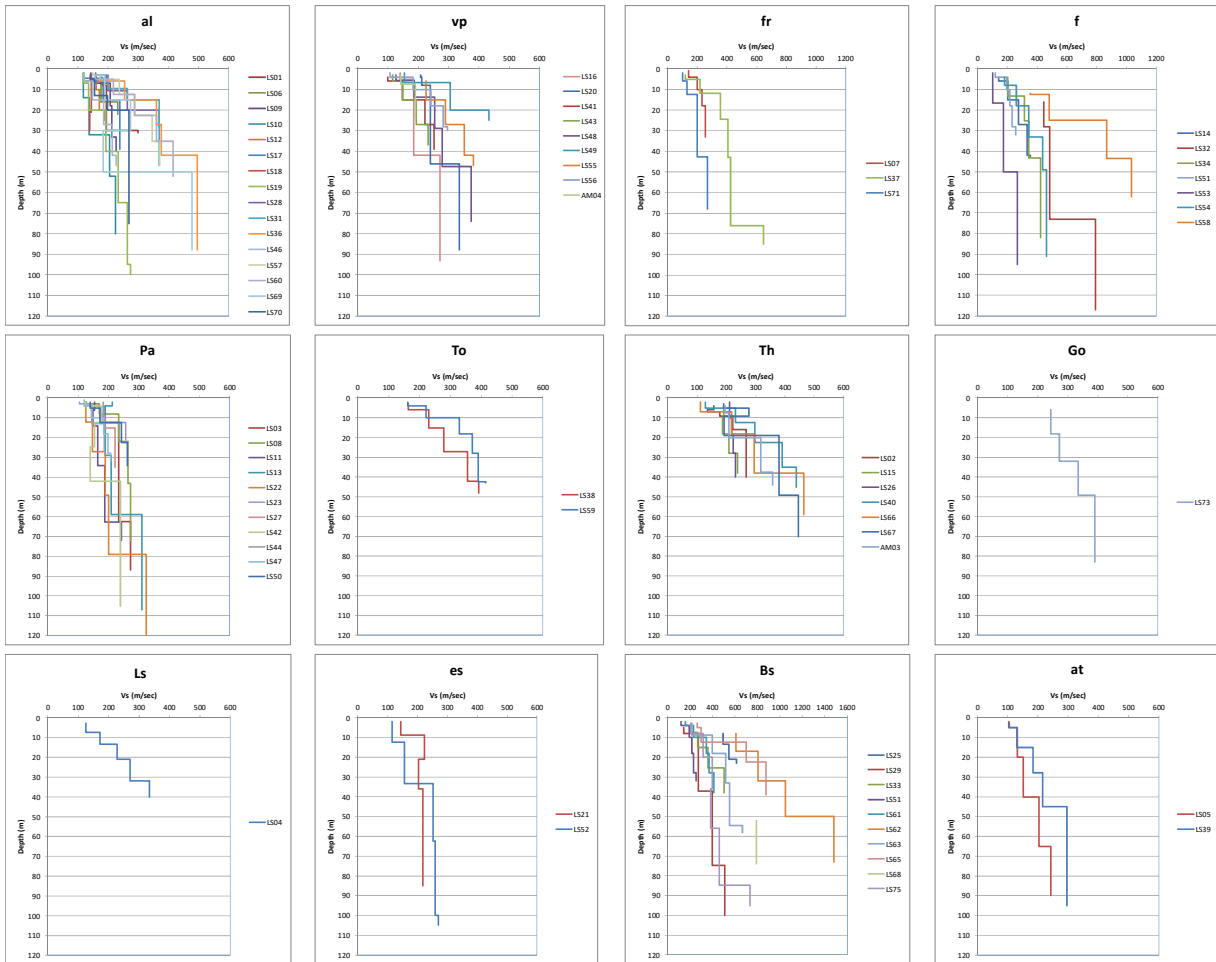
**Figure 3.4.4 Measurement Points of L-shape Microtremor Measurement**





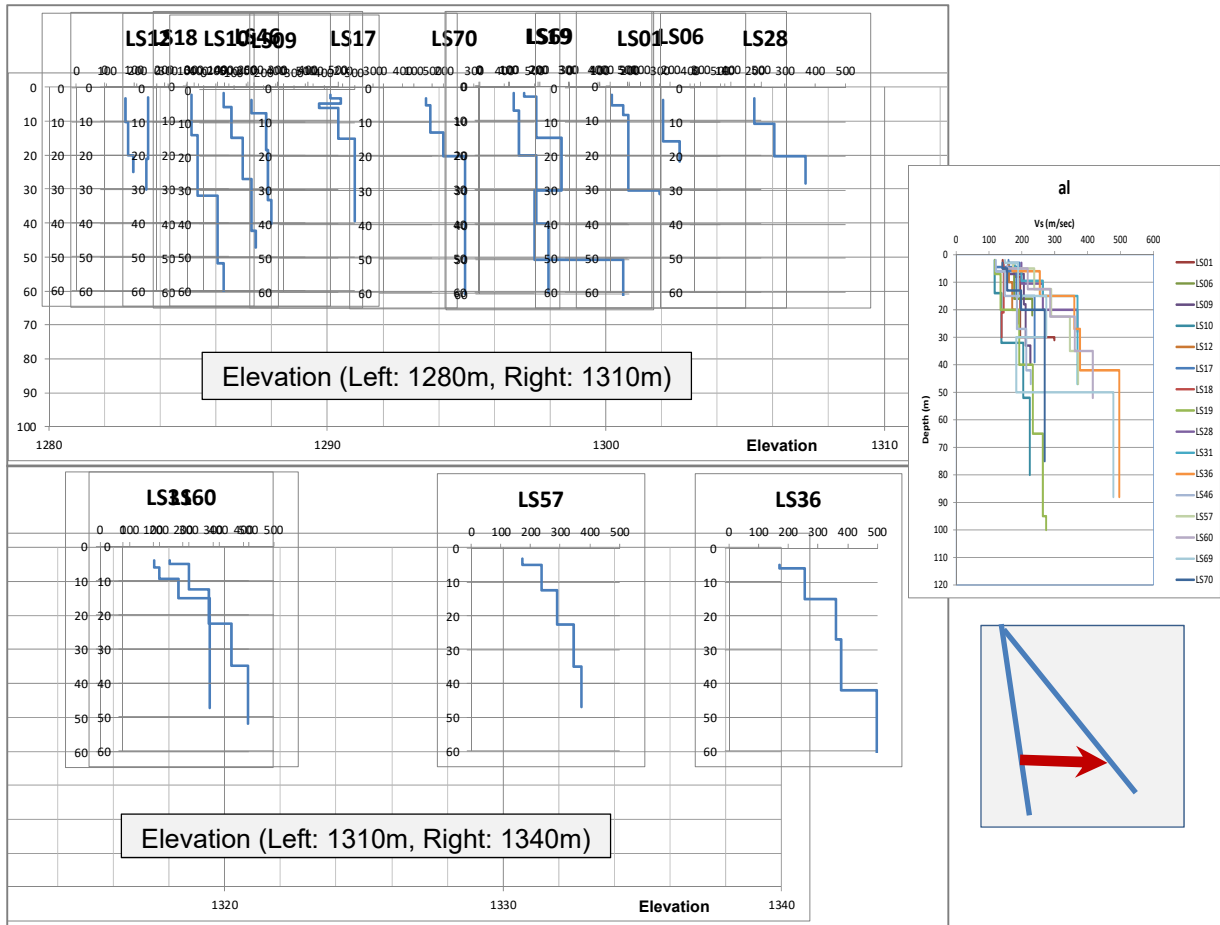
Source: JICA Project Team

**Figure 3.4.5 Relation of AVS30 and Elevation**



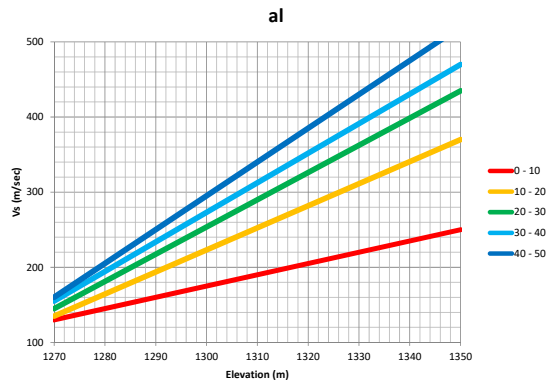
Source: JICA Project Team

**Figure 3.4.6 Observed S-wave Velocity Profile by Geomorphological Unit**



Source: JICA Project Team

**Figure 3.4.7** Relation of Observed S-wave Velocity Profile with Elevation for Alluvial Lowland (al)



Source: JICA Project Team

**Figure 3.4.8** Relation of S-wave Velocity Structure Model in 10m Depth Interval with Elevation for Alluvial Lowland (al)

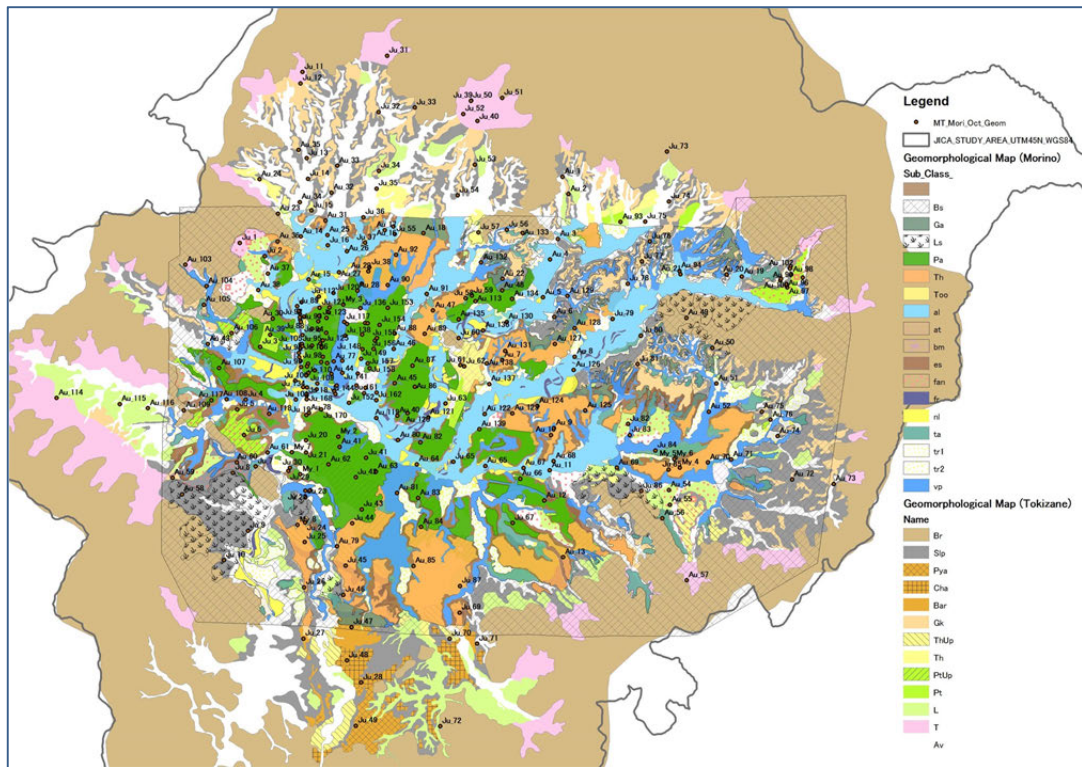
### 3.4.3 Single Point Microtremor Measurement

Among several scientific single point microtremor studies, the data by Paudyal (2012) and Kukidome et al. (2008) were available. The numbers of observation points are 172 and 38 respectively, 210 in total. In this project, 78 points were measured along with L-shape microtremor measurement and 308 points (Figure 3.4.9) were measured independently, 518 points in total.

Parts of the result are shown below. Three types of predominant periods are found. The peaks of 2~4 sec may correspond to the boundary between rock and sediment layer. The peak of around 1 sec and shorter peak of 0.3~0.5 sec, which may correspond to subsurface soft layers are also found (Figure 3.4.10, Figure 3.4.11 and Figure 3.4.12). The distribution of these peaks seems to be corresponding to the structure of ground.

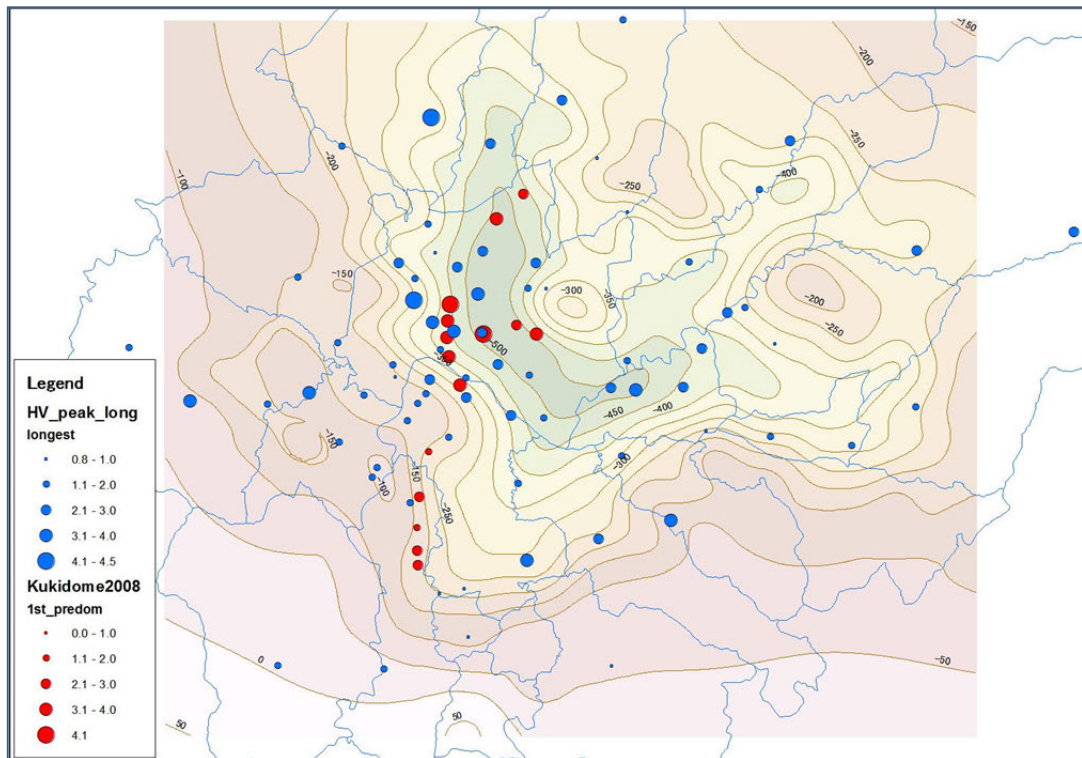
To confirm the ground model in clause 3.5, the 1st predominant period by single point microtremor (Figure 3.4.13) was compared with the calculated value by ground model (Figure 3.4.14). The calculated periods are the 1st and 2nd peak values of SH-wave transfer function by ground model. The observed 1st predominant periods are classified into two groups. The period of Group-A (blue ellipse in Figure 3.4.14) is 1-4 sec, and Group-B (red ellipse in Figure 3.4.14) is around 1 sec. Group-A roughly coincide with the calculated value of 1st peak value of SH-wave transfer function. The period of Group-B is roughly corresponding to the calculated value of 2nd peak value of SH-wave transfer function. This may mean that Group-B reflects the effect of K1m or shallower layers.

The weak point of a single point microtremor is that it is impossible to know which layer boundary is the cause of the observed predominant period by single point microtremor observation only. In other words, it is impossible to decide the velocity structure of the ground only by a single point microtremor measurement. The predominant period observed by a single point microtremor measurement should be carefully used paying attention to which layer is the cause of resonance in the future.



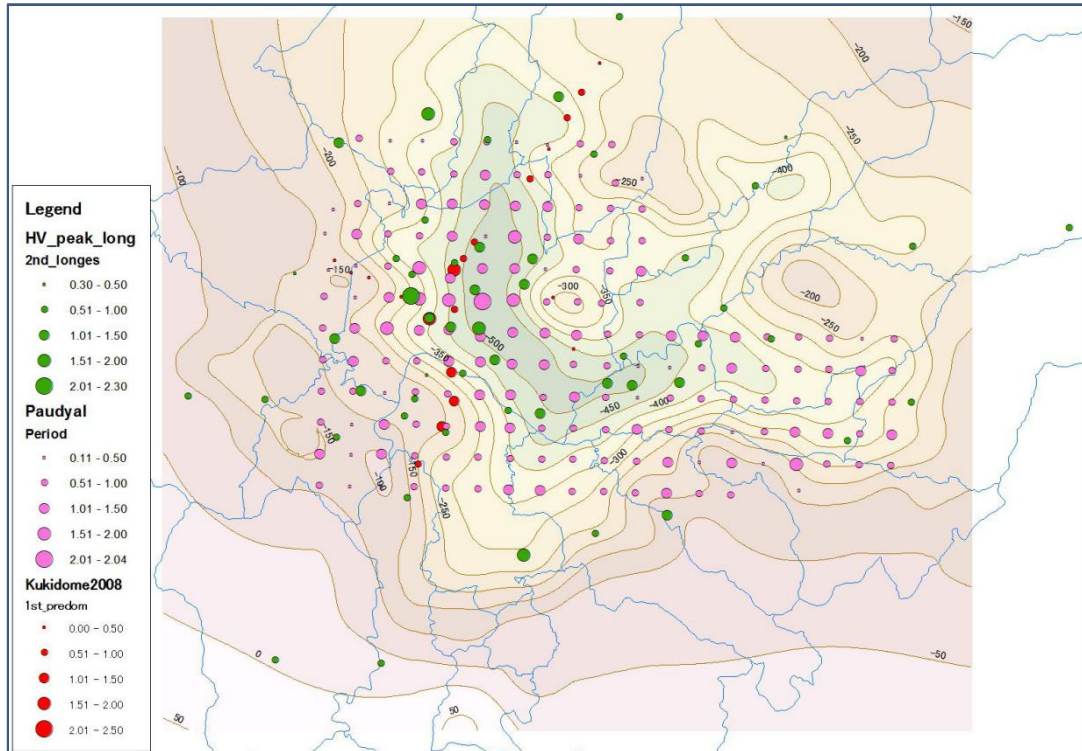
Source: JICA Project Team

**Figure 3.4.9 Measurement Points of Single Point Microtremor Measurement except Existing and L-shape Points**



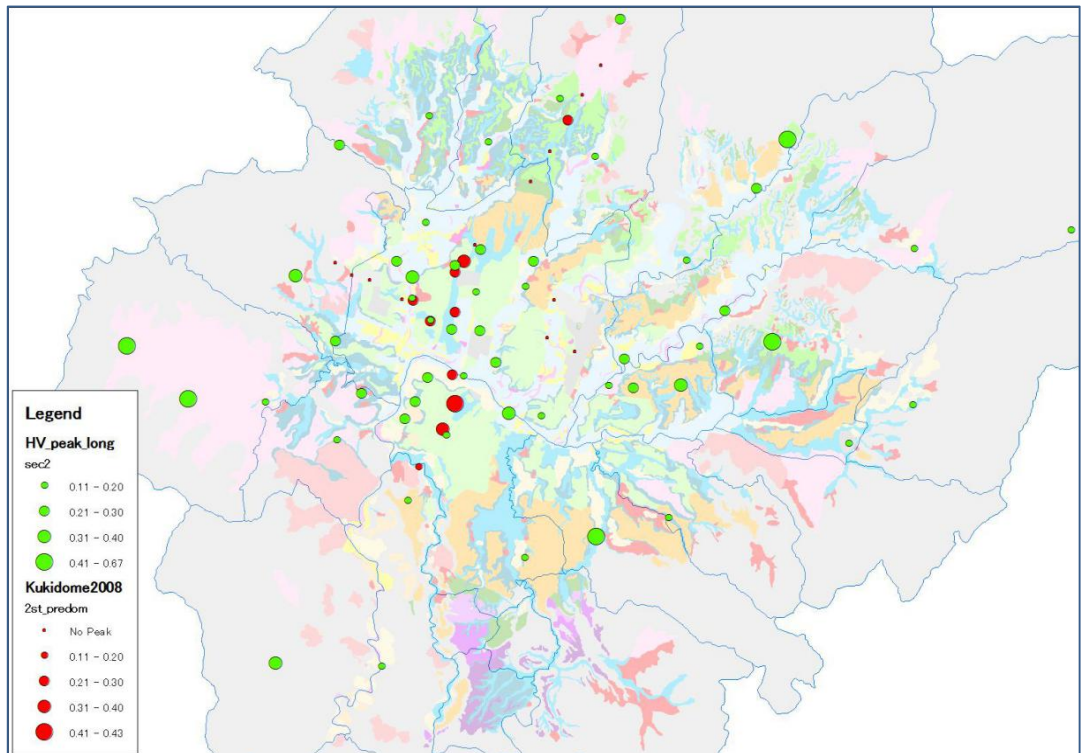
Source: JICA Project Team

**Figure 3.4.10 1st Predominant Period by Single Microtremor Measurement and Rock Depth by Gravity Anomaly**



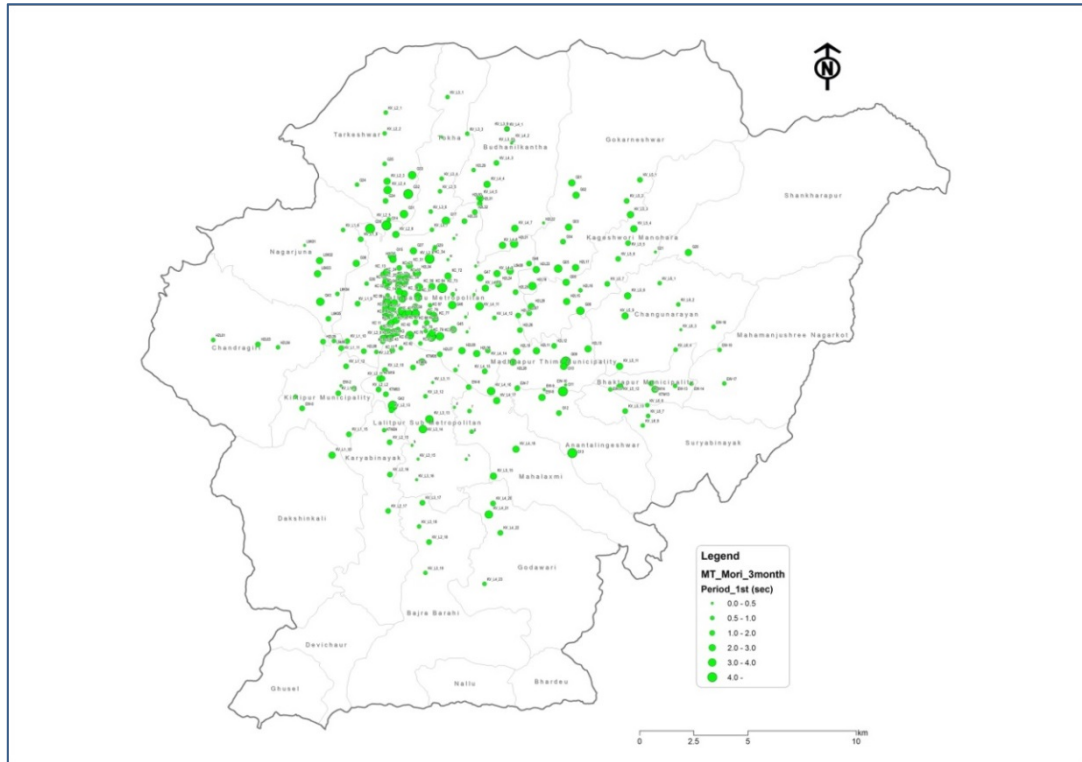
Source: JICA Project Team

**Figure 3.4.11** Predominant Period around 1~2 sec. by Single Microtremor Measurement and Rock Depth by Gravity Anomaly



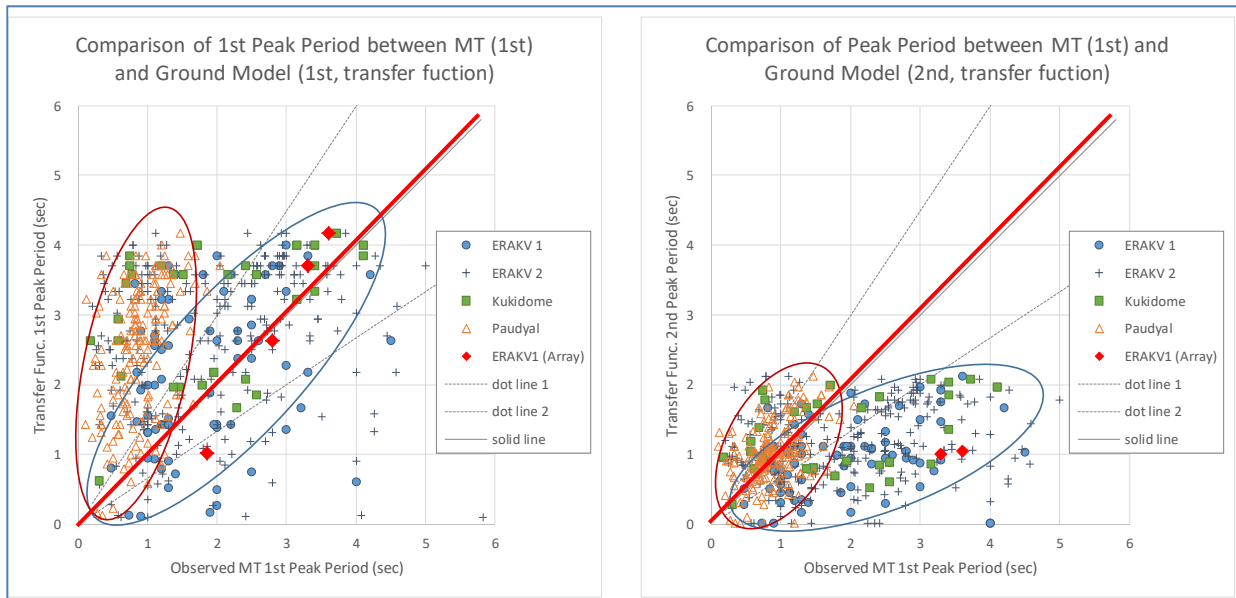
Source: JICA Project Team

**Figure 3.4.12** Predominant Period less than 1 sec. by Single Microtremor Measurement and Geomorphological Class



Source: JICA Project Team

**Figure 3.4.13 1st Predominant Period by Single Microtremor Measurement except Existing and L-shape Points**



Note: (left) 1st and (right) 2nd peak of SH-wave Transfer Function

Source: JICA Project Team

**Figure 3.4.14 Comparison of Predominant Period by Microtremor Measurement and by Ground Model**

### **References (3.4)**

- Kukidome, T., S. Mori and N. P. Bhandary (2009) The predominant period distribution in Kathmandu Valley ground by microtremors, 44th Japan National Conference on Geotechnical Engineering. (in Japanese)
- Paudyal, Y. R. (2012) Microtremor Based Earthquake Disaster Risk Evaluation of the Kathmandu Valley, Doctoral Thesis, School of Science and Engineering of Ehime University.

## **3.5 Modelling of the Ground**

The ground was modeled through three steps; modeling between the rock surface to the Kalimati layer (Klm), modeling between Klm to the ground surface and the integration of them.

### **3.5.1 Modeling between rock surface to Klm**

The 3D distribution of Rock surface, surface of Tarebhir layer, Lukundor layer (Lkl) and Kalimati layer (Klm) was estimated in this step. The depth of the rock surface was estimated from existing gravity survey and collected deep drilling logs (see Figure 3.3.21). The 3D distribution of Tarebhir, Lkl and Klm was modeled based on the 2km depth grid data taken from a geological cross section (Figure 3.3.22). The rock outcrop area, which is shown in the geomorphology map (Figure 3.3.6) was also considered.

The S-wave velocity of Rock, Tarebhir, Lkl and Klm layer was estimated from tripartite microtremor measurement (Figure 3.4.3).

### **3.5.2 Modeling between Klm to ground surface**

The geomorphology map (Figure 3.3.6) and L-shape array microtremor measurement (Figure 3.4.6) were used to model the subsurface ground structure. At first, one geomorphological unit which has the maximum area in the grid was assigned to each 250m grid. Next, 10m depth interval S-wave velocity structure was made for the grid, except the rock outcrop grid, based on The relation of S-wave velocity and elevation ( Figure 3.4.7 and Figure 3.4.8) was also considered to make the model of grid which was assigned to the geomorphological unit of al, bm, ta, nl, vp and fa.

### **3.5.3 Integration of ground model**

The average depth of Rock, Tarebhir, Lkl and Klm for 250m grid was set from 3D model. The total ground model can be created putting the subsurface ground model on it. The issue in connecting the two models is the difficulty to decide the top of Klm in the subsurface ground model. The subsurface ground model includes only the S-wave structure and the

geology is uncertain. The accuracy of depth of K<sub>lm</sub> in the geological cross section is not enough for modeling. Therefore, the deep structure and subsurface structure was connected at the depth where the S-wave velocity of the subsurface layer becomes the same as K<sub>lm</sub>.

The created ground model was confirmed by observed data. Figure 3.5.1 is the example of confirmation at the DMG office. The predominant frequency of amplification function derived from the observed earthquake wave (upper left), spectral ratio to the rock site at Phulchauki (PKI) (upper right), and microtremor measurement (lower left) are almost same to the one calculated (lower right) by the constructed ground model. This may be an evidence of a reasonable ground model.

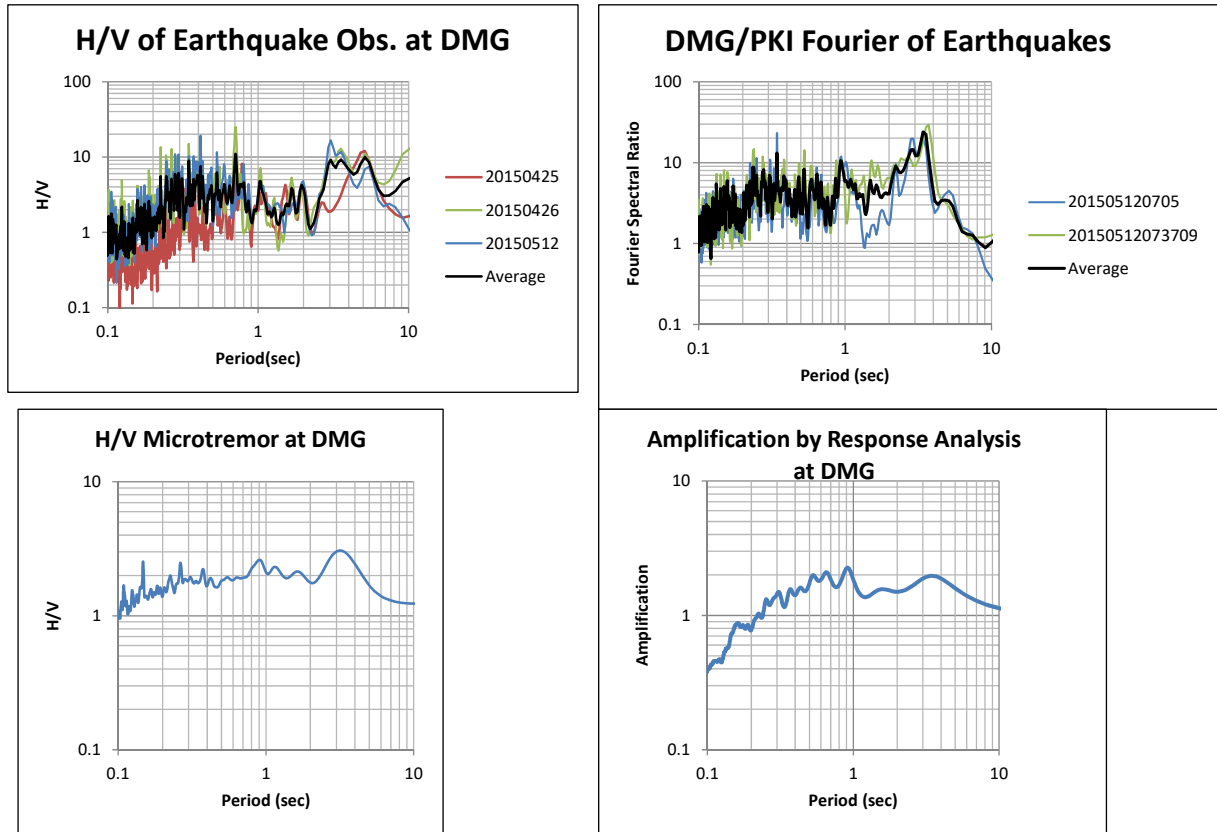
Several reasons are supposed for the difference of amplification value. Rather than rock, the response analysis considers the shallow layer, but, the earthquake record is also influenced by deeper layers. The ground of PKI observatory may be very hard and the S-wave velocity is much higher than the rock of the ground model. The two-dimensional effect of the Kathmandu Valley may have affected the ground motion but is not included in the response analysis. The strain levels between microtremor and earthquake is remarkably different. The amplification value by H/V (Horizontal vs Vertical ratio) microtremor measurement has quite a higher value of uncertainty. These are the examples of the considerable reasons and are necessary to be considered in the future revision of hazard assessment.

Ground model was made for each 250m grid. Examples of cross section of the ground model are shown in Figure 3.5.2. This map looks like a bundle of pencils. Several maps are made to check the ground model. Figure 3.5.3 shows the distribution of AVS30 (Average V<sub>s</sub> over 30m from surface). Figure 3.5.4 shows the difference of amplification for small and large input acceleration. The amplification factor in Kathmandu Valley is generally low. The low amplification is obvious in case of large input rather than small input especially in the center of the valley where the sediment layer is thick. The non-linearity<sup>1</sup> effect of K<sub>lm</sub> may be the main reason. The predominant period of the ground can be calculated from the ground model. Figure 3.5.5 shows the 1st peak of the transfer function by SH wave multiple reflection response analysis. The constructed ground model is shown in 3D view. The East-West view in almost runs along the four strong motion observatories of Hokkaido University and the North-South view runs through Pashpatinath. In Figure 3.5.7, the used drilling logs are shown.

---

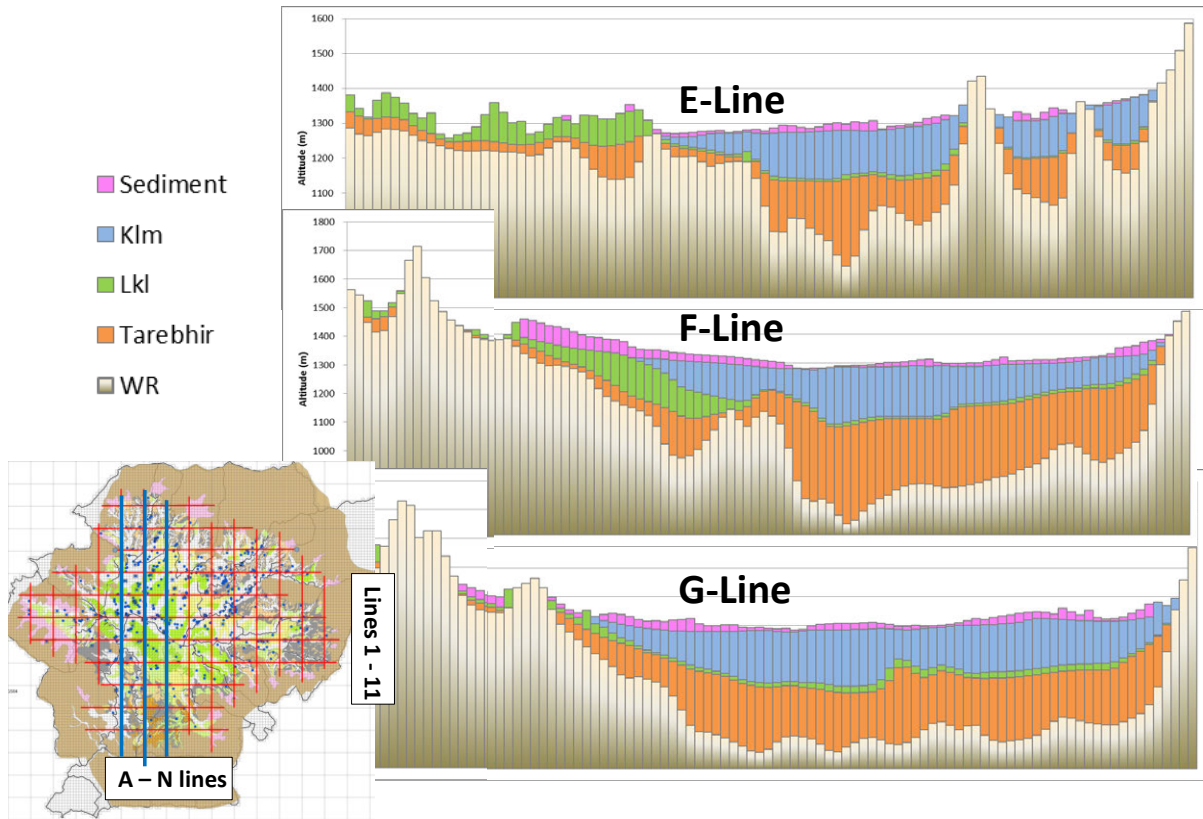
<sup>1</sup> Non-linearity of the ground: If input earthquake motion is large, the strain of the ground becomes large and the response becomes smaller as compared to the linear behaviour. In the case of the reproduction of the Gorkha Earthquake, if original input acceleration by GMPE (correction factor = 1.0) is used, non-linearity becomes eminent and the surface PGA becomes 1/4 of the actual observation. To get the observed PGA by response analysis, input PGA should be reduced to 1/5 of the value by GMPE. Non-linearity is prominent in the former case but not so obvious in the latter case. The difference of 1/5 and 1/4 may be attributed to the non-linearity of the soil. The dynamic soil test was first conducted recently by a local researcher to study the non-linearity (Chamlagain, 2016).  
GMPE: Ground Motion Prediction Equation





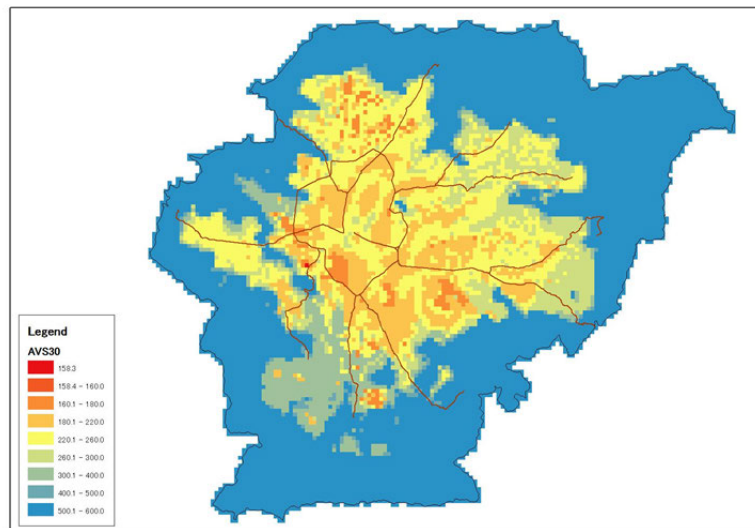
Source: JICA Project Team and DMG

**Figure 3.5.1 Comparison of Amplification Function Estimated from Earthquake Record (upper), Microtremor Measurement (lower left) and Ground Model (lower right) at DMG point**



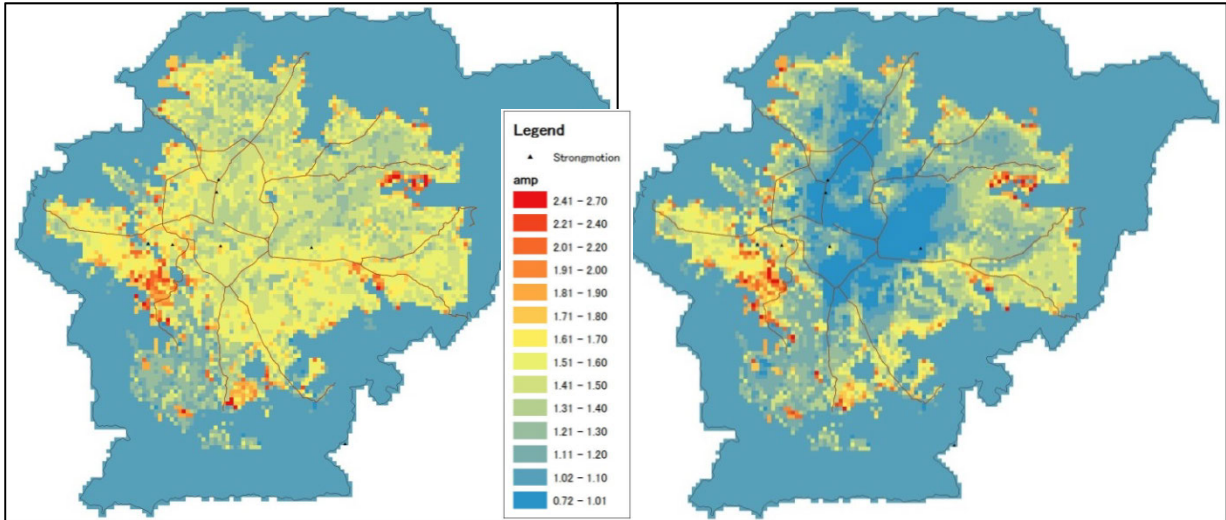
Source: JICA Project Team

**Figure 3.5.2** Examples of North-South Cross Section of Ground Grid Model



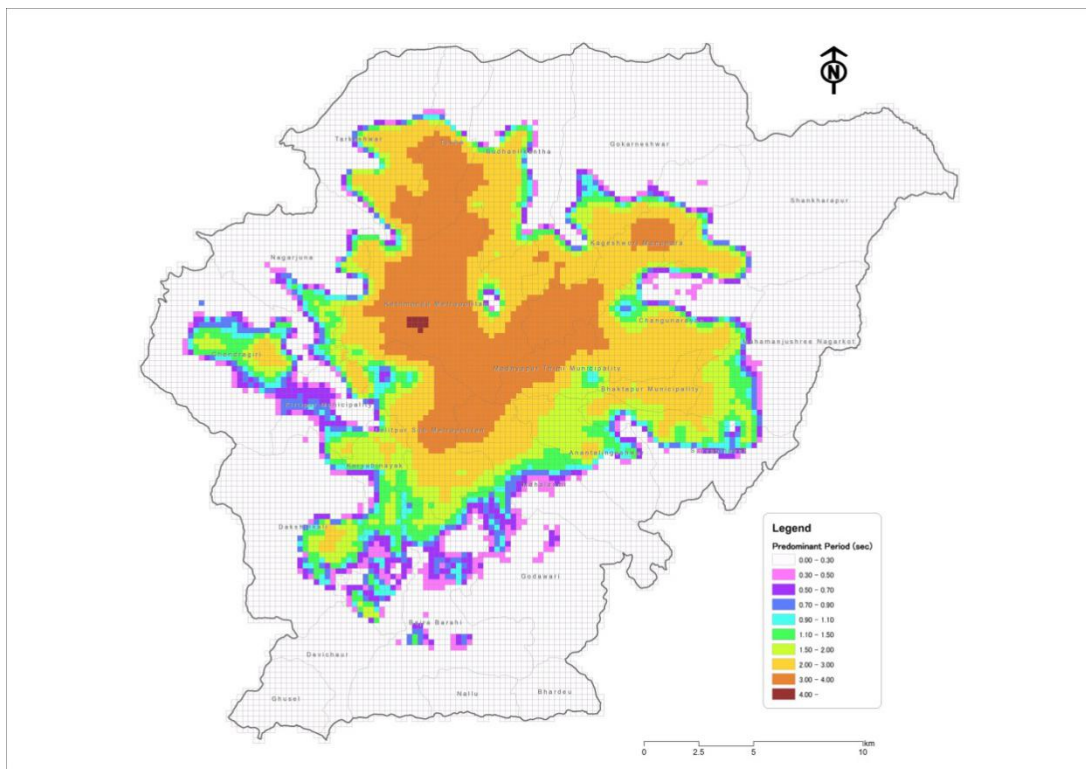
Source: JICA Project Team

**Figure 3.5.3** Estimated AVS30 from Ground Model



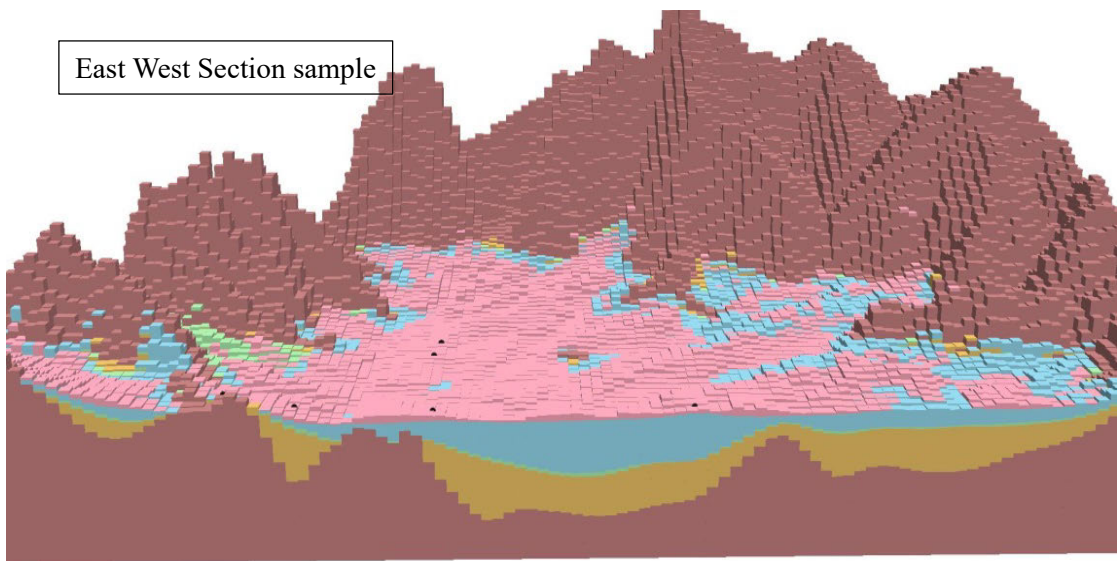
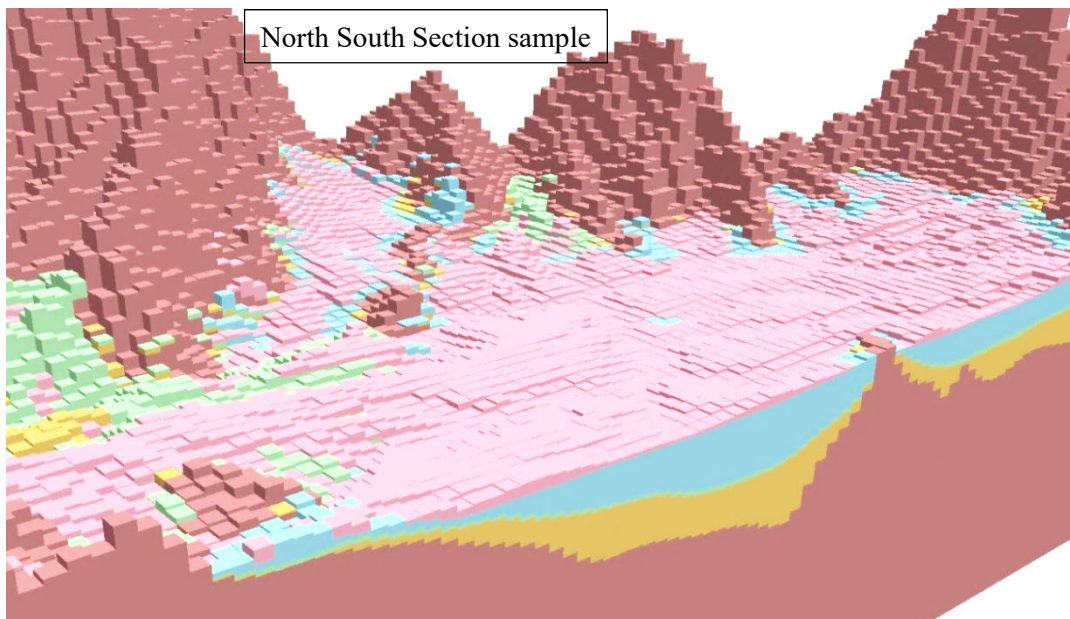
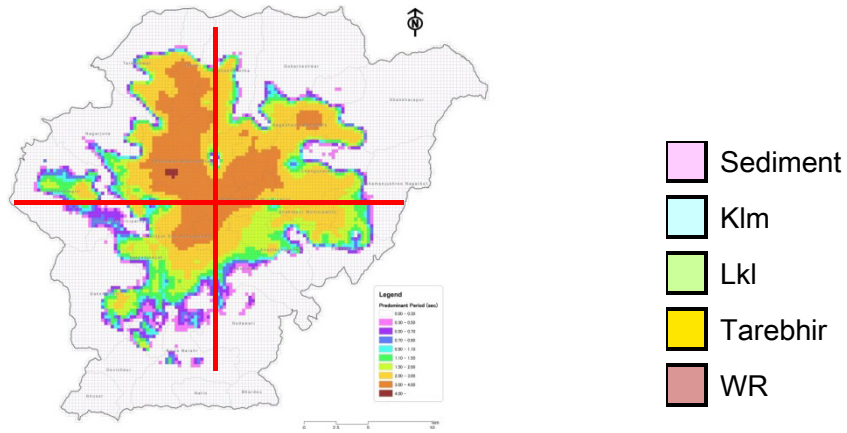
Source: JICA Project Team

**Figure 3.5.4 Amplification Factor by Subsurface Soil Layer for Small Input (left) and Large Input (right)**



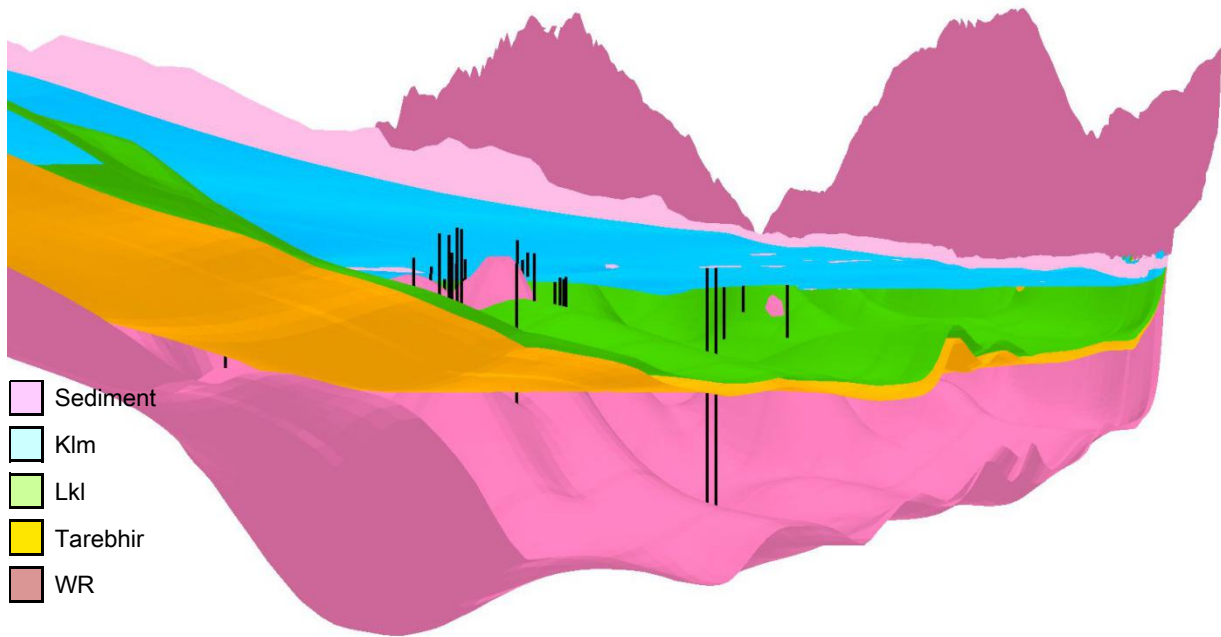
Source: JICA Project Team

**Figure 3.5.5 Predominant Period of the Ground by Response Analysis, 1st peak of the transfer function by SH wave multiple reflection theory**



Note: Black dots show the strong motion observatories at the time of Gorkha Earthquake  
 Source: JICA Project Team

**Figure 3.5.6 3D Expression of Grid Ground Model**



Source: JICA Project Team

**Figure 3.5.7 3D Expression of Soil Layer Boundary, Ground surface (pink), surface of Klm (light blue), Lkl (green), Tarebhir (camel) and Rock (purple). Black bars are drilling logs which reach to rock.**

### References (3.5)

- Chamlagain, D., G. Lamzo, A. Pagliaroli, N. Poovarodom, D. Gautam and B. Giri (2016) Cyclic Geotechnical Characterization of Soils from Kathmandu Valley with Reference to 2015 Gorkha Seismic Sequence, International Workshop on Gorkha Earthquake, Ministry of Industry and DMG, April 2016.

### 3.6 Calculation of Earthquake Motion at Bedrock

The earthquake motion generated at the earthquake source fault propagates to the deep ground and finally reaches the bedrock under the considered site. In this project, the earthquake motion at the bedrock was evaluated using the Ground Motion Prediction Equation (GMPE) because of the insufficiency of radiation property of the earthquake motion from the fault, propagation characteristic of the deep ground and resources for numerical simulation.

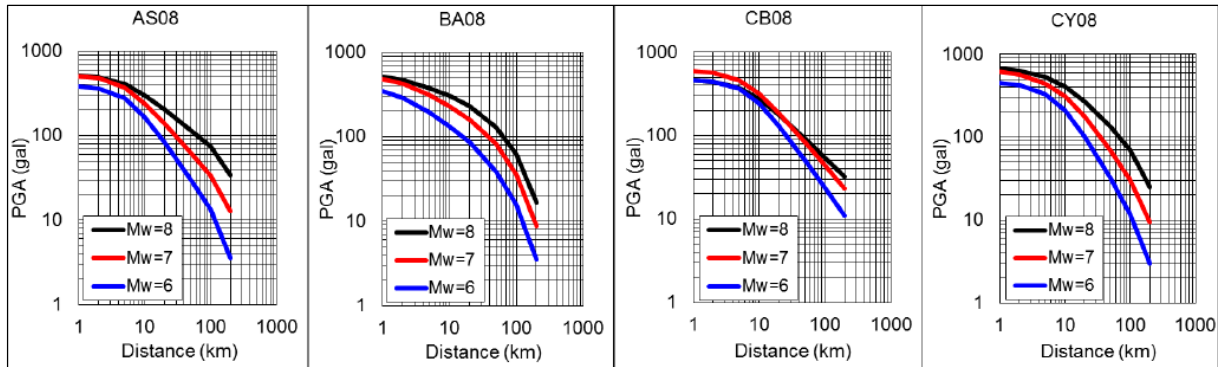
The earthquake motion of scenario earthquake at bedrock was calculated following the conditions below.

- Bedrock for the analysis in this project is defined as weathered rock ( $V_s=600\text{m/sec}$ ), which corresponds to the deepest layer of the ground model.
- Earthquake motion at the bedrock is calculated using existing GMPE.

- GMPE derived from the observed strong motion records in Nepal is not proposed so far because of the shortage of data. The up to date “New Generation Attenuation” (NGA) equations were used. NGA was studied based on the strong motion record from the world and introduces the effects of fault type, ground condition, etc.
- Used GMPE in this project and the 2002 JICA project are shown in Table 3.6.1 and Figure 3.6.1.

**Table 3.6.1 Used GMPE in this Project and 2002 JICA Project**

GMPE in this Project	GMPE in 2002 JICA Project
(AS08) Abrahamson N. and W. Silva (2008) (BA08) Boore D. M. and G. M. Atkinson (2008) (CB08) Campbell K. W. and Y. Bozorgnia (2008) (CY08) Chiou B. S.-J. and R. R. Youngs (2008) Developed in NGA project. Average of above four equations was used considering the uncertainty.	Boore, D. M., W. B. Joyner, and T. E. Fumal (1997) $\ln Y = 0.527(M-6) - 0.778 \ln R - 0.242 - 0.371 \ln$ (AVS30/1396)



Source: JICA Project Team

**Figure 3.6.1 NGA Attenuation Function for PGA**

PGA at bedrock was calculated by GMPE. Used GMPEs are developed in the NGA project in 2008 and the average of four GMPEs was adopted. The reliable GMPE reflecting the local conditions is usually adopted if available, otherwise the most appropriate GMPE for the resemble condition is selected from the existing formulas in the world. As no reliable GMPE is proposed for Nepal or the Himalayan region based on the local records so far, the GMPE reflecting the tectonics of these regions are selected. Many GMPEs are developed based on the Japanese strong motion but they are not suitable for Nepal because the used data are mainly oceanic plate related deep events. GMPEs developed in NGA project are applicable to the shallow (~30km) crustal earthquakes. NGA formulas are suitable for Nepal because they used enormous strong motion records from the world and can be applied to many conditions. The application of the formula by Youngs et al. (1997) was suggested in the 3rd JCC but it was agreed to adopt NGA because recent formulas reflect the current numerical approach more than the previous one. In the process of GMPE selection, the exchange of views with DMG was helpful.

PGA at bedrock was roughly calculated by the NGA formula. The calculated values are; 50 ~ 60 gal for Far-Mid Western Nepal Scenario, 70 ~ 100 gal for Western Nepal Scenario, 170 ~ 400 gal for Central Nepal South Scenario, 140 ~ 200 gal for 1934 Bihar-Nepal earthquake and 360 ~ 600 gal for the Gorkha Earthquake. The actual observed PGA of Gorkha Earthquake at Kirtipur, where the base rock is very shallow, was 150 gal (EW). The calculated PGA by the NGA formula is four times larger than the observed one. This preliminary analysis revealed the unusual character of the Gorkha Earthquake, namely the bedrock motion is very small compared to the experience.

### **References (3.6)**

- Abrahamson N. and W. Silva (2008) Summary of the Abrahamson & Silva NGA Ground-Motion Relations, *Earthquake Spectra*, Vol. 24, Issue 1, pp. 67-97.
- Boore D. M. and G. M. Atkinson (2008) Ground-Motion Prediction Equations for the Average Horizontal Component of PGA, PGV, and 5%-Damped PSA at Spectral Periods between 0.01 s and 10.0 s, *Earthquake Spectra*, Vol. 24, Issue 1, pp. 99-138.
- Boore, D. M., W. B. Joyner, and T. E. Fumal (1997) Equations for estimating horizontal response spectra and peak acceleration from western North American earthquakes: A summary of recent work, *Seismol. Res. Lett.*, 68, pp. 128-153.
- Campbell K. W. and Y. Bozorgnia (2008) NGA Ground Motion Model for the Geometric Mean Horizontal Component of PGA, PGV, PGD and 5% Damped Linear Elastic Response Spectra for Periods Ranging from 0.01 to 10 s, *Earthquake Spectra*, Vol. 24, Issue 1, pp. 139-171.
- Chiou B. S.-J, and R. R. Youngs (2008) NGA Model for the Average Horizontal Component of Peak Ground Motion and Response Spectra, *Earthquake Spectra*, Vol. 24, Issue 1, pp. 173-215.
- Youngs, R. R., S. J. Chiou, W. J. Silva, and J. R. Humphrey (1997) Strong ground motion attenuation relationships for subduction zone earthquakes, *Seismological Research Letters*, vol. 68, no. 1, pp. 58-73.

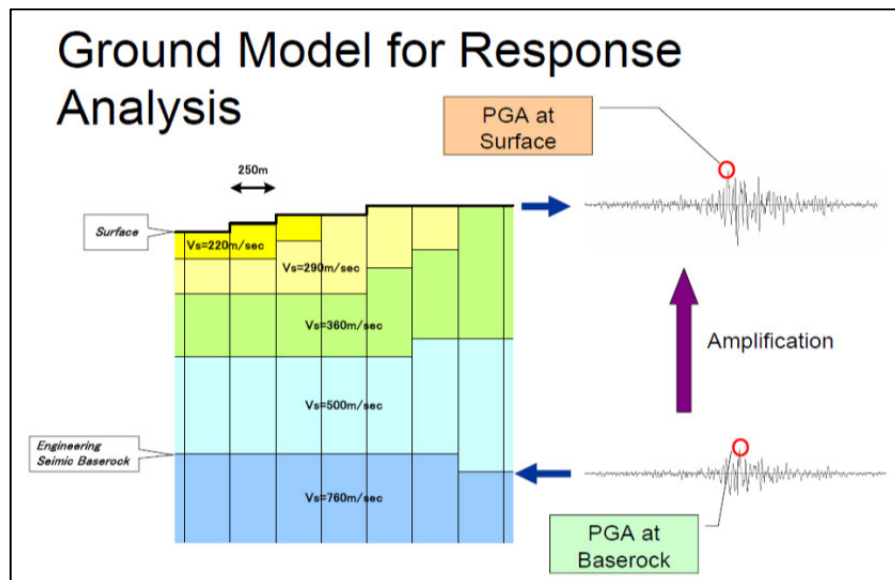
### **3.7 Calculation of Earthquake Motion at Ground Surface**

The earthquake motion (PGA) of the scenario earthquake at the ground surface was calculated following the conditions below.

- Amplification is evaluated by one dimensional response analysis (SHAKE). Flow of the analysis is shown in Figure 3.7.1.
- The waveform of the Gorkha Earthquake which was observed at Kirtipur is used for input motion to the ground model at the weathered base rock. The Kirtipur record is the only one waveform of shallow rock condition for the main shock of the Gorkha

Earthquake. The Kirtipur record is converted to the  $V_s=600\text{m/sec}$  site condition by inverse response analysis.

- Amplitude of input waveform is adjusted to the calculated PGA by GMPE at the base rock.
- Ground model for response analysis is constructed by drilling log, geomorphology map, microtremor survey, etc. in this project (Clause 4.6).
- The Japanese non-linearity property of soil (Central Disaster Management Council (2003)) is borrowed as no information is available in Nepal so far.
- PGV is calculated by integrating the surface acceleration waveform. Seismic Intensity in the MMI scale is estimated from existing empirical in relation with PGA. Acceleration Response Spectra (Sa) and Spectral Intensity (SI) are calculated following the definition from the acceleration waveform.



Source: JICA Project Team

**Figure 3.7.1 Flow of Response Analysis**

### 3.7.1 Input Waveform

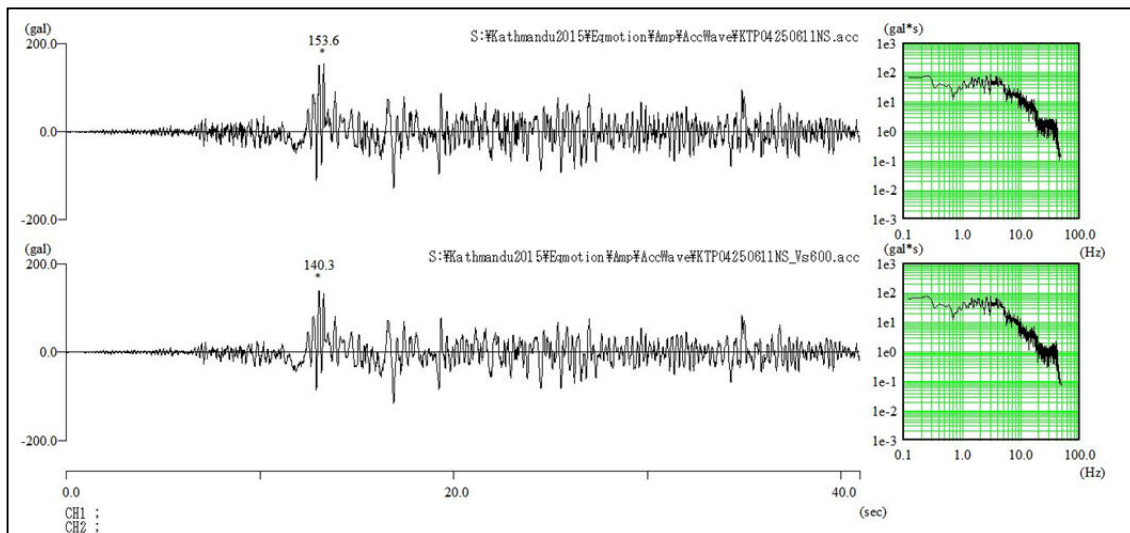
DMG provided the strong motion record<sup>2</sup> of the Gorkha Earthquake and largest aftershock observed at the DMG office and largest aftershock observed at Phulchauki (PKI) station on the hard rock located southeast of the Kathmandu Valley rim. The waveform observed at Kantipath (KATNP) by USGS, including the main shock, largest aftershock and other smaller aftershocks, is freely accessible on the website. The record of the main shock acquired at Kirtipur, Tribhuvan Univ., IoE and Sano Thimi through the joint research work of Hokkaido Univ. with Tribhuvan Univ. is open on the scientific paper (Takai et al.

<sup>2</sup> DMG provided the waveform of main shock at DMG and two aftershocks, which occurred on same day and the largest one, at DMG and PKI. USGS opens the waveform of main shock and ten aftershocks. The PGA by USGS observation shows a smaller value than the existing attenuation equations like the result of Dhakal et al. (2015). Recently DMG published the technical paper about strong motion records before the Gorkha Earthquake (Bhattarai et al., 2016).



(2016b)). The PGA and PGV values of the largest aftershock observed by Hokkaido University are also reported in Takai et al. (2016a).

The observed record at Kirtipur (KTP) was used as the input waveform for response analysis as the KTP record is the only waveform of the main shock observed at a semi-rock ground condition. The record observed at the rock site in or near the study area is usually used as the input waveform for the response analysis in earthquake engineering project. As thin sediment covers the rock at the Kirtipur site, the observed record was converted to  $V_s=600\text{m/sec}$  rock condition by inverse response analysis (Figure 3.7.2). The amplitude of the converted waveform was adjusted to the calculated PGA by GMPE at the base rock in each grid and used as the input waveform for the response analysis of each ground model. The acceleration waveform at ground surface in each grid is the output of response analysis.



Source: JICA Project Team

**Figure 3.7.2 Input Waveform for response Analysis, (upper) original, (lower) converted to  $V_s=600\text{m/sec}$  rock condition**

### 3.7.2 Ground Model for Response Analysis

The ground model for response analysis was constructed by drilling log, geomorphology map (newly created), microtremor survey (single point: 318 in this project and 210 existing, L-shape: 74, 3-point: 39, Tripartite: 5), etc. in this project (Clause 3.6). Grid size is  $250\text{m} \times 250\text{m}$  and maximum depth of the ground model is about 500m.

The Japanese non-linearity property of soil (Central Disaster Management Council (2003)) was used as no information is available in Nepal so far. The first dynamic soil test by a local researcher, which was presented in the Memorial Seminar of Gorkha Earthquake on 25 April 2016 (Chamlagain, 2016), suggests a gradual development in this field in Nepal.

### 3.7.3 Calculation for Verification Earthquake

The earthquake motion of two verification earthquakes was calculated. The largest aftershock of the Gorkha Earthquake was added in the analysis. The calculated PGA at the ground surface for the Gorkha Earthquake was 400 ~ 800 gal and 150 ~ 200 gal for largest aftershock, however the observed PGA was 150 ~ 200 gal and 60 ~ 110 gal respectively. The calculated PGA was extremely larger than the observed one. The estimated damage from the calculated PGA for the 1934 Bihar-Nepal Earthquake was compared with actual damage because strong motion data is not available for the 1934 event and they don't show a major discrepancy.

Based on the above phenomena and below verification analysis, and the fact that the seismic source and propagation characteristics have not yet been solidified in seismology, it became necessary to consider the correction factor (C.F.) for the earthquake motion estimation in Kathmandu.

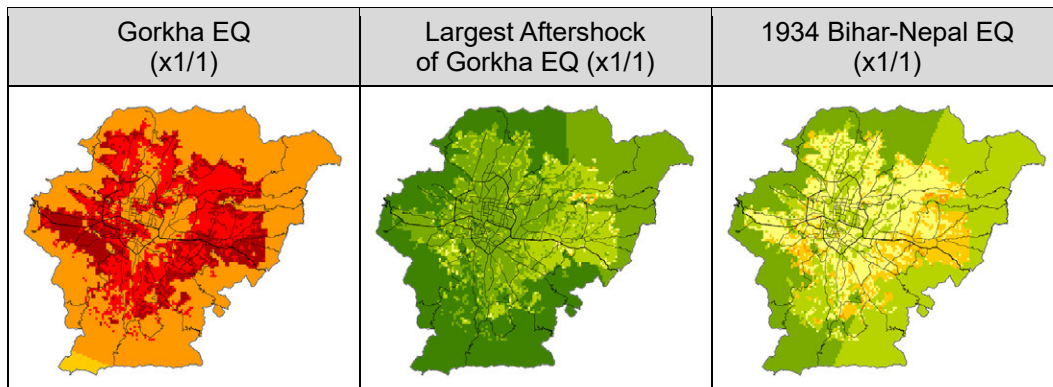
It is obvious that the Gorkha Earthquake deviates significantly from the average in terms of attenuation characteristic of PGA as shown by Takai et al. (2016), Dhakal et al. (2015) and this study, however, the reason is not scientifically identified so far. As little information can be found regarding the attenuation characteristics in Nepal, more study is necessary to create GMPE for Nepal based on not only the Gorkha Earthquake but many earthquakes in and around Nepal. To move ahead with the hazard/risk assessment and disaster risk reduction and management planning, even the reason of deviation is not clarified yet, so, introducing C.F. may be one option. Not so many examples of C.F. in the hazard assessment may be found, but it is a realistic measure to reproduce the observed value by C.F. and apply it to scenario earthquakes.

As for the special feature of the Gorkha Earthquake, Bilham (2015) said "The deviation from average is unique in the world and the bright spot in the tragedy". Prof. Koketsu commented as follows: "As PGA at the rock site is smaller than GMPE, the deviation may be the result of the singularity of the earthquake source around Kathmandu or the propagation path. The introduction of C.F. is unavoidable in engineering study for risk management planning."

One opinion for the Nepal side is that C.F. may be affected by the propagation path of the seismic wave and this effect should be considered in the calculation. However, it is an unrealistic option because the propagation path effect contains many issues and the structure or features of the deep ground are unknown. Another opinion is that the methodology in this project is the same as the process in the 2002 JICA project and no progress is found, but this opinion is not getting to the truth. The methodology to assess the earthquake motion; namely set up the earthquake source, calculate the base rock motion by GMPE using the magnitude and distance, and assess the amplification by response analysis in every grid with the created

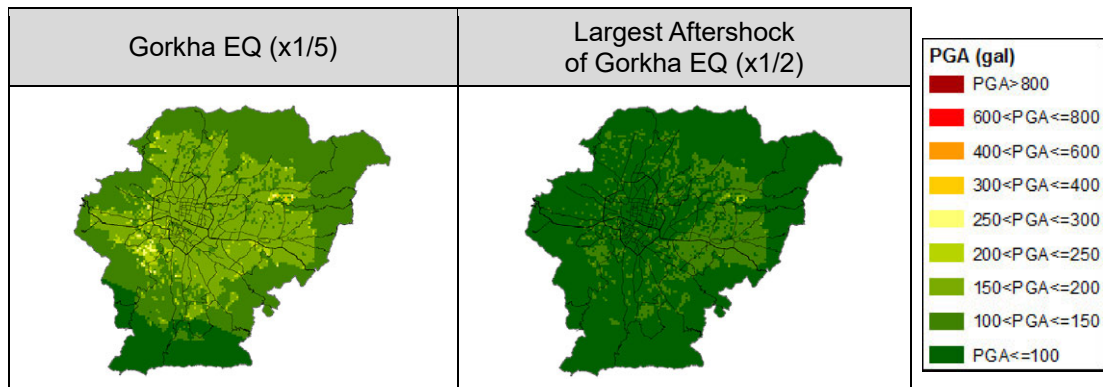
ground model, is the standard process in the engineering field. Actually, new measures are introduced to the scenario setting, base rock motion calculation, C.F. based on the actual observation and apply to the scenario, ground modeling, etc. (Clause 3.1).

At first, PGA of verification earthquakes was calculated in the condition of C.F. = x1/1, namely GMPE is applied without correction (Figure 3.7.3). Next, proper value of C.F. to reproduce the observed PGA of the Gorkha Earthquake was searched by trial-and-error method. C.F. = x1/5 could reproduce the actual value on average. The same study was applied to the largest aftershock and the proper value was x1/2 (Figure 3.7.4).



Source: JICA Project Team

**Figure 3.7.3 PGA of Verification Earthquake (C.F. = x1/1)**



Source: JICA Project Team

**Figure 3.7.4 PGA of Gorkha Earthquake (C.F. is set to reproduce the observed PGA)**

Next verification was done for the 1934 Bihar-Nepal Earthquake. The damage of buildings and casualties are shown in Table 3.7.1. The damage by the 1934 event is clearly larger than the 1833 event and the Gorkha Earthquake. PGA at the ground surface may have been larger than the 1833 or 2015 earthquakes. Recently, Sapkota (2016) shows the same view. Based on this consideration, C.F. = x1/2 was tried in order to reproduce the 1934 event, but the calculated PGA was smaller than the Gorkha Earthquake, which is not consistent with the damage data. After some trial study, the proper value of C.F. was x1/1. The PGA distribution for 1934 event was also calculated in the 2002 JICA project by different GMPE, different

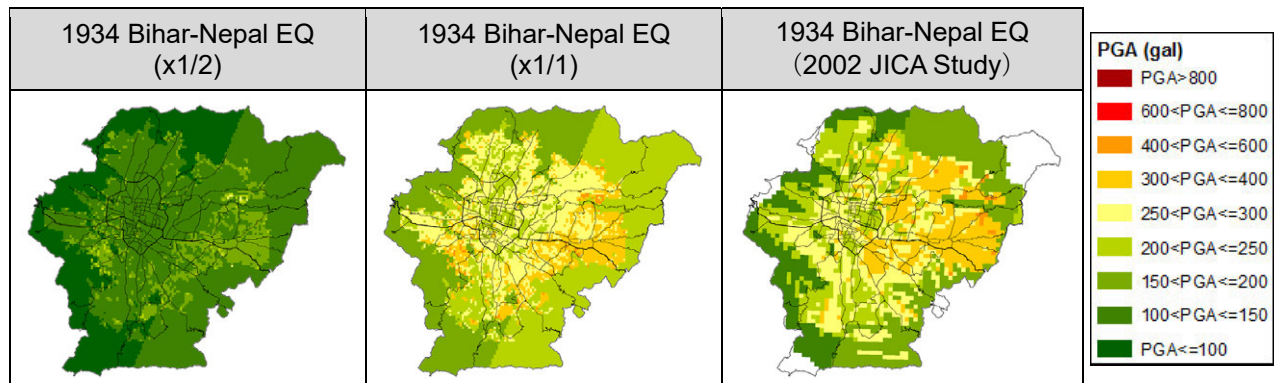
input waveform and different ground model. The PGA in the 2002 JICA project is consistent with the PGA in this project (Figure 3.7.5) and the estimated damage in the 2002 JICA project agrees with actual damage.

The seismic intensity distribution, damage distribution of buildings by structure and death ratio by the North Bagmati earthquake, one of the scenario earthquakes in the 2002 JICA project are comparable to those of the Gorkha Earthquake. The magnitude of North Bagmati Earthquake is 6.0 and the location is north of Kathmandu Valley and just south of the maximum slip of the Gorkha Earthquake by Kubo et al. (2015). The short period component of the wave of the Gorkha Earthquake, which is critical to the buildings in Nepal, is said to be radiated from the north of the Kathmandu Valley. This may indicate the validity of basic methodology and consequently the estimated PGA in this project for the 1934 event may agree with actual damage.

**Table 3.7.1 Damage by Historical Earthquakes and Gorkha Earthquake in Kathmandu**

Year		Damage to Buildings		Deaths		Total Buildings	Population	Remarks
1833	7.3-7.7	3,565	29%	296	0.59%	12,500	50,000	Masonry
1934	8.4	55,739	71%	4,296	1.36%	78,750	315,000	Masonry
2015	7.8	91,150	15%	1,713	0.07%	614,777	2,517,023	RC+Masonry
2015	7.8	72,920	39%	1,370	0.18%	188,750	755,000	Masonry

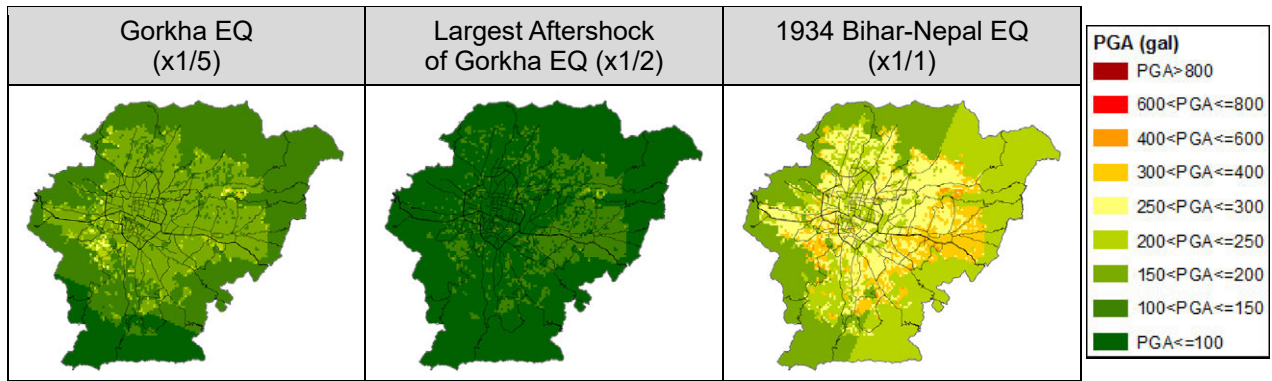
(references: Oldham(1883), Rana(1935), UNDP(1994), Bilham(1995, Web), NPC(2015), Ohsumi(2015), Sapkota(2016) and Bollinger(2016))



Source: JICA Project Team

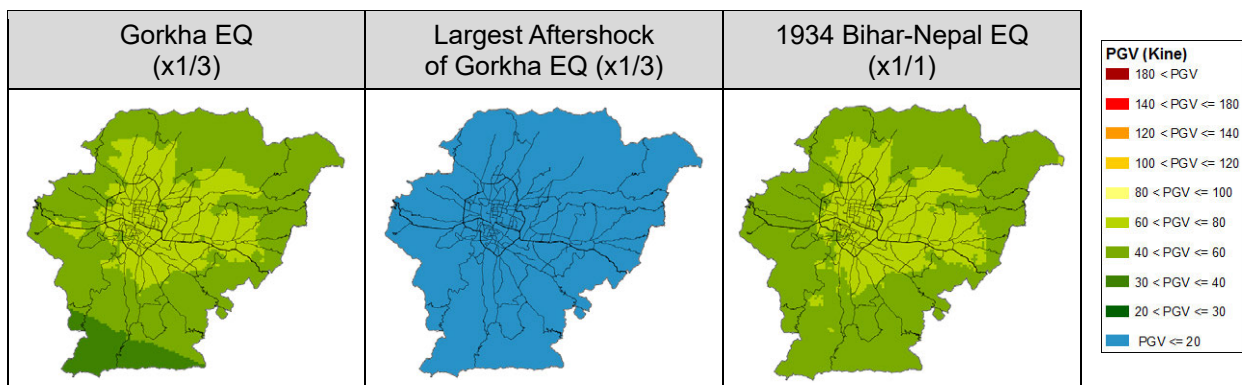
**Figure 3.7.5 PGA of 1934 Bihar-Nepal Earthquake, C.F. = x1/1 can explain damage**

In the same way, C.F. for PGV was studied. The C.F. for the Gorkha Earthquake, largest aftershock and the 1934 Bihar-Nepal Earthquake are x1/3, x1/3 and x1/1 respectively. The calculated PGA and PGV distribution with adopted C.F. are shown in Figure 3.7.6 and Figure 3.7.7.



Source: JICA Project Team

**Figure 3.7.6 PGA of Verification Earthquake (Adopted)**



Source: JICA Project Team

**Figure 3.7.7 PGV of Verification Earthquake (Adopted)**

### 3.7.4 Study of Correction Factor

To study the correction factor (C.F.) for a scenario earthquake, the calculated PGA and PGV for main shock of the Gorkha Earthquake by GMPE and response analysis with observed value at six strong motion stations in Kathmandu Valley, namely KANTP (USGS), DMG, Kirtipur, Tribhuvan University, IoE, SanoThimi (Hokkaido Univ.) were referred. The calculated PGA is around four times larger than observed and PGV is three times larger (Figure 3.7.8). The same study was conducted for the largest aftershock. The observed PGA is two times larger than the observed value. The calculated PGV is larger than observed but the ratio varies (Figure 3.7.8).

The summary of study is shown below.

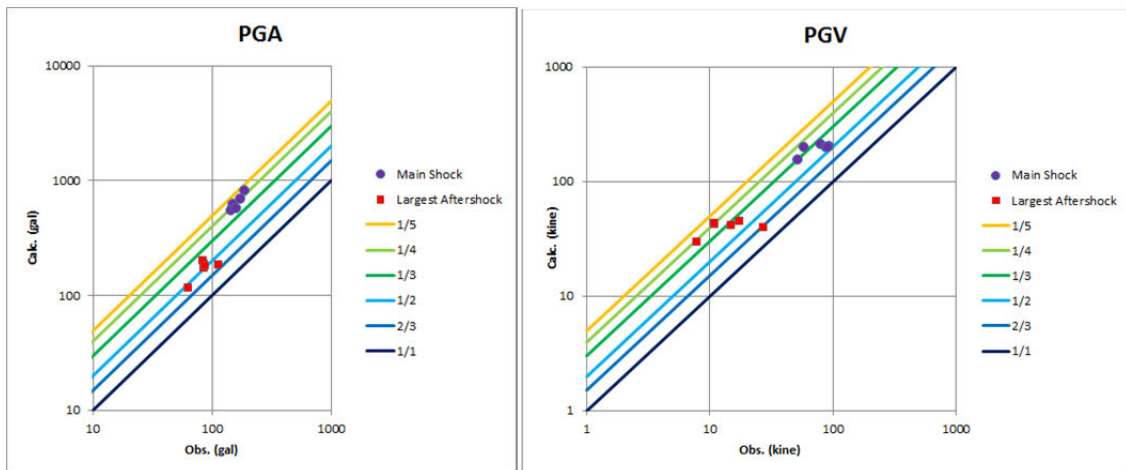
- Main shock: Observed PGA is 1/5 to 1/3 of calculated  
Observed PGV is 1/3 to 2/3 of calculated
- Largest aftershock: Observed PGA is 1/4 to 1/2 of calculated  
Observed PGV is 1/4 to 2/3 of calculated

As shown above, the characteristic of an earthquake differs site by site. The variation of the earthquake source or path effect may be one reason for the difference. The variation of the magnitude may be another reason of differences in the same region. There is very little information to study for the source and path effects for the two western scenario earthquakes, namely Far-Mid Western Nepal Scenario Earthquake and Western Nepal Scenario Earthquakes, therefore it is difficult to decide C.F. for these scenario earthquakes. For the Central Nepal South Scenario Earthquake, so far, not much data of middle to large earthquakes is available. However, because the source fault of this scenario earthquake is adjacent to the fault of the Gorkha Earthquake, it resembles the condition of source or path effect to Kathmandu valley and C.F. can be supposed based on the Gorkha Earthquake case study.

Because of the current situation of methodology, data and limitation of time, to show the possible range of C.F. may be the best solution of the hazard assessment in this project. The adopted C.F. is shown in Table 3.7.2.

These values were determined taking in mind that the earthquake motion is used for risk assessment and disaster management planning.

The scientific estimation of future earthquakes has its limits. The evaluated values usually have the conceivable extent. The studied C.F. is evaluated by currently available limited information and may be approved by additional data and analysis.



Source: JICA Project Team

**Figure 3.7.8 Comparison of Observed PGA/PGV and Calculated PGA/PGV; (left) PGA, (right) PGV**

**Table 3.7.2 Adopted Correction Factor**

Scenario Earthquake	Correction Factor (PGA)	Correction Factor (PGV)
Far-Mid Western Nepal Scenario Earthquake	x1/1 (Normal)	x1/1 (Normal)
Western Nepal Scenario Earthquake	x1/1 (Normal)	x1/1 (Normal)
Central Nepal South Scenario Earthquake	x1/1 (Normal) x2/3 (cover max. aftershocks) x1/2 (average of aftershock) x1/3 (cover max. main shock)	x1/1 (Normal) x2/3 (cover max. aftershocks) x1/2 (cover max. main shock)
Verification Earthquake	Correction Factor (PGA)	Correction Factor (PGV)
2015 Gorkha EQ.	x1/5 (observed average)	x1/3 (observed average)
Largest Aftershock of 2015 Gorkha EQ.	x1/2 (observed average)	x1/3 (observed average)
1934 Bihar-Nepal EQ.	x1/1 (Normal / damage level)	x1/1 (Normal / damage level)

Source: JICA Project Team

### 3.7.5 Calculation of Earthquake Motion at Ground Surface for Scenario Earthquake

For the verification earthquake, the C.F. of x1/5 and x1/2 were calculated to reproduce the PGA of the Gorkha main shock and largest aftershock respectively. The damage of the 1934 event was explained by C.F. = x1/1.

While, as little information about the observed earthquake motion or damage experience is available in the scenario fault area, the study of C.F. for the scenario earthquake was difficult. The calculation by C.F. = x1/1 is the first choice. For Central Nepal South Scenario Earthquake, based on the similarity of the source area to the Gorkha Earthquake, C.F. = x1/3, x1/2 and x2/3 were also used for PGA calculation, though, which C.F. is most probable is a very difficult question. For PGV, x1/2, x2/3 and x1/1 were used.

In answer to the question of when scenario earthquakes occur or how long is the occurrence interval is basically very difficult. Prof. Koketsu declared his opinion in the seminar on 25 May 2015 that “Only 10-20% of the plate boundary in western to central Nepal moved. Accumulated energy still remains in this area. The next large event may occur within several decades.” JICA reconstruction assistance including this project is standing on this estimation.

The hazard and risk assessment intend the application in the disaster management planning to promote the actual counter measurement. In this regard, it is one of the choices to select C.F. from the angle of planning or political measures.

In general, earthquakes which occur in the same area have resembled the mechanism in the influence of same seismo-tectonics condition. Historically, many huge earthquakes have occurred in Nepal, and the surrounding territory is divided by the source zone of them from west to east by the north-south boundary. For example, from the east, the 1934 event, 2015

event and 1505 event are recognized. The Central Nepal South Scenario Earthquake and Gorkha Earthquake may be included in the same zone.

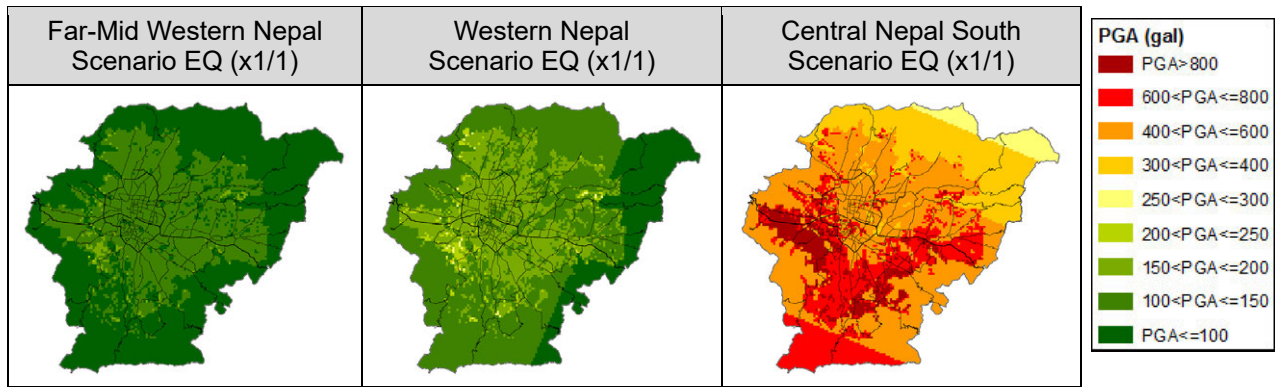
Several reasons are considered why C.F. is necessary to reproduce the Gorkha Earthquake. For example, the strong motion is produced less in the western part of the source fault because of some fracture property, or short period wave contents are reduced during propagation, or some special condition upon the hypocenter. Actually, the seismic intensity and damage in the Gorkha Area in the west is less than the Sindhupalchok in the east which is far from the epicenter. This may be evidence of an unequal condition of strong motion generation depending on the area. Several researchers pointed out the effects of asperity and directivity. The short period component of the wave might be less generated compared to the average earthquake, however, from the engineering point of view, a rather-long period component might be large enough because of the above-mentioned reasons, but this is still hypothesis. One can say that the Central Nepal South Scenario may be similar to the Gorkha Earthquake because of the source zone and magnitude analogy. On the contrary, it cannot be denied that C.F. should be  $\times 1/2$  same to largest aftershock or  $\times 1/1$  like 1934 event.

From the view point of disaster management, it is one idea to set the scenario earthquake to affect more severe than the Gorkha Earthquake. Some people may think that important infrastructures including bridges, governmental buildings, schools and hospitals should keep their functions in case of any earthquakes. This may also be from the point of politics.

If the Gorkha Earthquake had not yet occurred, the study of C.F. must be out of consideration. But this doesn't naturally mean that a huge PGA should be estimated for the scenario earthquakes. The scenario earthquakes themselves may not be same before and after the Gorkha Earthquake. Without the Gorkha Earthquake, Central South Nepal Scenario may not be considered.

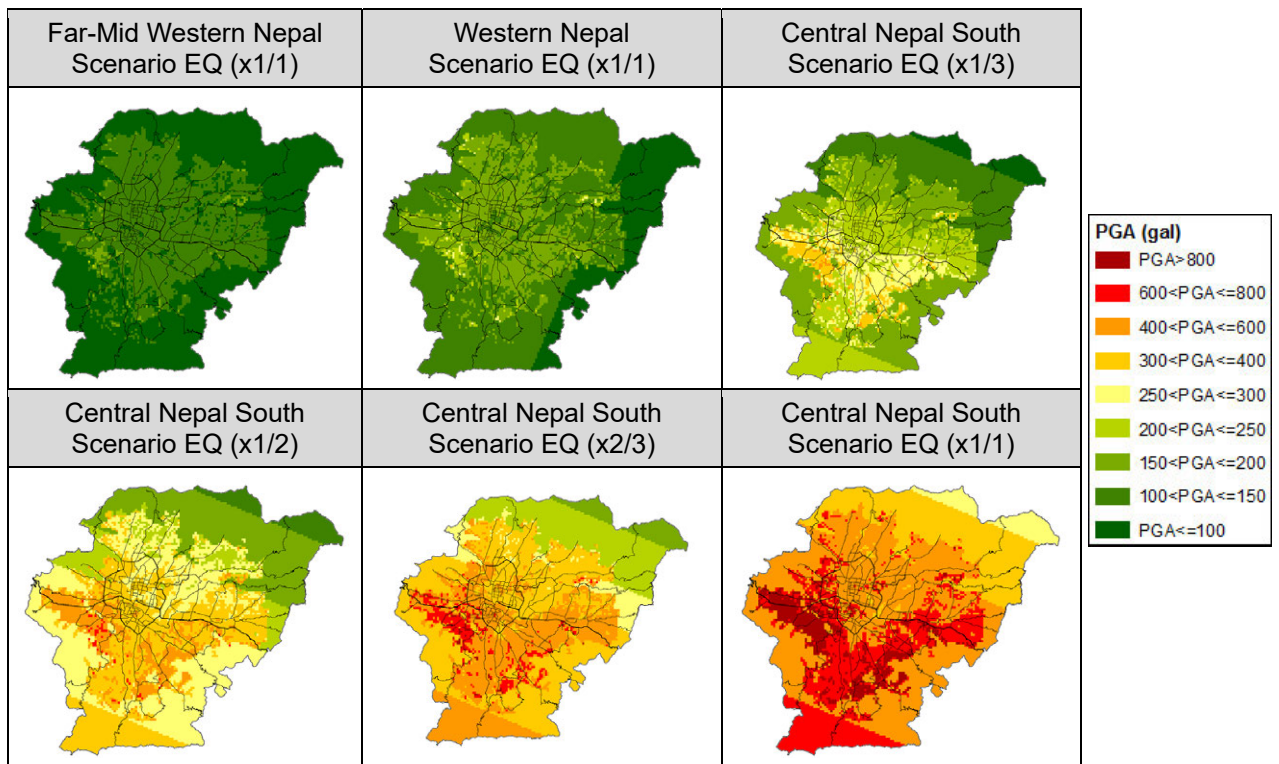
DMG pointed out that the magnitude of the Central Nepal South Scenario Earthquake is over estimated considering the magnitude of the 1866 event, which is supposed to be 6.5 to 7.4 (Szeliga et al. (2010), Bollinger (2016)). In this study, the magnitude is set 7.8, which is the same as the Gorkha Earthquake, based on the fault size and from the view point of disaster management.





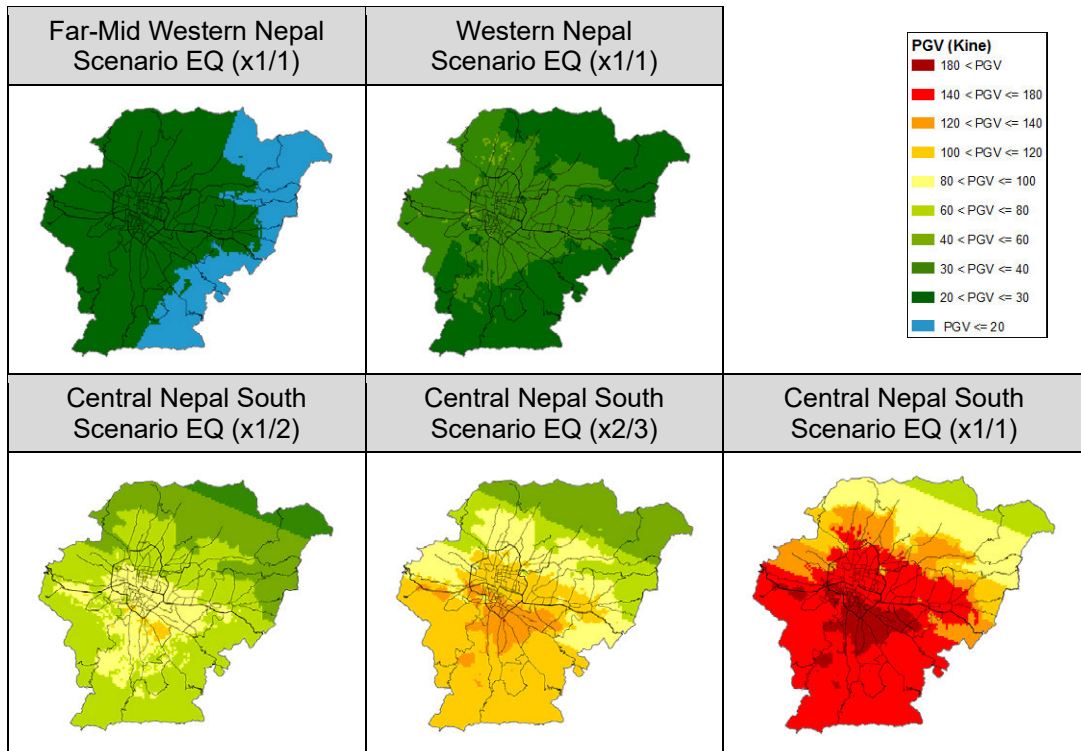
Source: JICA Project Team

**Figure 3.7.9 PGA of Scenario Earthquake (C.F. = x1/1)**



Source: JICA Project Team

**Figure 3.7.10 PGA of Scenario Earthquakes (Adopted)**



Source: JICA Project Team

**Figure 3.7.11 PGV of Scenario Earthquakes (Adopted)**

### 3.7.6 Calculation of Other Indexes for Earthquake Motion

Seismic intensity, acceleration response spectra and spectral intensity were calculated from PGA or acceleration waveform for risk assessment. The calculated cases are six for three scenario earthquakes and three for two verification earthquakes.

#### (1) Modified Mercalli Intensity (MMI)

Seismic intensity is the most popular index of earthquake motion. Among several intensity scales in the world, the MMI scale is most popularly used in many countries. Seismic intensity is not directly related to PGA, but several empirical relations are proposed. In this study, average of the following two equations was used. Figure 3.7.12 shows the MMI distribution of verification earthquakes and scenario earthquakes.

- $Imm = 3.66 \cdot \log(PGA) - 1.66$  ( $\sigma=1.08$ )     $V \leq Imm \leq VIII$     (Wald et al. , 1999)  
 (Imm: MMI, PGA: Peak Ground Acceleration (gal),  $\sigma$ : standard deviation)
- $\log(PGA) = 0.014 + 0.30 \cdot IMM$      $IV \leq IMM \leq X$     (Trifunac & Brady, 1975)  
 (PGA: Peak Ground Acceleration (gal), IMM: MMI)

#### (2) Acceleration Response Spectra (Sa)

Sa is usually related to the design of the buildings and seismic loading. When a building is

forced into earthquake motion, the response is different depending on the natural period of the building.  $S_a$  is a plot of peak response of a building, as modeled by a particle on a massless vertical rod having the same natural period of vibration as the building. Response of 5% damping within 0.01 to 10 sec was calculated from acceleration waveform.

### (3) Spectral Intensity (SI)

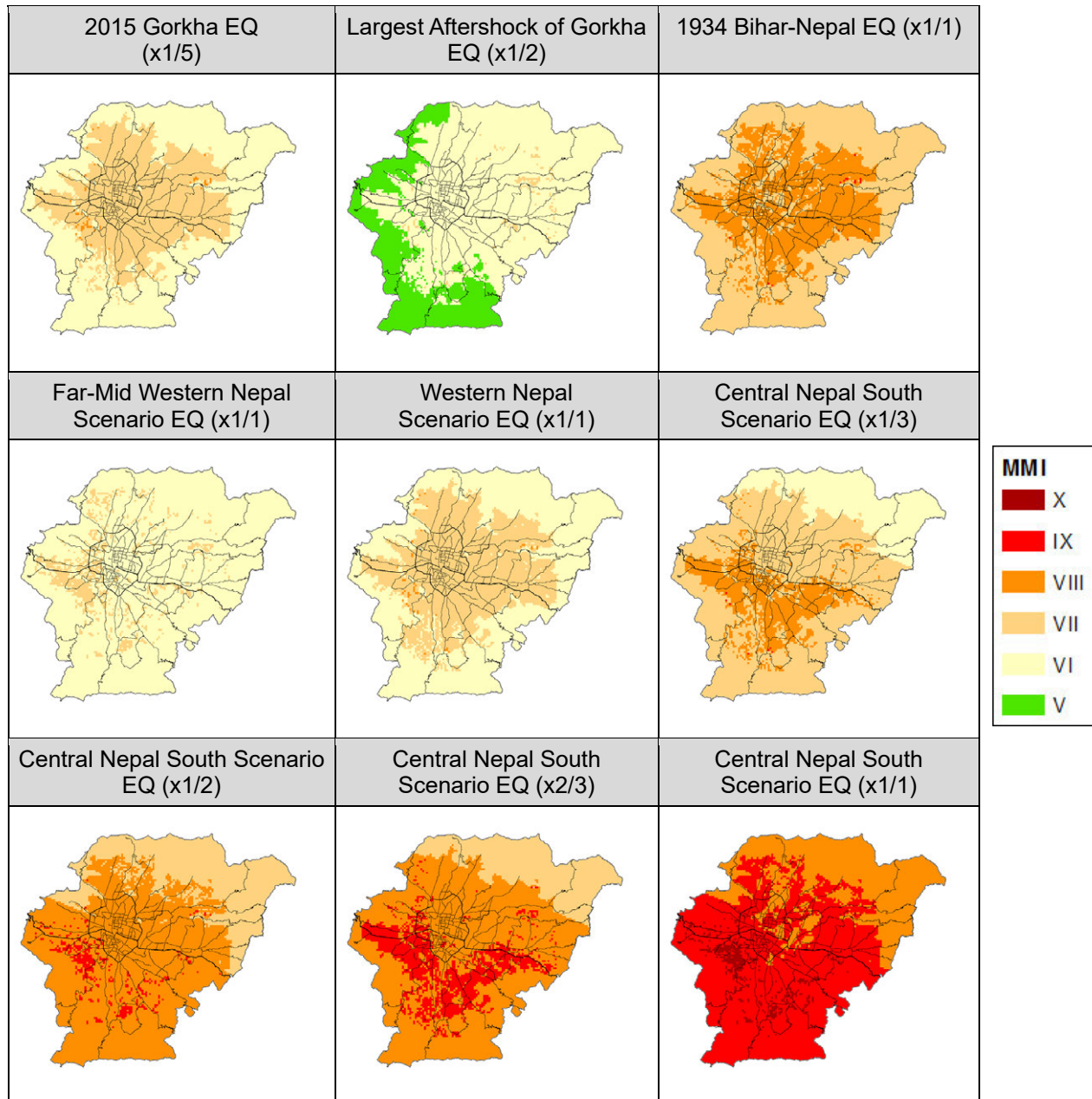
The most popular spectral intensity was calculated among several definitions. SI is available by integrating the velocity response spectra as the formula below. SI is used as the index indicating the total seismic force to the structure.

$$SI = \frac{1}{2.4} \int_{0.1}^{2.5} Sv(T, h) dT$$

Sv: velocity response spectra

T: period (sec)

h: damping factor (=0.2)



Source: JICA Project Team

**Figure 3.7.12 MMI of Verification and Scenario Earthquakes**

**References (3.7)**

- Bhattarai, M., L. B. Adhikari, U. P. Gautam, L. Bollinger, B. Hernandez, T. Yokoi and T. Hayashida (2016) Establishing a reference rock site for the site effect study in and around the Kathmandu Valley, Nepal, *Earth, Planets and Space*, 68:81.
- Bilham, R. (1995) Location and magnitude of the 1833 Nepal earthquake and its relation to the rupture zones of contiguous great Himalayan earthquakes, *Current Science*, Vol.69, No.2, 25, July 1995.
- Bilham, R. (2015) on the discussion, *International Symposium on the Gorkha Earthquake*, June 2015.

- Bilham, R., <http://cires1.colorado.edu/~bilham/1833Earthquake.html>
- Bollinger, L., P. Tapponnier, S. N. Sapkota, and Y. Klinger (2016) Slip deficit in central Nepal: omen for a repeat of the 1344 AD earthquake?, *Earth Planets Space*, 68, 12.
- Central Disaster Management Council (2003) 16th Meeting of Working Group for Tonankai and Nankai Earthquake, Reference Material No. 2-3 (in Japanese).
- Chamlagain, D., G. Lamzo, A. Pagliaroli, N. Poovarodom, D. Gautam and B. Giri, (2016) Cyclic Geotechnical Characterization of Soils from Kathmandu Valley with Reference to 2015 Gorkha Seismic Sequence, International Workshop on Gorkha Earthquake, Ministry of Industry and DMG, April 2016.
- Dhakal, Y.P., H. Kubo, W. Suzuki, T. Kunugi, S. Aoi and H. Fujiwara (2015) An analysis of strong-motion records and site amplification at Kantipath, Kathmandu from the 2015 Mw 7.8 Gorkha Earthquake, Nepal and its aftershocks, *Proceeding of JAE Annual Conference*.
- Kubo, H., Y. P. Dhakal, W. Suzuki, T. Kunugi, S. Aoi and H. Fujiwara (2016) Estimation of the source process of the 2015 Gorkha, Nepal, earthquake and simulation of long-period ground motions in the Kathmandu basin using a one dimensional basin structure model, *Earth, Planets and Space*, 68:16.
- Morikawa, N., and H. Fujiwara (2013) A New Ground Motion Prediction Equation for Japan Applicable up to M9 Mega-Earthquake, *JDR*, Vol.8 No.5, pp. 878-888.
- National Planning Commission (2015) Government of Nepal, Post Disaster Needs Assessment, Vol. A: Key Findings.
- Ohsumi, T., F. Kaneko, S. Segawa and H. Fujitani (2016) Situation of Damage in and around Kathmandu Valley due to the 2015 Gorkha Nepal Earthquake, *Journal of Japan Society of Civil Engineers*, Ser. A1, Vol. 72, No. 4, p. I\_22-I\_32.
- Oldham, T. (1883) A catalogue of Indian earthquakes from the earliest time to the end of AD 1869, *Memoirs of the Geological Survey of India*, 19, Part 3.
- Rana, J. B. (1934) *The Great Earthquake in Nepal (1934 A.D.)*, translated by Kesar Lall, Ratna Pustak Bhandar, Kathmandu, Nepal, pp. 136, reprint 2013.
- Sapkota, S.N., L. Bollinger and F. Perrier (2016) Fatality rates of the Mw~8.2, 1934, Bihar-Nepal earthquake and comparison with the April 2015 Gorkha earthquake, *Earth, Planets and Space*, 68:40.
- Szeliga, W., S. Hough, S. Martin, and R. Bilham (2010) Intensity, Magnitude, Location and Attenuation in India for Felt Earthquakes since 1762, *Bull. Seism. Soc. Am.*, Vol. 100, No. 2, pp. 570 - 584.
- Takai, N., M. Shigefuji, S. Bijukchen, M. Ichiyanagi and T. Sasatani (2016a) Strong Motion Characteristics of the Kathmandu Valley during the 2015 Nepal Gorkha Earthquake, Grants-in-Aid for Scientific Research, Special Research Promotion Expense (in Japanese).

- Takai, N., M. Shigefuji, S.Rajaure, S. Bijukchhen, M. Ichianagi, M.R. Dhital and T. Sasatani (2016b), Strong ground motion in the Kathmandu Valley during the 2015 Gorkha, Nepal, earthquake, *Earth, Planets and Space*, 68:10.
- Trifunac, M. D. and A. G. Brady (1975) On the Correlation of Seismic Intensity Scales with the Peaks of Recorded Ground Motion, *Bull. Seism. Soc. Am.*, 65, pp. 139 - 162.
- UNDP/HMG/UNCHS (Habitat) (1994) Seismic Hazard Mapping and Risk Assessment for Nepal.
- Wald, D. J., V. Quitoriano, T. H. Heaton and H. Kanamori (1999) Relationships between Peak Ground Acceleration, Peak Ground Velocity, and Modified Mercalli Intensity in California, *Earthquake Spectra*, 15, pp. 557 - 564.

### **3.8 Assessment of Liquefaction**

Liquefaction is a phenomenon in which the bondage of sand grains under the groundwater level are loosened in response to the increase of water pressure in sandy soil by the iteration of strong ground shaking caused by an earthquake. Due to liquefaction the sand layer turns into a liquid-like form, then, the boiling of sand, mud, or water takes place, ground settles, structures subside or underground structures float, thus causing damage. This is a common phenomenon in major earthquakes around the world. Also, liquefaction has occurred during past large earthquakes in Kathmandu.

However, in Kathmandu Valley, since accurate ground materials for liquefaction evaluation are very few, the evaluation in this project had to be implemented referencing the past history, assuming several logistical points and in consideration of the following disaster management activities. Thus, a simpler method was attempted to show an overall feature.

#### **3.8.1 Liquefaction history in Kathmandu Valley**

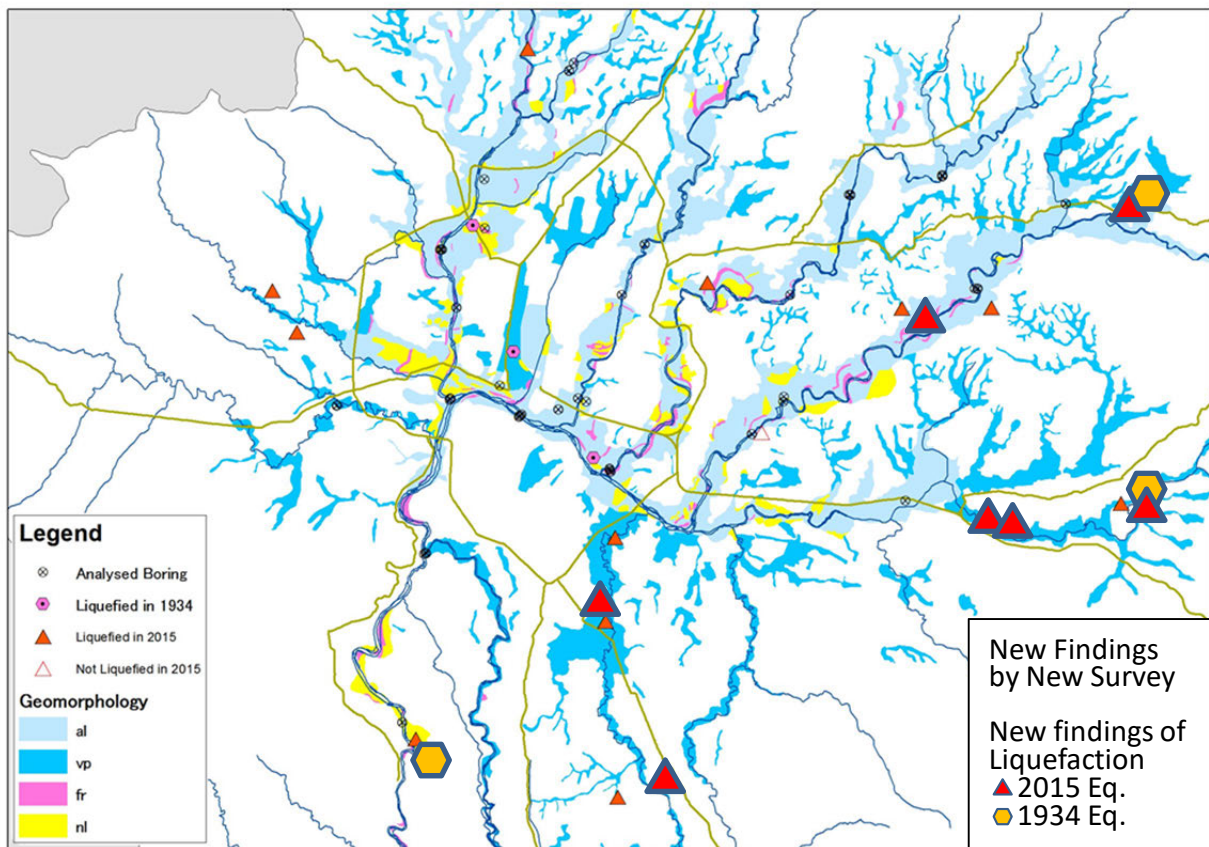
According to Rana (1935), in the 1934 Bihar-Nepal Earthquake, liquefaction seems to have occurred at various places in Kathmandu Valley, such as sand boiling, water sprouting and settlement. In particular, in Tundhikel and Nayabazar (way to Balaju), large-scale cracks and sand boils were observed. For the 2015 Gorkha Earthquake, for examination, seventeen sites have been surveyed by the ground survey of this project (Volume 5). Liquefaction was confirmed at five of the locations. Okamura et al. (2016) have confirmed the eleven liquefied locations (including the above five sites) in J-RAPID.

The actual liquefaction of past earthquakes is very important information for liquefaction analysis because liquefaction usually occurs at same place repeatedly during several earthquakes. The number of reported liquefaction point is only three for 1934 Bihar-Nepal Earthquake, but only part of liquefaction points may have been reported considering the estimated large earthquake motion. To know the liquefaction situation of 1934 Bihar-Nepal

Earthquake and also 2015 Gorkha Earthquake, interview survey to the residents was conducted in June 2017.

As a result, five liquefaction points during 2015 Gorkha Earthquake were found, namely, Indrayani near Sankhu, Thaiba, Kamalvinayak in east of Bhaktapur and two points in southwest Bhaktapur. The reported liquefaction points in Hattiban and Mulpani by J-RAPID were confirmed but the actual location was modified. The five new findings and two modified liquefaction points are plotted by big red colored triangle in Figure 3.8.1. The position of the existing boring points with *N* value is also plotted.

Also, three liquefaction points during 1934 Bihar-Nepal Earthquake were found by interviews. The newly found liquefied points are Kokhana (Bungmati), Indrayani and Kamalvinayak. These points are also liquefied during 2015 Gorkha Earthquake. This may be one an evidence of repeated liquefaction occurrence at same place. The three new findings are plotted by big orange colored hexagon in Figure 3.8.1.



Source: JICA Project Team

**Figure 3.8.1 Liquefaction history in Kathmandu Valley**

The above liquefied sites are mostly locating at “al” (alluvial lowland), “vp” (valley plain), “nl” (natural levee), and “fr” (former river course) of geomorphological units, in many cases in the peripheral portion of the valley. In addition, since the 1934 Bihar-Nepal Earthquake happened in January, and the 2015 Gorkha Earthquake occurred in April, both were in the

dry season with deeper groundwater level, but they were mostly shallow due to the communication with the local people. According to Okamura et al. (2016) and Marasini and Okamura (2014), fine fraction content  $F_c$  (%) of sand by boiled sand and soil survey are as high as 20% -40% containing more silty component in the central part of the Valley, but at the peripheral portion  $F_c$  is often less than 15% with less silt component.

Also, liquefaction has not been reported at any of the 121 existing borehole locations with  $N$  values.

### 3.8.2 Study of liquefaction assessment method

#### (1) Review assessment method

So far, several liquefaction assessments have taken place for Kathmandu Valley. They are UNDP (1994), Piya (2006), UNDP (2013) and so on. However, these examples have not provided seismic force, verification of used data and methods, consequently the results have not always been clear. Since this assessment is for disaster management planning, the trend of liquefaction will be clarified by as a trial using of simple method corresponding to the scenario earthquakes, based on limited collected materials.

Due to the preliminary investigation, as there are insufficient documents for ground properties in the Kathmandu Valley, the assessment was supplemented with materials from other regions. Since the  $N$  value, and fine fraction content ( $F_c$ ) have some information, the method of the Architectural Institute of Japan was adopted as an assessment method for this project. Although there are several highly precious approaches, the accuracy cannot be sufficiently increased when ground materials are insufficient. An outline of the method is shown in Section 3.8.5.

Materials necessary for the assessment are the position (latitude, longitude or 250m grid), altitude, depth of borehole, peak ground acceleration (PGA for verification earthquakes and scenario earthquakes),  $N$  value,  $F_c$  and overburden pressure, effective overburden pressure, density (unit weight), groundwater level, and the curve for the criteria.

At the start of the assessment, both the force of generating liquefaction and the force to resist at each depth of  $N$  value are calculated. Then, the  $F_L$  value, representing the ratio, will be calculated. If  $F_L$  value is below 1.0, then it is suggesting liquefaction at that depth. Furthermore, the value of  $(1 - F_L)$  at each depth will be summed up weighting along with depth, and the  $P_L$  value will be calculated as an evaluated value in each site. Finally,  $P_L$  value for each site will be judged as follows.



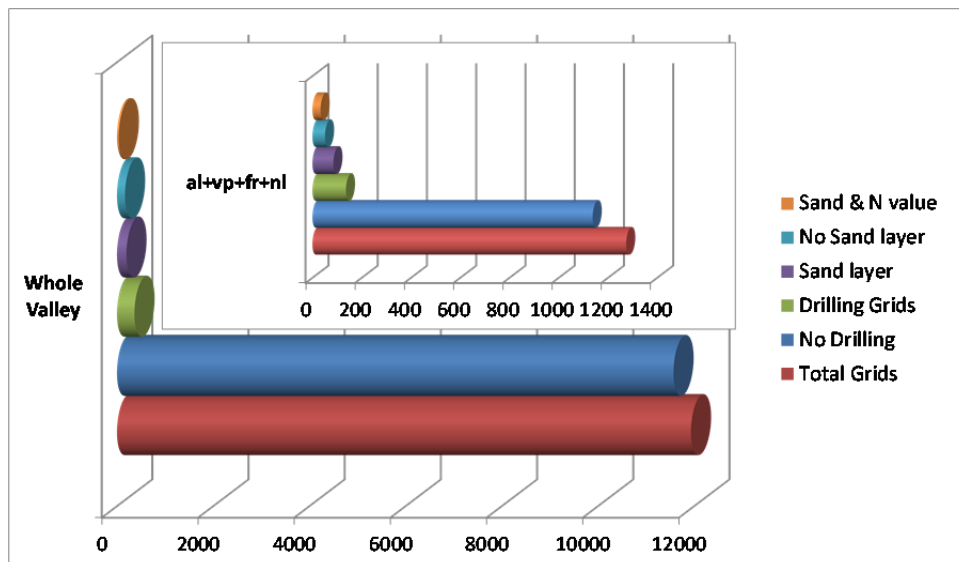
**Table 3.8.1 Adopted Correction Factor**

Judgement of liquefaction possibility	
$P_L=0$	(O) No possibility
$0 < P_L \leq 5$	(L) Low possibility
$5 < P_L \leq 15$	(M) Moderate possibility
$15 < P_L$	(H) High possibility

**(2) Ground to be evaluated**

Liquefaction occurs in sandy ground. On the other hand, the collected drilling data in this project are 449, in the total area of 722km<sup>2</sup>. Figure 3.8.2 represents this relation by grid. Out of the total grid number 11,934 of the entire Valley, the number of grids where boreholes exist is 363, with sand within 20m depth is 196, without sand is 167. Also, there are N values with sand in 38 grids. In other words, only 3% can know whether there is sand or not, and unknown is 97%. In addition, as for four geomorphological units where likely to have liquefaction, namely “al” (alluvial lowland), “vp” (valley plains), “nl” (natural levee), and “fr” (former river course), the total number of grid is 1,274, without borehole is 89% where it is unknown that sand exists or not.

Thus, around more than 90% of grids are unclear whether sand exists or not. Even though a borehole suggests sandy, it is unclear whether whole the grid has sand or not. Boreholes with *N* values are also very limited.



Source: JICA Project Team

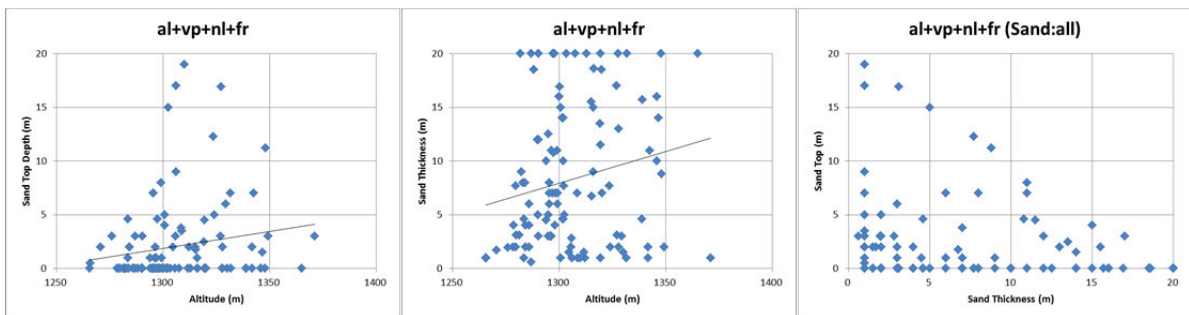
**Figure 3.8.2 Rate of grids with boreholes or sand layers**

### (3) Area division and soil properties

In order to organize the materials to be used for the assessment, geomorphology units, thickness of Holocene layers, sand layer distribution,  $N$  value distribution in sandy layers, altitudes, and the divisions of the above properties were studied, by using conceivable analogies.

First, with regard to geomorphological units, “al”, “vp”, “nl”, and “fr” are the targets. They are mostly distributed along the river. (See Figure 3.8.1)

As alluvium is the main target of liquefaction, from soil columns roughly 30 times of the  $N$  value will be the bottom of alluvium, on average, approximately a depth of 20m in the valley center, and it becomes shallower along the peripheral area. In the alluvium, the distribution of the sand layer, which is subject to liquefy, was arranged by what was shown in the soil columns. According to Figure 3.8.3, in the target areas, there are about 60 boreholes, and the sand layer are likely to start from relatively shallow depth, thicknesses in many cases can be up to about 5m to 10m.



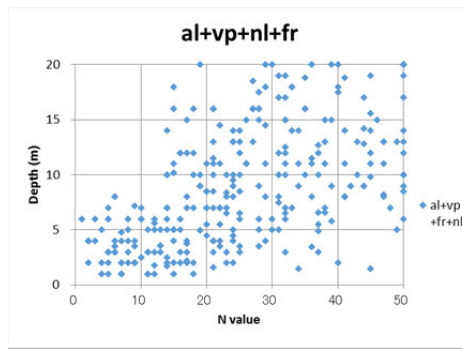
Source: JICA Project Team

**Figure 3.8.3 Top depth and thickness of alluvial sand layers**

The *N* value of sand layers, though only a few, indicates the high trends of increasing according to depth (Figure 3.8.4). Since the data of geomorphology is biased in alluvial lowlands “al”, it is difficult to see a trend by geomorphological units. Therefore, an attempt was made to subdivide the regional characteristics. Considering the sediment environment, the old Kathmandu Lake drained out of the valley at Chobar Canyon. Then upstream and downstream from there can be roughly divided to two, namely the lake basin deposited from the surrounding areas and the river basin exiting from the lake respectively. Next, the central portion, where is made from the sediment from the peripheral higher surroundings, would have the characteristics than that of the rougher particle size at the peripheral (upstream), and the particle size becomes finer closer to the center (downstream) and the river sides. Therefore, as there is a sedimentary environment in the lake, there is a possibility that it may show different characteristics along the altitude. After trial and error, an assumption was made which shows that it is appropriate to have the six divisions, as shown in Table 3.8.2, Figure 3.8.4 and Figure 3.8.5.

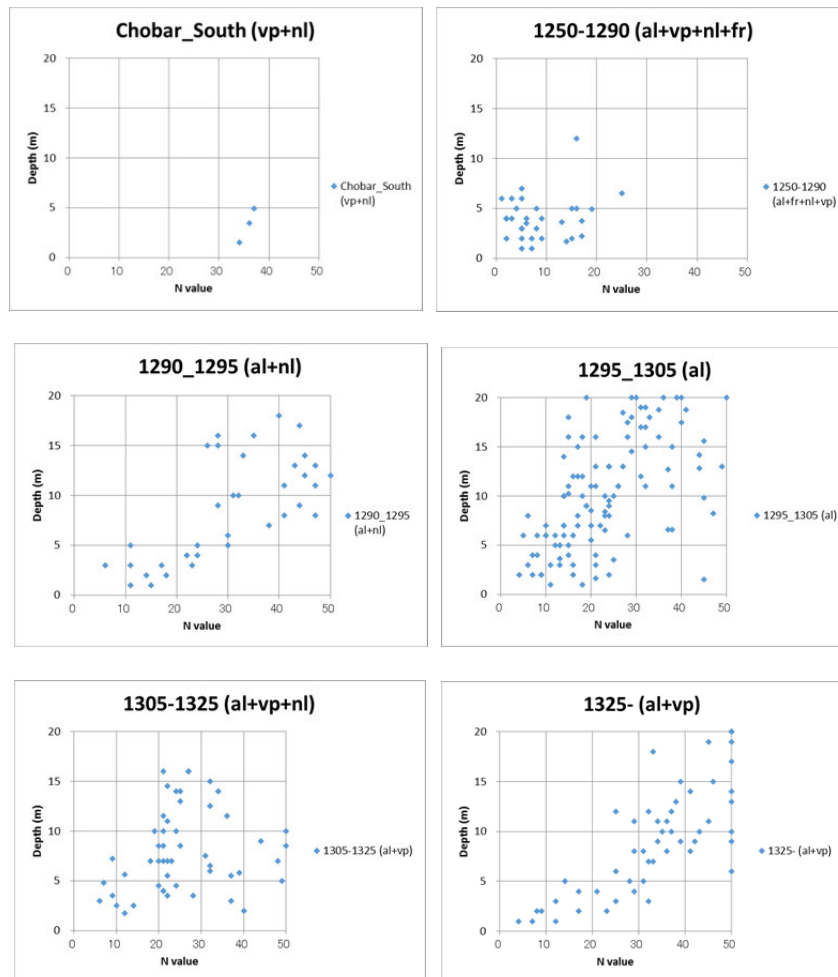
**Table 3.8.2 Area division for *N* value and depth relation**

<b>Area division</b>	<b>Contents</b>
1	South of Chobar, along Bagmati River
2	Up to 1290m (central region)
3	Up to 1295m (central region)
4	Up to 1305m (central region)
5	Up to 1325m (central region)
6	1325m and more (central region)



Source: JICA Project Team

**Figure 3.8.4 Relation between N value and depth (alluvial sand layers)**



Source: JICA Project Team

**Figure 3.8.5 Relation between N value and depth for area division**

**(4) Study of soil properties**

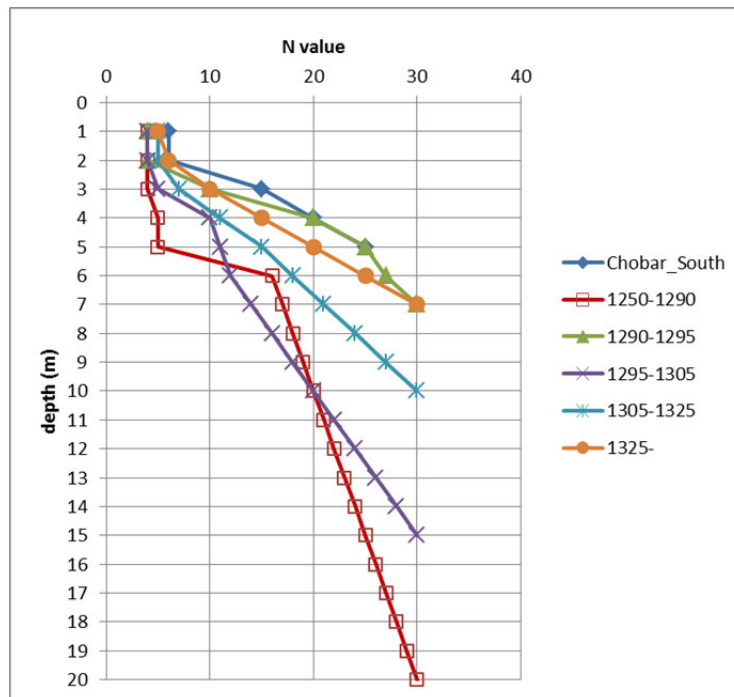
Among the soil properties, so far, positions, altitude, and PGA are based on the materials used in this project. Also, the curve for criteria is set in the original method.

**1) *N* value**

Around 60 existing boreholes including data by Okamura et al. (2016) were used. They have the sand layer *N* values, and the depth is more than 10m. Other physical properties were subjected to the following settings.

The 60 boreholes data could cover only 33 grids because of the duplication of the assigned 250m x 250m grid. In order to picture the whole target area, the typical relationship between the *N* value and depth (Figure 3.8.6) for each regional division was set with reference to Figure 3.8.5. Up to the depth where *N* value equal 30 times was modeled. Since these models are merely typical ones for assessing the tendency of liquefaction, it is noted that in some cases the actual ground does not always match them.

Moreover, since not all the grids of the target geomorphological units have sand layers, though not all the grids have sand layers actually, these models are assumed merely typical models of the cases only where sand layers are distributed. In other words, if there is no sand layer in an actually targeted grid, as it may be sometimes possible to have less of a sand layer than the typical model, this typical process may be corresponding to assuming a safer side or overestimated of disaster a management point of view.



Source: JICA Project Team

**Figure 3.8.6 N value along depth for each area division**

**2) Density (Unit Weight)**

As the information of the density of the sand layer is insufficient with variation, standard values in reference to the 2002 JICA study were adopted as below.

**Table 3.8.3 Assumed relation of N value and density**

<i>N</i> value	Density of sand (g/cm <sup>3</sup> )
$N < 10$	1.8
$10 \leq N < 20$	1.9
$20 \leq N$	2.0

**3) Fine fraction content (*F<sub>c</sub>*)**

As mentioned earlier, though information is limited, according to the boiling sand and field survey, the fine fraction content of the sand layer is as high as 20 - 40% in the central part of the basin, and contains more of a silt portion. Although the *F<sub>c</sub>* of the sand layer at the periphery is frequently less than 15% with less finer component. Fine fraction content is an important factor of sand layer for the liquefaction of Kathmandu, and should be evaluated carefully after accumulation in the future. Based on these information as reference, the following values were set.

**Table 3.8.4 Assumed *F<sub>c</sub>* for area division**

Fine fraction content ( <i>F<sub>c</sub></i> ) of sand layer	
Area division 1, 6	$F_c = 5-10\%$
Area division 2, 3, 4, 5	$N < 10$ $F_c = 20-40\%$
	$N \geq 10$ $F_c = 5-20\%$

**4) Ground water level**

Groundwater level is also a major element of the liquefaction assessment. It commonly differs by seasons, and also by the distance from the river. As underground water level of the existing drilling data has considerable variation, the levels were set as below by referring to them.

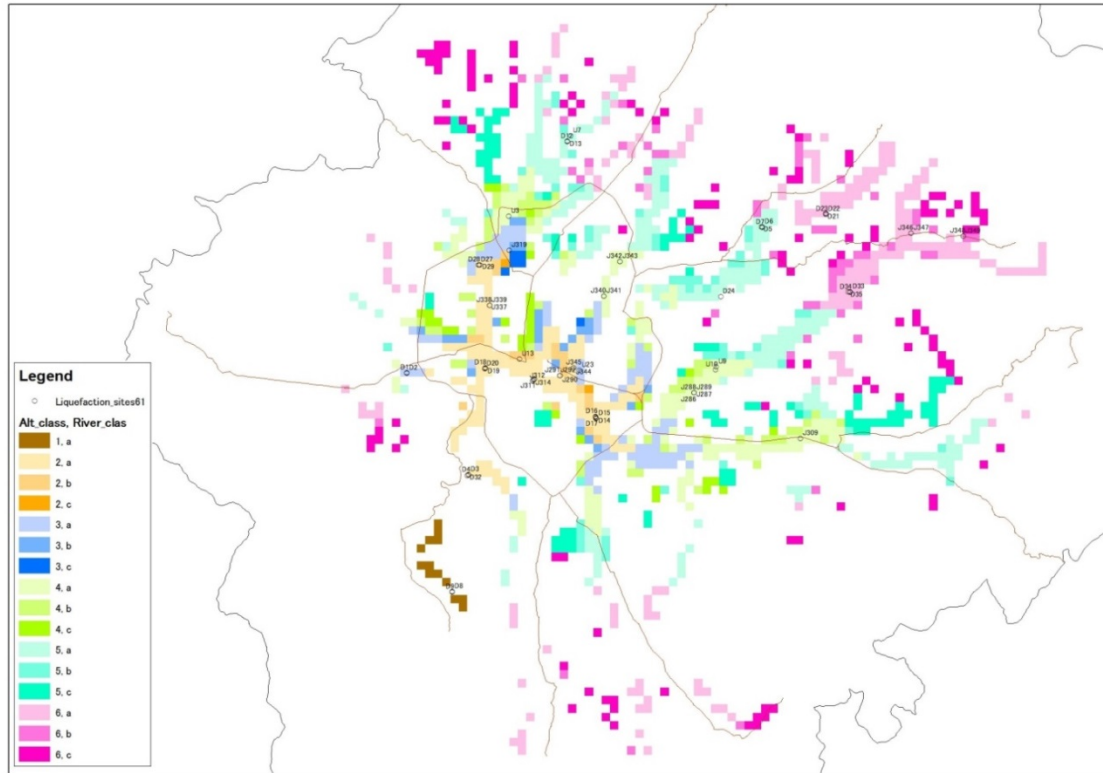
**Table 3.8.5 Assumed ground water level according to the distance from river**

Distance from river (m)	Dry season	Rainy season
a. within 250m	1m	0m
b. 250 - 500m	3m	2m
c. more than 500m	5m	4m

**5) Overburden pressure and effective overburden pressure**

Overburden pressure and effective overburden pressure can be calculated using above properties of density and underground water level.

Therefore, it is possible to calculate the liquefaction assessment using the above conditions. Then, the distribution of the area division and groundwater level based on the above setting of areas is shown in Figure 3.8.7. It should be noted that the assessment unit is a 250m grid.



Source: JICA Project Team

**Figure 3.8.7** Liquefaction assessment target grids with area division and ground water level

### 3.8.3 Verification of liquefaction assessment

For verification, the liquefaction assessment was tried using 60 borehole data for nine patterns of verification earthquakes and scenario earthquakes. Table 3.8.6 shows the results.

As per the results, out of the 60 examples, the rainy season case of the Gorkha Earthquake showed three sites of “M: moderate possibility of liquefaction, and eight sites of “L”: low possibility of liquefaction. Further, out of four of actual liquefied sites, three sites were calculated “L”, one non-liquefied site showed “O”: no possibility of liquefaction. Actually, the Gorkha Earthquake happened in late April during the end of the dry season, but according to the interview at sites, the underground water level was mostly shallow. Therefore, the evaluation fit at most point of no liquefaction, it can be said that the estimation roughly explained the condition. There was no report of liquefaction due to the largest aftershock of the Gorkha Earthquake, and the estimation showed the same. In the case of the 1934 Bihar-Nepal Earthquake, “H”: high possibility of liquefaction may appear, as well as nearly half of the examples showed “L” or “M”. This also conforms to the information from history.

From the above, it was judged that the actual situation of liquefaction in case of the verification earthquake is approximately described by the method adopted in this project. That is, in general for the history of liquefaction for the Gorkha Earthquake, although liquefaction did not occur, it may be judged that liquefaction occurred at some particularly likely sites.

**Table 3.8.6 Assessment result of liquefaction for borehole data with N value**

Model Division	Geo Morphology	Altitude (m)	River Distance (m)	Liquefaction History (2015)	Gorkha		Largest Aftershock of Gorkha		1934 Bihar-Nepal		Far-Mid West (1505)		West		Central Nepal South (x1/3)		Central Nepal South (x1/2)		Central Nepal South (x1/1)			
					M7.8		M7.3		M8.3		M8.6		M7.8		M7.8		M7.8		M7.8		M7.8	
					Wet	Dry	Wet	Dry	Wet	Dry	Wet	Dry	Wet	Dry	Wet	Dry	Wet	Dry	Wet	Dry	Wet	Dry
1	vp	1264.8	a		O	O	O	O	O	O	O	O	O	O	O	O	O	O	O	O	O	
1	nl	1265.8	a		O	O	O	O	O	O	O	O	O	O	O	O	O	O	O	O	O	
2	vp	1265.9	a		O	O	O	O	O	O	O	O	O	O	O	O	O	O	O	O	O	
2	vp	1265.9	a		O	O	O	O	O	O	O	O	O	O	O	O	O	O	O	O	O	
2	al	1275.9	a		O	O	O	O	O	O	O	O	O	O	O	O	O	O	O	O	O	
2	al	1275.9	a		O	O	O	O	O	O	O	O	O	O	O	O	O	O	O	O	O	
2	al	1276.1	a		O	O	O	O	O	O	O	O	O	O	O	O	O	O	O	O	O	
2	al	1276.7	a		M	L	O	O	O	M	M	L	L	M	L	M	M	M	M	H	M	
2	fr	1277.1	a		O	O	O	O	O	O	O	O	O	O	O	O	O	O	O	O	O	
2	al	1287.7	a		O	O	O	O	O	O	O	O	O	O	O	O	O	O	O	O	O	
2	al	1287.3	a		O	O	O	O	O	O	O	O	O	O	O	O	O	O	O	O	O	
2	al	1283.7	b		L	L	O	O	H	M	O	O	L	O	M	M	H	H	H	H	H	
2	al	1283.9	a		O	O	O	O	O	O	O	O	O	O	O	O	O	O	O	O	O	
2	al	1283.9	a		O	O	O	O	O	O	O	O	O	O	O	O	O	O	O	O	O	
2	al	1283.9	a		O	O	O	O	O	O	O	O	O	O	O	O	O	O	O	O	O	
2	al	1284.4	b		L	L	O	O	M	M	O	O	L	O	M	M	M	M	M	M	M	
2	al	1284.4	b		L	L	O	O	H	M	L	O	L	L	M	M	H	H	H	H	H	
2	al	1286.0	a		M	O	O	O	H	M	O	O	M	O	H	L	H	M	H	H	H	
2	al	1286.0	a		L	L	O	O	M	M	L	O	L	L	M	M	H	M	H	H	H	
2	al	1289.2	a		O	O	O	O	O	O	O	O	O	O	O	O	O	O	O	O	O	
2	nl	1289.3	a		O	O	O	O	O	O	O	O	O	O	O	O	O	O	O	O	O	
2	nl	1289.5	a		O	O	O	O	O	O	O	O	O	O	O	O	O	O	O	O	O	
2	al	1289.8	a	Yes	L	O	O	O	L	L	O	O	L	O	L	L	L	L	L	L	M	
3	nl	1290.1	b		O	O	O	O	L	O	O	O	O	O	O	O	O	O	O	O	O	
3	vp	1292.6	a		O	O	O	O	L	L	O	O	O	O	L	L	M	M	H	H	H	
3	vp	1292.8	a		O	O	O	O	O	O	O	O	O	O	O	O	O	O	O	O	O	
3	al	1294.9	a		O	O	O	O	O	O	O	O	O	O	O	O	O	O	O	O	O	
3	al	1294.9	a		O	O	O	O	O	O	O	O	O	O	O	O	O	O	O	O	O	
4	al	1295.5	a		O	O	O	O	L	L	O	O	O	O	L	L	L	L	M	M	M	
4	al	1295.5	a		O	O	O	O	L	L	O	O	O	O	L	L	L	L	M	M	M	
4	al	1295.5	a		O	O	O	O	L	L	O	O	O	O	L	L	L	L	M	M	M	
4	al	1295.5	a		O	O	O	O	L	L	O	O	O	O	L	L	L	L	M	M	M	
4	al	1296.2	a		O	O	O	O	L	L	O	O	O	O	L	L	L	L	M	M	M	
4	al	1296.2	a		O	O	O	O	L	L	O	O	O	O	L	L	L	L	M	M	M	
4	al	1295.4	a		M	O	O	O	H	H	L	O	L	O	H	M	H	H	H	H	H	
4	al	1300.0	a		O	O	O	O	L	L	O	O	O	O	L	L	L	L	M	M	M	
4	al	1300.0	a		O	O	O	O	L	L	O	O	O	O	L	L	L	L	L	L	M	
4	al	1300.0	a	No	O	O	O	O	L	L	O	O	O	O	L	L	L	L	L	L	M	
4	al	1301.4	a		O	O	O	O	O	O	O	O	O	O	O	O	O	O	O	O	O	
4	al	1302.4	a		O	O	O	O	O	O	O	O	O	O	O	O	O	O	O	O	O	
4	al	1304.2	a		O	O	O	O	O	O	O	O	O	O	O	O	O	O	O	O	O	
4	al	1304.8	a		O	O	O	O	O	O	O	O	O	O	O	O	O	O	O	O	O	
5	al	1305.9	a		O	O	O	O	O	O	O	O	O	O	O	O	O	O	O	O	O	
5	vp	1312.4	a	Yes	O	O	O	O	L	L	O	O	O	O	O	L	L	L	L	M	L	
5	al	1315.1	a		O	O	O	O	O	O	O	O	O	O	O	O	O	O	O	O	O	
5	al	1319.3	a		O	O	O	O	O	O	O	O	O	O	O	O	O	O	O	O	O	
5	al	1319.4	a		O	O	O	O	O	O	O	O	O	O	O	O	O	O	O	O	O	
5	al	1319.5	a		O	O	O	O	O	O	O	O	O	O	O	O	O	O	O	O	O	
6	al	1329.2	a		O	O	O	O	O	O	O	O	O	O	O	O	O	O	O	O	O	
6	al	1329.8	a		O	O	O	O	O	O	O	O	O	O	O	O	O	O	O	O	O	
6	al	1329.9	a		O	O	O	O	O	O	O	O	O	O	O	O	O	O	O	O	O	
6	al	1330.1	a		O	O	O	O	O	O	O	O	O	O	O	O	O	O	O	O	O	
6	al	1330.4	b	Yes	L	O	O	O	M	M	O	O	O	O	L	L	M	M	M	M	H	
6	al	1330.9	a		O	O	O	O	O	O	O	O	O	O	O	O	O	O	O	O	O	
6	al	1331.8	a		O	O	O	O	O	O	O	O	O	O	O	O	O	O	O	O	O	
6	al	1341.8	b		O	O	O	O	L	O	O	O	O	O	O	O	O	O	O	O	O	
6	al	1341.8	b		O	O	O	O	O	O	O	O	O	O	O	O	O	O	O	O	O	
6	vp	1343.1	b	Yes	L	O	O	O	M	M	O	O	L	O	M	L	H	M	H	H	H	
6	vp	1346.2	a		O	O	O	O	M	M	O	O	L	O	M	M	M	M	M	M	M	
6	vp	1346.2	a		O	O	O	O	L	L	O	O	O	O	O	O	O	O	O	O	O	

Area Division		Ground Water Level		
1	Bagmati River drainage (South of Chobar)	Distance from River	Dry Season	Rainy Season
2	lower than 1290m (Valley central)	a. within 250m	1m	0m
3	1290-1295m (Valley central)	b. 250m - 500m	3m	2m
4	1295-1305m (Valley central)	c. More than 500m	5m	4m
5	1305-1325m (Valley central)			
6	higher than 1325m (Valley central)			
Geomorphology		Judgment of Liquefaction Possibility		
al	Alluvial Low land	(O)	No possibility	
fr	Former River Course	(L)	Low possibility	
nl	Natural Levee	(M)	Moderate possibility	
vp	Valley Plain	(H)	High possibility	

Source: JICA Project Team

### 3.8.4 Liquefaction assessment results for scenario earthquakes

The assessment was conducted assuming ground model to each 250m grid in target area. If



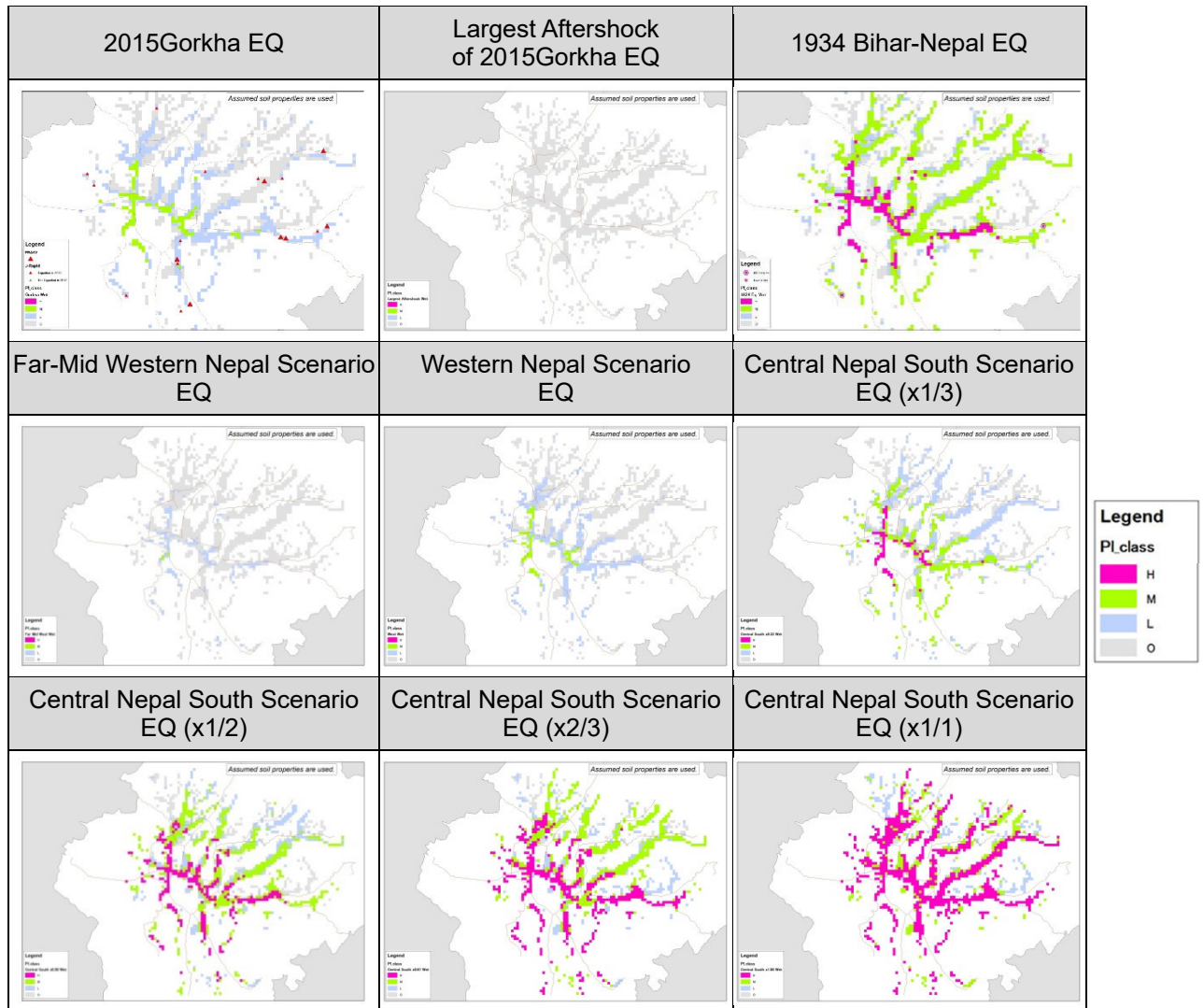
multiple results are available in one grid, the result based on the existing borehole data is prioritized. The assessed results of both the rainy season and dry season are shown in and respectively.

Note that with rainy season with a higher groundwater level is more likely to have liquefaction than the dry season. Also, the rainy season result could explain the history of liquefaction in the 2015 Gorkha Earthquake. Thus, from the viewpoint of disaster management, the results of rainy season are recommended to be prioritized. As described above, since the ground information is insufficient, the assumption that there is a sand layer in each grid is set, which provides overestimated results.

The feature of each earthquake is described below. First, for the largest aftershock of the 2015 Gorkha Earthquake, occurrence of liquefaction is not expected. For the Gorkha Earthquake and Far-Mid Western Nepal Scenario earthquake and Western Nepal Scenario earthquake, the result of liquefaction is assumed to have a rare occurrence. In the case of the Gorkha event, it is confirmed that there was some occurrence of liquefaction, but they did not bring actual damage. And, in the 1934 Bihar-Nepal Earthquake and Central Nepal South Scenario earthquake of correction coefficient  $x1/3$ , the possibility of the occurrence of liquefaction was assumed as some liquefaction possibility at central part of valley. The assumed results conform to the actual historical information due to the 1934 earthquake. In other cases ( $x1/2$ ,  $x2/3$ ,  $x1/1$ ) of the Central Nepal South Scenario earthquake, the possibility of liquefaction occurrence is assumed to gradually spread toward the peripheral region of the valley.

The occurrence of liquefaction is sensitive to soil characteristics at each point and the underground water level. Further, whether or not sand or water boils to the surface is strongly affected by the ground situation in the vicinity of the ground surface. For this reason, the liquefaction phenomena observed in reality shows mostly a shape such as boiled sand cones or fissures. This assessment of liquefaction was conducted setting a typical ground model even if there was a sand layer and underground water level for each 250m grid from data constraints. However, even in a 250m grid, both the situation of the ground and the status of the groundwater level have a variety. Therefore, even though the liquefaction possibility is judged to be “H”: possibility of liquefaction is high at any grid, it must be reasonable to have the possibility of sand or water boiling at somewhere in the grid, rather than the occurrence of liquefaction in the whole grid area.

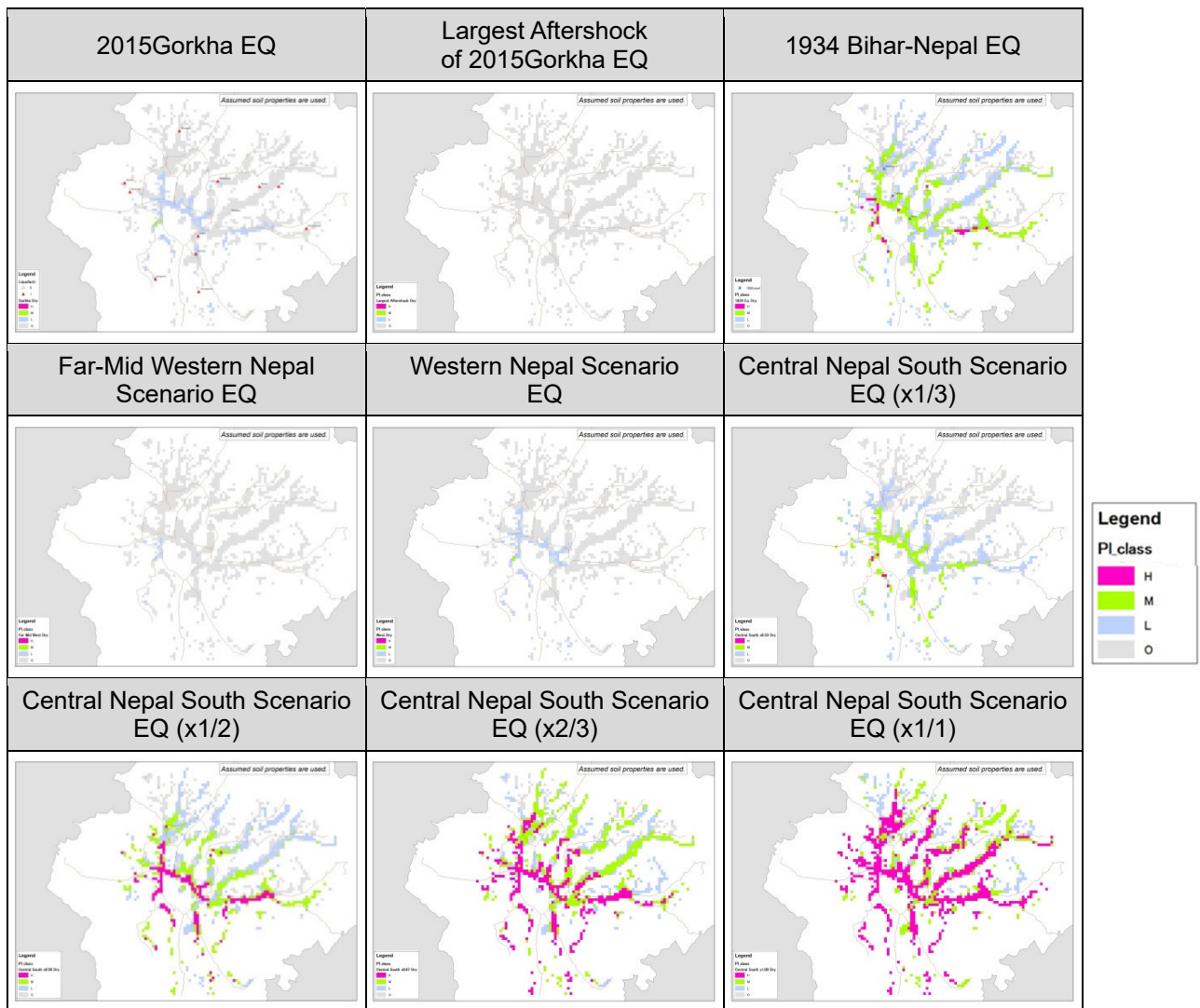
Although repeating again, the above evaluation is under setting the assumption that there is a sand layer to each target grid according to the insufficiency of ground information. Then, actually when there is no sand, or when sand is partly not whole, it may become overestimated in such cases.



Note: assumed soil properties are used according to their shortage

Source: JICA Project Team

**Figure 3.8.8 Assumed result of liquefaction (rainy season)**



Note: assumed soil properties are used according to their shortage

Source: JICA Project Team

**Figure 3.8.9 Assumed result of liquefaction (dry season)**

### 3.8.5 Evaluation method for liquefaction by Architectural Institute of Japan

The evaluation method of liquefaction by the Architectural Institute of Japan (AIJ, 2001) is shown below. It should be noted that the term, charts, number of expressions as remains as the original, but translated into English.

Section 4.5 Liquefaction of ground (page 61 - 71 of original copy) in “Recommendations for Design of Building Foundations (AIJ) 2001” is originally translated as below,

### **Concept**

1. Evaluate the possibility of liquefaction occurrence in an earthquake by appropriate means for saturated sand soil.
2. Evaluate the degree of liquefaction, deformation of ground after liquefaction, degree of deformation and ground rigidity, fall in sub-grade reaction, etc. For the ground where the possibility of liquefaction has been judged to be high.
3. In foundation design for the ground where the possibility of liquefaction has been judged to be high, the foundation design methods considering the effects of liquefaction must be selected as well as providing measures as required.

Grounds that have liquefied will cause settling and leaning of the spread foundation by its complete loss of bearing capacity or the apparent loss of rigidity. Furthermore, dynamic and residual lateral displacement and settling by liquefaction and lateral flow ground may lead to damage to the pile foundation. For retaining walls and sub-structures, the soil pressure will increase by liquefaction and could result in possible damage. In addition, liquefied soil will behave like a liquid with unit weight of almost double that of water, and by this, underground installations with small unit weight will float with the increase in buoyancy and reduced friction. To prevent these kinds of damage, in the basic design for liquefied ground, in addition to predicting the possibility of liquefaction, the decrease in ground rigidity and sub-grade reduction, increase in ground deformation, changes in soil pressure, buoyancy and friction must be determined, and its effects appropriately considered and measures be taken appropriately as required.

The degree of liquefaction and damage will vary widely with the density of the soil. In loose sand, deformation will progress while strength and rigidity will remain small, leading to severe damage, while with compacted sand, the ground strength will recover when the deformation reaches a certain extent, and the damage will be relatively smaller. This phenomenon, to distinguish it from liquefaction, shall be named “cyclic mobility.” The extent of damage will also differ with the depth of the liquefied stratum. In this guideline, as an index to evaluate the degree of liquefaction, dynamic lateral displacement of the ground surface caused by the shear deformation of the liquefied stratum shall be applied.

The design flow for the foundation structure for liquefied ground shall be divided into 1) Liquefaction judgment and ground deformation forecast and 2) Design of foundation considering liquefaction. Liquefaction judgment, ground deformation forecast, evaluation of sub-grade reaction and rigidity, and the concept of foundation design are described hereunder.

**(1) Liquefaction judgment**

**1) Soil stratum to be considered**

The saturated soil stratum requiring liquefaction judgment is of an alluvial formation, generally located in a depth of around 20m or less below the ground surface, and the type of soil to be considered is soil with a fine fraction content of 35% or less. However, there have been reports where liquefaction has occurred in artificially created ground such as reclaimed ground, ultra plastic silt with fine fraction content of 35% or higher and silt with soil water content close to its liquid limit, therefore a liquefaction study must be made for soil with clay content (soil fraction of soil diameter of 0.005 mm or less) of 10% or less, or reclaimed or filled ground with a plasticity index of 15% or less. The possibility of liquefaction cannot be denied for gravel with fine fractions or surrounded by a soil stratum of low permeability, and a study for liquefaction must also be made in these cases.

**2) Liquefaction risk forecast**

Liquefaction judgment may be in accordance with the following procedure, using Figure 3.8.10 through Figure 3.8.14.

- (a) Equivalent cyclic shear stress ratio generated at each depth of the ground concerned shall be obtained from the following equation:

$$\begin{aligned} \frac{\tau_d}{\sigma_z} &= \gamma_n \frac{\alpha_{\max} \tau_d}{g \sigma_z} \gamma_d \frac{\tau_d}{\sigma_z} = \gamma_n \frac{\alpha_{\max} \tau_d}{g \sigma_z} \gamma_d \frac{\tau_d}{\sigma_z} = \gamma_n \frac{\alpha_{\max} \tau_d}{g \sigma_z} \gamma_d \\ \frac{\tau_d}{\sigma_z} &= \gamma_n \frac{\alpha_{\max} \tau_d}{g \sigma_z} \gamma_d \frac{\tau_d}{\sigma_z} = \gamma_n \frac{\alpha_{\max} \sigma_z}{g \sigma_z} \gamma_d \end{aligned} \quad (3.8.10)$$

Where,  $\tau_d$  is the amplitude of equivalent constant cyclic shear stress ( $\text{kN/m}^2$ ) generated on the lateral plane;  $\sigma'_z$  is the effective overburden pressure (effective vertical stress) ( $\text{kN/m}^2$ );  $\gamma_n$  is the correction coefficient concerning the equivalent number of cycles and is  $0.1 (M-1)$ ;  $M$  is the seismic magnitude;  $\alpha_{\max}$  is the design lateral acceleration at ground surface ( $\text{cm/s}^2$ );  $g$  is the gravity acceleration ( $980 \text{ gal} = \text{cm/s}^2$ );  $\sigma_z$  is the total overburden pressure at the depth concerned (total vertical stress) ( $\text{kN/m}^2$ ); and  $\gamma_d$  is the reduction coefficient of the ground not being a rigid body, and expressed by the following:

$$\gamma_d = 1 - 0.015z \quad (3.8.11)$$

Where,  $z$  is the depth from the ground surface expressed in meters.

- (b) Corrected N-value ( $N_a$ ) corresponding to the depth is obtained from the following equation:

$$N_1 = C_N * N \quad (3.8.12)$$

$$C_N = \sqrt{98/\sigma'_z} \quad (3.8.13)$$

$$N_a = N_1 + \Delta N_f \quad (3.8.14)$$

Where,  $N_1$  is the reduced  $N$ -value,  $C_N$  is the conversion coefficient concerning confining pressure,  $\Delta N_f$  is the corrected  $N$ -value increment corresponding to fine fraction content  $F_C$  as per Figure 3.8.11.  $N$  shall be actually measured  $N$ -value by the pigtail-hook drop method or the automatic drop method.

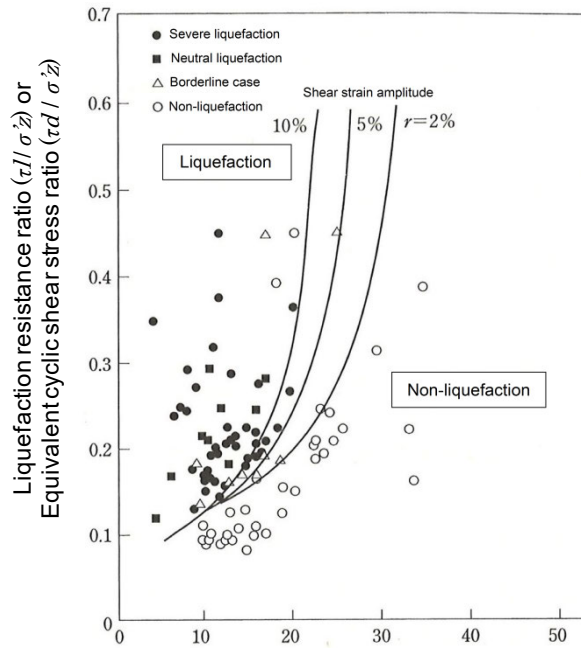


**Figure 3.8.10 Relationship Between Corrected  $N$ -Value, Liquefaction Resistance and Dynamic Shear Strain**

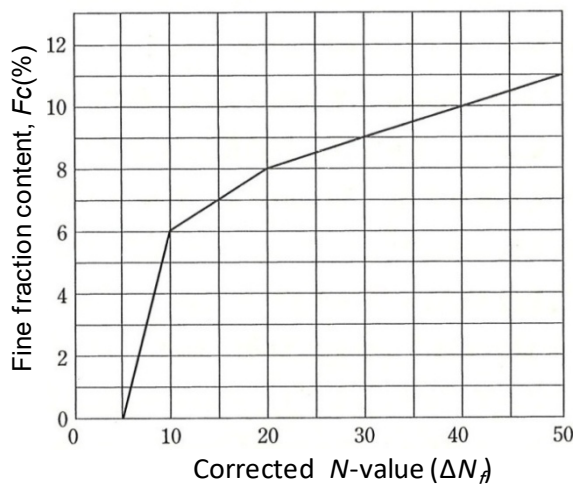


**Figure 3.8.11 Fine Fraction Content and Correction Coefficient for  $N$ -Value**

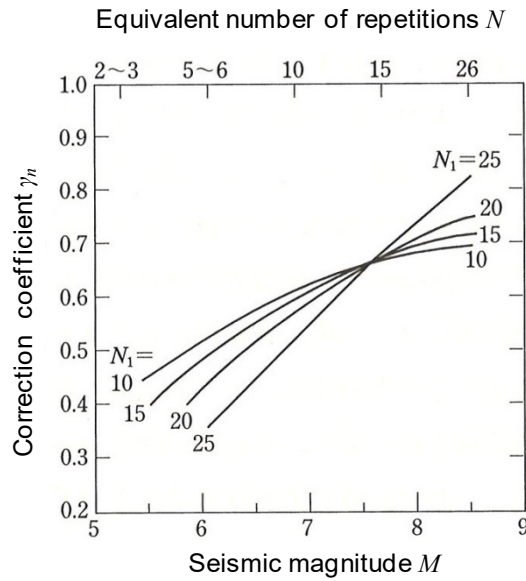


**Figure 3.8.12 Relationships Among Corrected N-Value, Magnitude, Number of Repetitions and Correction Coefficient**

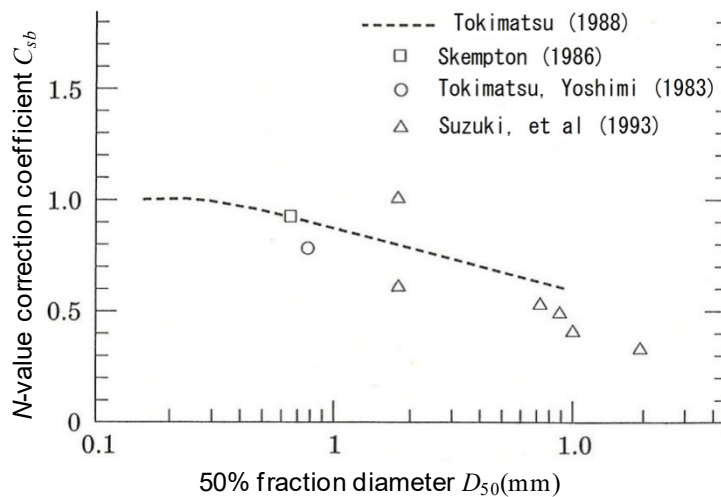


**Figure 3.8.13 N-Value Correction Coefficient for Sand/Gravel Ground**

- (c) Using the limit shear strain curve at 5% in Figure 3.8.10, liquefaction resistance ratio  $R = \tau_l / \sigma'_z$  for saturated soil layer corresponding to corrected N-value ( $N_a$ ) is obtained. Here,  $\tau_l$  is the liquefaction resistance at the lateral plane.
- (d) Safety factor  $F_l$  against the generation of liquefaction at each depth shall be calculated by the following equation:

$$F_l = \frac{\tau_l / \sigma'_z}{\tau_d / \sigma'_z} \quad (3.8.15)$$

It is judged that there shall be no liquefaction for soil stratum where  $F_l$  is greater than one, but on the other hand, if it is one or less, the possibility exists and the smaller the number,

the larger the risk of liquefaction, and the greater the depth of the soil stratum where  $F_l$  is one or less, the greater the risk.

In the above procedure, the lateral acceleration at the ground surface in the calculation of cyclic shear stress ratio ( $\tau_d / \sigma'_z$ ) is the result of ground response, and is greatly influenced by the ground properties. However, we recommend the use of 150 to 200 cm/s<sup>2</sup> hereunder, for check of the damage limits, and 350 cm/s<sup>2</sup> for the check of ultimate limit study. 350 cm/s<sup>2</sup> corresponds almost to the maximum value observed on liquefied ground in the 1995 South Hyogo Prefecture Earthquake. If shear stress needs to be obtained more appropriately, it can be obtained by defining the input seismic vibrations against the engineering foundation by maximum velocity and spectrum and (1) obtain the depth distribution of shear stress through response analysis or (2) obtain shear stress by the method indicated in (a) above after assuming ground surface acceleration. The accuracy of  $\gamma_d$  in Eq. (3.8.10) will worsen with the increase in depth. When this situation is to be assumed, the use of response analysis is recommended. Equivalent linearization analysis may be permitted for this analysis and in such a case, it can be done by factoring  $\gamma_n$  in Eq. (3.8.10) to the maximum shear stress ratio to obtain ( $\tau_d / \sigma'_z$ ) and following the procedures in the guideline, as follows. In addition, it is also possible to determine  $\gamma_n$  from Figure 3.8.12 considering the calculated effective number of repetitions of the seismic wave and the ground density.

For gravel type soil where the  $N$ -value tends to be large,  $N$ -value correction coefficient  $C_{sb}$  in Figure 3.8.13 may be used temporarily for its 50% fraction diameter  $D_{50}$ . However, in view of its reliability, it is desirable that it be studied in a comprehensive manner together with estimation method using large-scale penetration tests and an estimation method using  $S$ -wave velocity. Furthermore, for soil with relatively high fine-fraction with low reliability  $N$ -value, the use of estimation method to use cone penetration test or indoor-testing method for undisturbed samples to obtain liquefaction resistance, without relying on estimation method using  $N$ -value, is recommended.

### References (3.8)

- Architectural Institute of Japan (AIJ), 2001, Recommendation for Design of Building Foundations (in Japanese).
- Iwasaki, T., F. Tatsuoka, K. Tokita and S. Yasuda, 1980, Estimation of Soil Liquefaction during Earthquakes, Soil and Foundation, Vol.28, No.4, 23-29 (in Japanese).
- Marasini, N.P. and M. Okamura, 2014, Liquefaction Potential Analysis and Possible Remedial Measure for Existing Structure in Kathmandu Valley, International Journal of Landslide and Environment, Vol.2, No.2 & 3, pp.32-44.



- Okamura, M., N.P. Bhandary, N.P. Marasini, I. Towhata, S.N.Shrestha, I.P. Acharya, S.R. Adhikari and D.Pathak, 2016, Investigation of soil liquefaction and geotechnical properties in Kathmandu, J-RAPID.
- Piya1, B., C.J.Van Westen, T. Woldai, 2006, Generation of Geological Database for Liquefaction Hazard Analysis in Kathmandu Valley, Nepal, International Symposium on Geo-Disasters, Infrastructure Management and Protection of World Heritage Sites, pp.9-25.
- Rana, J. B., The Great Earthquake in Nepal (1934 A.D.), 1935, translated by Kesar Lal, Ratna Pustak Bhandar, Kathmandu, Nepal, pp 136, reprint 2013.
- UNDP/HMG/UNCHS (Habitat) (1994) Seismic Hazard Mapping and Risk Assessment for Nepal.
- United Nations Development Program (UNDP), Nepal, Comprehensive Disaster Risk Management Program (Report for MoUD/KVDA), 2013.

### **3.9 Earthquake Induced Slope Failure**

The susceptibility map for earthquake induced slope failure is shown in Figure 3.3.18 It shows the related Geomorphological units including Ls (landslide), ta (talus), es (eroded slope), fa (fan) and Bs (geomorphological base rock), and elevation contour lines of 20-meter intervals as well as locations of slope failure history which were collected from field survey after the 2015 Gorkha Earthquake and Environmental Engineering Geology Map of DMG, 1998.

In this section, the hazard map for slope failure potential was prepared considering PGA (peak ground acceleration) due to the scenario earthquakes as an external force to slope. The methodologies for this purpose commonly refer Wilson et al. (1979), Tanaka (1982) and so on. These methods require soil parameters of  $C$  (cohesion),  $\phi$  (internal friction angle) and density, as well as slope angles.

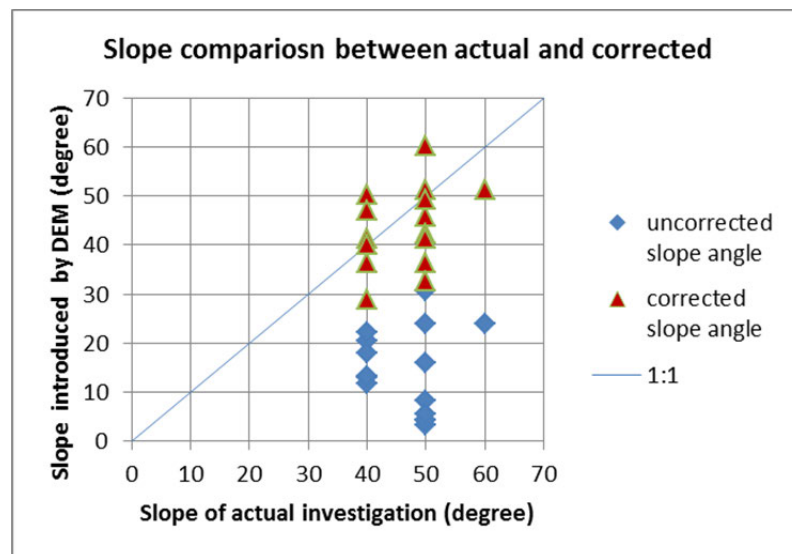
Although the above parameters for slope sites in Kathmandu Valley are not sufficiently available, a suitable method that can show the trend of damage to slope due to earthquake is adopted with assumed soil properties.

#### **3.9.1 Existing Data Collection**

##### **(1) Slope Angle**

Slope angle is one of the most important parameters contributing slope stability. For this, the digital elevation model (DEM) of 10-meter intervals provided from the UNDP project was used.

According to Figure 3.3.3, slope angles of the central region of KV are relatively more moderate than those of peripheral region. As the resolution of altitude is limited to 10-meter units, slope angles may be underestimated as compared to the actual small scale slopes less than the DEM interval. Considering this, a correction of slope calculation was applied to the original DEM. shows the comparison between the slope angles of the corrected DEM and the actual slope angles from the field survey. From this figure, it is clearly confirmed that the corrected slope angles match the actual one better than those of original DEM. Thus, the corrected slope angles were used for the following evaluation of slope failure due to earthquakes.



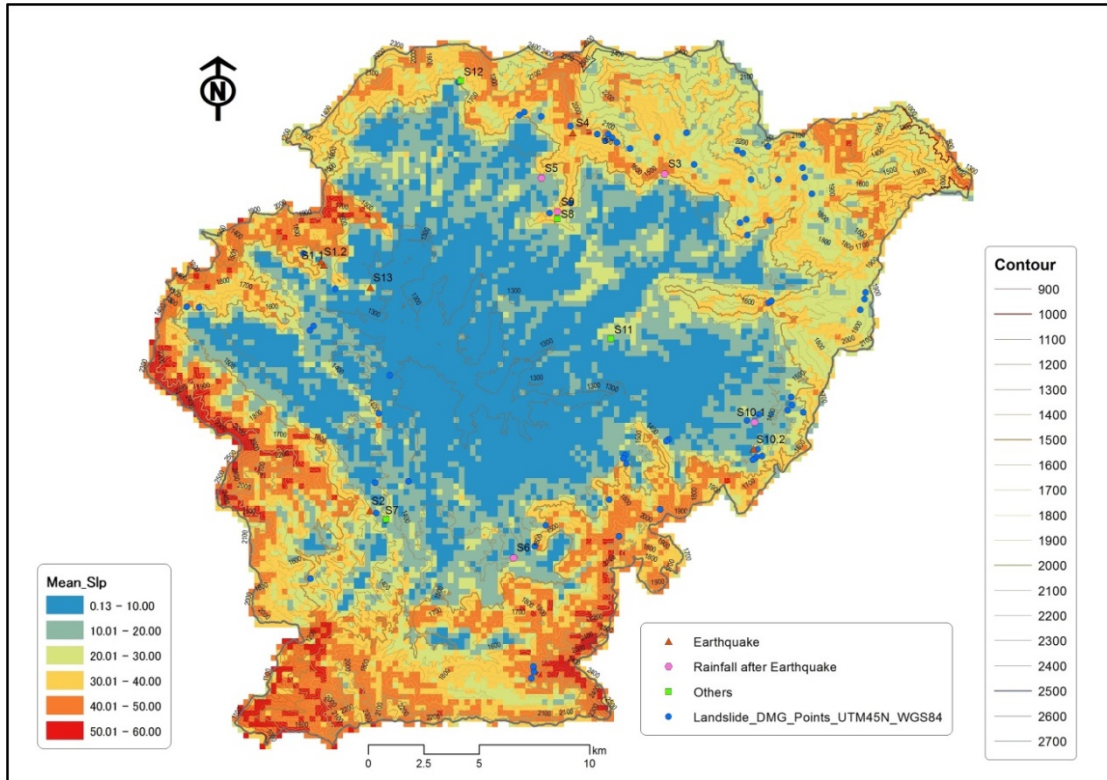
Source: JICA Project Team

**Figure 3.9.1 Slope angle comparison between actual and corrected**

Figure 3.9.2 presents the distribution of the corrected slope angle for 250meter grid. This figure shows the trend that the peripheral region is steeper than central.

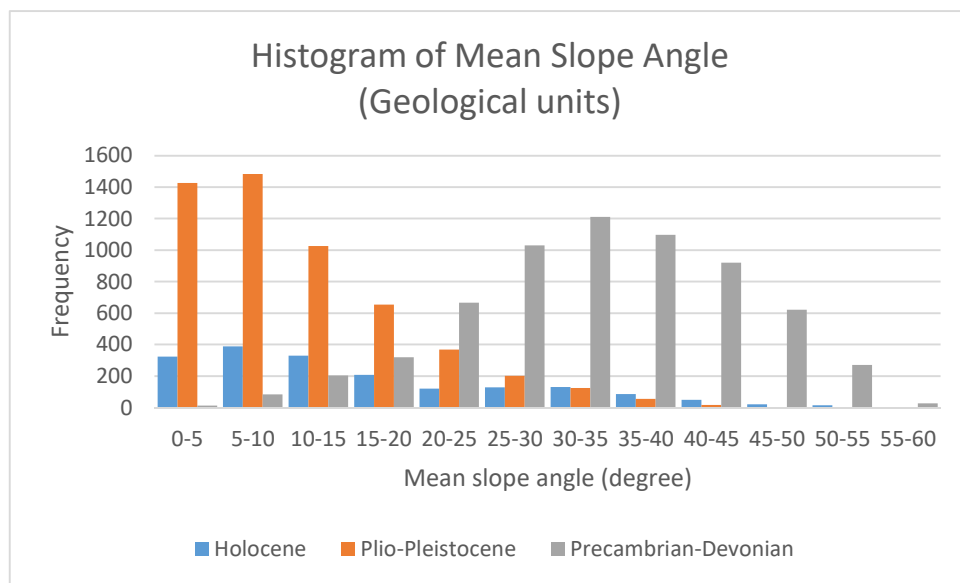
Figure 3.9.3 and Figure 3.9.4 show the histograms of corrected slope angles classified by geological units or geomorphological units respectively. From the histograms, the slope angles of geological ages during Precambrian to Devonian are distributed in the range of 20 to 50 degrees which are steeper than other geological ages. On the other hand, that of Tertiary to Quaternary mainly consisted of lake deposits distributed in the range of less than 20 degrees, which trend resembles that of the Holocene along rivers and in low lands.

The geomorphological units which are related to surface slip or landslide like Ls (landslide), ta (talus) and es (eroded slope) in distribute less than 20 degrees. Since it is also observed that some of eroded slopes are steeper than the trend of the histogram, the distribution of eroded slopes is shown in another layer of the result maps.



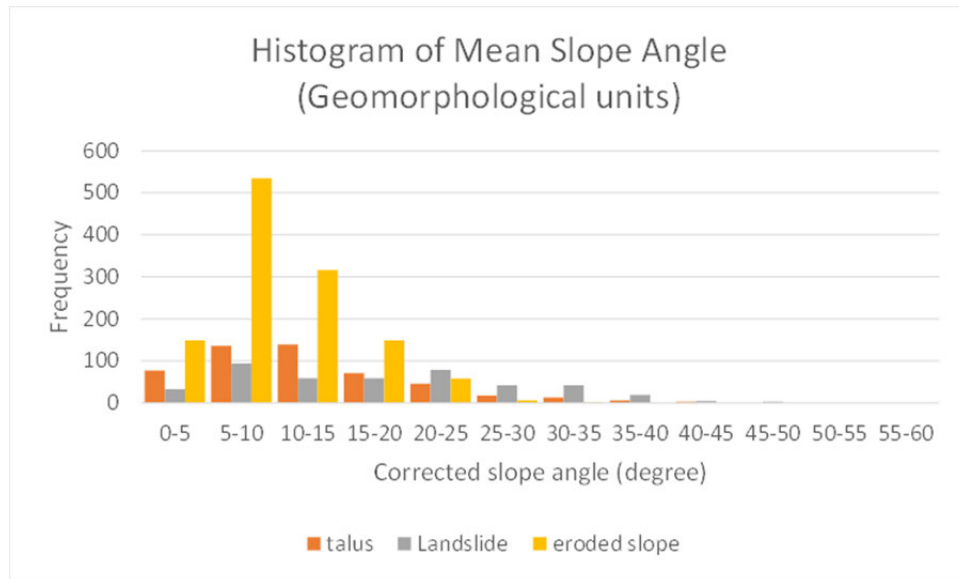
Source: JICA Project Team

**Figure 3.9.2 Distribution of Corrected Slope Angle**  
 (average of the slope angles at the points of 10-meter interval in 250 meter grid, with elevation contour and slope failure history)



Source: JICA Project Team

**Figure 3.9.3 Histogram of Mean Slope Angle classified by Geological Age**



Source: JICA Project Team

**Figure 3.9.4 Histogram of Mean Slope Angle for Geomorphological units relating to Surface Slip and Landslide**

**(2) Soil Properties of Slope**

In order to evaluate slope failure, soil properties of  $C$  (cohesion),  $\phi$  (internal friction angle) and  $N$  value were collected and analyzed. Especially, the  $N$  value was classified by geological units and examined to estimate  $C$  and  $\phi$ .

Among the collected data, the shear stress test and compression test are available for  $C$  and  $\phi$ . The disturbed and undisturbed soil samples are included. Figure 3.9.1 summarizes the total 29 data list from Department of Roads. As the values of  $C$  are distributed to a range more than 4 KN/m<sup>2</sup>, and the values of  $\phi$  distributed in the range of 20 to 30 degrees. However, since most of the  $N$  values are over 5, they do not correspond to samples at slope failure sites.

Next,  $N$  value data with less than 10 in the depth of less than 5 meters are screened, classifying by geological, geomorphological units or soil types (Figure 3.9.5).

Consequently, as these collected soil test data are for designing bridges, it is found that their sampling sites locate mostly in and around terraces with less slope hazard. Furthermore, a less weathered soil sample was found. Thus, it is difficult to grasp the trend of soil properties of slope from this data set.

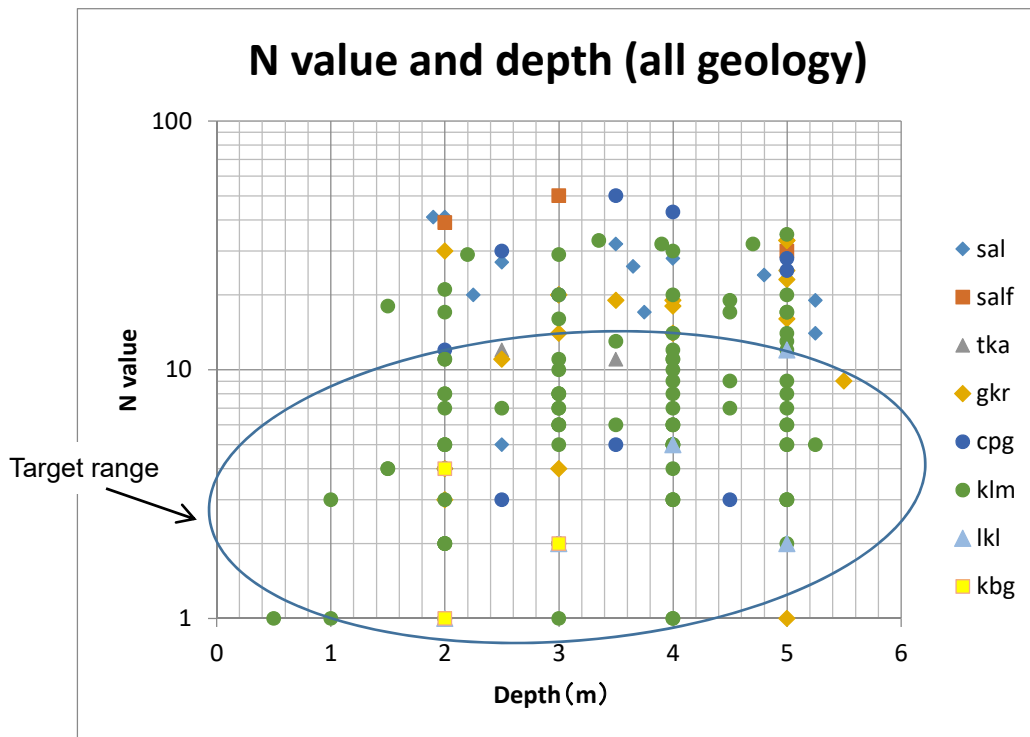
Within the selected data where the  $N$  value is less than 10 and the depth is less than 5 meters, the statistical result of  $N$  value is; average “ $X$ ” is 4.59, standard deviation “ $\sigma$ ” is 2.47. If taking the safety side,  $N$  value by the calculation of ( $X - \sigma$ ) is 2.12.

**Table 3.9.1 Summary Table of Soil Properties (including  $C$  and  $\phi$ )**

No	Depth of sample		geology	geomor	Soil		Sample	density	Shear test		Compression strength (kN/m <sup>2</sup> )	N value
	From	to	symbol	phology	Type	WL			type	C(kN/m <sup>2</sup> )		
1	4.5	4.95	klm	vp	C-Si	2.8	SPT	1.877	0.0	30	-	25
2	12	12.45	klm	vp	C-Si	2.8	UDS	1.800	61.7	-	123.6	17-31
3	4.5	4.95	klm	vp	C-Si	1.5	SPT	1.872	0.0	30	-	11
4	5	5.5	klm	vp	C-Si	1.5	UDS	1.820	60.3	-	120.7	11-12
5	4.5	4.8	sal	vp	G	2.8	SPT	-	0.0	33	-	>50
6	7	7.5	sal	vp	C-Si	2.8	UDS	1.880	57.9	-	115.8	20-20
7	3	3.45	sal	vp	S	2.5	SPT	1.856	0.0	31	-	33
8	8	8.5	sal	vp	C-Si	2.5	UDS	1.790	58.9	-	117.7	8-18
9	9.5	10	nl	kgb	C-Si	3	UDS	1.400	121.6	-	243.3	34-36
10	9.5	10	nl	kgb	C-Si	2.5	UDS	1.450	133.4	-	266.8	40-36
11	7.5	8	sal	Bs	C-Si	3.5	UDS	1.540	186.4	-	372.8	36->50
12	8	8.5	sal	Bs	C-Si	3	UDS	1.390	146.2	-	292.3	42-46
13	4	4.5	tka	al	S-Si	6	UDS	1.674	9.0	27.5	-	11-13
14	6	6.45	tka	al	S	6	SPT	1.819	8.0	33	-	38
15	4	4.5	tka	al	S-Si	6.3	DS	1.662	14.0	26	-	14-23
16	9.75	10	tka	al	Si-S	6.3	UDS	1.674	4.0	29.5	-	45-32
17	7	7.5	sal	fr	Si	2.2	UDS	1.315	7.0	24.5	-	9-8
18	13	13.5	sal	fr	Si	2.2	UDS	1.305	29.0	21	-	9-6
19	6.5	7	klm	fr	Si	12.5	UDS	1.424	6.0	23.5	-	6-9
20	12.5	13	klm	fr	Si	12.5	UDS	1.448	4.0	21.5	-	7-7
21	8	8.5	klm	al	Si	11.5	UDS	1.474	30.0	17.5	-	9-11
22	15	15.5	klm	al	Si	11.5	UDS	1.373	17.0	23.5	-	11-11
23	3.5	4	klm	al	Si	2.1	UDS	1.419	17.0	23.5	-	5-11
24	9.5	10	klm	al	Si	2.1	UDS	1.364	15.0	19	-	12-12
25	11		klm	tr2	CSi	2	UDS	1.920	51.0	-	102.0	10-9
26	9.5		klm	tr2	CSi	5.6	UDS	1.910	47.5	-	95.0	8-9
27	9.5		klm	at	CSi	3.4	UDS	1.900	43.0	-	86.0	10-6
28	7	7.45	klm	tr2	C	4.2	UDS	2.015	12.3	28	-	9-6
29	12	12.45	klm	tr2	CSi	4.45	UDS	2.105	7.5	36	-	5-12

$q_u = 2 \cdot c \cdot \tan(45^\circ + \phi/2)$

Source: JICA Project Team



Source: JICA Project Team

**Figure 3.9.5  $N$  values classified by Geological units (surface 5 meters)**

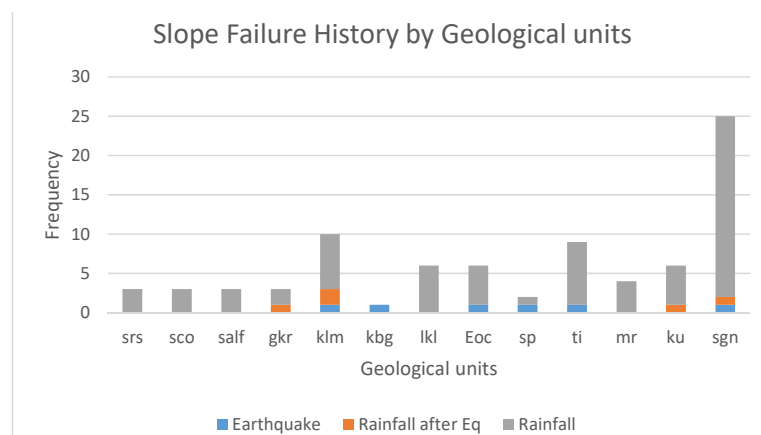
### (3) History of Slope Failure

As the historical data of slope failure in Kathmandu Valley, DMG published “Engineering and Environmental Geological Map” in 1998 where about 70 slope failure sites were mapped. It is noticeable that these data are due to rainfall, not ground shaking. Then, a field survey was carried out at the slope failure sites after the 2015 Gorkha Earthquake in this project. The total number of survey sites is fifteen; six slope failures are due to the earthquake, five are due to rainfall after earthquake, and the others are unknown.

Figure 3.9.6 presents the histogram of the history data of slope failure classified by geological units. It is found that slope failures occurred in many geological units and especially klm (Kalimati Formation) and sgn (Sheopuri gneiss) show high frequency. But klm and sgn are distributed widely in the geological map, and the ratio of sites per area is not higher than the other geological units. As shown in Figure 3.9.2, most of the slope failures are located in the peripheral region and less in the central region.

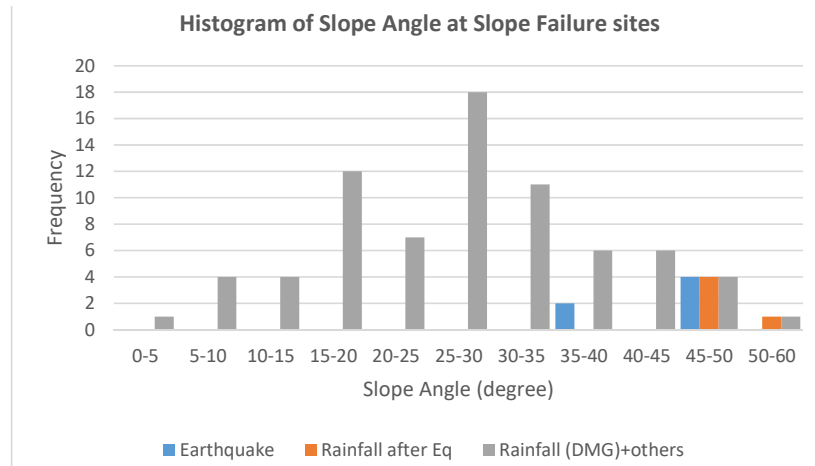
Figure 3.9.7 is the histogram of slope angle at the location of slope failure history. Slope angles due to rainfall commonly distribute in the range of 15 to 45 degrees, whereas the ones due to earthquakes are distributed in the range of 40 to 50 degrees. The historical sites in the slopes of less than 20 degrees mainly tend to surface failure or landslide. And it is worthy of special notice that no existing slope sites with a history of failure due to rainfall collapsed during the 2015 Gorkha Earthquake.

Figure 3.9.8 shows the relation between the slope angle and peak ground acceleration (PGA, gal) at the sites of slope failure. The following points are known from this figure: slope failure sites with moderate slope angle didn’t collapse even by 200 gal of PGA; there are no slope failures in less than 100 gal; and, there are no slope failures at sites with more than 50 degrees, which may be caused by a very shallow surface soft soil layer.



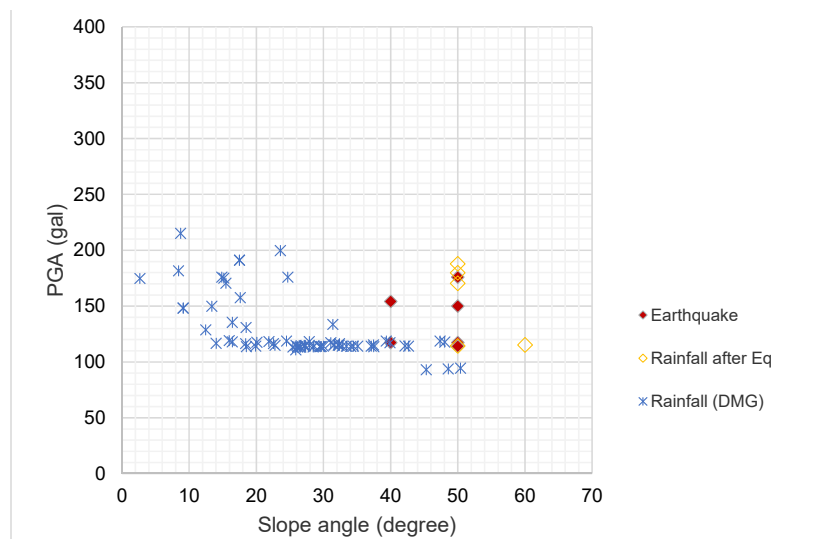
Source: JICA Project Team

**Figure 3.9.6 Histogram of Slope Failure History by Geological Units**



Source: JICA Project Team

**Figure 3.9.7 Histogram of Slope Failure History by Slope Angle**



Source: JICA Project Team

**Figure 3.9.8 Relationship between PGA and Slope Angle at Slope Failure History Sites**





During the 1934 Bihar-Nepal Earthquake, it was described that there were more moderate slope failures outside the Kathmandu Valley than inside. Furthermore, the document described as follows; “There were cracks in the roads as a result of the earthquake. No motor-car could go to Bhaktapur, Sankhu, Chapagaon and Godavari. But, as the main bridge was only slightly damaged, the roads to Bhaktapur and Sankhu became motorable from the 19th and 22nd January (EQ happened 15th) respectively. ... As other roads in the hill were used by men or horses only, despite landslides at different places, they did not become a problem for the people and the postal service. The roads within the three cities in the valley were full of debris.” (Rana, 1935, p.19). Unfortunately, the actual locations could not be identified from the above description.

In the 2015 Gorkha Earthquake, some small fallen rocks or road failures have been reported. But major slope failure damage was not reported.

Peak ground accelerations for the scenario earthquakes were estimated in Clause 3.7. The results were used for external force in slope stability assumption. The estimated PGAs of the 2015 Gorkha Earthquake are 100 to 150 gal in the central to northern region, 150 to 200 gal in the central region, and around 100 gal in the southern region. Also for the 1934 Bihar-Nepal Earthquake, PGAs are 100 to 150 gal in the western region, 200 to 250 gal in the eastern region, and 250 to 300 or 350 gal in the central region.

Some pictures in the field survey after the 2015 Gorkha Earthquake are shown in Figure 3.9.9 to Figure 3.9.11. After the earthquake, in case of Budhanilkantha Municipality, surface failures were observed which resulted in debris flow during monsoon season. The debris flow started from a surface failure upstream. It is a good example that the ground surface failure happened and expanded downstream due to rainfall with the increasing river water level. This kind of disaster would affect human activity, although in this case there were no houses in the area (Figure 3.9.9).

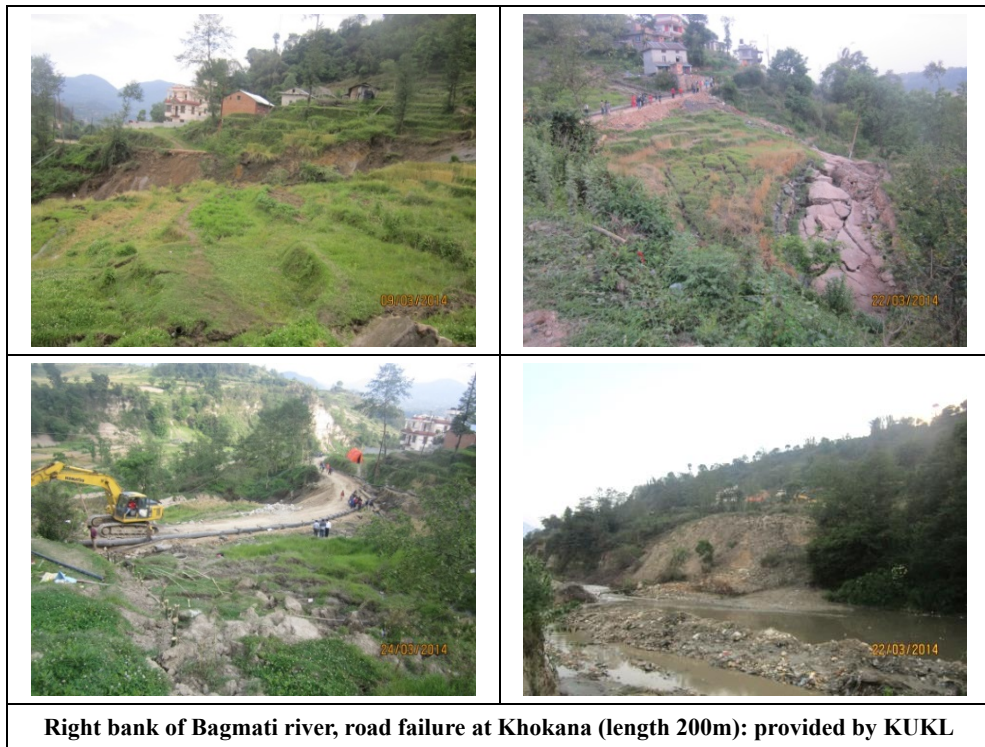
A couple of slope failures and road failures were pointed out along the Bagmati River and Bhaktapur Road during the earthquake. Figure 3.9.10 and Figure 3.9.11 show them respectively.

	
<p><b>The white bear soil in mountain looks to be the starting point of debris flow</b></p>	<p><b>White sand deposits along the stream at higher level can be detected to be debris flow deposits</b></p>
	
<p><b>Surface failure (Budhanilkantha)</b></p>	<p><b>Southern side at LS62 (near the MT Array site)</b></p>

Source: JICA Project Team

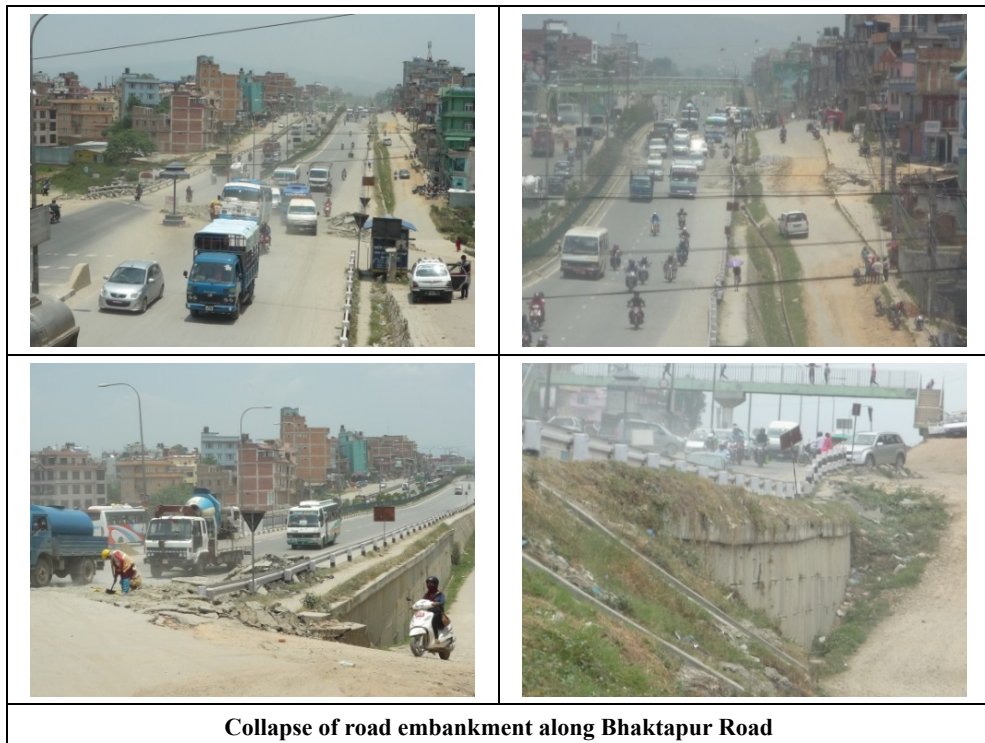
**Figure 3.9.9 Slope failure example by the 2015 Gorkha Earthquake (Budhanilkantha)**





Source: KUKL: Kathmandu Upatyaka Khanepani Limited

**Figure 3.9.10 Road failure by the 2015 Gorkha Earthquake (Bagmati River)**



Source: JICA Project Team

**Figure 3.9.11 Road embankment failure by the 2015 Gorkha Earthquake (Bhaktapur road)**

### 3.9.2 Types of Slope Failure

In general, slope failures due to earthquakes are divided into two types: landslide type and surface failure type.

#### (1) Landslide type

Landslide type slope failure occur at relatively moderate slope sites (angles are 5 to 20 degrees at most; JASDiM). The main cause is not only ground shaking but the vulnerable soil condition and underground water level. Therefore, it is difficult to foresee the location of landslide type failure using only the slope angle and PGA.

However, this landslide type shows typical topographical features. Ls in the Geomorphological Map created in this project (see Section 3.3.3) correspond to the landslides sites. Ls area can be vulnerable for slope stability during earthquakes. Actually, in Ls zones, any countermeasures cannot be seen. Some zones can be seen moving due to rainfall.

The Ls unit is identified as one of the hazardous slope zone in the Slope Susceptible Map along with ta (talus) and es (eroded slope) units.

#### (2) Surface failure type

As surface soil on the steep slope site is unstable, it is assumed to be fragile to ground shaking. To estimate this kind of slope failure certain macroscopic methods have been proposed by Wilson et al. (1979) or Tanaka (1982). For these kinds of methods, it is necessary to give (or estimate)  $C$ ,  $\phi$ , density and thickness of the slope surface soil.

Considering the above soil parameters,  $N$  value in such fragile surface soil may be in the range of 1 to 5. And  $C$  and  $\phi$  can be estimated from  $N$  value. The representative equations are as following;

$$\begin{aligned} C &= 12.5 * N / 2 \quad (\text{kN/m}^2) && \text{Terzaghi and Peck (1948)} \\ \phi &= (N * 15) (1/2) + 15 \quad (\text{degree}) && \text{Japan Road Association (2002)} \end{aligned}$$

For example, if  $N=4.59$  is given, then  $C=0.287$  ( $\text{kN/m}^2$ ) and  $\phi=23.3$  (degree). If  $N=2.12$  is given, then  $C=0.132$  ( $\text{kN/m}^2$ ) and  $\phi=20.6$  (degree). Regarding thickness of the vulnerable surface soil layer, it is assumed up to 1.5 m. Density is given as  $1.9$  ( $\text{g/cm}^3$ ) which is typical value from laboratory test. Target geological units are basically Plio-Pleistocene and Precambrian to Devonian.

### 3.9.3 Case Study of Surface Failure using Slope Angle and PGA

The equation of Wilson et al. (1979) or Tanaka (1982) for safety factor  $F = 1.0$  can introduce

relations between slope angle and PGA, if values of  $C$  and  $\phi$  are given. Figure 3.9.12 shows the two relations, blue line is for  $N=2.12$  ( $X-\sigma$ ) and orange line is for  $N=4.59$  (Average  $X$ ) if the thickness of the sliding layer is 1.5m.

Tanaka's equation is shown below;

Tanaka (1982)'s equation

$$a_c = g * (C / \gamma * h + (\cos \theta * \tan \phi - \sin \theta))$$

Where,

$a_c$ : critical acceleration including the slide

$g$ : acceleration of gravity

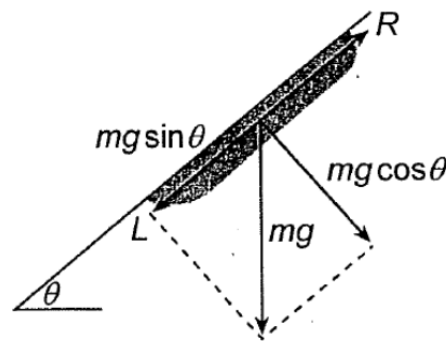
$C$ : cohesion of soil

$\phi$ : internal friction angle of the layer

$\gamma$ : unit weight of soil

$\theta$ : angle of slope

$h$ : thickness of the sliding layer



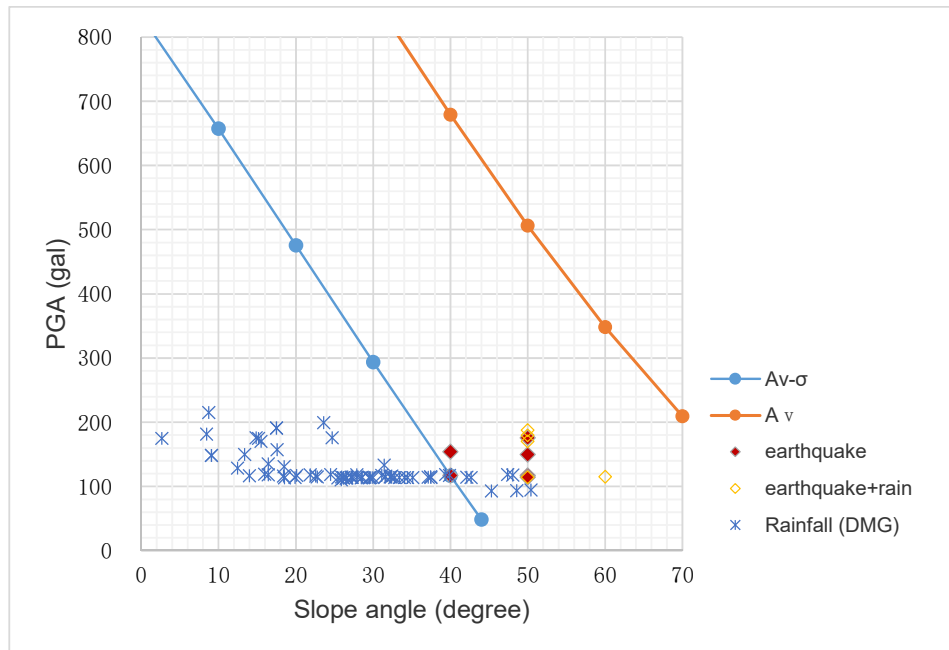
If the condition data (slope angle, PGA) of a grid is plotted in lower left side of the line, the slope is stable. On the other hand, if the data is plotted in upper right side of the line, the slope is unstable.

The historical slope failures caused by rainfall, where no slope failure occurred by 2015 Gorkha Earthquake, are also plotted in by a blue cross. By comparing these data and line, the blue line looks like separating the unstable slope from the stable slope due to the earthquake, however, the blue line can't separate the slope failure due to the earthquake motion and due to the rainfall after earthquake.

Secondly, the boundary of no slope failure due to the Gorkha Earthquake has been searched changing  $N$  value and  $h$  (thickness). The orange line ( $N=3$ ,  $h=1.6$ ) in can separate no slope failure data from the Gorkha Earthquake slope failure records. The green line ( $N=3$ ,  $h=1$ ) in can be applied to the case of slope angle over 50 degrees reflecting the fact that there is little history of slope failure due to the earthquake because of the thin surface sliding soil layer.

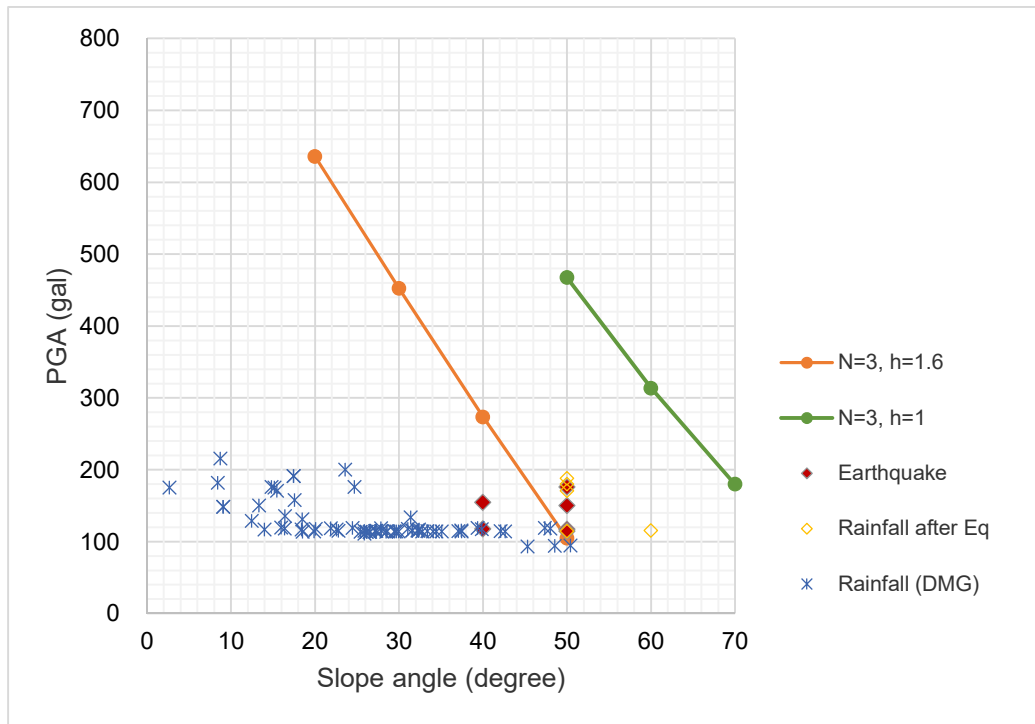
Additionally, following facts are considered in the analysis; there is no slope failure in the history where PGA is less than 100 gal, and slope failure is little and surface slide is dominant if slope angle is less than 20 degrees. Also in this study, target is the failure of natural slope due to the surface collapse. The landslides are not considered.

The slope failure evaluation method was applied to scenario earthquakes considering the additional conditions above. The calculation was done at each 10m grid point and slope failure potential was judged by the ratio of unstable 10m grid points in 250m grid.



Source: JICA Project Team

**Figure 3.9.12 Relationship between Slope Angle and PGA for Safety Factor (F=1.0)**



Source: JICA Project Team

**Figure 3.9.13 Proposed Surface Failure Evaluation Criteria**

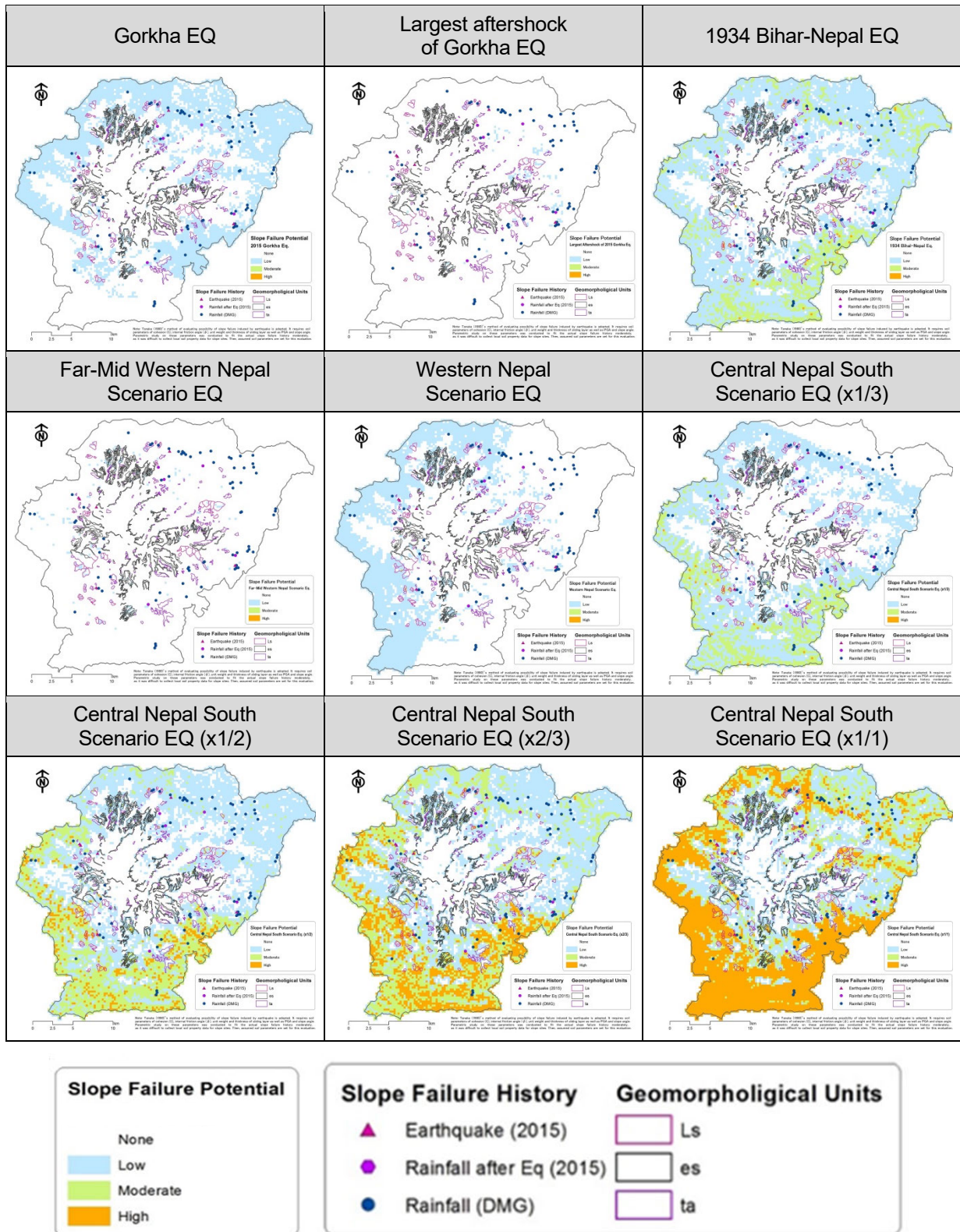
### 3.9.4 Slope Failure Evaluation Results

Figure 3.9.14 summarizes the results of earthquake induced slope failure evaluation for scenario earthquakes. In these maps, the slope failure relating geomorphological units, namely, Ls, ta and es are overlaid.

These maps describe the following situation: 1) Regarding Gorkha, Largest Aftershock, Far-Mid Western Nepal Scenario, and Western Nepal Scenario, very little slope failure potentials are estimated which corresponds to the actual condition of the 2015 earthquake. 2) Regarding 1934 Bihar-Nepal, Central Nepal South Scenario (x1/3), low potentials are estimated widely in the peripheral regions of KV. This situation corresponds to the description of the 1934 earthquake damage. 3) Regarding Central Nepal South Scenario (x1/2), (x2/3), (x1/1), slope failure potential increases gradually from southern part of KV where is nearer to the epicenter.

As described above, during the evaluation of earthquake induced slope failure, the existing information regarding ground condition ( $C$ ,  $\phi$ ,  $h$ ,  $N$  value) was very few. Therefore, the methodology of evaluation and ground properties were set or estimated as they will suit to the history of slope failure as much as possible.

In order to achieve the evaluation of slope stability with higher accuracy in the future, it is necessary to have more accurate ground information and methodologies.



Note: assumed soil properties are used according to their shortage  
 Source: JICA Project Team

Figure 3.9.14 Assumed results of earthquake induced slope failure due to scenario earthquakes

### 3.9.5 Slope Failure after Earthquake

It is reported that the surface soil became unstable due to the seismic motion of Gorkha Earthquake and after that, in some cases, slope failure occurred due to the rainfall. Slope failure is a usual natural disaster in Japan. Japanese are always warned about this kind of slope failure due to multiple causes, earthquake and rainfall. Not only the ground shaking but also rainfall after ground shaking sometimes cause slope failure. It is quite natural that rainfall after earthquake raise the potential of slope failure.

As shown above for an example, it is difficult to foresee slope failure using only slope angle and PGA. In this study, the general aspect of slope failure potential was evaluated.

In the case of rainfall after an earthquake, it is desirable for the people in vulnerable slope zones to move to safer places, or evacuation shelters. To enhance this kind of early warning and evacuation for the people, countermeasures by government is inevitable. Collaboration of the people with the government must be much more effective. To support this kind of activity, monitoring system of soil conditions and water level using gauges in the individual slope hazardous sites must be effective.

We would like to express our gratitude to KUKL, DoR for providing soil data, and local people for their cooperation during our field survey.

#### References (3.9)

- DMG (Department of Mines and Geology; Shrestha, O.M, A. Koirala, S.L. Karmacharya, U.B. Pradhan, and R. Karmacharya) (1998) Engineering and environmental geological map of the Kathmandu Valley, scale 1: 50,000.
- Japan Road Association (2002) Specifications for Highway Bridges, Part IV Substructures.
- JASDiM: Japan Association for Slope Disaster Management web site
- Rana, B.J.B. (1935). Nepal ko MahaBhukampa (Great Earthquake of Nepal); Jorganesh Press, Kathmandu. (Translated into English)
- Tanaka, K. (1982) Seismic Slope Stability Map (Present situation and several mooted points), Journal of Japan Landslide Society, 19-2, 12-19. (in Japanese).
- Terzaghi. K and Peck R.B. (1948) Soil Mechanics in Engineering Practice, John Wily & Sons.
- Wilson, R.C., Wieczorek, G.F., and Horp, E.L. (1979) Development of Criteria for regional Mapping of Seismic Slope Stability, Abstract, 1979 Annual Meeting of the Geological Society of America.

### **3.10 Considerations and Recommendations for the Future in the Seismic Hazard Assessment Performance**

In the practice of seismic hazard assessment, the challenges, which are the lack of necessary data and lack of human resources in the associated field, often appear. Furthermore, in the current project, the specific Gorkha Earthquake occurred just before the commencement of the project. The earthquake had significant characteristics in seismology and earthquake engineering fields. Therefore, the interpretation and reproduction of the Gorkha Earthquake as well as how to apply the scenario earthquakes were added as the major issues to be struggled.

Originally, the assessment method and necessary data were in a complimentary relationship of combination. Even if only one or the other is excellent, the total operation cannot always work sufficiently. If the reasonable method of assessment is made without the sufficient necessary data available, practically, the way to follow would be to select the supplementary estimates or change the method. The main items of seismic hazard assessment are earthquakes and the ground. The faced challenges, correspondence, notes for mainly earthquake and ground related matters during seismic hazard assessment are described in the following.

#### **3.10.1 Data and assessment method regarding earthquake**

With regard to the earthquake information, the results of the conventional seismic observation and research by DMG, the counterpart, was referred to. In addition, though not enough, several observations which were recorded by DMG and other institutions at the time of the 2015 Gorkha Earthquake has been provided. These achievements and observation records could be effectively utilized to verify the validity in ground motion evaluation method etc. In addition, actual statistical damage data also became an important document for the verification of the assumed result.

However, the PGA (peak ground acceleration) caused by the Gorkha Earthquake and its aftershocks appeared quite lower than the values than given by empirical attenuation equations, which was a remarkably different characteristic. On the other hand, long-period components showed a relatively larger value compared to the short-period components. The results were examined from a variety of information, which is believed to be caused by both complex phenomena of the seismic source characteristics of the Gorkha Earthquake and the effects of ground structure of the Kathmandu Valley. In this project, the "correction factor" is adopted for seismic motion in order to adjust the special phenomena, and the seismic ground motion is to be presented using the "potential range". Actually, in order to appropriately assess the seismic ground motion in Kathmandu, the empirical relation on site has to be used, but it is not available. So, currently the existing relations in another region of the world have



been adopted. These measures were taken because there is no attenuation equation in Kathmandu. In Nepal, it is recommended to study the attenuation equation of strong ground motion as well as it is proposed to implement more study of the historical earthquakes.

As an example, the 1505 earthquake of  $M = 8.6$  has to be a huge earthquake, though actual damage information in Nepal is hardly existent. According to the Chinese historical material, there is an article that Nepal village has been destroyed. However, there are fewer articles and more unknown factors because of fewer residential areas. In some cases, although the magnitude is larger than that of the Gorkha Earthquake, ground acceleration can sometimes be low. However, as currently the information is insufficient, it would be reasonable to consider a huge earthquake from the disaster management policy point of view.

Although the seismic ground motion in Kathmandu Valley will be low due to Far-Mid Western Nepal Scenario earthquake and Western Nepal Scenario earthquake, rather than that due to the Gorkha Earthquake in Kathmandu, it should not be forgotten that a major disaster can occur with respect to the region near the epicenter. In addition, "It should be considered more for the disaster management of Nepal that in the case of Central Nepal South Scenario earthquake, Terai area, closer to the epicenter with soft ground, would affect further intense damage", as Prof. Koketsu and Dr. Sapkota, Deputy Director General of DMG, pointed out.

### **3.10.2 Active fault investigation**

This project proposed the active fault investigation and its activity realistically for the first time in Kathmandu Valley. Up until now, DMG has conducted the trench survey at MFT, but has not implemented the survey in the Kathmandu Valley. If this survey is carried out, the scientists and engineers in the metropolitan area can directly refer to a real survey. And, if the knowledge can be obtained that an active fault lies directly under the capital, it can not only be a motivation, but also can be much important for disaster management.

On the other hand, to carry out active fault investigation of the MFT in SATREPS or the joint research between France and Nepal will be interesting.

### **3.10.3 Ground model**

In this project, taking into account the fact that long-period component is dominant in the Gorkha Earthquake, a ground model was prepared to a maximum depth of 500m. However, in practice, the number of deep drilling is small and the soil properties information was very less. Therefore, the current ground model can be improved with the increase of ground data in the future.

In the Kathmandu Valley, though the drilling had been carried out for the purpose of groundwater development, the description of the geological column is poor, which shows the

difficulty of using the existing drilling information for ground modeling. Each relating implementing agency should understand the importance of the drilling data and should be enforced to carry out ground surveys to grasp the ground properties steadily. Further, it is proposed that the DMG plays a central role to continue accumulating, storing and publicizing the data.

On the other hand, considering the fact that only the drilling cannot provide the physical property values, physical tests such as microtremor measurement to obtain the S-wave velocity information that was carried out in this project is also necessary. In this project, a large scale tripartite array microtremor measurement at five points, and a smaller scale array measurement at 74 points were implemented. In the future, it is expected that if microtremor measurement is conducted at more points mainly by the DMG, the ground model will become more accurate.

#### **3.10.4 Assessment for slope failure and liquefaction**

In order to assess slope failure and liquefaction during earthquake, currently both the soil property information and the history research are insufficient. Since the Gorkha Earthquake caused less damage by these two hazards, there were fewer disaster investigations immediately after the earthquake. Therefore, this project had to understand the damage history through interviews.

For soil physical properties, since there are less data of  $C$  and  $\phi$  that are necessary for slope failure assessment, they are assumed from  $N$ -value in this project. Also, regarding the parameters required for the liquefaction assessment, data of water level, particle size and so on are lacking significantly rather than the  $N$ -value data. Therefore, liquefaction for the entire Kathmandu Valley was evaluated by a very little data of only 60 drilling points with  $N$ -value. It is expected that the assessment accuracy can be further enhanced, after the property information is added in the future. By all means, it is highly desirable to study the detail history of the earthquake damage before the people who has the experience and information has faded away, especially for the 1934 earthquake case.

As described above, though the understanding of the soil physical properties is a challenge in future, during the project, dynamic soil testing was started and carried out outside of Nepal; tested in Japan. This is meaningful for dynamic geotechnical engineering in Nepal. Such a trend of consciousness to enhance the relevant technical personnel is to be developed.

#### **3.10.5 Human resource development**

In this project, the geomorphological map and the geological cross-sections are newly developed. Through the experience, the number of the engineers and human resources in the

field of relevant geotechnical and earthquake engineering in Nepal seemed extremely small. Also, the system to continue and develop the technology is lacking.

As it would be similar for the risk assessment techniques as well, it is recommended that Nepal should prepare a comprehensive education system for disaster management.

### **3.10.6 Results of seismic hazard assessment**

With respect to scenario earthquakes, although the tectonic information was referred to, it is natural that the exactly same earthquakes will not take place in actuality, and also it cannot be predicted when they will occur. As mentioned above, the physical properties in the ground model are estimated from less data. In addition, the ground models at 11,934 grids are based on only around 449 data per approximately 722 square kilometers. It is not enough density of data to cover the study area. In this project, ground models are assumed based on newly produced geomorphology map, geological cross-sections and microtremor measurement results. Therefore, some deviations associated with the assumption of the ground model should be understood in the seismic hazard assessment results.

There are various matters in the 250m grid models that cannot be interpreted and described during the liquefaction and slope failure assessment process, such as the presence of a sand layer below water level, or the presence of slip boundaries underground. For example, in this liquefaction assessment, the typical ground model and water level model are set for each 250m grid due to the restriction of data availability, but the underground soil and water level situation varies even within the 250m grid ground. Therefore, even if the liquefaction assessment result is "H: possibility of liquefaction is high" for a certain grid, rather than all the grid area is to liquefy, the grid has a high possibility that somewhere in that grid where there may be the occurrence of sand boiling or water boiling.

As described above, in this project, the seismic hazard assessment quantitatively presents incorporating several estimations and assumptions, on the basis of the limited and less information and data. Therefore, compared with the results observed in Japan incorporating more information, the results of this project are expected to have more uncertainty.

Compared to the 2002 JICA Study, additional information, in particular by comparison with the phenomena actually caused by the Gorkha Earthquake, accuracy is remarkably improved. However, still it is necessary to pay attention to the deviations in results due to the lack of soil information, etc.